Introduction to Molecular Dynamics Simulation

Gerald Kneller

Centre de Biophysique Moléculaire CNRS and Université d’Orléans
Laboratoire des Biomolécules CNRS and Ecole Normale Supérieure Paris

Presentation for the MDANSE 2024 school
Grenoble, 6 November 2024

Short history of Molecular Dynamics simulation

Monte Carlo Simulation of hard disks

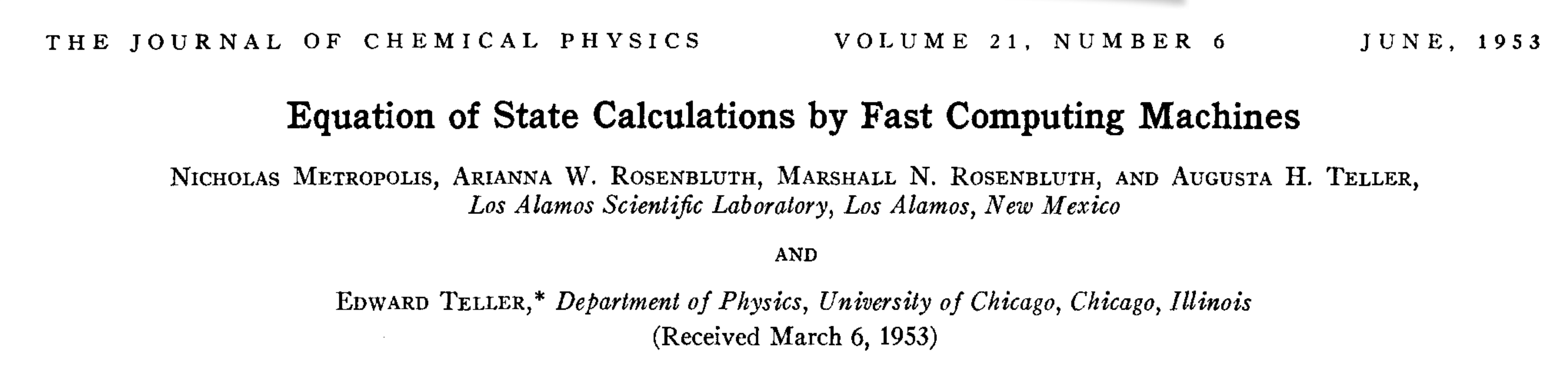

THE JOURNAL OF CHEMICAL PHYSICS VOLUME 21, NUMBER 6 JUNE, 1953

Equation of State Calculations by Fast Computing Machines

NICHOLAS METROPOLIS, ARIANNA W. ROSENBLUTH, MARSHALL N. ROSENBLUTH, AND AUGUSTA H. TELLER,
Los Alamos Scientific Laboratory, Los Alamos, New Mexico

AND

EDWARD TELLER,* *Department of Physics, University of Chicago, Chicago, Illinois*
(Received March 6, 1953)

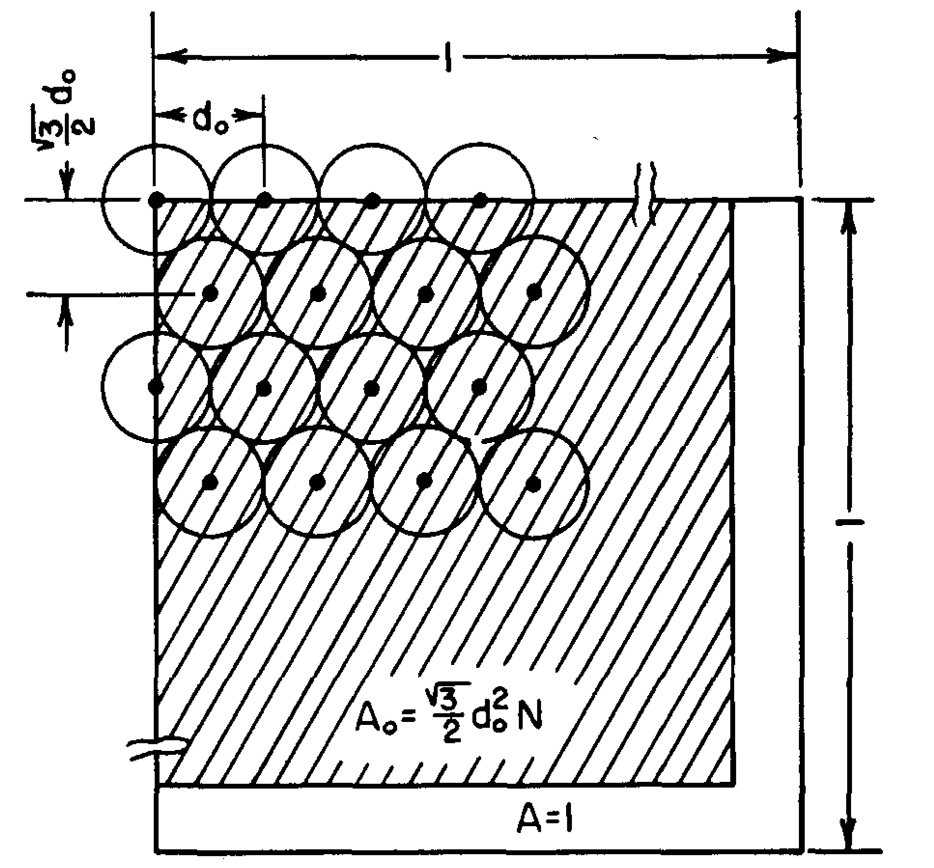

FIG. 3. The close-packed arrangement for determining A_0.

☞ Short-ranged repulsive forces

Molecular Dynamics Simulation of hard spheres

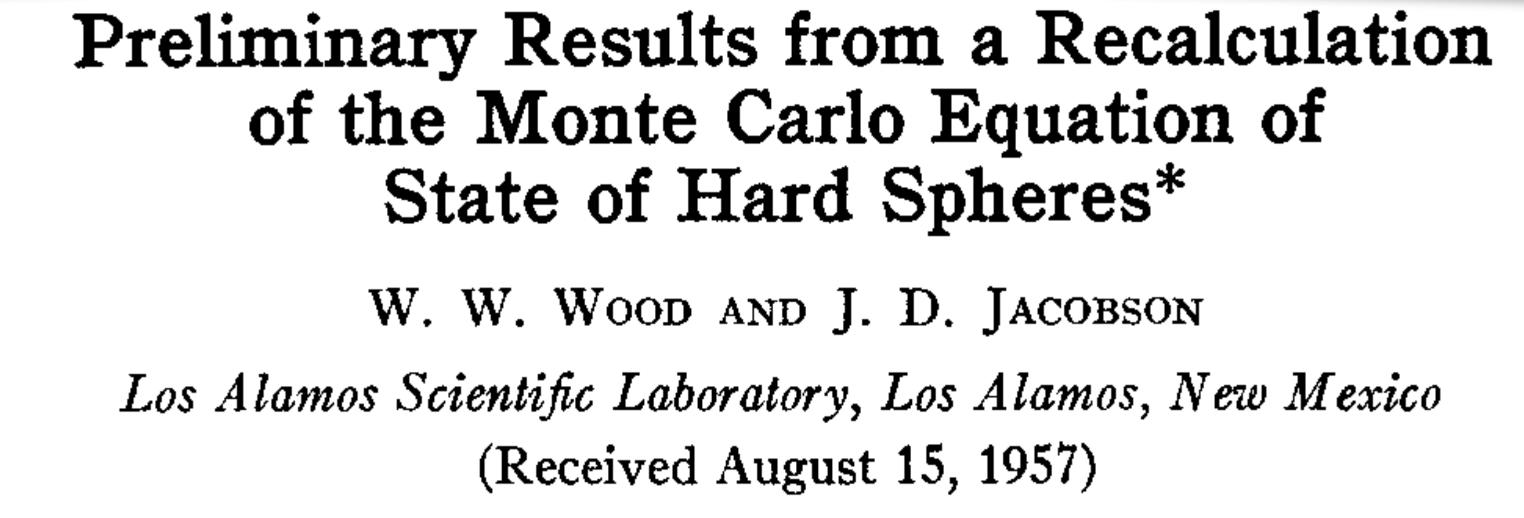

Preliminary Results from a Recalculation of the Monte Carlo Equation of State of Hard Spheres*

W. W. WOOD AND J. D. JACOBSON
Los Alamos Scientific Laboratory, Los Alamos, New Mexico
(Received August 15, 1957)

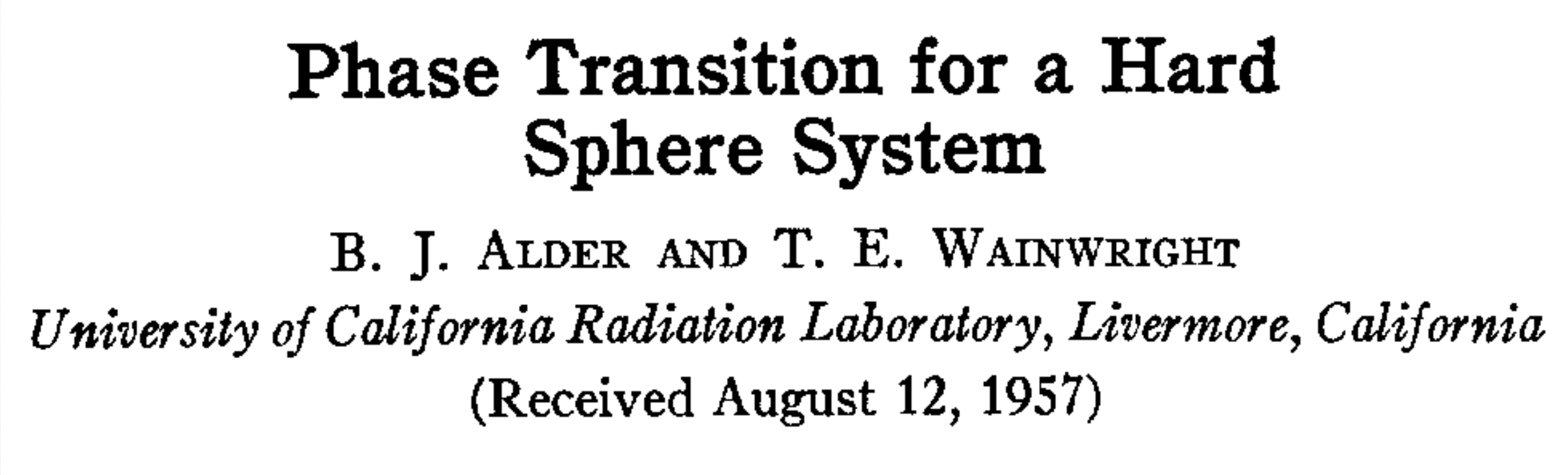

Phase Transition for a Hard Sphere System

B. J. ALDER AND T. E. WAINWRIGHT
University of California Radiation Laboratory, Livermore, California
(Received August 12, 1957)

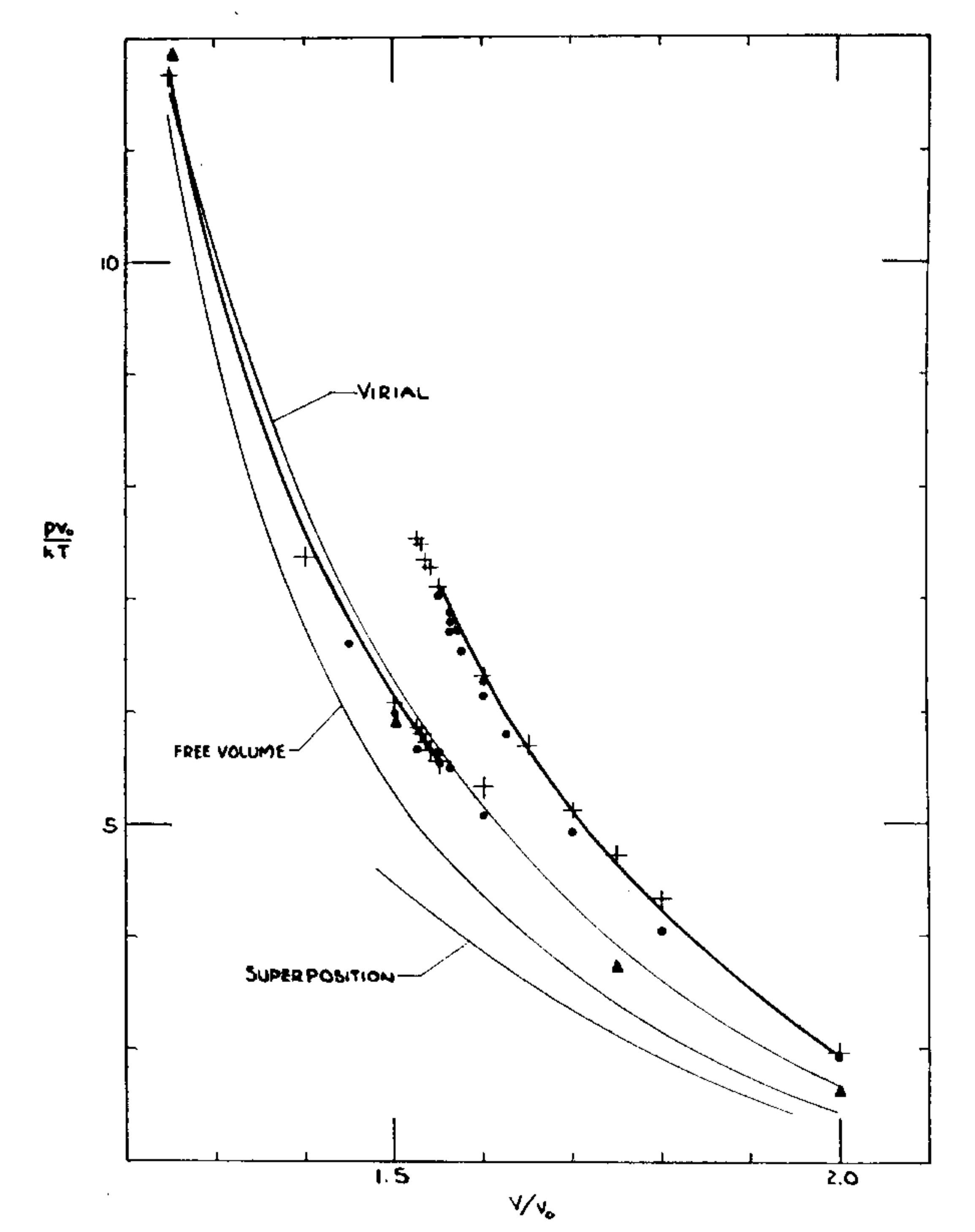

Pressure

Volume

What are MD simulations ?

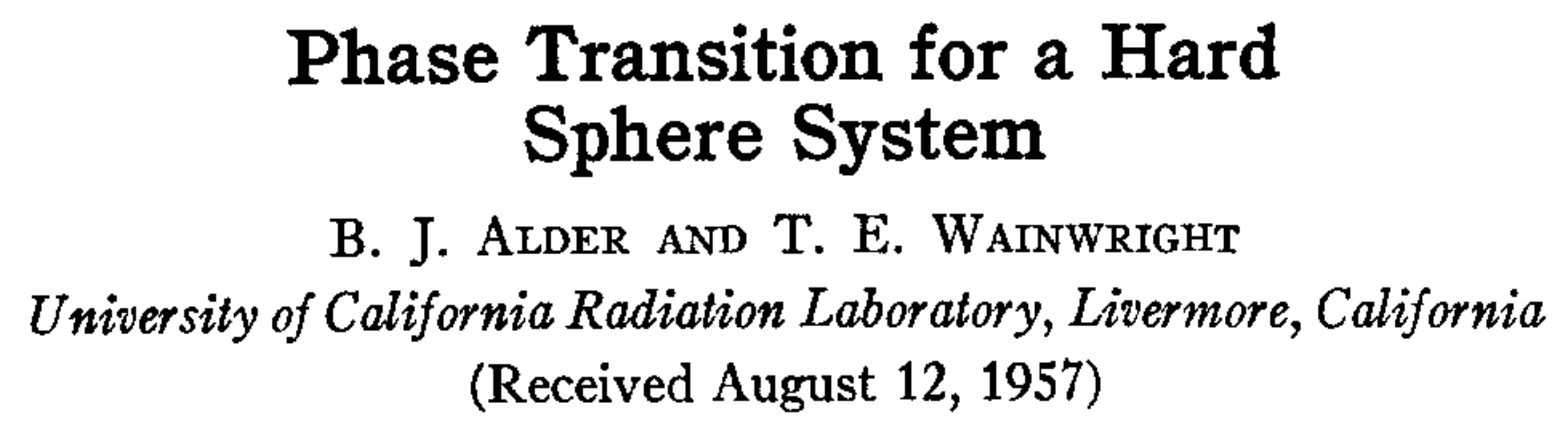

Phase Transition for a Hard Sphere System

B. J. Alder and T. E. Wainwright

University of California Radiation Laboratory, Livermore, California

(Received August 12, 1957)

CALCULATION of molecular dynamic motion has been designed principally to study the relaxations accompanying various nonequilibrium phenomena. The method consists of solving exactly (to the number of significant figures carried) the simultaneous classical equations of motion of several hundred particles by means of fast electronic computors. Some of the details as they relate to hard spheres and to particles having square well potentials of attraction have been described. The method has been used also to calculate equilibrium properties, particularly the equation of state of hard spheres where differences with previous Monte Carlo results appeared.

Berni Alder, Mary Ann Mansigh, T.E Wainwright

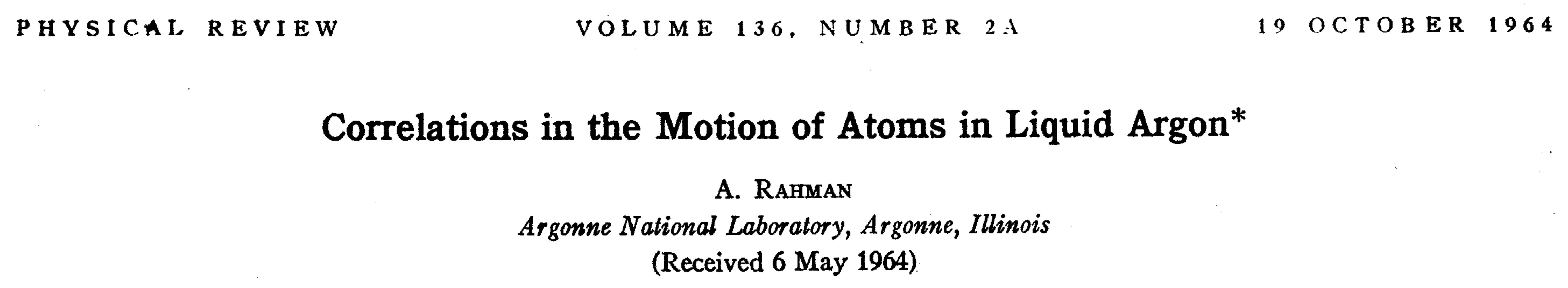

PHYSICAL REVIEW VOLUME 136, NUMBER 2A 19 OCTOBER 1964

Correlations in the Motion of Atoms in Liquid Argon*

A. Rahman
Argonne National Laboratory, Argonne, Illinois
(Received 6 May 1964)

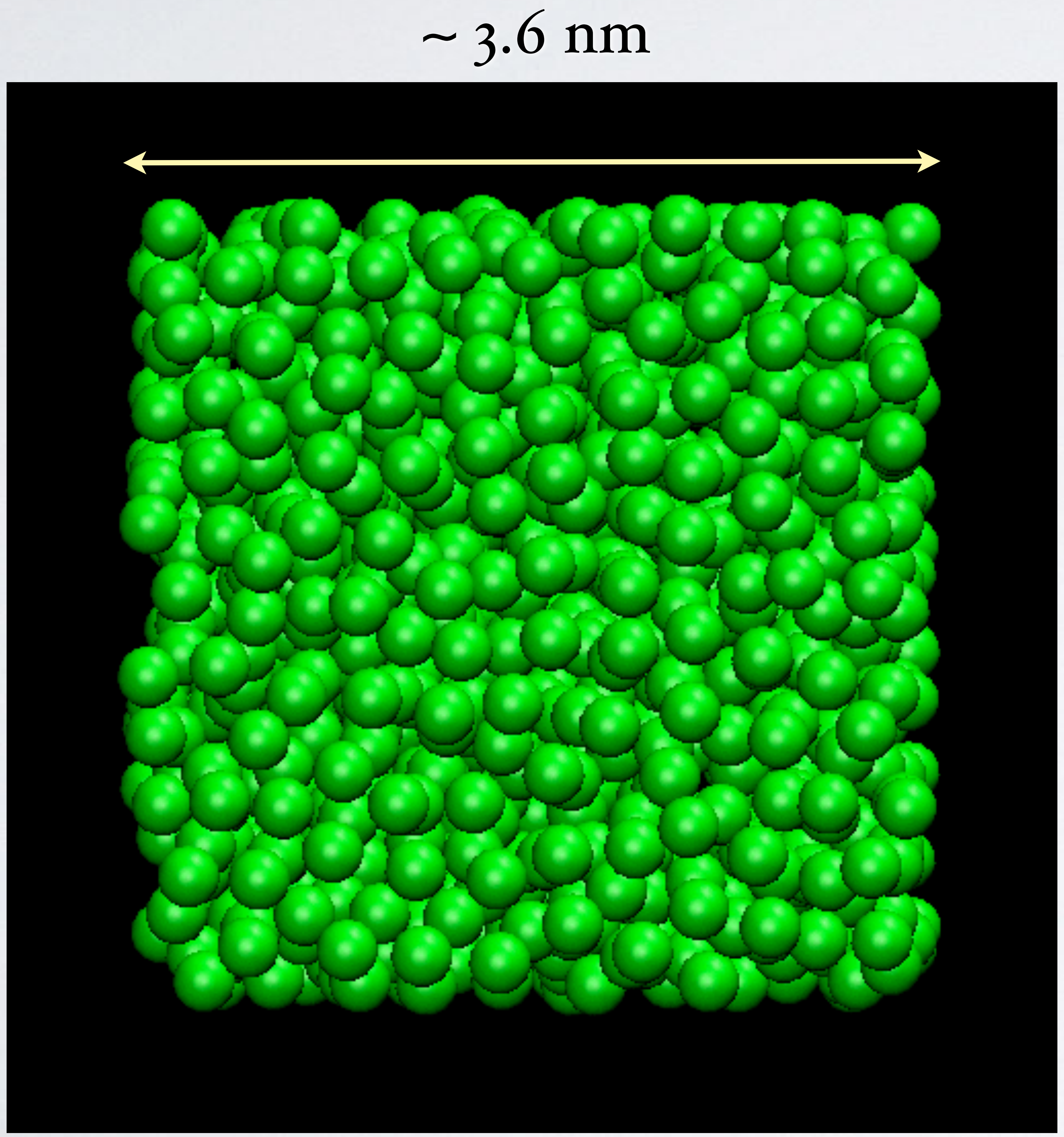

- Solve Newton's equations of motion

$$M_i \ddot{\mathbf{r}}_i = -\frac{\partial U}{\partial \mathbf{r}_i}$$

$$U = \sum_{ij} 4\epsilon \left(\left[\frac{\sigma}{r_{ij}}\right]^{12} - \left[\frac{\sigma}{r_{ij}}\right]^{6} \right)$$

- Discretization and iterative solution yields trajectories = time series (< 100 ns)

$$\mathbf{r}_i(n+1) \;\leftarrow\; 2\mathbf{r}_i(n) - \mathbf{r}_i(n-1) + \frac{\Delta t^2}{M_i}\mathbf{F}_i(n)$$

$$\mathbf{v}_i(n) \;\leftarrow\; \frac{\mathbf{r}_i(n+1) - \mathbf{r}_i(n-1)}{2\Delta t}.$$

$$\text{Forces:} \quad \mathbf{F}_i = -\frac{\partial U}{\partial \mathbf{r}_i}$$

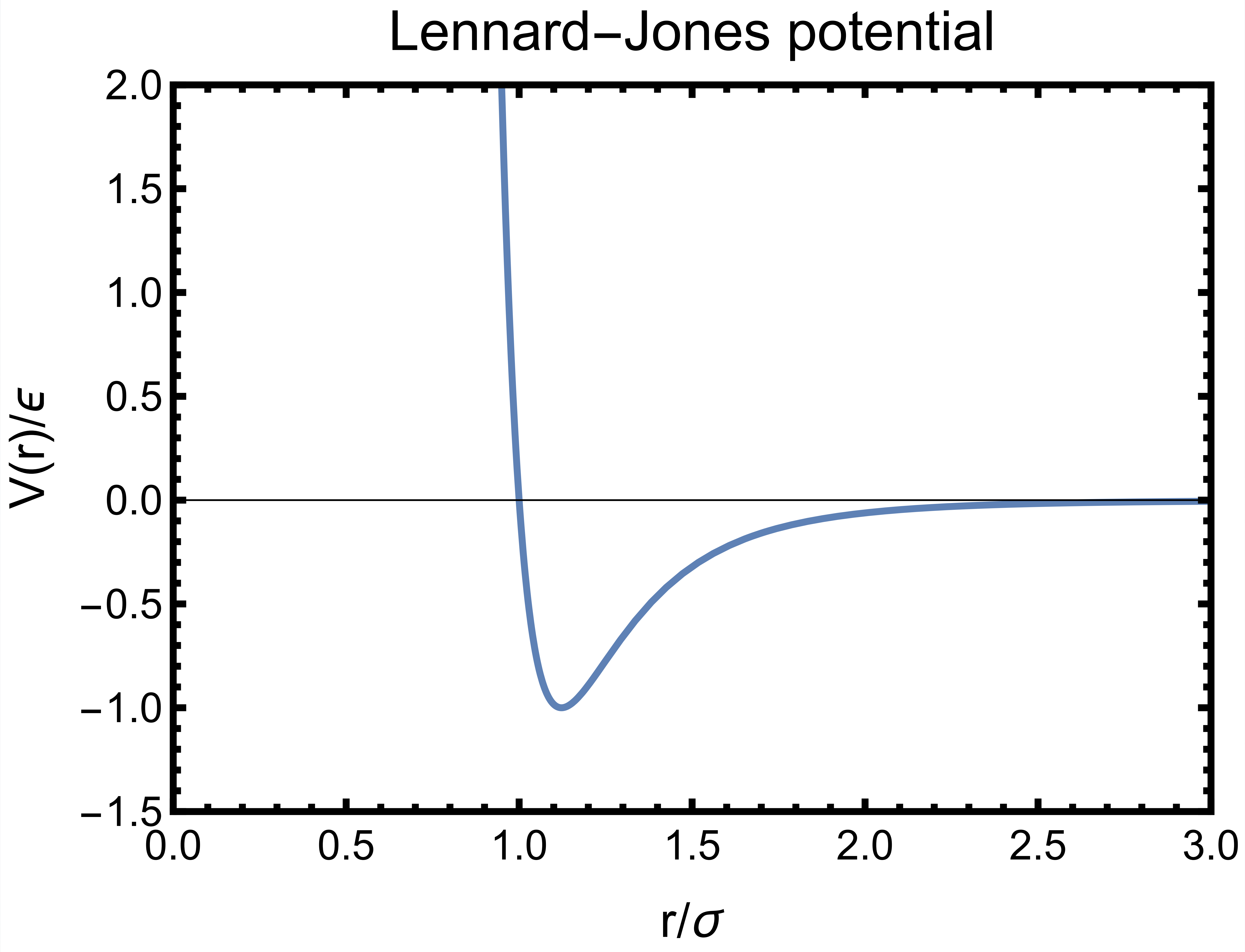

$$U = \sum_{ij} 4\epsilon \left(\left[\frac{\sigma}{r_{ij}} \right]^{12} - \left[\frac{\sigma}{r_{ij}} \right]^{6} \right)$$

Soft sphere repulsion

Induced dipole attraction

Simulating a quasi infinite system with a finite number of particles

Periodic boundary conditions and minimum image convention

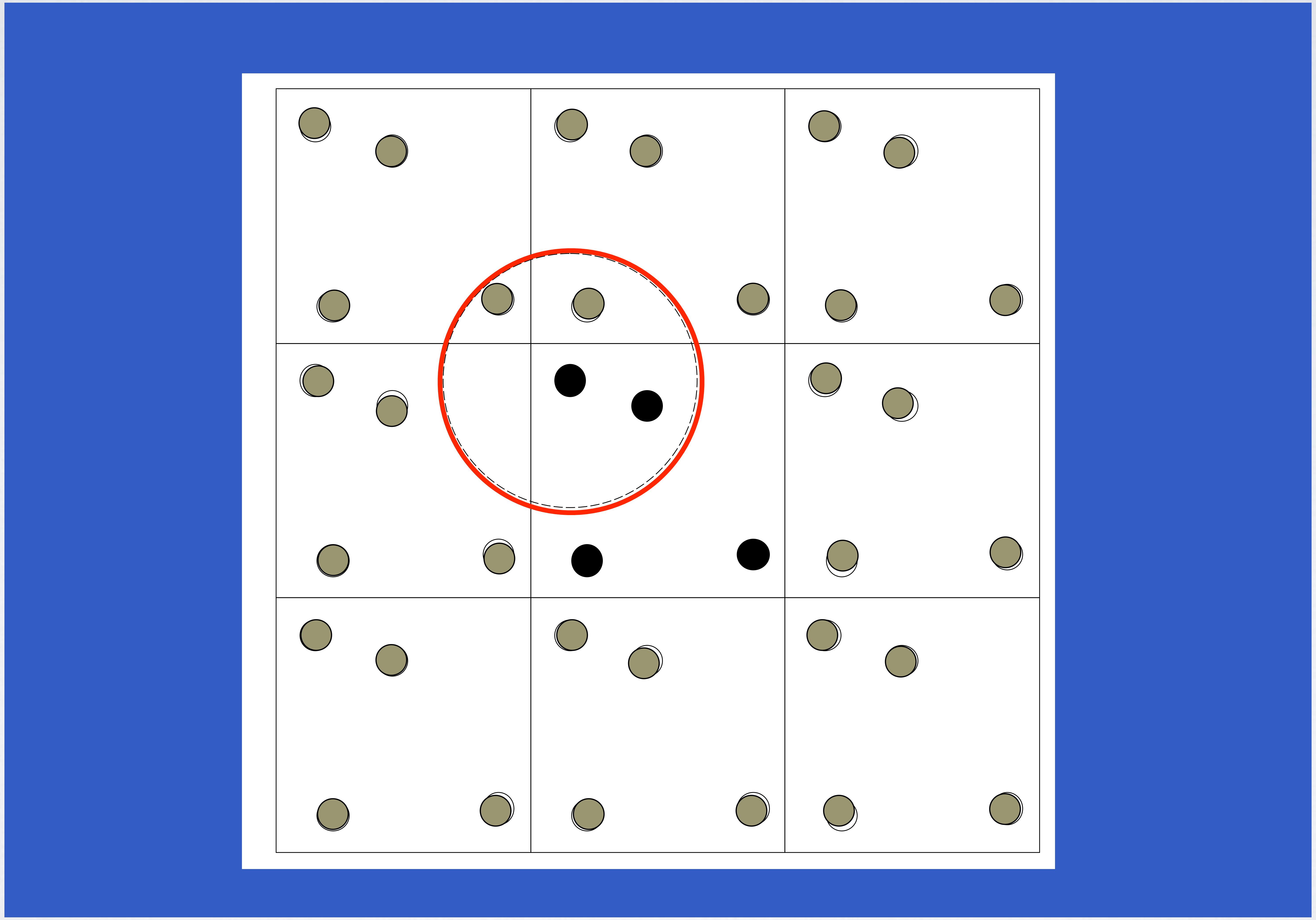

Discretize Newton's equations of motion

Central difference scheme — Verlet algorithm

$$x(t+\Delta t) \approx \frac{1}{2}\Delta t^2 \boxed{\ddot{x}(t)} + \Delta t \boxed{\dot{x}(t)} + x(t)$$

$$x(t-\Delta t) \approx \frac{1}{2}\Delta t^2 \boxed{\ddot{x}(t)} - \Delta t \boxed{\dot{x}(t)} + x(t)$$

$$\dot{x}(t) \approx \frac{x(t+\Delta t) - x(t-\Delta t)}{2\Delta t}$$

$$\ddot{x}(t) \approx \frac{x(t+\Delta t) - 2x(t) + x(t-\Delta t)}{\Delta t^2}$$

$$m\ddot{x}(t) = F(t)$$

$$x(t+\Delta t) \approx 2x(t) - x(t-\Delta t) + \Delta t^2 \frac{F(t)}{m}$$

Analysis of structure **and** dynamics

Static quantities

Maxwell velocity distribution

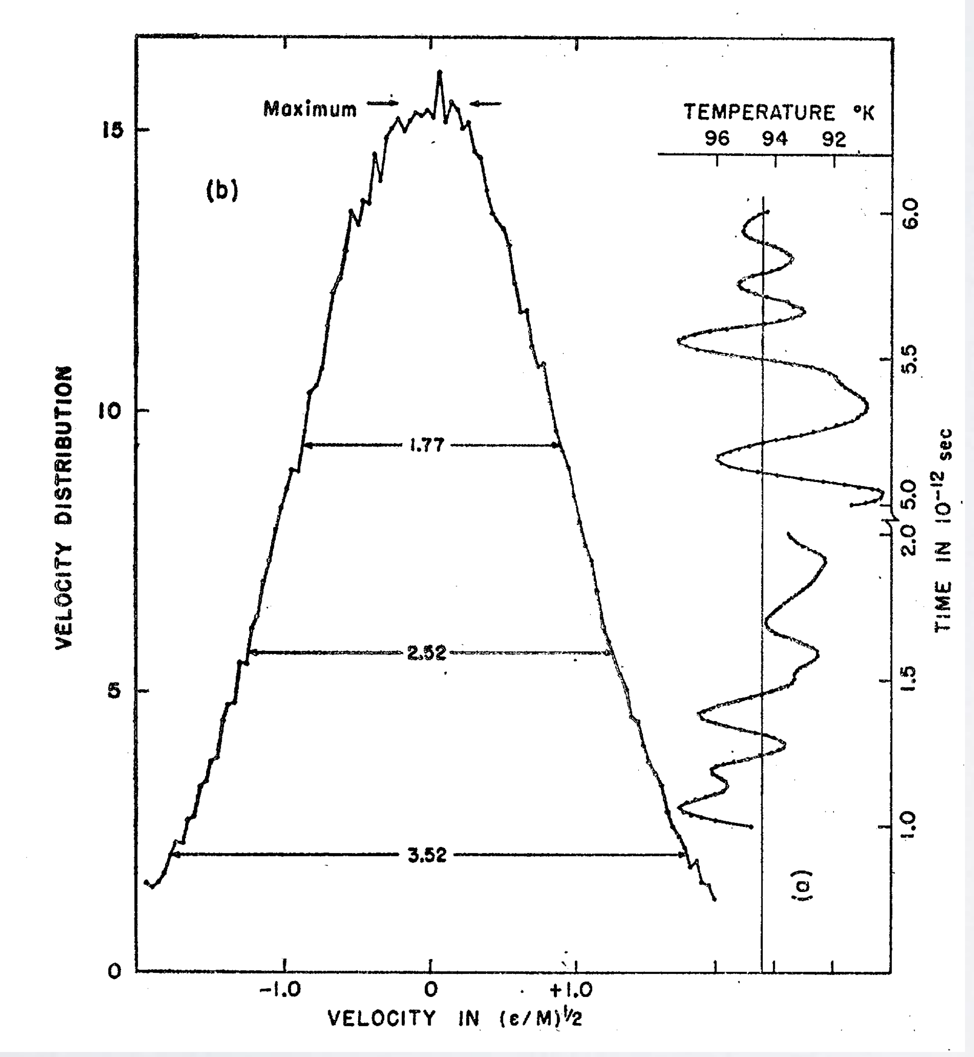

Pair correlation function

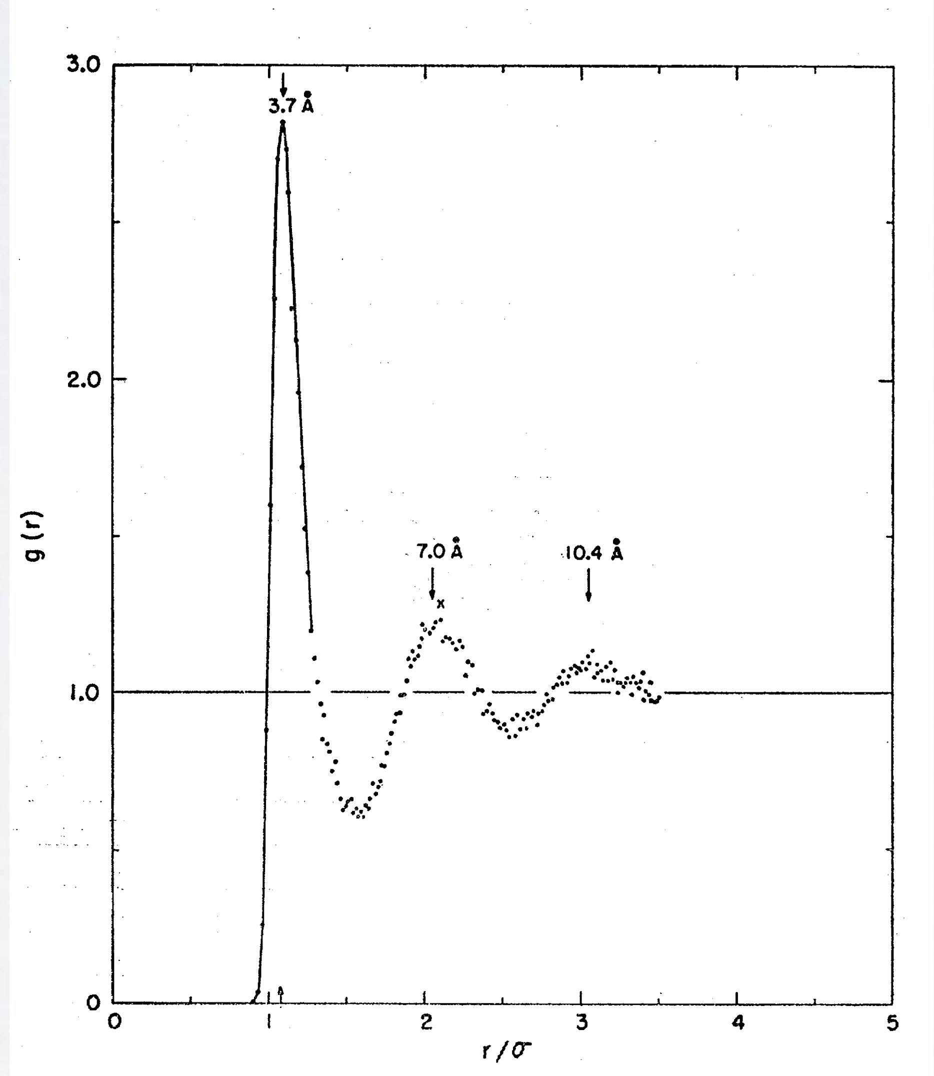

☞ *X-ray and neutron diffraction*

Dynamic quantities

Mean squared displacement

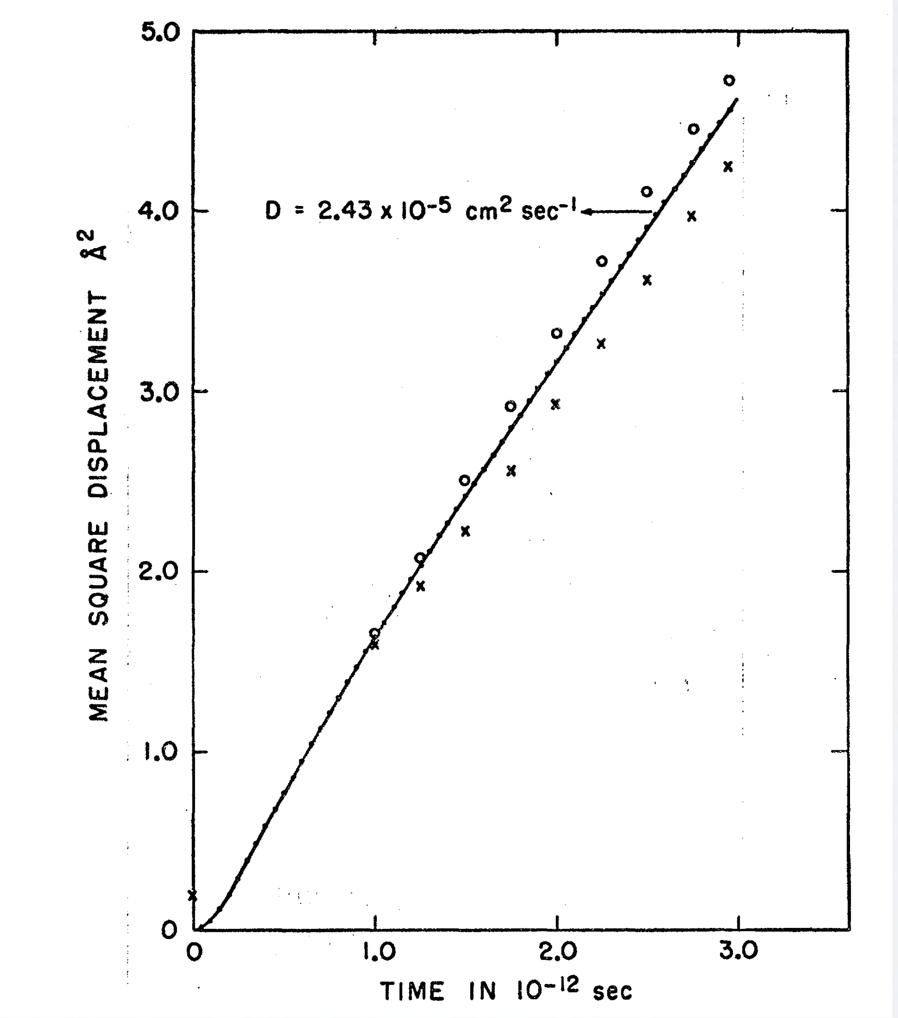

Velocity autocorrelation function

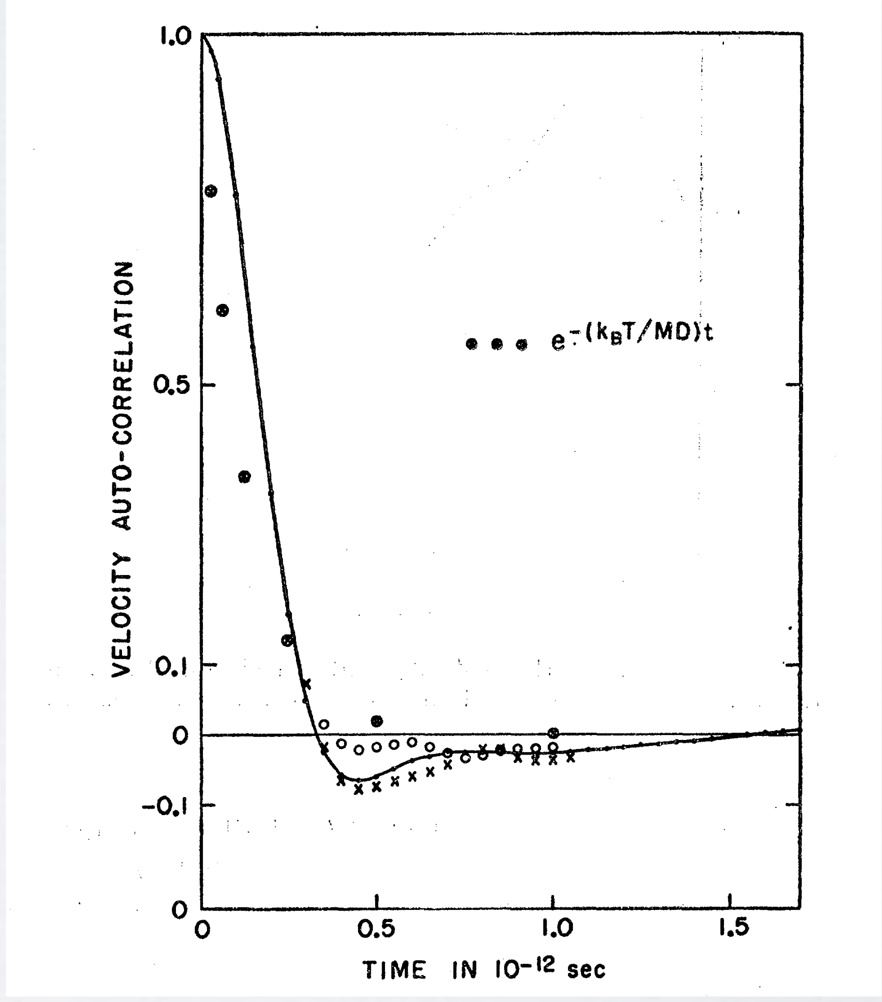

☞ *Quasielastic neutron scattering*

Orsay school of MD simulation

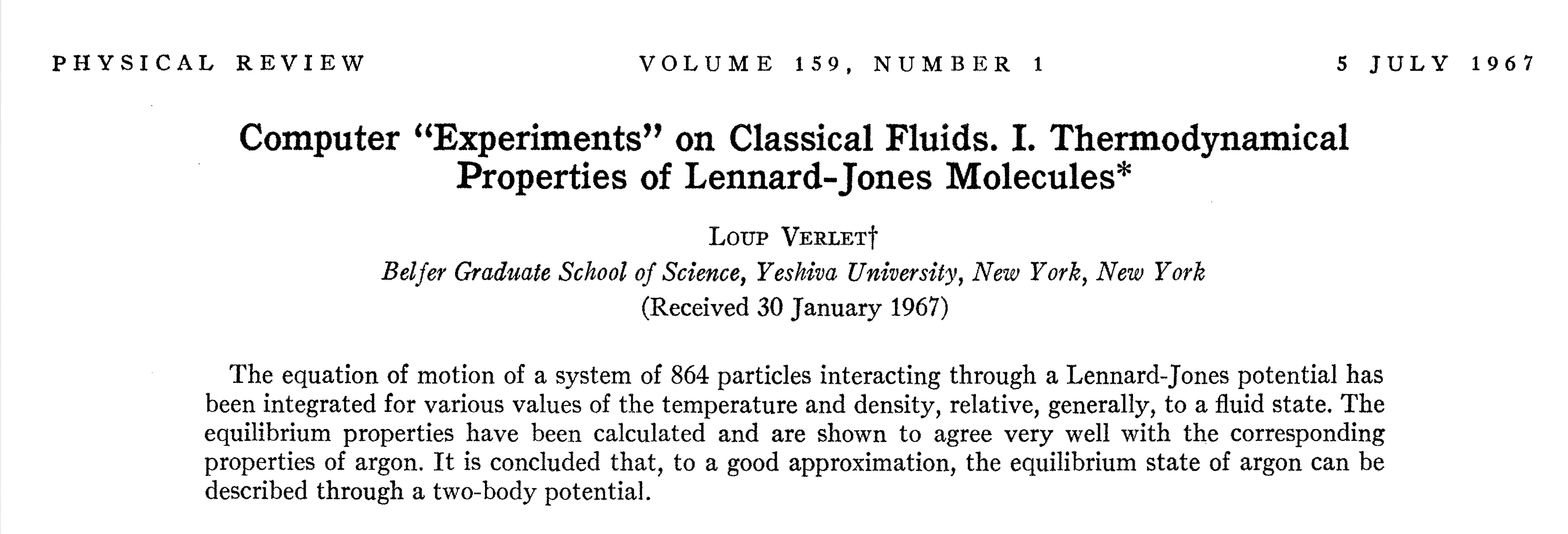

PHYSICAL REVIEW VOLUME 159, NUMBER 1 5 JULY 1967

Computer "Experiments" on Classical Fluids. I. Thermodynamical Properties of Lennard-Jones Molecules*

LOUP VERLET†
Belfer Graduate School of Science, Yeshiva University, New York, New York

(Received 30 January 1967)

The equation of motion of a system of 864 particles interacting through a Lennard-Jones potential has been integrated for various values of the temperature and density, relative, generally, to a fluid state. The equilibrium properties have been calculated and are shown to agree very well with the corresponding properties of argon. It is concluded that, to a good approximation, the equilibrium state of argon can be described through a two-body potential.

Loup Verlet

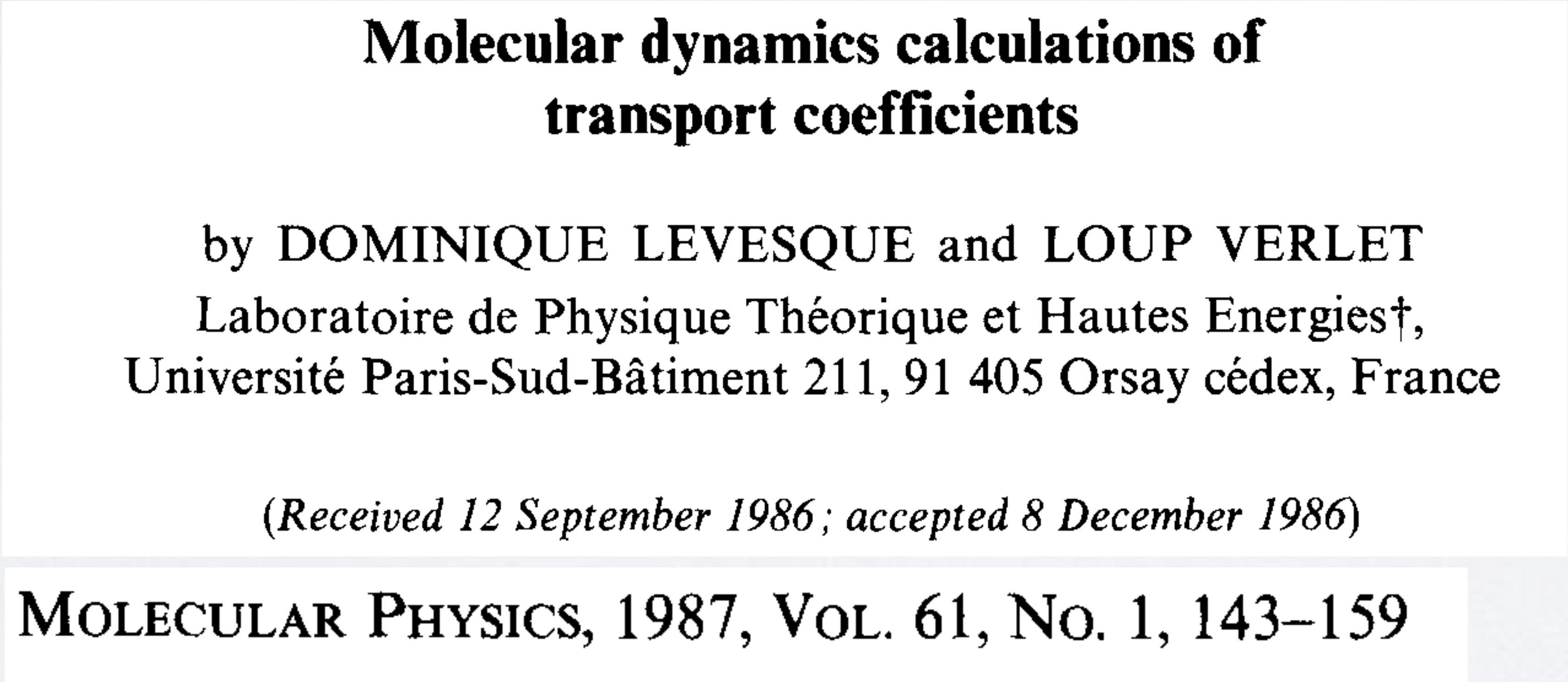

Molecular dynamics calculations of transport coefficients

by DOMINIQUE LEVESQUE and LOUP VERLET
Laboratoire de Physique Théorique et Hautes Energies†,
Université Paris-Sud-Bâtiment 211, 91 405 Orsay cédex, France

(*Received 12 September 1986; accepted 8 December 1986*)

MOLECULAR PHYSICS, 1987, VOL. 61, NO. 1, 143–159

Dominique
Levesque

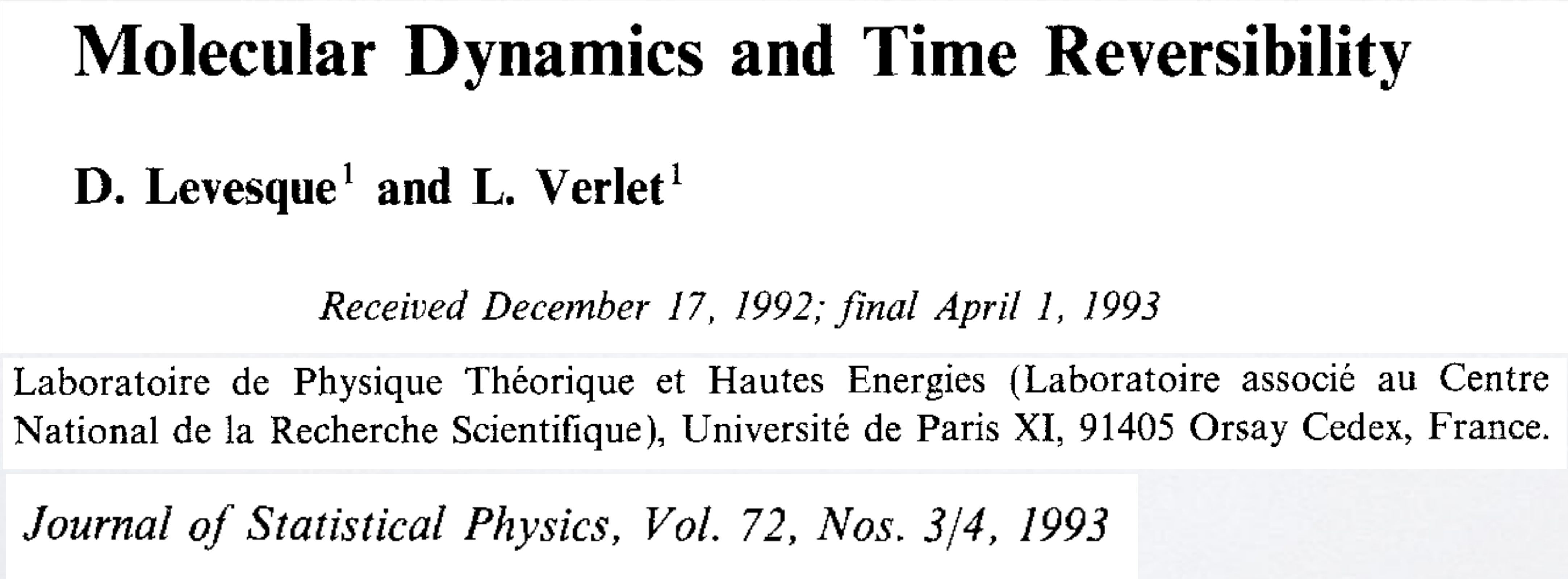

Molecular Dynamics and Time Reversibility

D. Levesque[1] and L. Verlet[1]

Received December 17, 1992; final April 1, 1993

Laboratoire de Physique Théorique et Hautes Energies (Laboratoire associé au Centre National de la Recherche Scientifique), Université de Paris XI, 91405 Orsay Cedex, France.

Journal of Statistical Physics, Vol. 72, Nos. 3/4, 1993

MD simulation of liquid water

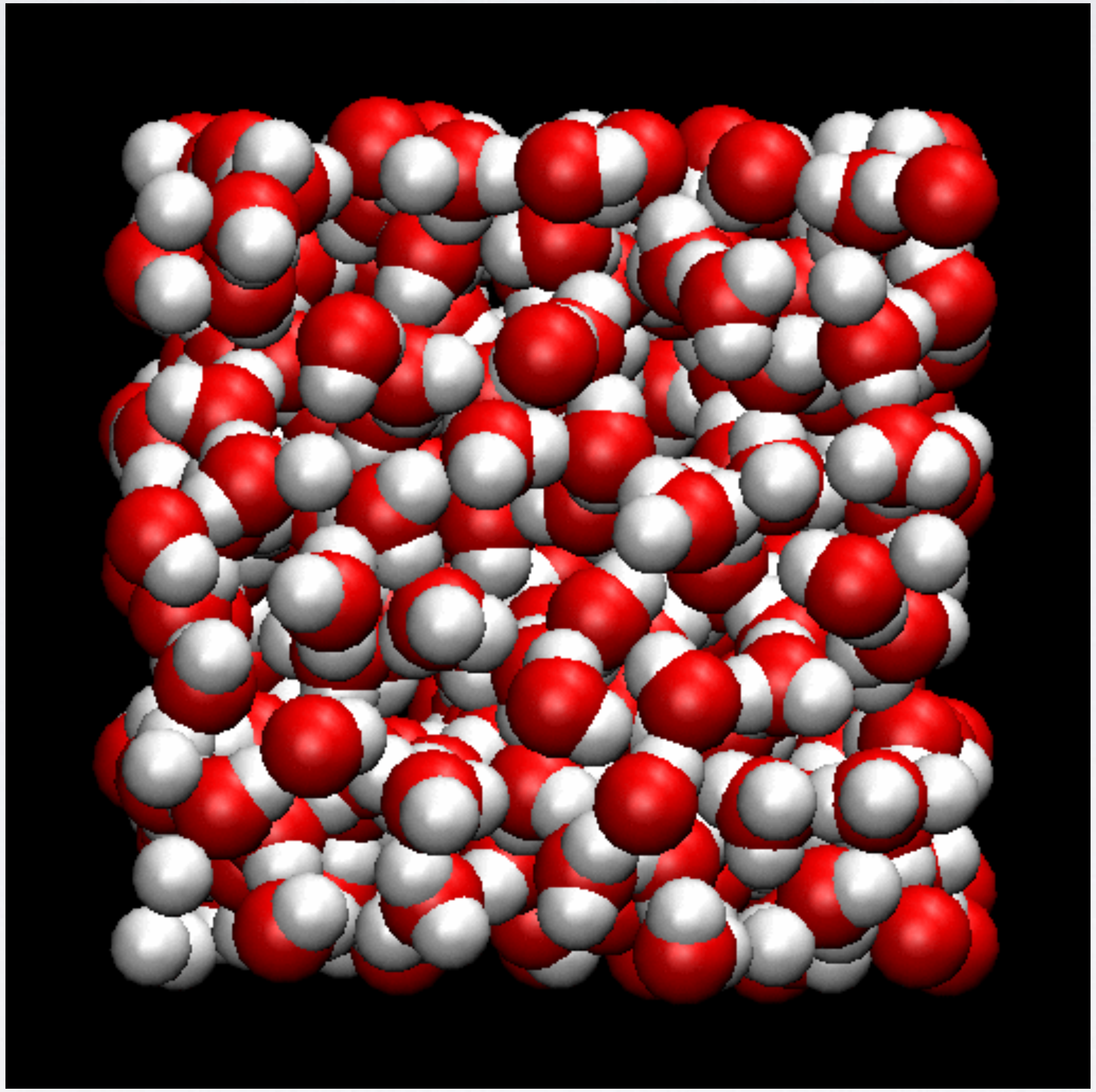

Simulation of liquid water with an effective electrostatic model

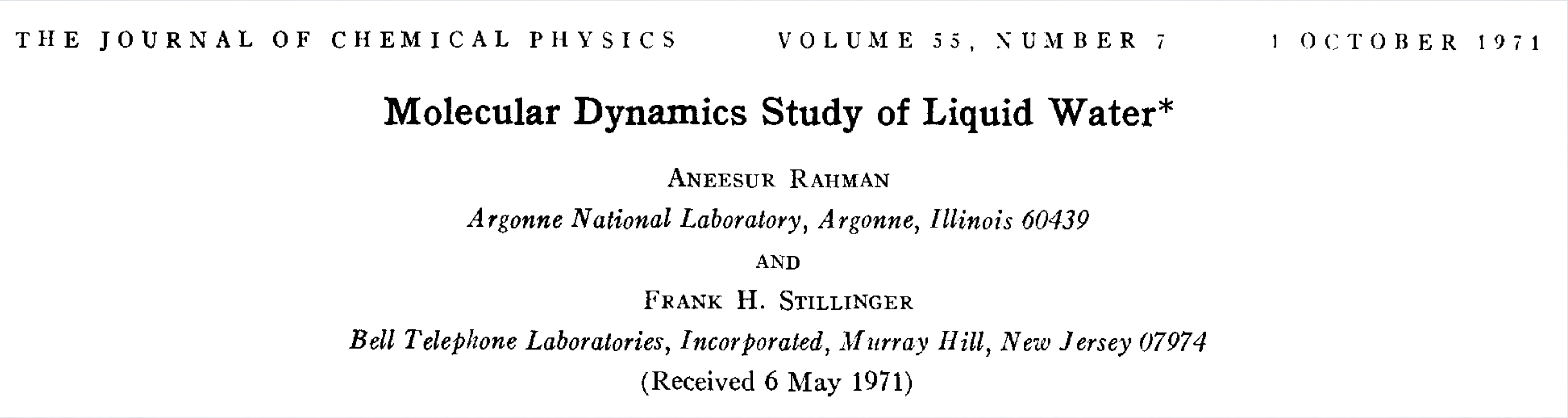

THE JOURNAL OF CHEMICAL PHYSICS VOLUME 55, NUMBER 7 1 OCTOBER 1971

Molecular Dynamics Study of Liquid Water*

ANEESUR RAHMAN
Argonne National Laboratory, Argonne, Illinois 60439
AND
FRANK H. STILLINGER
Bell Telephone Laboratories, Incorporated, Murray Hill, New Jersey 07974
(Received 6 May 1971)

Charged mass-less force centers

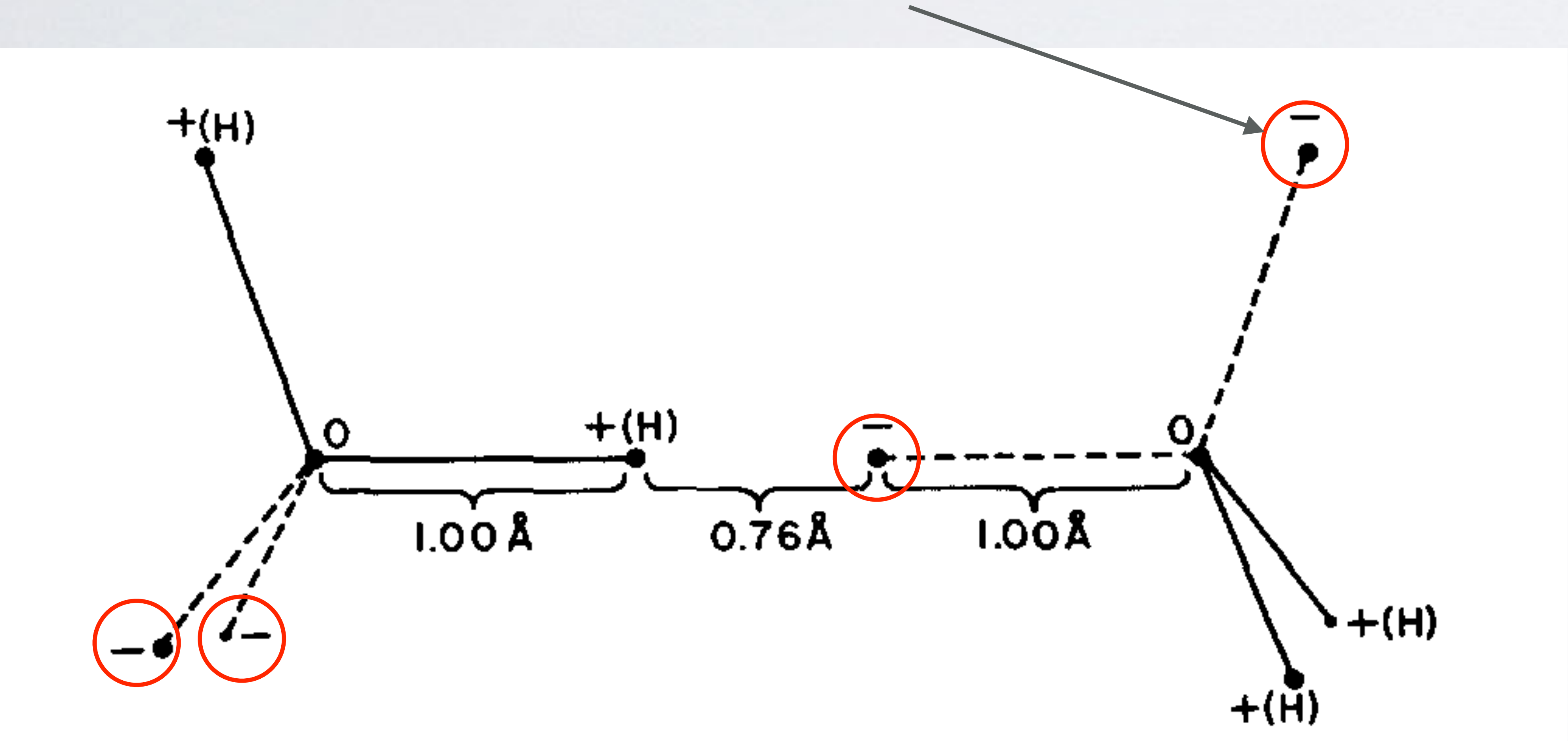

FIG. 1. Minimum energy configuration for two water molecules, according to potential (2.5). Each oxygen nucleus is symmetrically surrounded by a tetrad of four-point charges ($\pm 0.19e$), the positive members of which represent partially shielded protons. The configuration shown has a plane of symmetry and incorporates a single linear H bond.

$$\boxed{V_{\text{eff}}^{(2)}(\mathbf{x}_i,\, \mathbf{x}_j)=v_{\text{LJ}}(r_{ij})+S(r_{ij})\,v_{\text{el}}(\mathbf{x}_i,\, \mathbf{x}_j)}$$

Effective pair potential

$$v_{\text{LJ}}(r_{ij})=4\epsilon[(\sigma/r_{ij})^{12}-(\sigma/r_{ij})^{6}].$$

Lennard-Jones term

$$v_{\text{el}}(\mathbf{x}_i,\, \mathbf{x}_j)=(0.19e)^2\sum_{\alpha_i,\alpha_j=1}^{4}(-1)^{\alpha_i+\alpha_j}/d_{\alpha_i\alpha_j}(\mathbf{x}_i,\, \mathbf{x}_j)$$

Electrostatic sum

$$\begin{aligned} S(r_{ij}) &= 0 && (0\leq r_{ij}\leq R_L),\\ &=(r_{ij}-R_L)^2(3R_U-R_L-2r_{ij})/(R_U-R_L)^3 && \\ & && (R_L\leq r_{ij}\leq R_U),\\ &=1 && (R_U\leq r_{ij}<\infty), \end{aligned}$$

“Switching function”

Simulation of liquid water with a simple point charge model

HJC. Berendsen, J. R. Grigera, and T. P. Straatsma, J Phys Chem, vol. 91, no. 24, pp. 6269–6271, 1987.

- Rigid molecule
- O-O interactions via Lennard-Jones potential
- Point charges on the atoms - interaction via the **Coulomb potential**

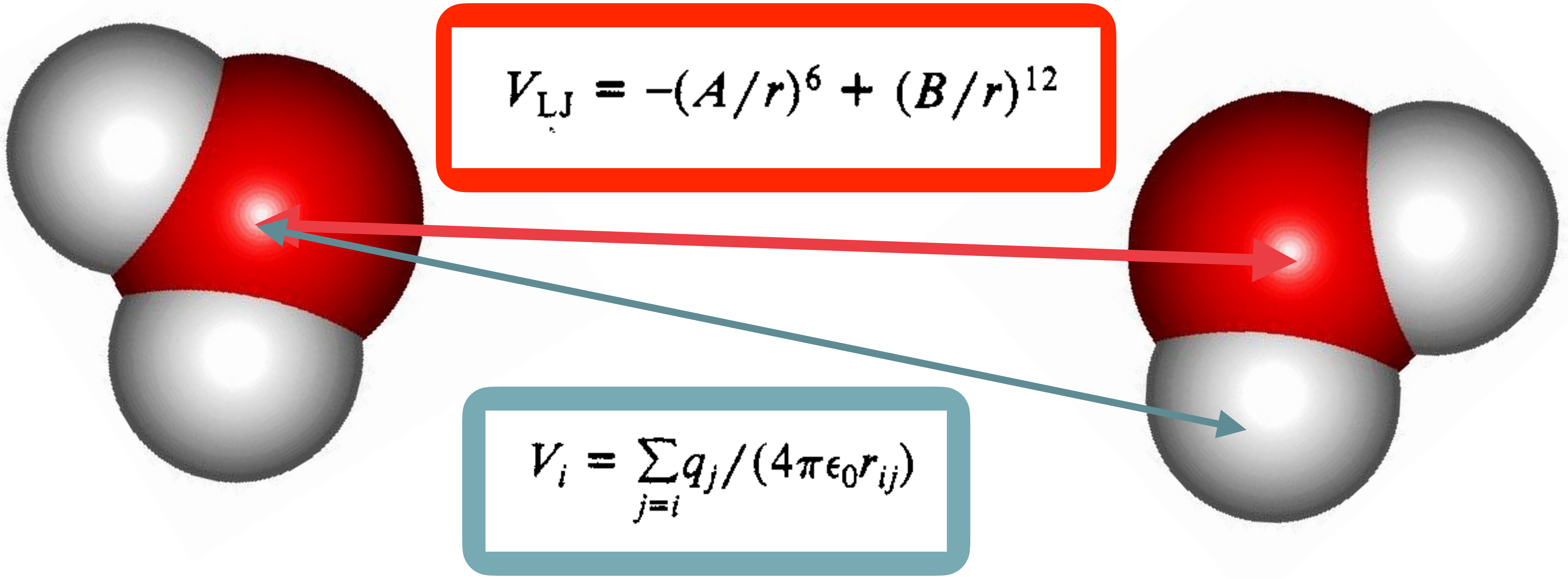

$$V_{\mathrm{LJ}} = -(A/r)^6 + (B/r)^{12}$$

$$V_i = \sum_{j=i} q_j/(4\pi\epsilon_0 r_{ij})$$

Long-ranged Coulomb interactions → Ewald summation, PME, …

Long-ranged Coulomb interactions in a pseudo crystal through Ewald summation

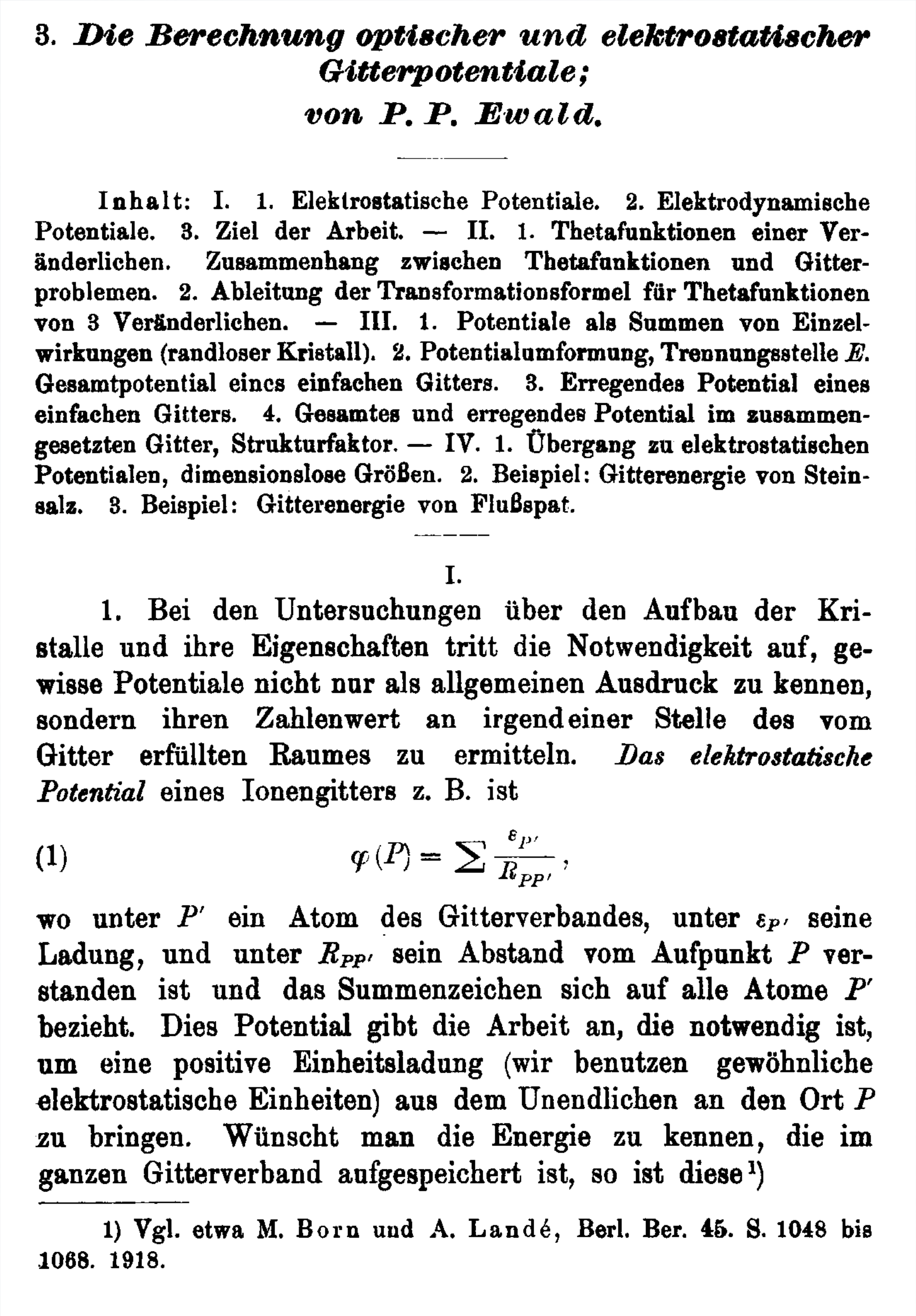

3. *Die Berechnung optischer und elektrostatischer Gitterpotentiale;*

von P. P. Ewald.

Inhalt: I. 1. Elektrostatische Potentiale. 2. Elektrodynamische Potentiale. 3. Ziel der Arbeit. — II. 1. Thetafunktionen einer Veränderlichen. Zusammenhang zwischen Thetafunktionen und Gitterproblemen. 2. Ableitung der Transformationsformel für Thetafunktionen von 3 Veränderlichen. — III. 1. Potentiale als Summen von Einzelwirkungen (randloser Kristall). 2. Potentialumformung, Trennungsstelle *E*. Gesamtpotential eines einfachen Gitters. 3. Erregendes Potential eines einfachen Gitters. 4. Gesamtes und erregendes Potential im zusammengesetzten Gitter, Strukturfaktor. — IV. 1. Übergang zu elektrostatischen Potentialen, dimensionslose Größen. 2. Beispiel: Gitterenergie von Steinsalz. 3. Beispiel: Gitterenergie von Flußspat.

I.

1. Bei den Untersuchungen über den Aufbau der Kristalle und ihre Eigenschaften tritt die Notwendigkeit auf, gewisse Potentiale nicht nur als allgemeinen Ausdruck zu kennen, sondern ihren Zahlenwert an irgendeiner Stelle des vom Gitter erfüllten Raumes zu ermitteln. *Das elektrostatische Potential* eines Ionengitters z. B. ist

$$\varphi(P) = \sum \frac{\varepsilon_{P'}}{R_{PP'}}, \tag{1}$$

wo unter P' ein Atom des Gitterverbandes, unter $\varepsilon_{P'}$ seine Ladung, und unter $R_{PP'}$ sein Abstand vom Aufpunkt P verstanden ist und das Summenzeichen sich auf alle Atome P' bezieht. Dies Potential gibt die Arbeit an, die notwendig ist, um eine positive Einheitsladung (wir benutzen gewöhnliche elektrostatische Einheiten) aus dem Unendlichen an den Ort P zu bringen. Wünscht man die Energie zu kennen, die im ganzen Gitterverband aufgespeichert ist, so ist diese[1])

---

1) Vgl. etwa M. Born und A. Landé, Berl. Ber. 45. S. 1048 bis 1068. 1918.

P. P. Ewald, Annalen der Physik, vol. 369, pp. 253–287, Jan. 1921

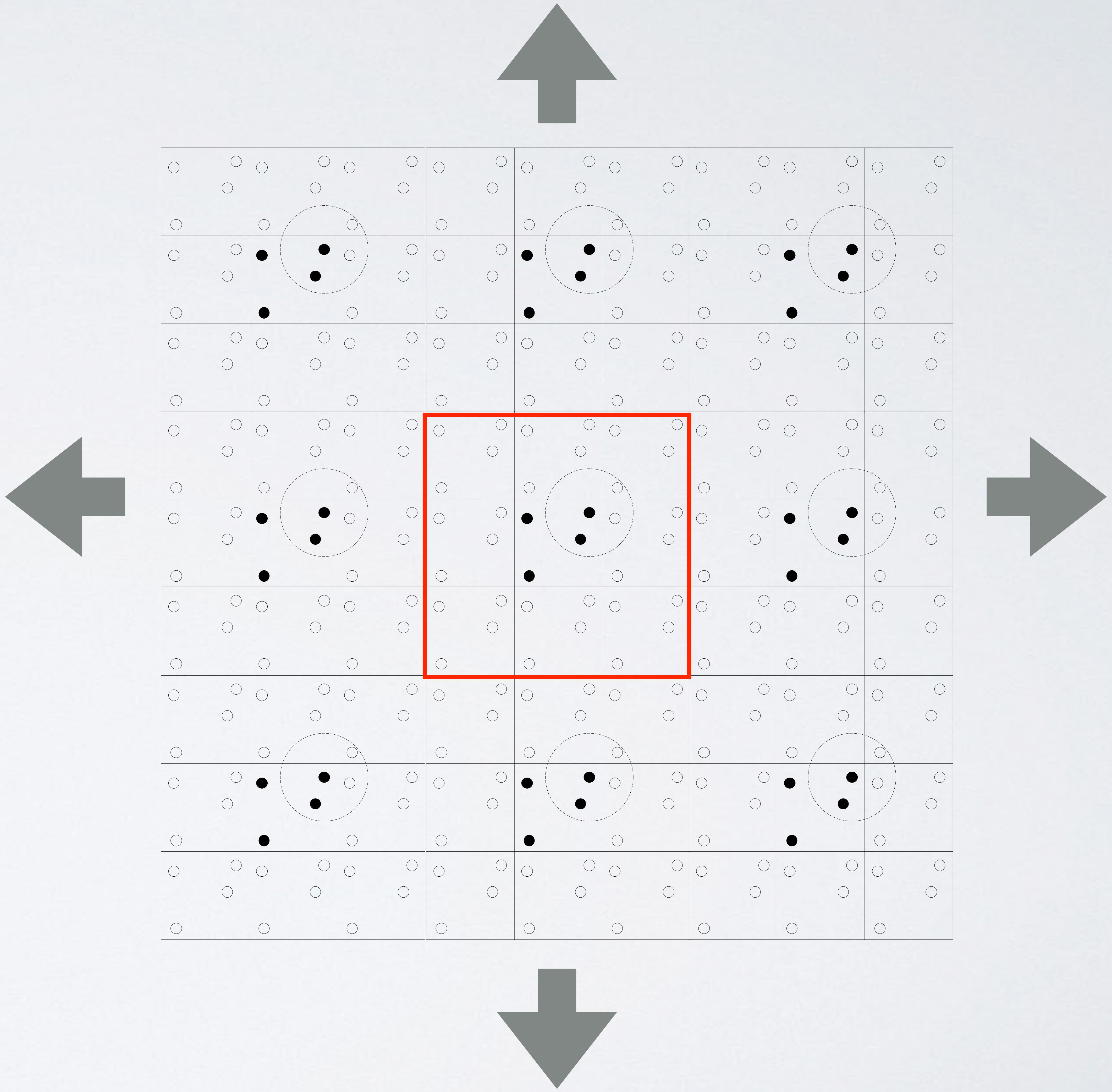

Convergence of the Coulomb energy: Split the latter into contributions from direct and reciprocal space, respectively, which are each converging, and a surface term, J(D), describing the boundary conditions at infinity (from Darden, York, Pedersen, J. Chem. Phys. **98**(12), 10089 (1993)).

Direct space (basis vectors $\mathbf{a}_1, \mathbf{a}_2, \mathbf{a}_3$)

$$\boxed{\Phi_{\text{dir}}(\mathbf{r};\beta) = \sum_{n} \frac{\operatorname{erfc}(\beta|\mathbf{r}+\mathbf{n}|)}{|\mathbf{r}+\mathbf{n}|}}$$

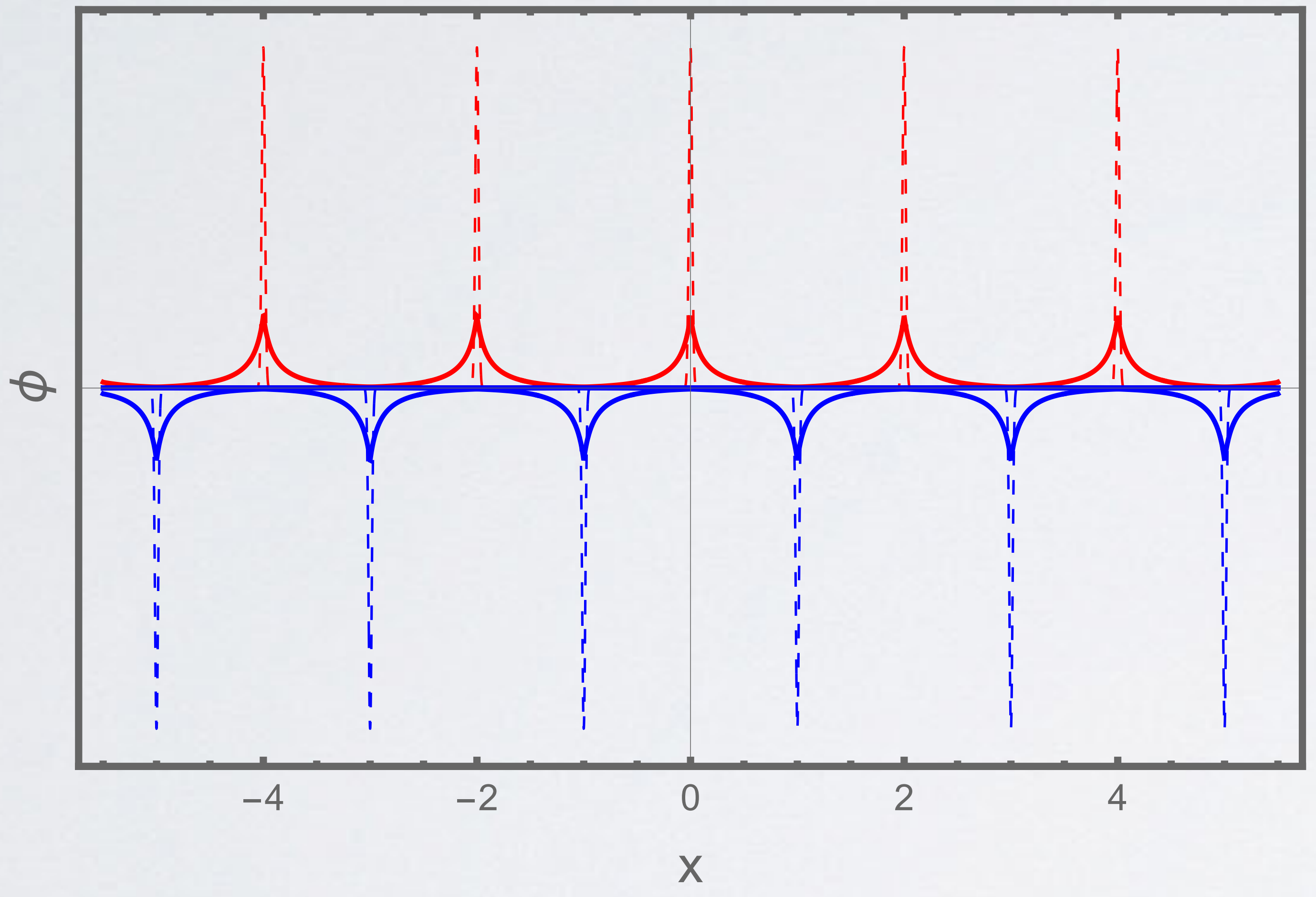

Reciprocal space (basis vectors $\mathbf{a}^1, \mathbf{a}^2, \mathbf{a}^3$)

$$\boxed{\Phi_{\text{rec}}(\mathbf{r};\beta) = \frac{1}{\pi V} \sum_{m\neq 0} \frac{\exp(-\pi^2\mathbf{m}^2/\beta^2)}{\mathbf{m}^2} \exp(2\pi i\mathbf{m}\cdot\mathbf{r})}$$

$$E = \sum_{i=1}^{N} \sum_{j=i+1}^{N} q_i q_j \boxed{\frac{\operatorname{erfc}(\beta r_{ij})}{r_{ij}}} - \frac{\beta}{\sqrt{\pi}} \sum_{i=1}^{N} q_i^2 + \frac{1}{2} \sum_{i=1}^{N} \sum_{j=1}^{N} q_i q_j \boxed{\Phi_{\text{rec}}(\mathbf{r}_j - \mathbf{r}_i;\beta)} + \boxed{J(\mathbf{D})}$$

The parameter β determines the repartition between real and imaginary space contributions.

Force field for biomolecular simulations

Chemistry-driven force fields

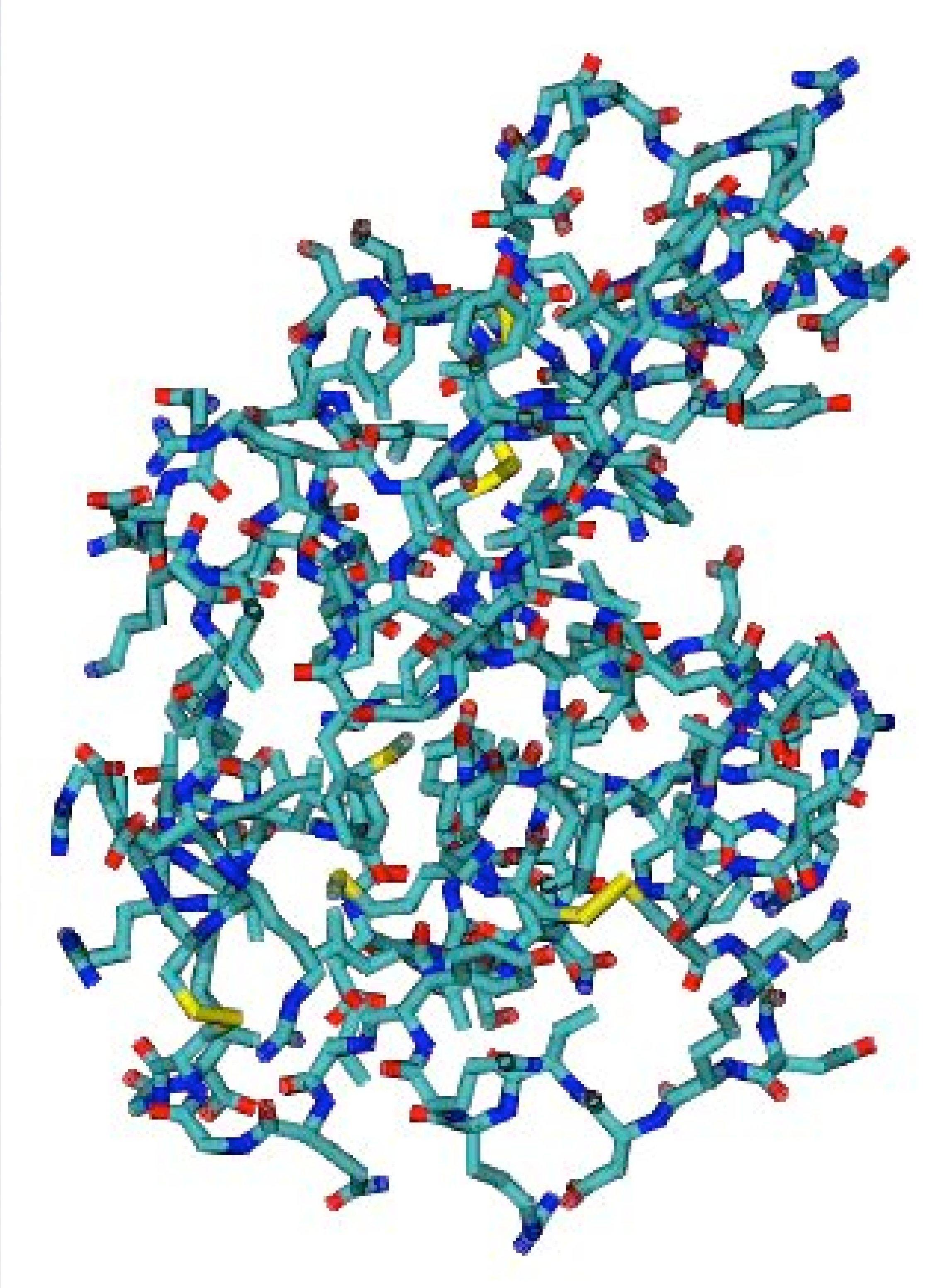

Lysozyme

$$U = \sum_{\text{bonds } ij} k_{ij}(r_{ij} - r_{ij}^{(0)})^2 + \sum_{\text{angles } ijk} k_{ijk}(\phi_{ijk} - \phi_{ijk}^{(0)})^2$$

$$+ \sum_{\text{dihedrals } ijkl} k_{ijkl} \cos(n_{ijkl}\theta_{ijkl} - \delta_{ijkl})$$

$$\left.\begin{aligned} &+ \sum_{\text{all pairs } ij} 4\epsilon_{ij}\left(\frac{\sigma_{ij}^{12}}{r^{12}} - \frac{\sigma_{ij}^{6}}{r^{6}}\right) \\ &+ \sum_{\text{all pairs } ij} \frac{q_i q_j}{4\pi\epsilon_0 r_{ij}} \end{aligned}\right\} \text{non-bonded.}$$

The force field (Amber)

Long-ranged Coulomb interactions in big systems through Particle-Mesh-Ewald (PME) approach

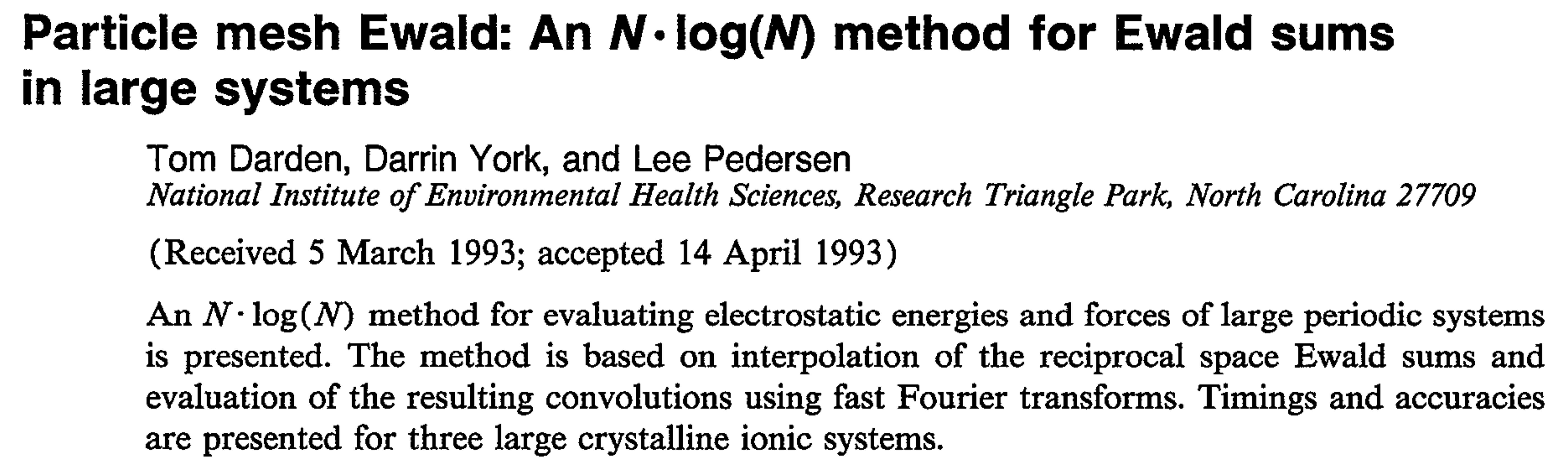

Particle mesh Ewald: An $N \cdot \log(N)$ method for Ewald sums in large systems

Tom Darden, Darrin York, and Lee Pedersen
National Institute of Environmental Health Sciences, Research Triangle Park, North Carolina 27709

(Received 5 March 1993; accepted 14 April 1993)

An $N \cdot \log(N)$ method for evaluating electrostatic energies and forces of large periodic systems is presented. The method is based on interpolation of the reciprocal space Ewald sums and evaluation of the resulting convolutions using fast Fourier transforms. Timings and accuracies are presented for three large crystalline ionic systems.

☞ Solve the Poisson equation on a grid by FFT and interpolate the forces at the atomic positions

Dynamics of proteins

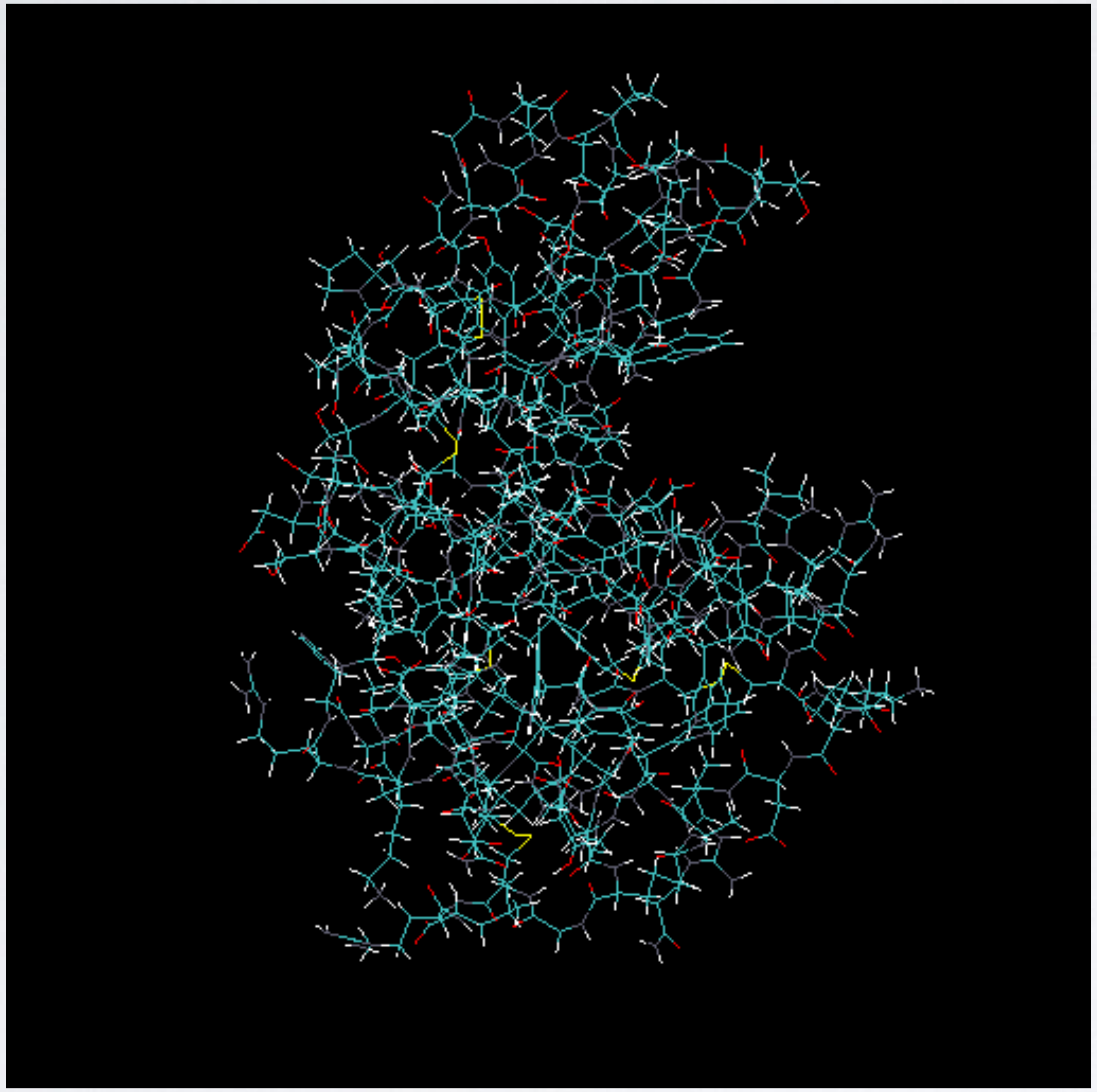

Lysozyme (all atoms)

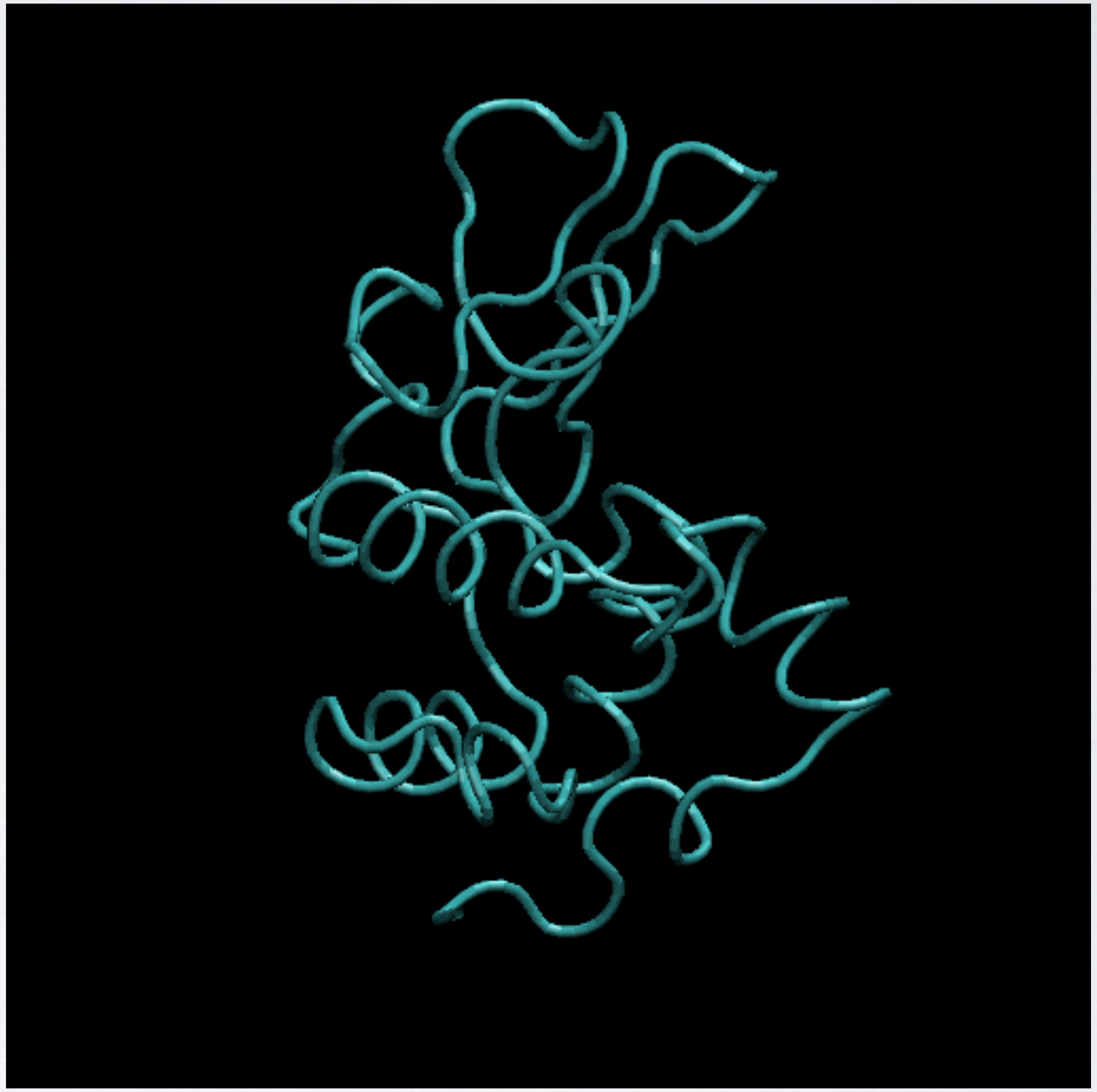

Lysozyme (backbone)

Liquid-like side chain motions in myoglobin

G. R. Kneller and J. C. Smith, “Liquid-like Side-Chain Dynamics in Myoglobin,” J Mol Biol, vol. 242, no. 3, pp. 181–185, 1994.

Backbone

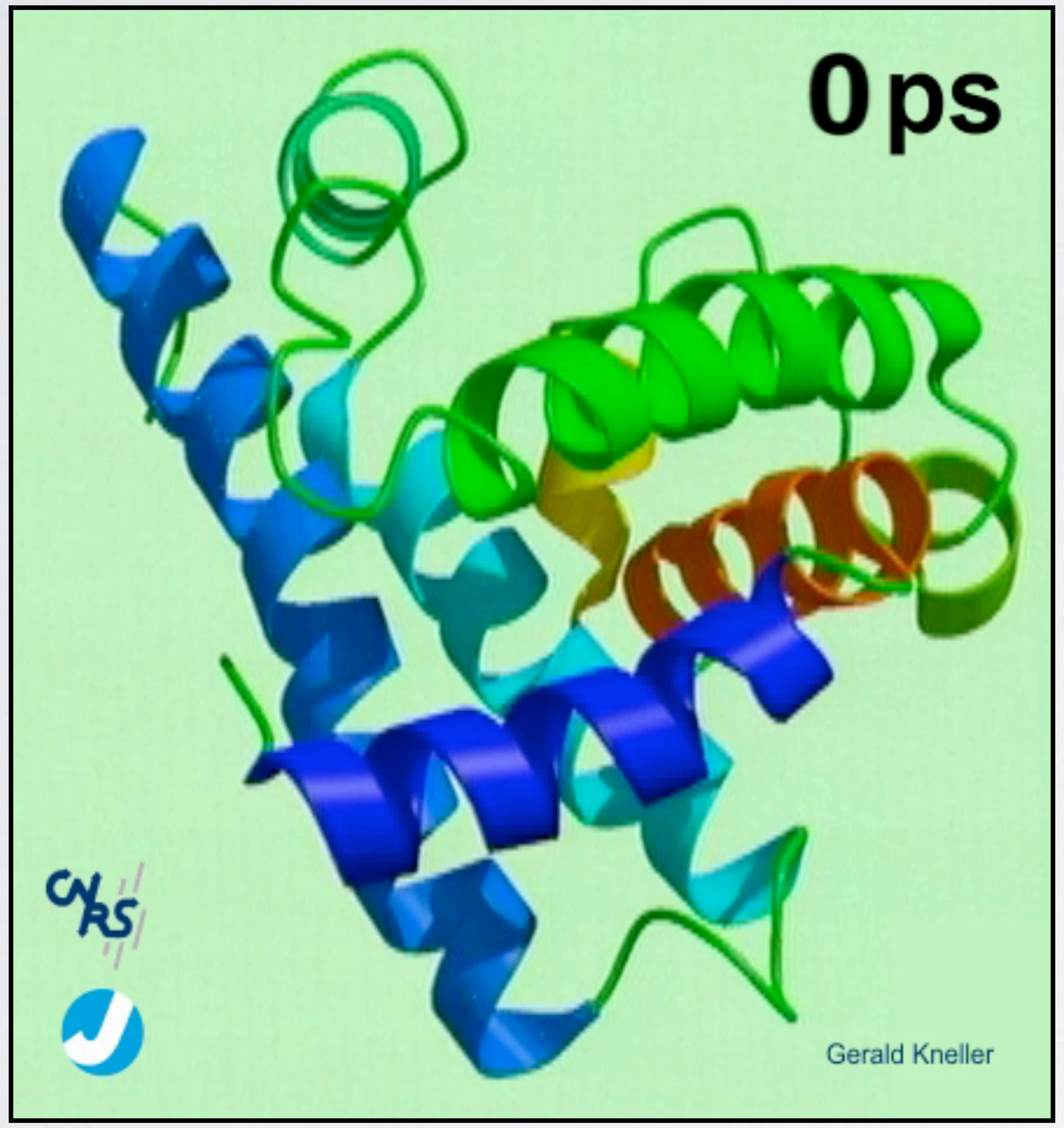

The "side-chain liquid"

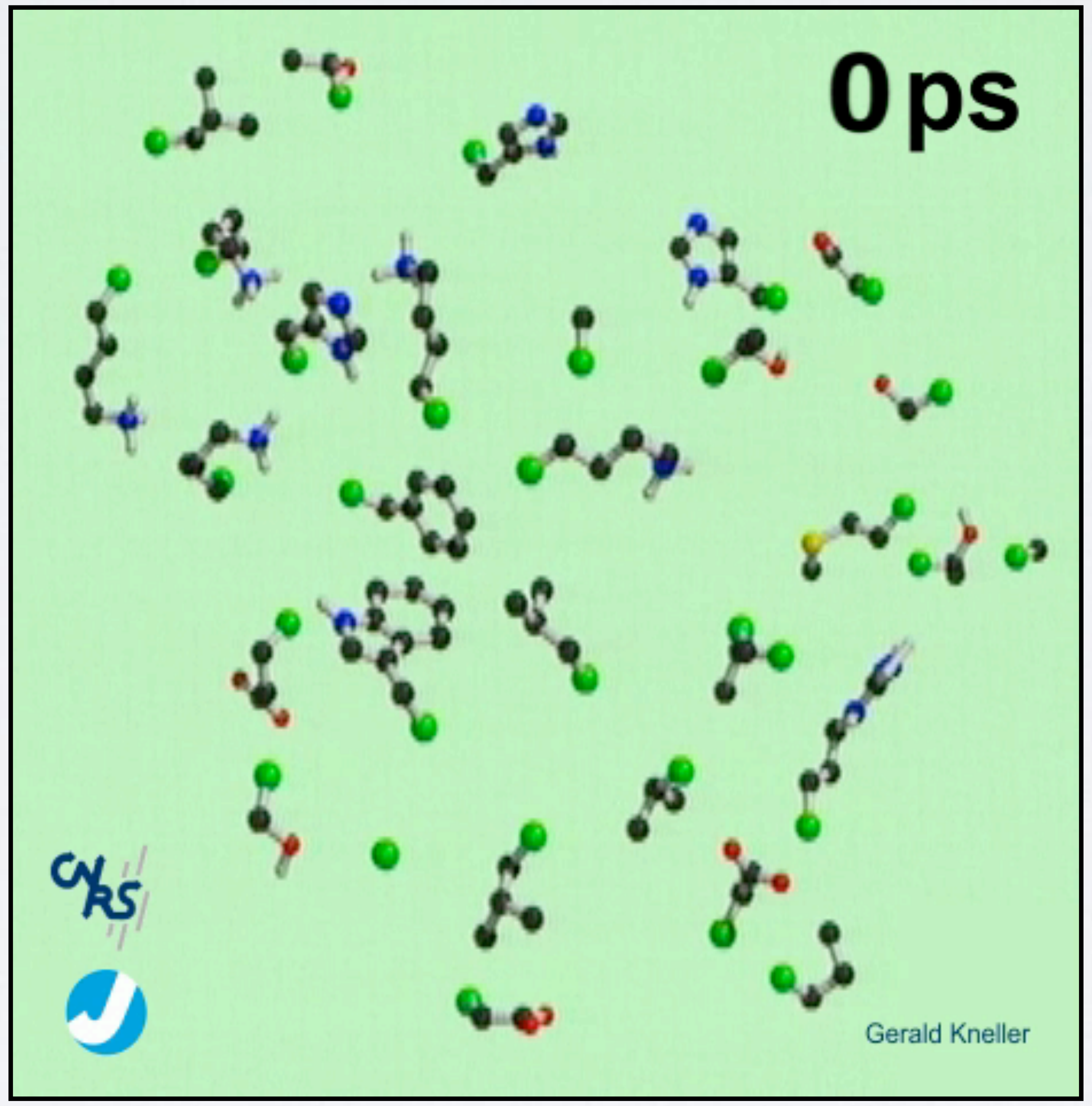

Flexible

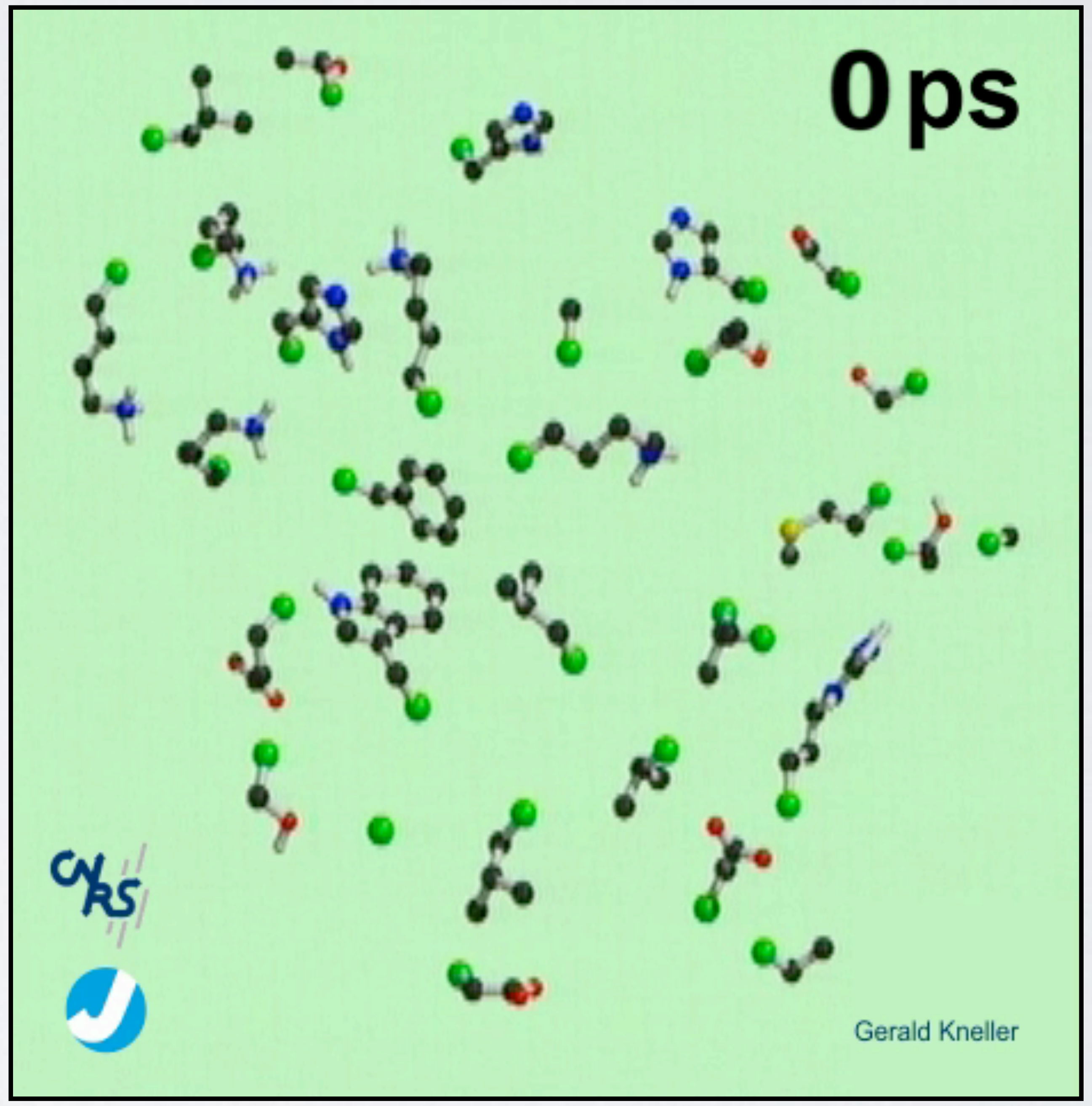

Rigid: Internal motions of the side-chains have been filtered out by quaternion-based rigid-body fits of the initial side-chain conformations (GR Kneller Mol. Sim. **7**(1),113-119).

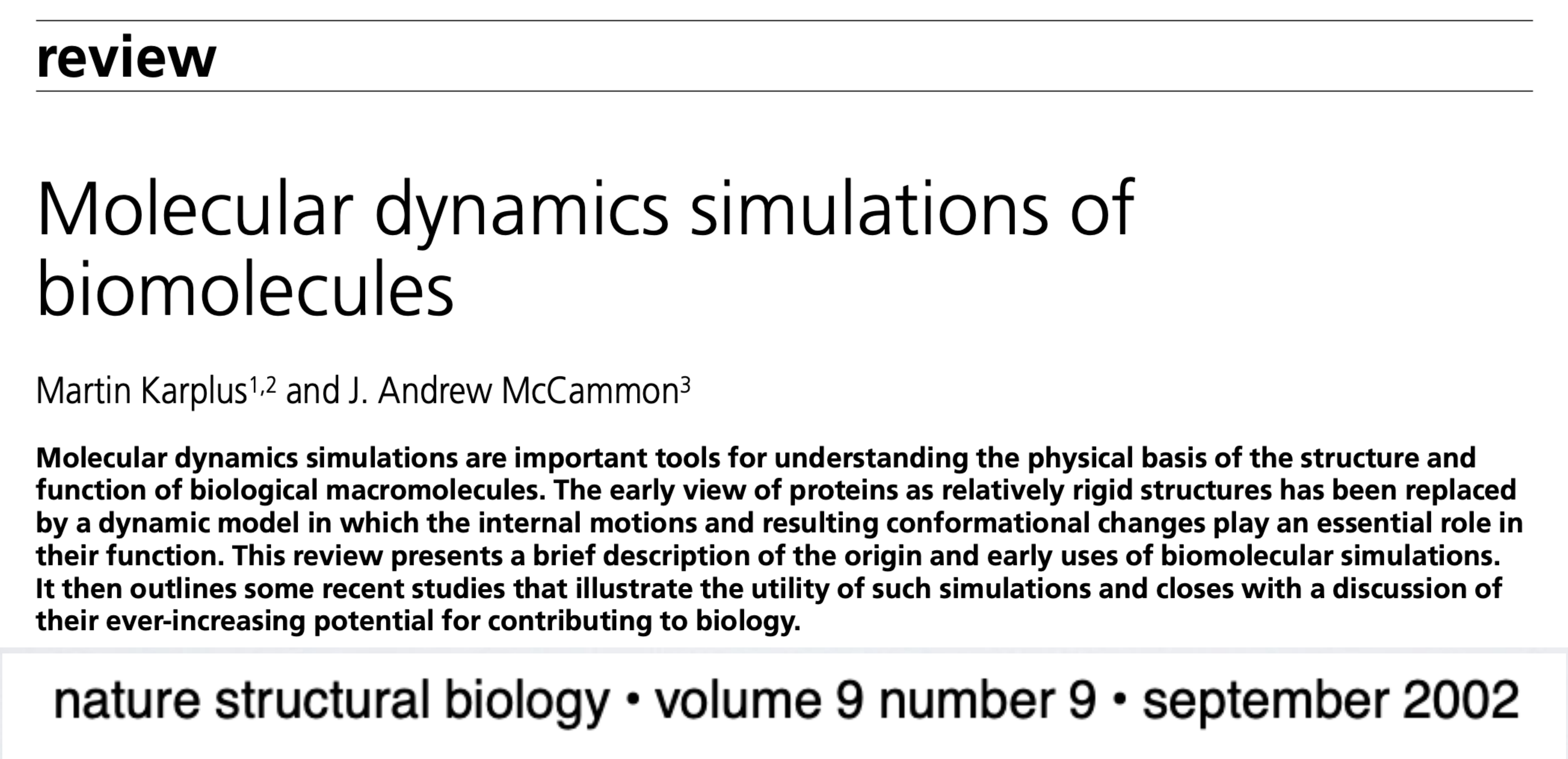

review

Molecular dynamics simulations of biomolecules

Martin Karplus[1,2] and J. Andrew McCammon[3]

Molecular dynamics simulations are important tools for understanding the physical basis of the structure and function of biological macromolecules. The early view of proteins as relatively rigid structures has been replaced by a dynamic model in which the internal motions and resulting conformational changes play an essential role in their function. This review presents a brief description of the origin and early uses of biomolecular simulations. It then outlines some recent studies that illustrate the utility of such simulations and closes with a discussion of their ever-increasing potential for contributing to biology.

nature structural biology • volume 9 number 9 • september 2002

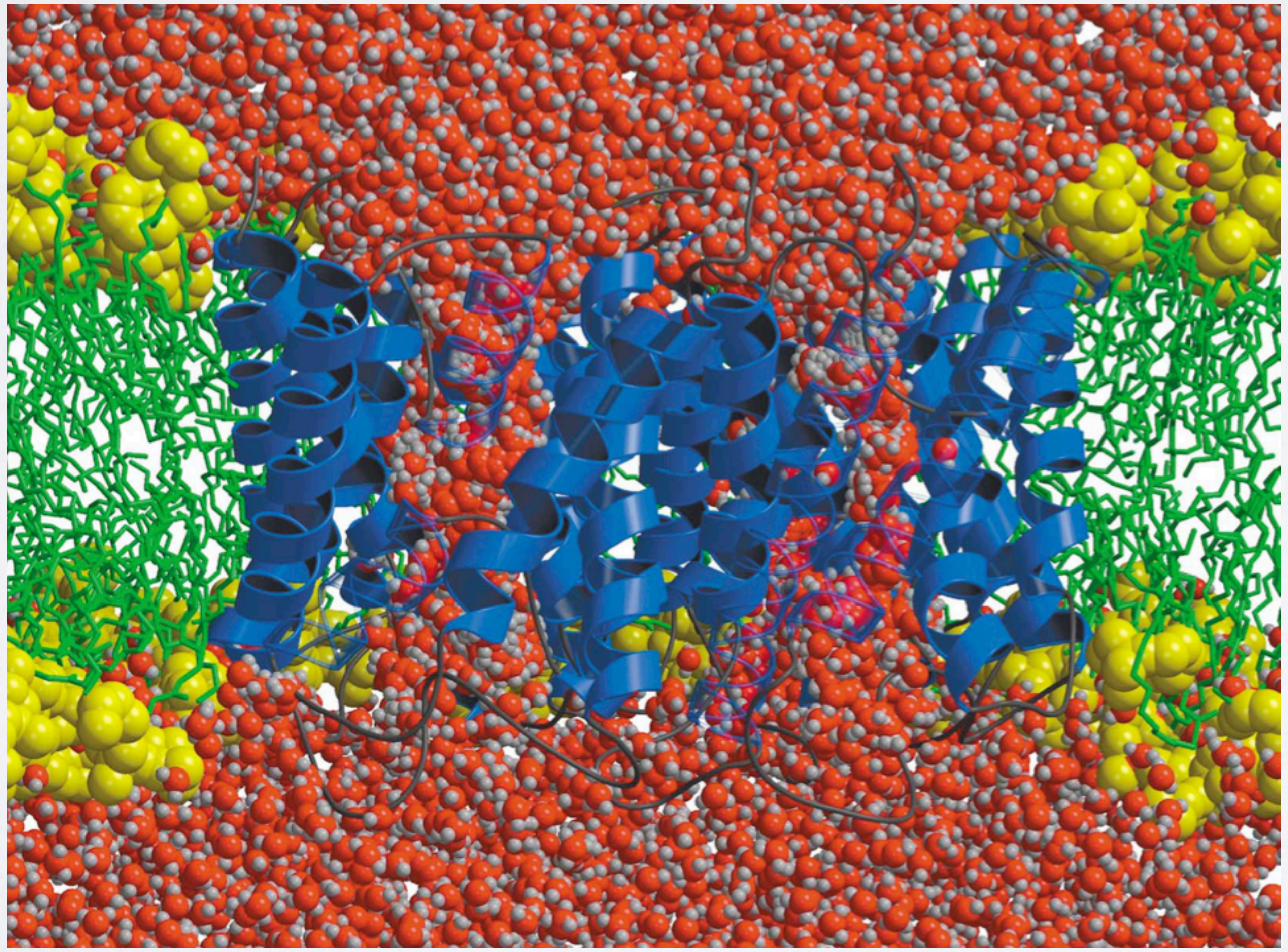

MD simulation of aquaporin

Dynamics of liquid bilayers / membranes

POPC bilayer

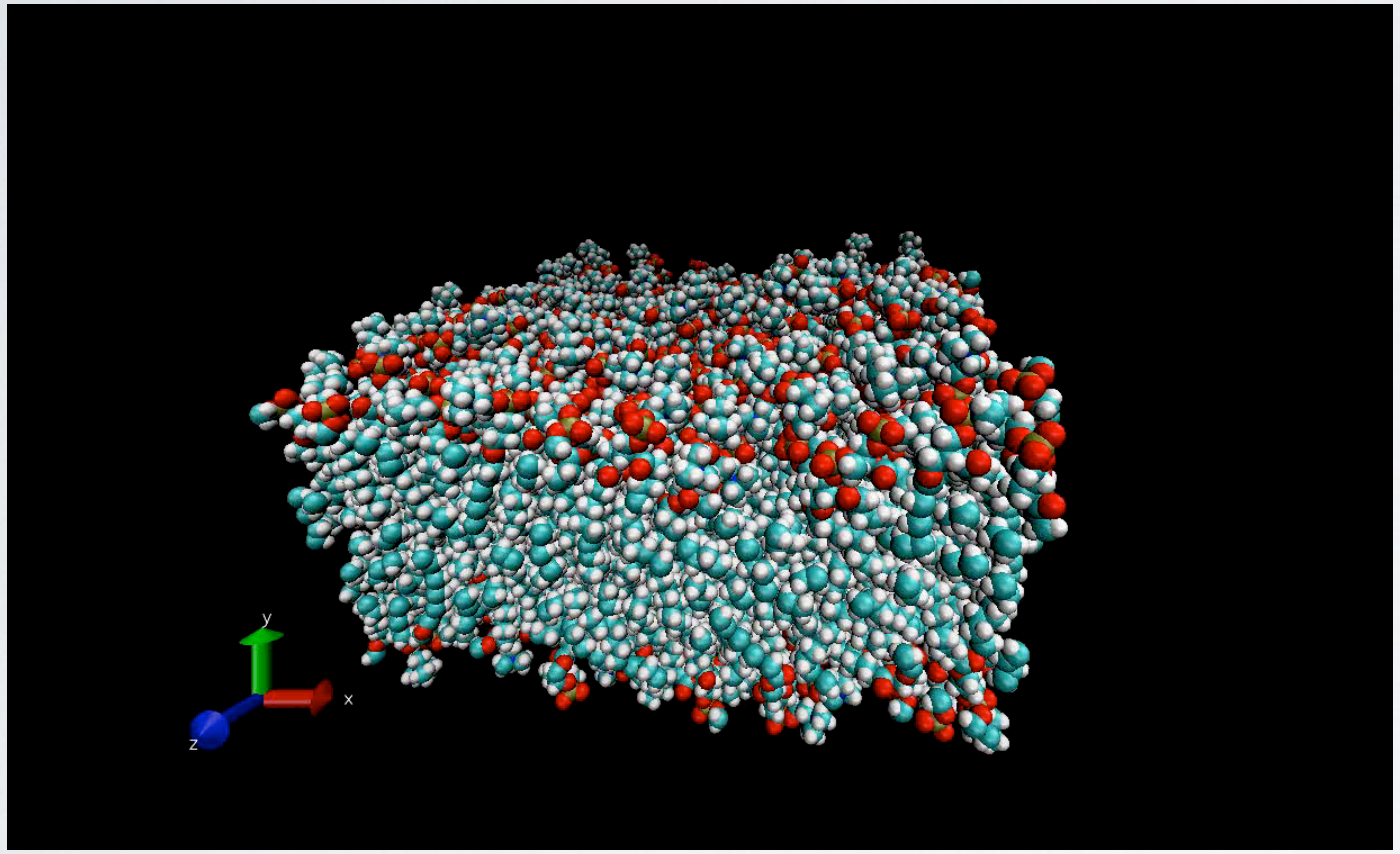

In-plane motion

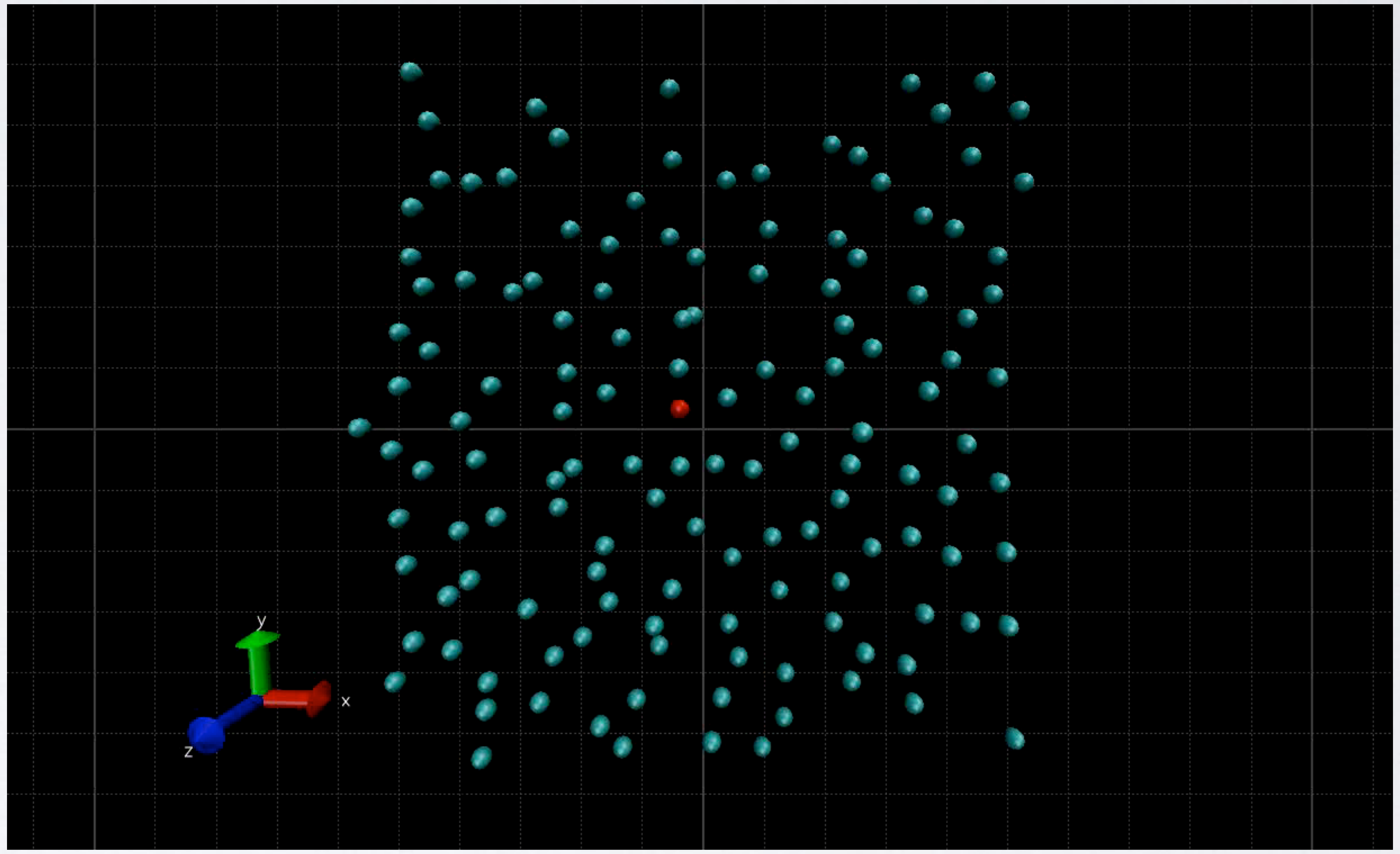

Some codes

- CHARMM (Chemistry at HARvard Macromolecular Mechanics)
  M. Karplus, Charles Brooks, Bernie Brooks et al., Harvard University

- AMBER (Assisted Model Building with Energy Refinement)
  Peter Kollman *et al*. UC San Francisco

- NAMD (Nanoscale Molecular Dynamics)
  Klaus Schulten *et al*., University of Illinois Urbana–Champaign

- GROningen MOlecular Simulation (GROMOS)
  Herman Berendsen & W. Van Gunsteren *et al*.,
  U. Groningen, NL & ETH Zürich

- GROMACS (GROningen MAchine for Chemical Simulations),
  Spin-off from GORMOS since 2001 Royal Institute of Technology
  and Uppsala University

- LAMMPS (Large-scale Atomic/Molecular Massively Parallel Simulator)
  Steve Plimpton *et al*. Sandia National Laboratories & Temple University
  Philadelphia

- MMTK (Molecular Modeling Toolkit)
  Konrad Hinsen, CNRS CBM Orléans
- …..

Basic steps in force field development

Born-Oppenheimer approximation

Hamilton operator for nuclei and electrons :

$$\hat{H} = \hat{H}_{nn} + \hat{H}_{ee} + \hat{V}_{ne}$$

The components are

$$\begin{aligned}
\hat{H}_{nn} &= \sum_i \frac{-\hbar^2}{2M_i}\frac{\partial^2}{\partial \mathbf{R}_i^2} + \frac{1}{4\pi\epsilon_0}\sum_i \sum_{i<j} \frac{Z_i Z_j e^2}{|\mathbf{R}_i - \mathbf{R}_j|}, \\
\hat{H}_{ee} &= \sum_i \sum_\alpha \frac{-\hbar^2}{2m_e}\frac{\partial^2}{\partial \mathbf{r}_{i,\alpha}^2} + \frac{1}{4\pi\epsilon_0}\sum_{i,\alpha} \sum_{j<i,\beta} \frac{e^2}{|\mathbf{r}_{i,\alpha} - \mathbf{r}_{j,\beta}|} + \frac{1}{4\pi\epsilon_0}\sum_i \sum_{\alpha<\beta} \frac{e^2}{|\mathbf{r}_{i,\alpha} - \mathbf{r}_{i,\beta}|}, \\
\hat{V}_{ne} &= \frac{1}{4\pi\epsilon_0}\sum_i \sum_{j,\alpha} \frac{-Z_i e^2}{|\mathbf{R}_i - \mathbf{r}_{j,\alpha}|}.
\end{aligned}$$

Notation: n = nuclei $(i, j, \ldots)$, e = electrons $(\alpha, \beta, \ldots)$.

Stationary problem for the electrons

Time scale separation between the time scales of the motions of the "light" and the "heavy" atoms ($M_i \gg m_e$). The electron dynamics follows instantaneously the motions of the nuclei.

- *Electron wave function :*

$$\psi_e(\{\mathbf{r}_{i,\alpha}\}, t|\{\mathbf{R}_i\}) = u_e(\{\mathbf{r}_{i,\alpha}\}|\{\mathbf{R}_i\})e^{-\frac{i}{\hbar}E_e t}.$$

- *Stationary Schrödinger equation :*

$$\left\{\hat{H}_{ee} + \hat{V}_{ne}\right\} u_e = E_e(\{\mathbf{R}_i\})u_e.$$

The eigenvalues are implicit functions of the configuration of the nuclei!

Schrödinger Equation of the nuclei:

$$\begin{aligned} i\hbar\frac{\partial\psi_n}{\partial t} &= \hat{H}_n\psi_n, \\ \hat{H}_n &= \sum_i \frac{-\hbar^2}{2M_i}\frac{\partial^2}{\partial\mathbf{R}_i^2} + \underbrace{\hat{V}_{nn} + E_e(\{\mathbf{R}_i\})}_{V_n(\{\mathbf{R}_i\})}. \end{aligned}$$

The potential of the nuclei is the superposition of the repulsive coulombic terms repulsive terms, V_{nn}, and the Born-Oppenheimer electronic energy, $E_e(\mathbf{R}_i\})$, which depends in a parametric way on the positions of the nuclei.

Classical MD

Concept

Instead of solving the Schrödinger equation with the potential $V_n(\{\mathbf{R}_i\})$ for the nuclei, we solve the Newton equations,

$$M_i\ddot{\mathbf{R}}_i = -\frac{\partial U(\{\mathbf{R}_i\})}{\partial \mathbf{R}_i},$$

where $U(\{\mathbf{R}_i\})$ is an *empirical potential* which is fitted to to $V_n(\{\mathbf{R}_i\})$,

$$U(\{\mathbf{R}_i\}) \approx V_n(\{\mathbf{R}_i\}).$$

The simplest example is the Lennard-Jones potential, which is used for simple liquids

$$U(r) = 4\epsilon\left(\frac{\sigma^{12}}{r^{12}} - \frac{\sigma^6}{r^6}\right).$$

Representative sampling of the QM force field is a non-trivial task for non-pairwise additive potentials!

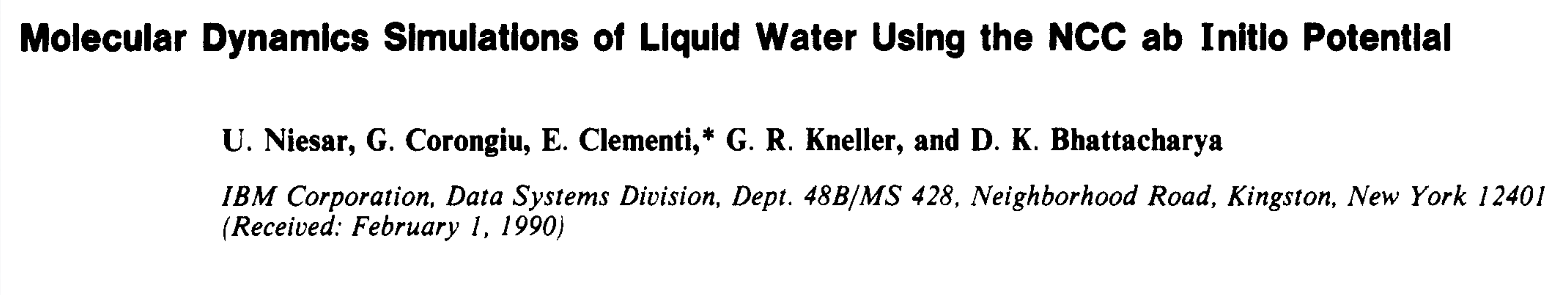

Molecular Dynamics Simulations of Liquid Water Using the NCC ab Initio Potential

U. Niesar, G. Corongiu, E. Clementi,* G. R. Kneller, and D. K. Bhattacharya

IBM Corporation, Data Systems Division, Dept. 48B/MS 428, Neighborhood Road, Kingston, New York 12401

(Received: February 1, 1990)

Include many-body effects due to polarization into the force field.

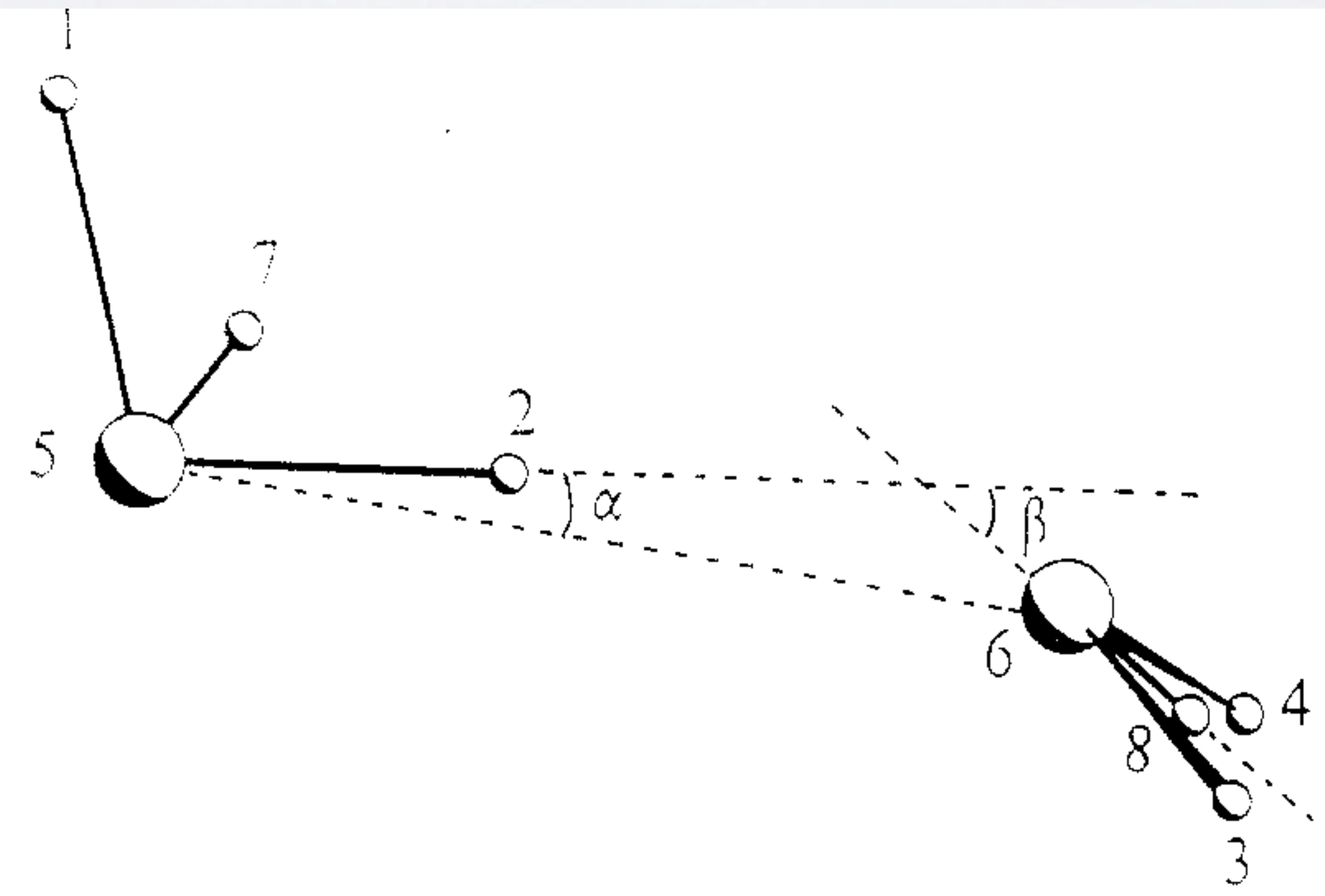

Figure 1. Definition of the water dimer geometry.

The limit of classical MD

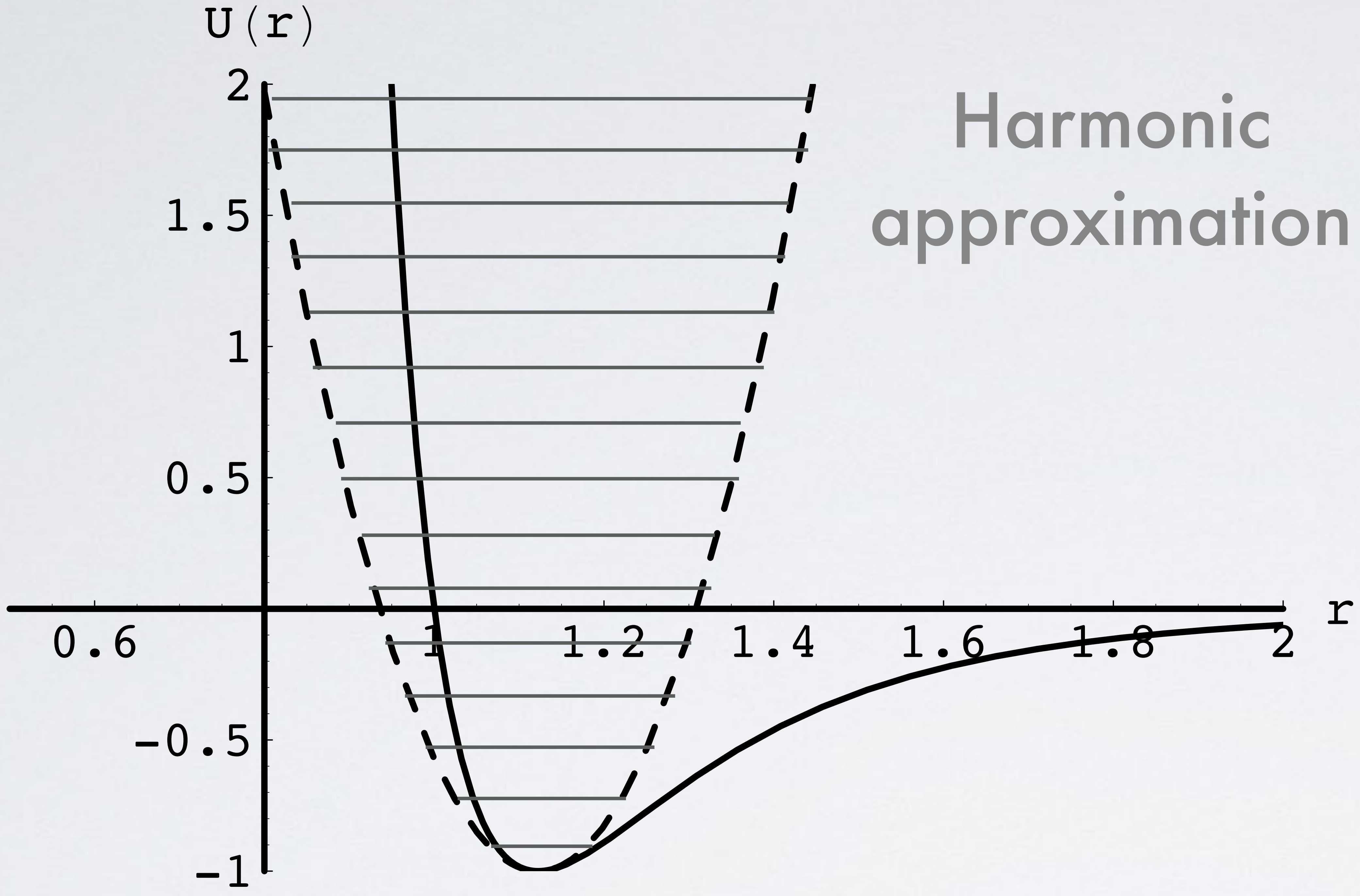

$$\boxed{\hbar\omega_0 \ll k_B T}$$

Argon :

$$T = 94.4\,K$$

$$\hbar\omega_0 \approx 0.2\,k_B T$$

$$U_{LJ}(r) = 4\epsilon\left(\left[\frac{\sigma}{r}\right]^{12} - \left[\frac{\sigma}{r}\right]^{6}\right) \approx -\epsilon + \frac{18\cdot 2^{2/3}\epsilon\left(r-r_0\right)^2}{\sigma^2} \qquad r_0 = 2^{1/6}\sigma$$

$$\omega_0 = \left(\frac{V''(r_0)}{2M}\right)^{1/2} \approx 2.49\times 10^{12}\,\mathrm{Hz}$$

For macromolecules like proteins only a small part of the motional frequency spectrum is accessible to classical MD!

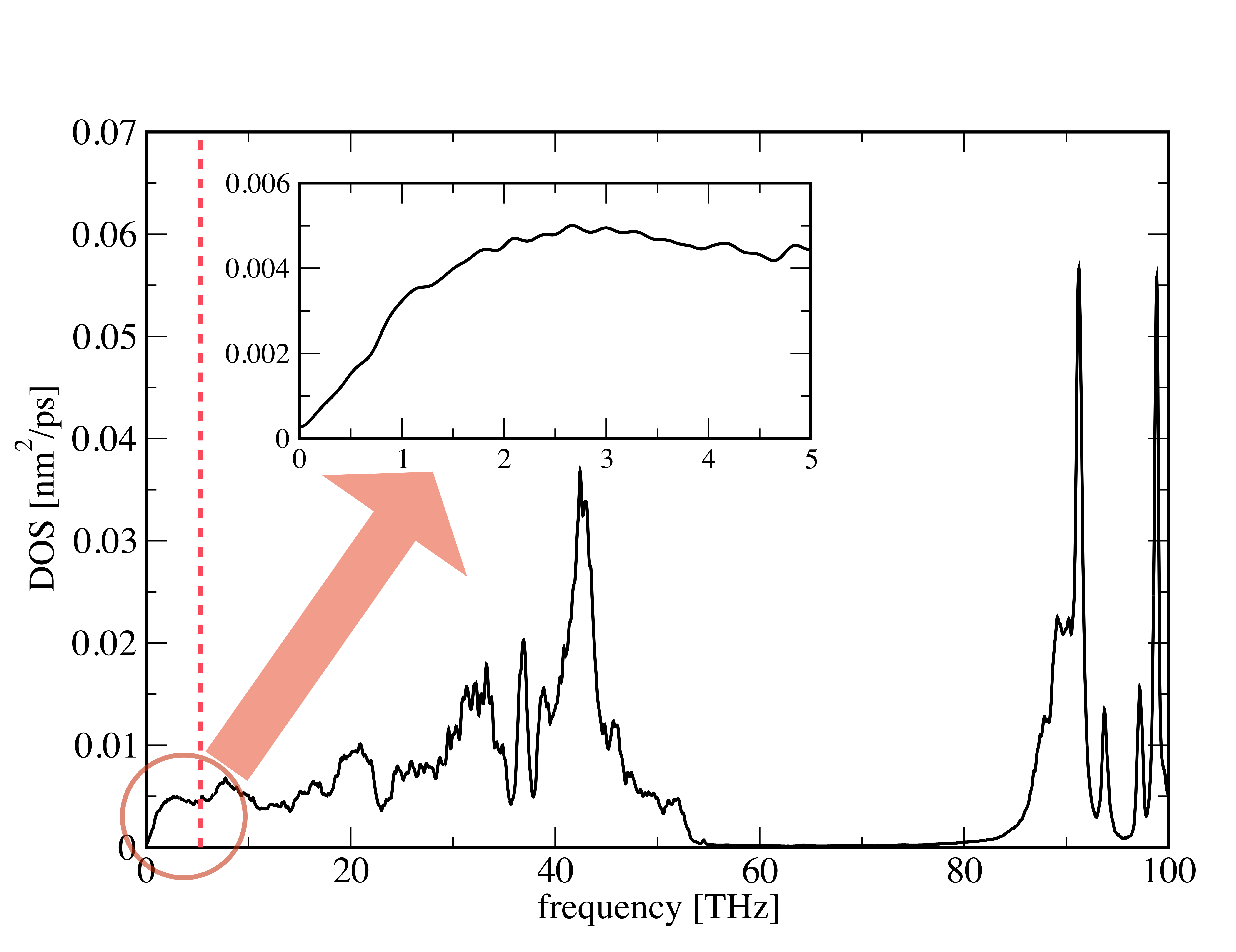

Conducting MD simulations

Some integration algorithms

Verlet:

Only the positions are used.

$$\mathbf{R}_i(t+\Delta t) \leftarrow 2\mathbf{R}_i(t) - \mathbf{R}_i(t-\Delta t) + \frac{\Delta t^2}{M_i}\mathbf{F}_i(t).$$

Accelerations and valocities are approximated by

$$\begin{aligned}\dot{\mathbf{R}}_i &\approx \frac{\mathbf{R}_i(t+\Delta t) - \mathbf{R}_i(t-\Delta t)}{2\Delta t},\\ \ddot{\mathbf{R}}_i &\approx \frac{\mathbf{R}_i(t+\Delta t) - 2\mathbf{R}_i(t) + \mathbf{R}_i(t-\Delta t)}{\Delta t^2}.\end{aligned}$$

Stable, but velocities are constructed a posteriori and velocity-dependent forces cannot be treated.

“Leap-frog”:

Velocities and positions are used.

$$\mathbf{V}_i(t + \Delta t/2) \leftarrow \mathbf{V}_i(t - \Delta t/2) + \frac{\Delta t}{M_i}\mathbf{F}_i(t)$$

Velocities at $t = (n + 1/2)\Delta t$

$$\mathbf{R}_i(t + \Delta t) \leftarrow \mathbf{R}_i(t) + \mathbf{V}_i(t + \Delta t/2)$$

Positions at $t = n\Delta t$

“Velocity-Verlet”:

Again velocities and positions are used.

$$\mathbf{R}_i(t + \Delta t) \leftarrow \mathbf{R}_i(t) + \mathbf{V}_i(t)\Delta t$$

Positions at $t = n\Delta t$

$$\mathbf{V}_i(t + \Delta t) \leftarrow \mathbf{V}_i(t) + \frac{\Delta t}{M_i}\left(\frac{\mathbf{F}_i(t + \Delta t) + \mathbf{F}_i(t)}{2}\right)$$

Velocities at $t = n\Delta t$

Velocities and positions are available at the same time.

Geometric constraints

Goal: ”Freeze” the fastest movements, such as the vibrations of the bonds, in order to allow the use of longer integration steps.

Holonomic constraints

It is required that

$$\sigma^{\alpha}(\mathbf{R}, t) = 0, \qquad \alpha = 1 \ldots l,$$

where $\mathbf{R} = (\mathbf{R}_1^T, \ldots, \mathbf{R}_N^T)^T$. An example of a constraint is a fixed bond length:

$$\sigma(\mathbf{R}, t) := (\mathbf{R}_1 - \mathbf{R}_2)^2 - l_{12}^2 \equiv 0.$$

Frequency spectrum of a protein

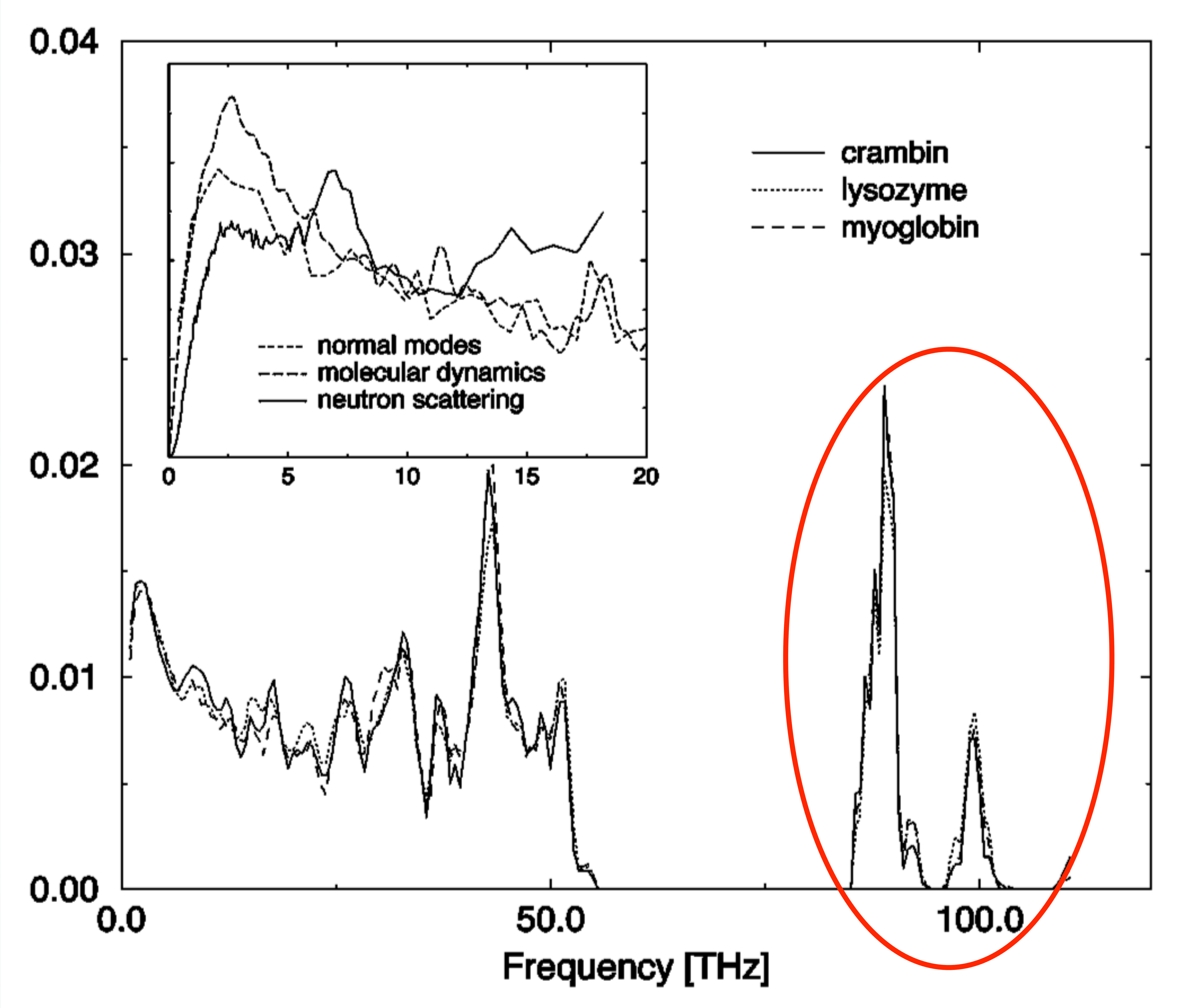

JOURNAL OF CHEMICAL PHYSICS VOLUME 111, NUMBER 24 22 DECEMBER 1999

A simplified force field for describing vibrational protein dynamics over the whole frequency range

Konrad Hinsen[a] and Gerald R. Kneller[b]
Centre de Biophysique Moléculaire (UPR 4301 CNRS), Rue Charles Sadron, 45071 Orléans Cedex 2, France

Freeze fast N-H and O-H bond vibrations

➡ The time step can increased from 1 fs to 2 fs.

Lagrangian mechanics without constraints

With the *Lagrange function*

$$\boxed{\mathcal{L} = \frac{1}{2}\dot{\mathbf{R}}^T \cdot \mathbf{M} \cdot \dot{\mathbf{R}} - \mathcal{U}(\mathbf{R})},$$

we obtain the equations of motion by postulating that the variation

$$\mathcal{S} = \int_{t_0}^{t_1} dt\, \mathcal{L}(\dot{\mathbf{R}}, \mathbf{R}, t) = Min.$$

for the true trajectory. This gives

$$\delta\mathcal{S} = \int_{t_0}^{t_1} dt\, \boldsymbol{\delta}\mathbf{R}^T \cdot \left(\frac{d}{dt}\frac{\partial\mathcal{L}}{\partial\dot{\mathbf{R}}} - \frac{\partial\mathcal{L}}{\partial\mathbf{R}}\right) = 0.$$

Without constraints the variations $\boldsymbol{\delta}\mathbf{R}$ are *arbitrary* and

$$\boxed{\frac{d}{dt}\frac{\partial\mathcal{L}}{\partial\dot{\mathbf{R}}} = \frac{\partial\mathcal{L}}{\partial\mathbf{R}}} \qquad \Longrightarrow \qquad \mathbf{M} \cdot \ddot{\mathbf{R}} = -\frac{\partial\mathcal{U}}{\partial\mathbf{R}} \equiv \mathbf{f}.$$

Lagrange mechanics with holonomic constraints

Since

$$\sigma^\alpha(\mathbf{R}_0 + \boldsymbol{\delta}\mathbf{R}, t) - \sigma^\alpha(\mathbf{R}_0, t) = 0$$

for a differential variation, it follows that

$$\mathbf{A}\cdot\boldsymbol{\delta}\mathbf{R} = \mathbf{0}, \qquad A_i^\alpha = \frac{\partial \sigma^\alpha}{\partial r^i}.$$

The allowed variations are in the nullspace of $\mathbf{A}$, $\boldsymbol{\delta}\mathbf{R} \in \mathbb{V}_\parallel$. We know that

$$\delta\mathcal{S} = \int_{t_0}^{t_1} dt \; \underbrace{\boldsymbol{\delta}\mathbf{R}^T}_{\in\mathbb{V}_\parallel} \cdot \underbrace{\left(\frac{d}{dt}\frac{\partial \mathcal{L}}{\partial \dot{\mathbf{R}}} - \frac{\partial \mathcal{L}}{\partial \mathbf{R}}\right)}_{\in\mathbb{V}_\perp} = 0.$$

Therefore

$$\mathbf{M}\cdot\ddot{\mathbf{R}} = \mathbf{f} + \mathbf{z}, \qquad \mathbf{z} = \mathbf{A}^T\boldsymbol{\mu} \in V_\perp.$$

Here $\mathbf{z}$ is the *constraint force*, and $\boldsymbol{\mu} = (\mu_1, \ldots, \mu_l)^T$ contains the Lagrangian parameters.

Avoid “melting” of rigid structures due to numerical errors

18574 citations

The SHAKE algorithm

For the computation of the μ_k parameters J.-P. RYCKAERT *et al.* have proposed the SHAKE algorithm which guarantees that the constraints are verified in the presence of unavoidable numerical errors.[1] In the Verlet integration scheme one writes

Lagrange parameters to be determined from the constraints

$$\mathbf{R}_{n+1} = \mathbf{R}^{(0)}_{n+1} + \Delta t^2 \mathbf{M}^{-1} \cdot \mathbf{A}^T(\mathbf{R}_n) \cdot \boldsymbol{\mu}_n,$$

where $\mathbf{R}^{(0)}_{n+1}$ is the new position *without* the presence of constraints

$$\mathbf{R}^{(0)}_{n+1} = 2\mathbf{R}_n - \mathbf{R}_{n-1} + \Delta t^2 \mathbf{M}^{-1} \cdot \mathbf{f}(\mathbf{R}_n).$$

We require that the constraints are exactly verified for the *new* positions,

$$\boldsymbol{\sigma}(\mathbf{R}_{n+1}) = \mathbf{0}, \qquad \text{où} \quad \boldsymbol{\sigma} := (\sigma^1, \dots, \sigma^l)^T.$$

Remark: In the Verlet scheme one should compute the μ_α from $\boldsymbol{\sigma}(\mathbf{R}_n) = \mathbf{0}$.

Implementation of SHAKE:

1. Given $\mathbf{R}_{n+1}^{(0)}$, compute $\sigma^\alpha(\mathbf{R}_{n+1}^{(0)})$, and initialize $j = 0$.
2. Compute $d_\alpha^j = \Delta t^2 \left(\mathbf{A}(\mathbf{R}_{n+1}^{(j)}) \cdot \mathbf{M}^{-1} \cdot \mathbf{A}^T(\mathbf{R}_n)\right)_{\alpha\alpha}$
3. Compute the estimations $\mu_\alpha^{(j)} = -\sigma^\alpha(\mathbf{R}_{n+1}^{(j)})/d_\alpha^j$
4. Compute corrected estimations
   $\mathbf{R}_{n+1}^{(j+1)} = \mathbf{R}_{n+1}^{(j)} + \Delta t^2 \mathbf{M}^{-1} \cdot \mathbf{A}^T(\mathbf{R}_n) \cdot \boldsymbol{\mu}^{(j)}$
5. Compute $\sigma^\alpha(\mathbf{R}_{n+1}^{(j+1)})$ and verify that $|\sigma^\alpha(\mathbf{R}_{n+1}^{(j+1)})| \leq \epsilon$ for all constraints

   for all the constraints. If the result is OK, stop. Otherwise, start over with 2

Here ϵ is a tolerance parameter. We notice that the constraints are considered *independent* in the computation of $\mu_\alpha^{(j)}$ estimates.

Simulate open thermodynamic systems

Scale the **velocities** to
adjust the **temperature**
(NVT ensemble)

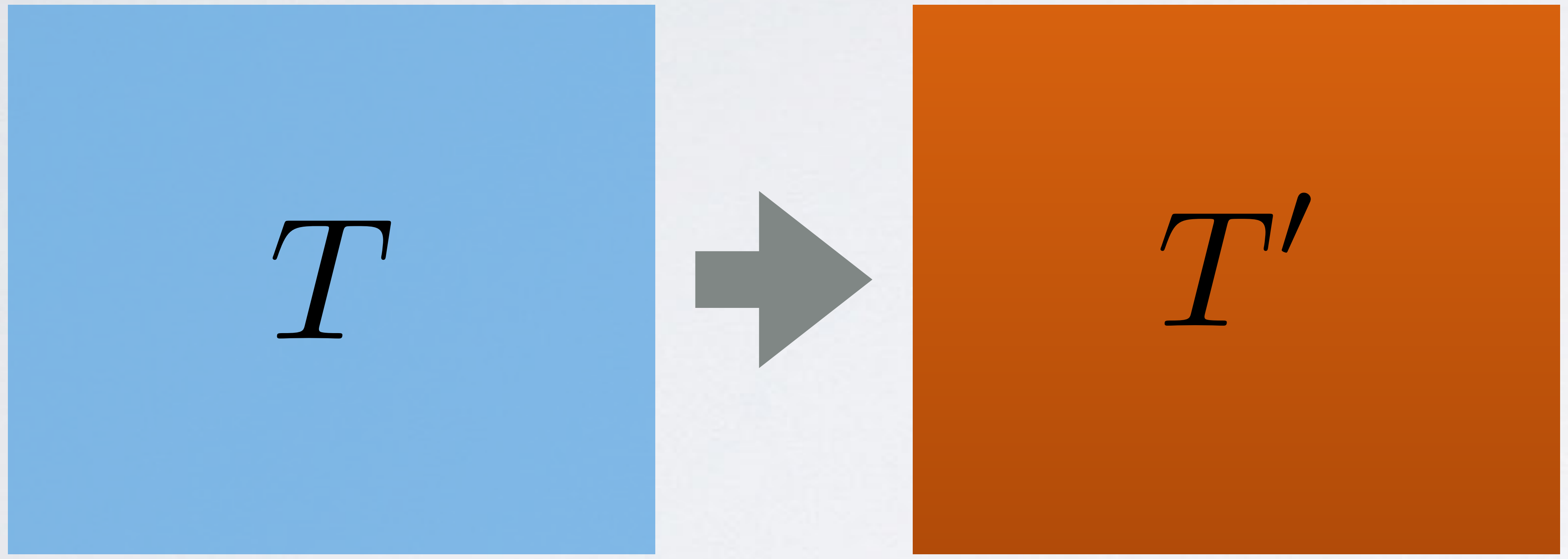

Real variables

$$
\begin{aligned}
\mathbf{r} &= \boldsymbol{\rho} \\
\dot{\mathbf{r}} &= s\dot{\boldsymbol{\rho}} \\
dt &= \frac{d\tau}{s}
\end{aligned}
$$

“Virtual” variables

Scale the **positions** to
adjust the **pressure**
(NpH ensemble)

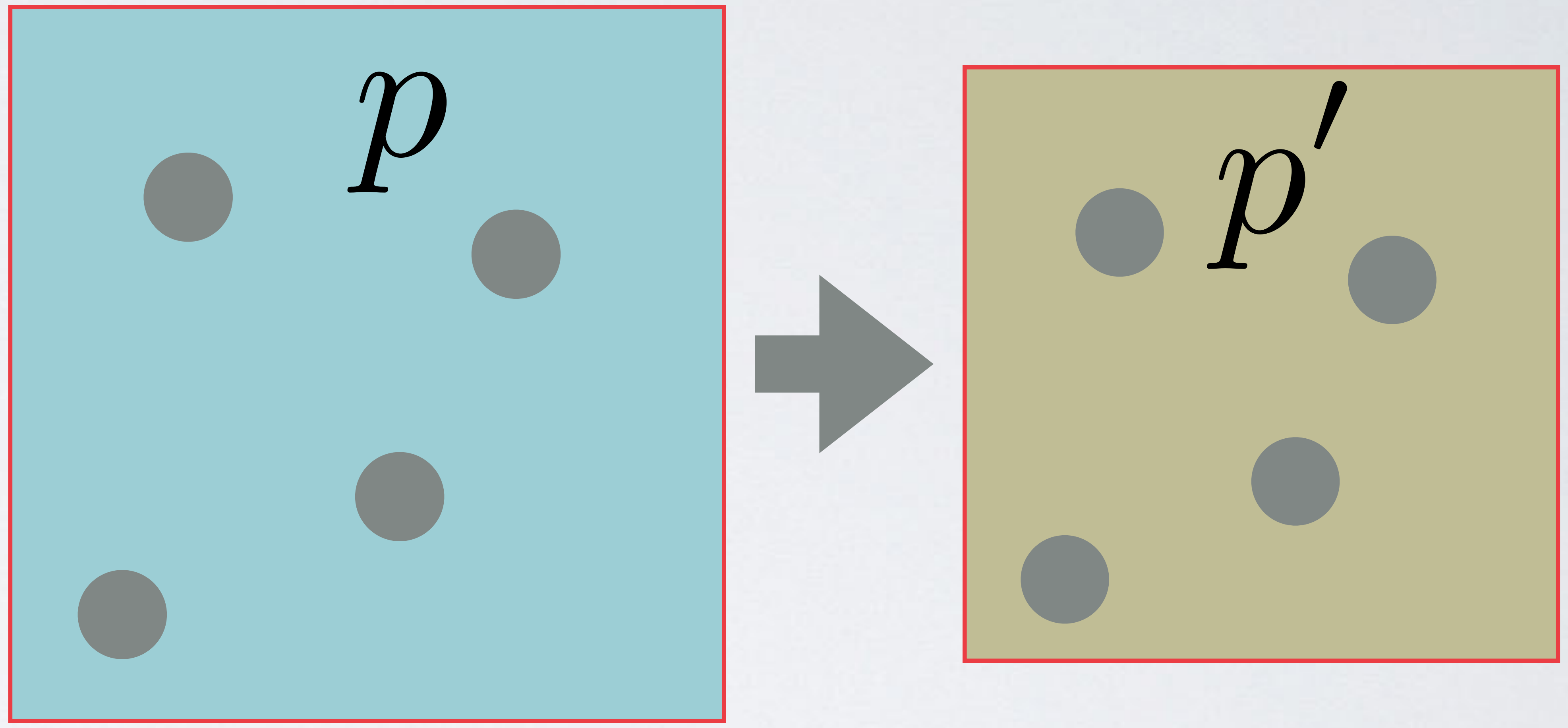

Real variables

$$
\begin{aligned}
V &= Q, \\
\mathbf{r} &= Q^{1/3}\boldsymbol{\rho} \\
\dot{\mathbf{r}} &= Q^{1/3}\dot{\boldsymbol{\rho}} \\
dt &= d\tau
\end{aligned}
$$

“Virtual” variables

The extended system approach

Extended system = physical system + thermostat and/or barostat

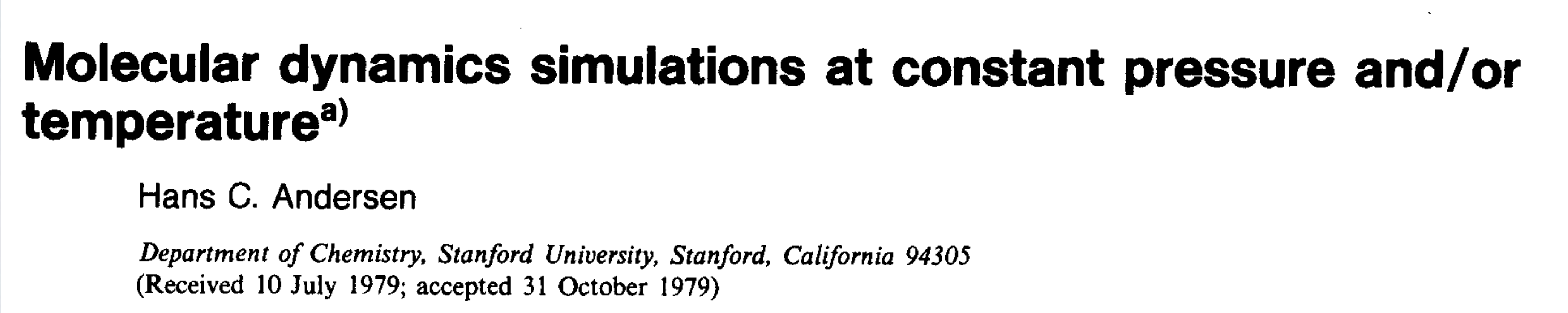

Molecular dynamics simulations at constant pressure and/or temperature[a)]

Hans C. Andersen

Department of Chemistry, Stanford University, Stanford, California 94305
(Received 10 July 1979; accepted 31 October 1979)

The Journal of Chemical Physics **72**, 2384 (1980);

A unified formulation of the constant temperature molecular dynamics methods

Shuichi Nosé[a)]
Division of Chemistry, National Research Council of Canada, Ottawa, Ontario, Canada, K1A OR6

J. Chem. Phys. **81**, 511 (1984)

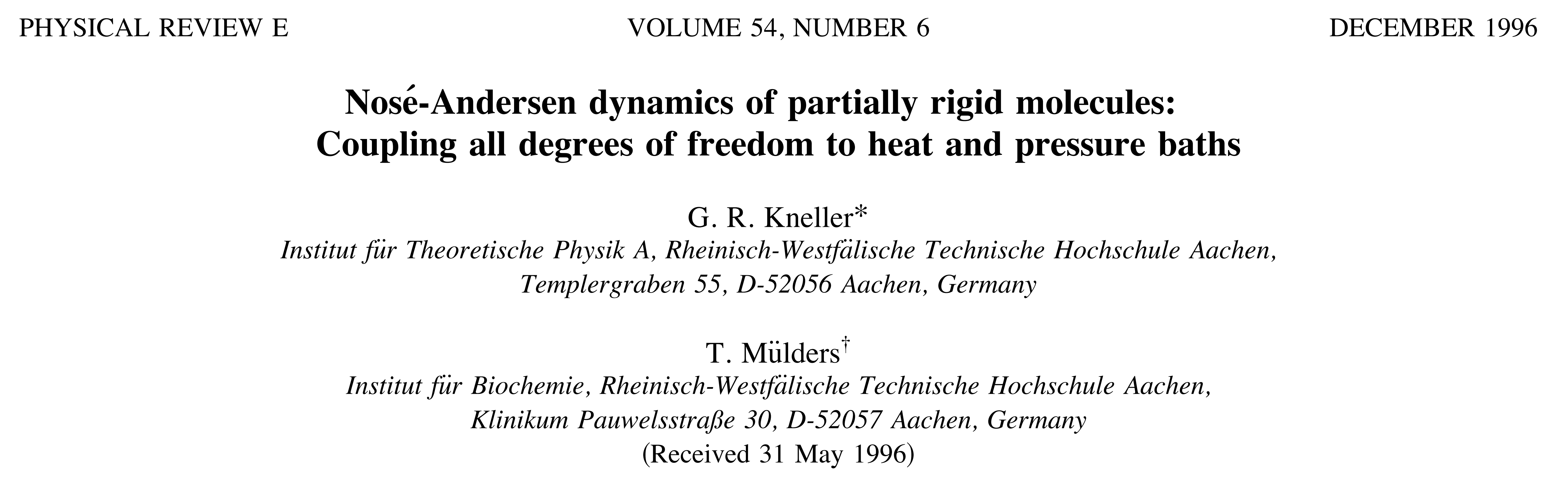

PHYSICAL REVIEW E VOLUME 54, NUMBER 6 DECEMBER 1996

**Nosé-Andersen dynamics of partially rigid molecules:
Coupling all degrees of freedom to heat and pressure baths**

G. R. Kneller*
*Institut für Theoretische Physik A, Rheinisch-Westfälische Technische Hochschule Aachen,
Templergraben 55, D-52056 Aachen, Germany*

T. Mülders†
*Institut für Biochemie, Rheinisch-Westfälische Technische Hochschule Aachen,
Klinikum Pauwelsstraße 30, D-52057 Aachen, Germany*
(Received 31 May 1996)

Combine geometric and thermodynamic constraints

Simulations in the NVT ensemble

Extended system

We define a "virtual" dynamic system of N particles having virtual positions $\boldsymbol{\rho}_i$ and virtual velocities $\dot{\boldsymbol{\rho}}_i$. The relation to the "real" system is given by

$$\begin{aligned} \mathbf{r}_i &= \boldsymbol{\rho}_i, \\ \dot{\mathbf{r}}_i &= s\dot{\boldsymbol{\rho}}_i. \end{aligned}$$

Lagrange function

$$\mathcal{L}_e = \sum_i \frac{1}{2} m_i s^2 \dot{\boldsymbol{\rho}}_i^2 - \mathcal{U}(\boldsymbol{\rho}_1, \ldots, \boldsymbol{\rho}_N) + \frac{1}{2} M_s \dot{s}^2 - g k_B T \ln s.$$

M_s is a fictitious "mass" for s, and g is still to be determined.

Hamilton function

$$\mathcal{H}_e = \underbrace{\sum_i \frac{\boldsymbol{\pi}_i^2}{2m_i s^2} + \mathcal{U}(\boldsymbol{\rho}_1, \ldots, \boldsymbol{\rho}_N)}_{\mathcal{H}(\boldsymbol{\pi},\boldsymbol{\rho})} + \frac{p_s^2}{2M_s} + gk_BT\ln s.$$

Partition function

$$\begin{aligned}\omega_e(NVE) &= \frac{1}{N!}\int_{-\infty}^{+\infty} dp_s \int_0^{\infty} ds \int_{\mathbb{R}_{3N}} d^{3N}\pi \int_V d^{3N}\rho\, \delta(E - \mathcal{H}_e) \\ &= \frac{1}{g}\left(\frac{2\pi M_s}{k_BT}\right)^{1/2} \exp\left[\frac{E}{k_BT}\right] \cdot Z_c(N,V,T).\end{aligned}$$

Here $Z_c(N,V,T)$ is the partition function of the canonical ensemble:

$$Z_c(N,V,T) = \frac{1}{N!}\int_{\mathbb{R}_{3N}} d^{3N}\pi \int_V d^{3N}\rho\, \exp\left[-\frac{\mathcal{H}(\boldsymbol{\pi},\boldsymbol{\rho})}{k_BT}\right].$$

Equations of motion for virtual and physical variables

Hamilton equations for the virtual variables

$$\begin{aligned}
\dot{\boldsymbol{\rho}}_i &= \frac{\partial \mathcal{H}_e}{\partial \boldsymbol{\pi}_i} &&= \frac{\boldsymbol{\pi}_i}{m_i s^2} \\
\dot{\boldsymbol{\pi}}_i &= -\frac{\partial \mathcal{H}_e}{\partial \boldsymbol{\rho}_i} &&= -\frac{\partial \mathcal{U}}{\partial \boldsymbol{\rho}_i} \\
\dot{s} &= \frac{\partial \mathcal{H}_e}{\partial p_s} &&= \frac{p_s}{M_s} \\
\dot{\pi}_s &= -\frac{\partial \mathcal{H}_e}{\partial s} &&= \sum_i \frac{\boldsymbol{\pi}_i^2}{m_i s^3} - \frac{g k_B T}{s}
\end{aligned}$$

Equations of motion for the physical variables

We use that

$$s\frac{d}{d\tau} = \frac{d}{dt},$$

where τ is the "virtual" time. This gives

$$\begin{aligned}
\dot{\mathbf{r}}_i &= \frac{\mathbf{p}_i}{m_i} \\
\dot{\mathbf{p}}_i &= -\frac{\partial \mathcal{U}}{\partial \mathbf{r}_i} - \zeta \mathbf{p}_i \\
\dot{\zeta} &= \frac{1}{M_s}\left(\sum_i \frac{\mathbf{p}_i^2}{m_i} - g k_B T\right)
\end{aligned}$$

We choose $g = 3N$. The variable ζ plays the role of a "friction constant" which can be positive or negative.

Simulations in the NpT ensemble

Extended system

virtual	real	relation
Q	V	$Q = V$
$\boldsymbol{\pi}_Q$	p_V	$\frac{\boldsymbol{\pi}_Q}{s} = p_V$
s	S	$s = S$
$\boldsymbol{\pi}_s$	p_S	$\frac{\boldsymbol{\pi}_s}{s} = p_s$
$\boldsymbol{\rho}$	$\mathbf{r}$	$Q^{1/3}\boldsymbol{\rho} = \mathbf{r}$
$\boldsymbol{\pi}$	$\mathbf{p}$	$\frac{\boldsymbol{\pi}}{Q^{\frac{1}{3}}s} = \mathbf{p}$
$d\tau$	dt	$\frac{d\tau}{s} = dt$

Lagrange function

$$\mathcal{L}_e = \sum_i \frac{m_i Q^{2/3} s^2}{2} \dot{\boldsymbol{\rho}}_i^2 - \mathcal{U}(Q^{1/3}\boldsymbol{\rho}_1, \ldots, Q^{1/3}\boldsymbol{\rho}_N)$$

$$+ \frac{1}{2} M_Q s^2 \dot{Q}^2 - P_{ext} Q + \frac{1}{2} M_s \dot{s}^2 - g k_B T \ln s .$$

M_Q and M_s are the fictitious "masses" for Q and s, respectively, and P_{ext} is the desired pressure.

Hamilton function

$$\mathcal{H}_e = \sum_i \frac{\boldsymbol{\pi}_i^2}{2 Q^{2/3} m_i s^2} + \mathcal{U}(Q^{1/3}\boldsymbol{\rho}_1, \ldots, Q^{1/3}\boldsymbol{\rho}_N)$$

$$+ \frac{1}{2 M_Q s^2} p_Q^2 + P_{ext} Q + \frac{1}{2 M_s} p_s^2 + g k_B T \ln s .$$

Partition function

Here we have

$$\omega_e(NVE) = \frac{1}{N!}\int_{-\infty}^{+\infty} dp_Q \int_0^{\infty} dQ \int_{-\infty}^{+\infty} dp_s \int_0^{\infty} ds \int_{\mathbb{R}_{3N}} d^{3N}\pi \int_V d^{3N}\rho\, \delta(E - \mathcal{H}_e)$$

$$= \frac{1}{g}\left(\frac{4\pi^2 M_s M_Q}{k_B T}\right)^{1/2} \exp\left[\frac{E}{k_B T}\right] \cdot Z_c(N,p,T).$$

$Z_c(N,p,T)$ is the partition function of the NpT ensemble:

$$Z_c(N,p,T) = \frac{1}{N!}\int_0^{\infty} dV \int_{\mathbb{R}_{3N}} d^{3N}\pi \int_V d^{3N}\rho\, \exp\left[-\frac{\mathcal{H}(\boldsymbol{\pi},\boldsymbol{\rho}) + P_{ext}V}{k_B T}\right].$$

Equations of motion for physical variables:

In the following we replace the indices “Q” by “V”.

$$
\begin{aligned}
\dot{\mathbf{r}}_i &= \frac{\dot{V}}{3V}\mathbf{r}_i + \frac{\mathbf{p}_i}{m_i} \\
\dot{\mathbf{p}}_i &= -\frac{\partial \mathcal{U}}{\partial \mathbf{r}_i} - \frac{\dot{V}}{3V}\mathbf{p}_i - \zeta \mathbf{p}_i \\
\dot{V} &= \frac{p_{_V}}{M_{_V}} \\
\dot{p}_{_V} &= -P_{ext} + \frac{1}{3V}\left\{\sum_i \left(\frac{\mathbf{p}_i^2}{m_i} - \mathbf{r}_i \cdot \frac{\partial \mathcal{U}}{\partial \mathbf{r}_i}\right)\right\} \\
\dot{\zeta} &= \frac{1}{M_s}\left(\sum_i \frac{\mathbf{p}_i^2}{m_i} - g k_B T\right)
\end{aligned}
$$

Berendsen thermostat

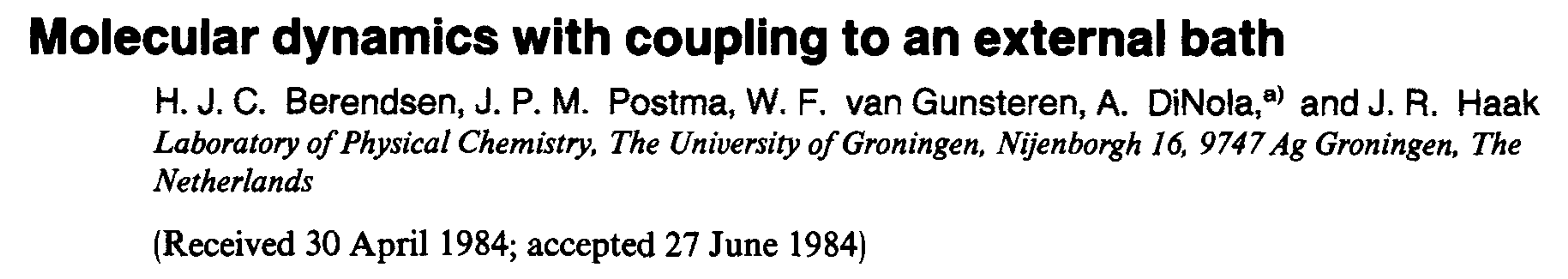

Molecular dynamics with coupling to an external bath

H. J. C. Berendsen, J. P. M. Postma, W. F. van Gunsteren, A. DiNola,[a] and J. R. Haak
Laboratory of Physical Chemistry, The University of Groningen, Nijenborgh 16, 9747 Ag Groningen, The Netherlands

(Received 30 April 1984; accepted 27 June 1984)

J. Chem. Phys. **81**, 3684 (1984)

$$m_i \dot{v}_i = F_i + m_i \gamma \left(\frac{T_0}{T} - 1 \right) v_i$$

This thermostat is widely used, in particular for the simulation of biomolecular systems, but it does not correspond to a standard thermodynamic ensemble.

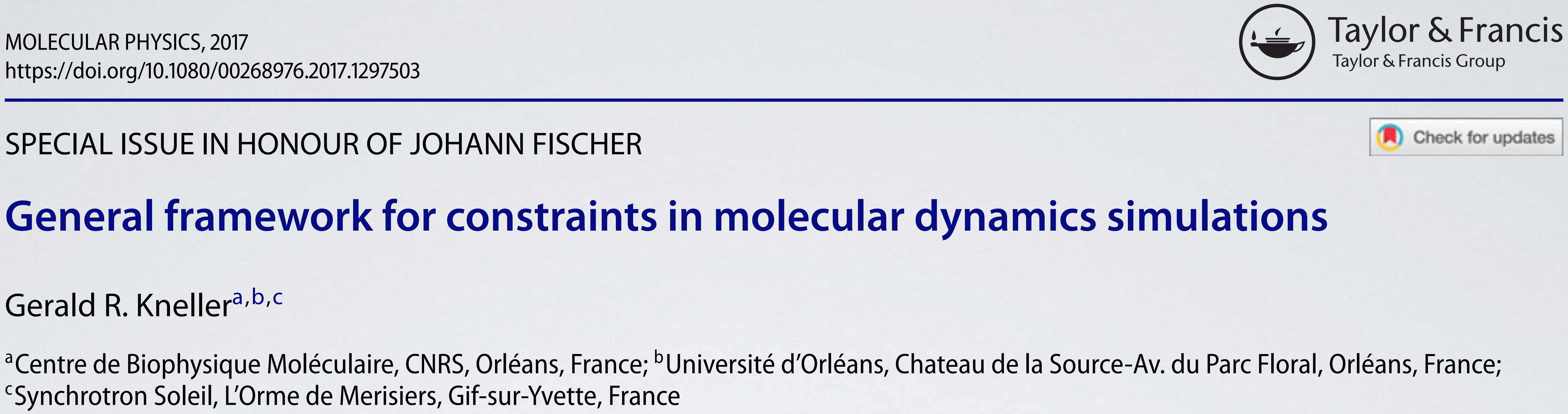

MOLECULAR PHYSICS, 2017
https://doi.org/10.1080/00268976.2017.1297503

SPECIAL ISSUE IN HONOUR OF JOHANN FISCHER

General framework for constraints in molecular dynamics simulations

Gerald R. Kneller[a,b,c]

[a]Centre de Biophysique Moléculaire, CNRS, Orléans, France; [b]Université d'Orléans, Chateau de la Source-Av. du Parc Floral, Orléans, France; [c]Synchrotron Soleil, L'Orme de Merisiers, Gif-sur-Yvette, France

Use Gauss' least-constraint principle as a framework for MD simulations in presence of holonomic and non-holonomic constraints.

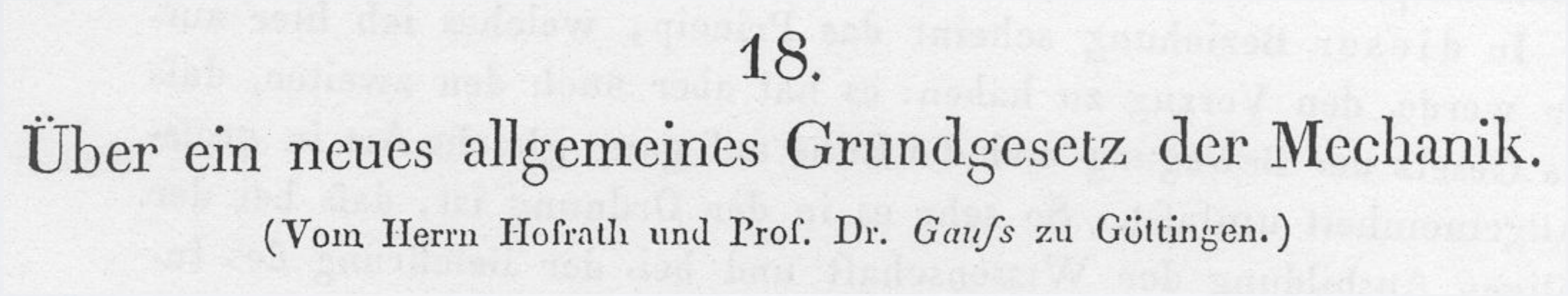

18.

Über ein neues allgemeines Grundgesetz der Mechanik.

(Vom Herrn Hofrath und Prof. Dr. Gauſs zu Göttingen.)

J. Reine und Angewandte Mathematik (Crelle's Journal) **1829**(4) 232-235

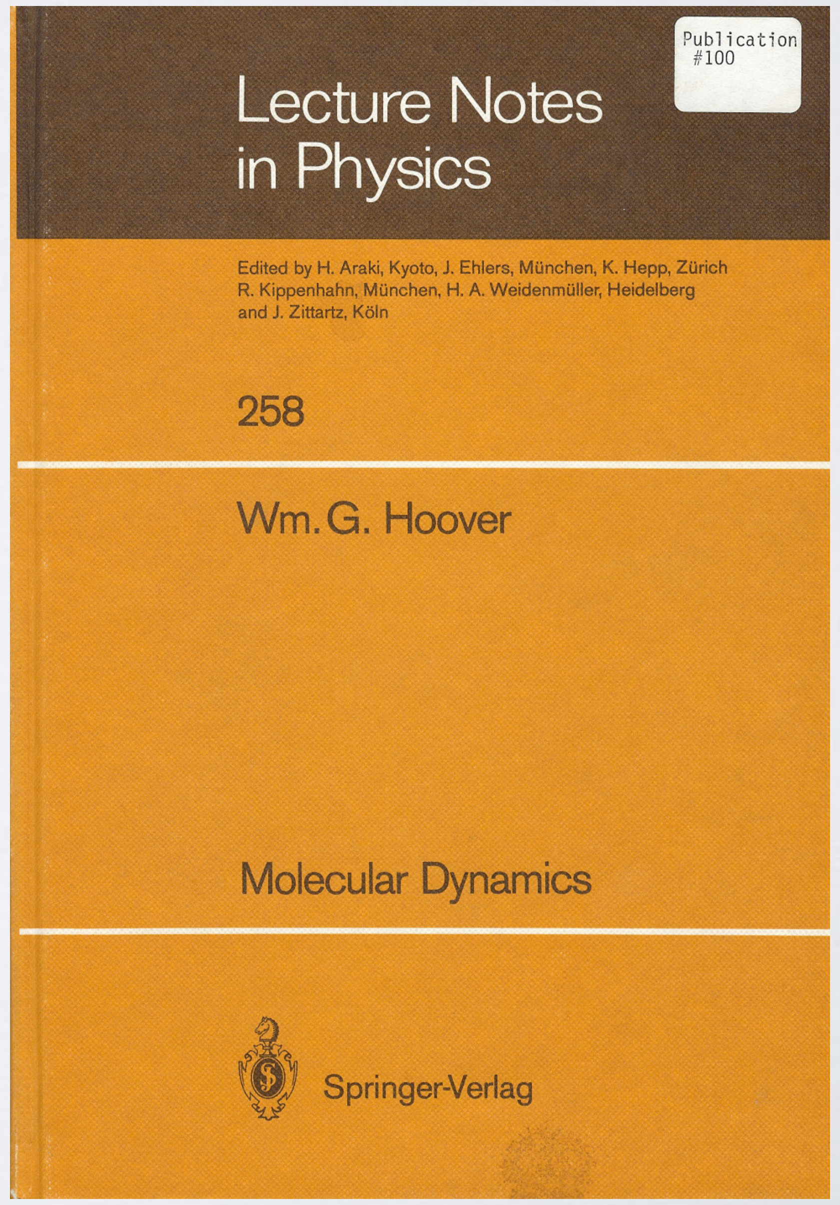

Lecture Notes in Physics

Publication #100

Edited by H. Araki, Kyoto, J. Ehlers, München, K. Hepp, Zürich
R. Kippenhahn, München, H. A. Weidenmüller, Heidelberg
and J. Zittartz, Köln

258

Wm.G. Hoover

Molecular Dynamics

Springer-Verlag

Molecular dynamics simulations of open systems can be considered as the numerical solution of the Newtonian equations of motion of a many-body system in presence of non-holonomic, **velocity-dependent** contraints.

$$\mathbf{M} \cdot \ddot{\mathbf{x}} = \mathbf{f}(\mathbf{x}) + \mathbf{z}(\mathbf{x}, \dot{\mathbf{x}}, t)$$

The constraint forces can be obtained from Gauß' principle of least constraint:

$$G(\ddot{\mathbf{x}}) = \frac{1}{2}\|\mathbf{M}^{-1/2} \cdot \mathbf{z}\|^2 = \mathrm{Min.}, \quad \text{subject to} \quad \mathbf{A}(\mathbf{x}, \dot{\mathbf{x}}, t) \cdot \ddot{\mathbf{x}} = \mathbf{b}$$

Set of linear constraints
for the accelerations

Impose n_c linear constraints for $3N$ accelerations

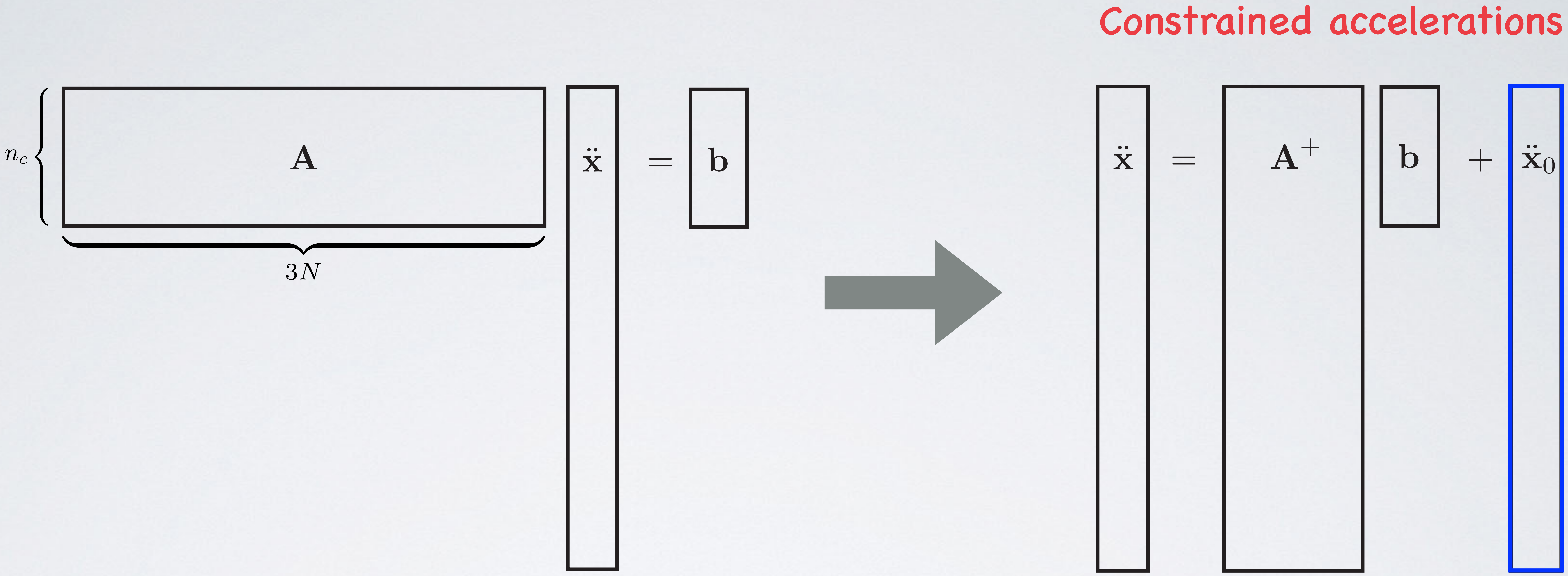

Number of degrees of freedom:

$$f = 3N - \operatorname{rank}(\mathbf{A})$$

$$\mathbf{A} \cdot \ddot{\mathbf{x}}_0 = \mathbf{0}$$

$$\mathbf{A} \cdot \mathbf{A}^+ \cdot \mathbf{b} = \mathbf{b}$$

R. Penrose, “A Generalized Inverse for Matrices,” Proc. Cambridge Philos. Soc, vol. 51, no. 406-413, p. C655, 1955.

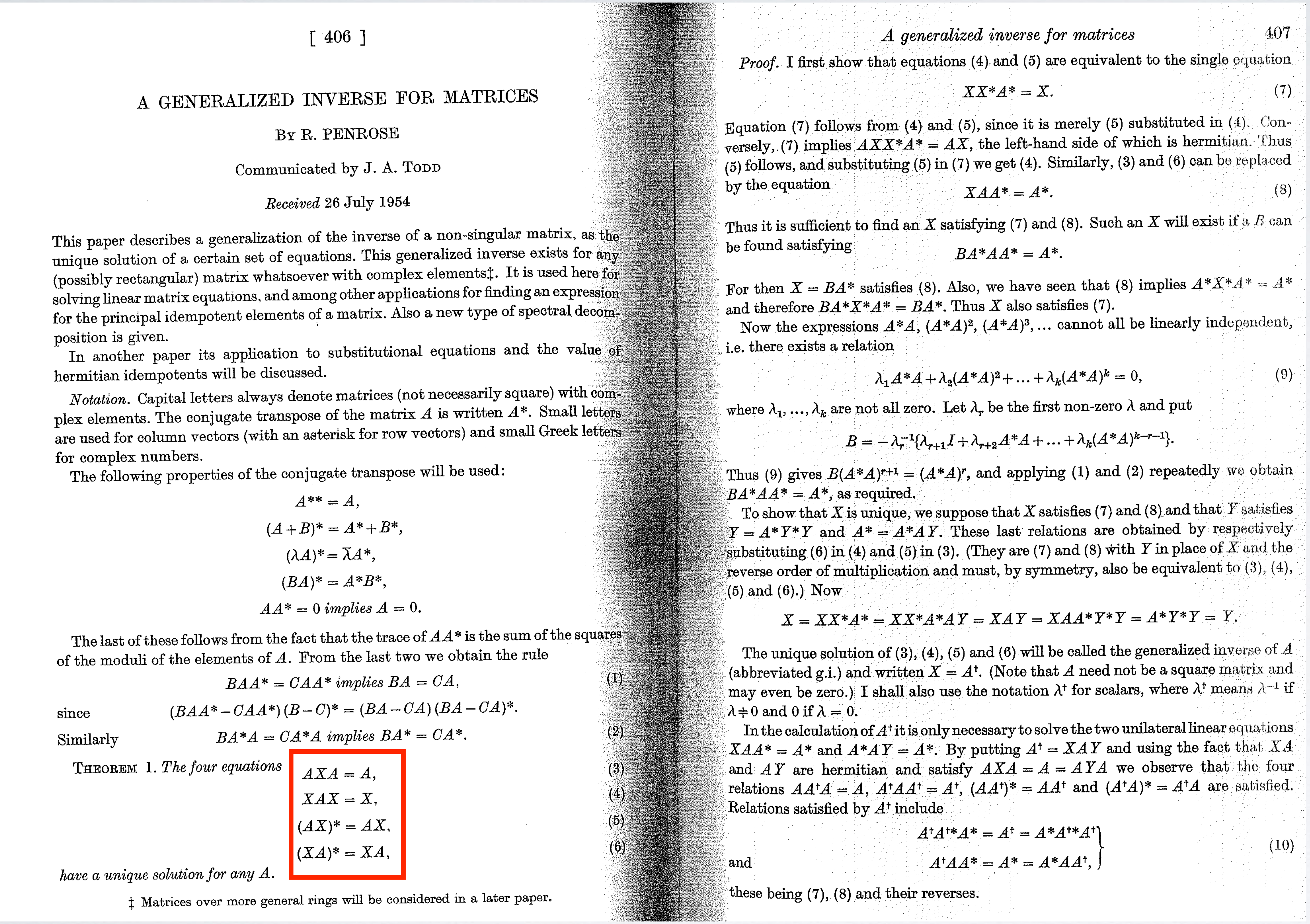

[406]

A GENERALIZED INVERSE FOR MATRICES

By R. PENROSE

Communicated by J. A. Todd

Received 26 July 1954

This paper describes a generalization of the inverse of a non-singular matrix, as the unique solution of a certain set of equations. This generalized inverse exists for any (possibly rectangular) matrix whatsoever with complex elements‡. It is used here for solving linear matrix equations, and among other applications for finding an expression for the principal idempotent elements of a matrix. Also a new type of spectral decomposition is given.

In another paper its application to substitutional equations and the value of hermitian idempotents will be discussed.

Notation. Capital letters always denote matrices (not necessarily square) with complex elements. The conjugate transpose of the matrix A is written A^*. Small letters are used for column vectors (with an asterisk for row vectors) and small Greek letters for complex numbers.

The following properties of the conjugate transpose will be used:

$$A^{**} = A,$$
$$(A+B)^* = A^* + B^*,$$
$$(\lambda A)^* = \bar{\lambda} A^*,$$
$$(BA)^* = A^* B^*,$$
$$AA^* = 0 \textit{ implies } A = 0.$$

The last of these follows from the fact that the trace of AA^* is the sum of the squares of the moduli of the elements of A. From the last two we obtain the rule

$$BAA^* = CAA^* \textit{ implies } BA = CA, \tag{1}$$

since $$(BAA^* - CAA^*)(B-C)^* = (BA-CA)(BA-CA)^*.$$

Similarly $$BA^*A = CA^*A \textit{ implies } BA^* = CA^*. \tag{2}$$

Theorem 1. *The four equations*

$$\boxed{\begin{aligned} AXA &= A, & (3)\\ XAX &= X, & (4)\\ (AX)^* &= AX, & (5)\\ (XA)^* &= XA, & (6)\end{aligned}}$$

have a unique solution for any A.

---

‡ Matrices over more general rings will be considered in a later paper.

A generalized inverse for matrices 407

Proof. I first show that equations (4) and (5) are equivalent to the single equation

$$XX^*A^* = X. \tag{7}$$

Equation (7) follows from (4) and (5), since it is merely (5) substituted in (4). Conversely, (7) implies $AXX^*A^* = AX$, the left-hand side of which is hermitian. Thus (5) follows, and substituting (5) in (7) we get (4). Similarly, (3) and (6) can be replaced by the equation

$$XAA^* = A^*. \tag{8}$$

Thus it is sufficient to find an X satisfying (7) and (8). Such an X will exist if a B can be found satisfying

$$BA^*AA^* = A^*.$$

For then $X = BA^*$ satisfies (8). Also, we have seen that (8) implies $A^*X^*A^* = A^*$ and therefore $BA^*X^*A^* = BA^*$. Thus X also satisfies (7).

Now the expressions A^*A, $(A^*A)^2$, $(A^*A)^3$, … cannot all be linearly independent, i.e. there exists a relation

$$\lambda_1 A^*A + \lambda_2 (A^*A)^2 + \dots + \lambda_k (A^*A)^k = 0, \tag{9}$$

where $\lambda_1, \dots, \lambda_k$ are not all zero. Let λ_r be the first non-zero λ and put

$$B = -\lambda_r^{-1}\{\lambda_{r+1} I + \lambda_{r+2} A^*A + \dots + \lambda_k (A^*A)^{k-r-1}\}.$$

Thus (9) gives $B(A^*A)^{r+1} = (A^*A)^r$, and applying (1) and (2) repeatedly we obtain $BA^*AA^* = A^*$, as required.

To show that X is unique, we suppose that X satisfies (7) and (8) and that Y satisfies $Y = A^*Y^*Y$ and $A^* = A^*AY$. These last relations are obtained by respectively substituting (6) in (4) and (5) in (3). (They are (7) and (8) with Y in place of X and the reverse order of multiplication and must, by symmetry, also be equivalent to (3), (4), (5) and (6).) Now

$$X = XX^*A^* = XX^*A^*AY = XAY = XAA^*Y^*Y = A^*Y^*Y = Y.$$

The unique solution of (3), (4), (5) and (6) will be called the generalized inverse of A (abbreviated g.i.) and written $X = A^\dagger$. (Note that A need not be a square matrix and may even be zero.) I shall also use the notation $\lambda^\dagger$ for scalars, where $\lambda^\dagger$ means λ^{-1} if $\lambda \neq 0$ and 0 if $\lambda = 0$.

In the calculation of $A^\dagger$ it is only necessary to solve the two unilateral linear equations $XAA^* = A^*$ and $A^*AY = A^*$. By putting $A^\dagger = XAY$ and using the fact that XA and AY are hermitian and satisfy $AXA = A = AYA$ we observe that the four relations $AA^\dagger A = A$, $A^\dagger AA^\dagger = A^\dagger$, $(AA^\dagger)^* = AA^\dagger$ and $(A^\dagger A)^* = A^\dagger A$ are satisfied. Relations satisfied by $A^\dagger$ include

$$\left.\begin{aligned} &A^\dagger A^{\dagger *} A^* = A^\dagger = A^* A^{\dagger *} A^\dagger \\ \text{and}\qquad &A^\dagger AA^* = A^* = A^*AA^\dagger, \end{aligned}\right\} \tag{10}$$

these being (7), (8) and their reverses.

Moore-Penrose conditions

$\mathbf{X} = \mathbf{A}^+$ iff

$$\mathbf{A} \cdot \mathbf{X} \cdot \mathbf{A} = \mathbf{A}$$
$$\mathbf{X} \cdot \mathbf{A} \cdot \mathbf{X} = \mathbf{X}$$
$$(\mathbf{A} \cdot \mathbf{X})^\dagger = \mathbf{A} \cdot \mathbf{X}$$
$$(\mathbf{X} \cdot \mathbf{A})^\dagger = \mathbf{X} \cdot \mathbf{A}$$

If **A** is full rank and of dimension $m \times n$ $(n < m)$

$$\mathbf{A}^+ = \mathbf{A}^T \cdot (\mathbf{A} \cdot \mathbf{A}^T)^{-1}$$

If **A** is full rank and of dimension $m \times n$ $(n > m)$

$$\mathbf{A}^+ = (\mathbf{A}^T \cdot \mathbf{A})^{-1} \cdot \mathbf{A}^T$$

Determine the constraint forces from Gauss' principle

Minimisation of the constraint forces with the side constraints $\mathbf{A}\cdot\ddot{\mathbf{x}}_0=\mathbf{0}$

$$\left\|\mathbf{M}^{-1/2}\cdot\left(\underbrace{\mathbf{M}\cdot(\mathbf{A}^{+}\cdot\mathbf{b}+\ddot{\mathbf{x}}_0)-\mathbf{f}}_{\mathbf{z}}\right)\right\|^2-{\ddot{\mathbf{x}}_0}^T\cdot\mathbf{A}^T\cdot\boldsymbol{\lambda}=\mathrm{Min}(\ddot{\mathbf{x}}_0,\boldsymbol{\lambda})$$

⇒ $\mathbf{M}\cdot\ddot{\mathbf{x}}=\mathbf{f}(\mathbf{x})+\mathbf{z}(\mathbf{x},\dot{\mathbf{x}},t)$ and $\mathbf{z}=\mathbf{A}^T\cdot\boldsymbol{\lambda}$

The Lagrange multipliers can be determined using the side constraints:

$(\mathbf{A}\cdot\mathbf{M}^{-1}\cdot\mathbf{A}^T)\cdot\boldsymbol{\lambda}=\mathbf{b}-\mathbf{A}\cdot\mathbf{M}^{-1}\cdot\mathbf{f}$ ⇒ $\ddot{\mathbf{x}}=\mathbf{M}^{-1}\cdot(\mathbf{f}+\mathbf{A}^T\cdot\boldsymbol{\lambda})$

Example: Isokinetic ensemble — fixed temperature <u>without fluctuations</u>:

$$\frac{1}{2}\dot{\mathbf{x}}^T \cdot \mathbf{M} \cdot \dot{\mathbf{x}} = \frac{3Nk_BT}{2}$$

$$\mathbf{M} \cdot \ddot{\mathbf{x}} = \mathbf{f}(t) \underbrace{-\xi(t)\mathbf{M} \cdot \dot{\mathbf{x}}}_{\mathbf{z}(t)}$$

$$\xi(t) = \frac{\dot{\mathbf{x}}^T \cdot \mathbf{f}(t)}{3Nk_BT}$$

Linear acceleration constraint

$$\underbrace{\dot{\mathbf{x}}^T \cdot \mathbf{M}}_{\mathbf{A}} \cdot \ddot{\mathbf{x}} = \underbrace{0}_{\mathbf{b}}$$

All thermostats as non-holonomic constraints

Equation of motion

$$\mathbf{M}\cdot\ddot{\mathbf{x}} = \mathbf{f}\underbrace{-\xi(t)\,\mathbf{M}\cdot\dot{\mathbf{x}}}_{\mathbf{z}=\mathbf{A}^T\cdot\lambda}$$

Constraints

$$\underbrace{\dot{\mathbf{x}}^T\cdot\mathbf{M}}_{\mathbf{A}}\cdot\ddot{\mathbf{x}} = \underbrace{-\dot{\mathbf{x}}^T\cdot\mathbf{M}\cdot\dot{\mathbf{x}}\,\xi(t)+\dot{\mathbf{x}}^T\cdot\mathbf{f}}_{\mathbf{b}}$$

$$\Updownarrow$$

$$\frac{d}{dt}\left(E_{\text{kin}}(t)+U(\mathbf{x}(t))\right) = -2\xi(t)E_{\text{kin}}(t)$$

“Friction terms”

$$\xi_G(t) = \frac{\dot{\mathbf{x}}^T\cdot\mathbf{f}(t)}{3Nk_BT}$$

Isokinetic

Differential controller

$$\xi_B(t) = \frac{1}{\tau_B}\left(\frac{2E_{kin}(t)}{3Nk_BT}-1\right)$$

Berendsen

Proportional Controller

$$\xi_{NH}(t) = \frac{1}{\tau_{NH}^2}\int_0^t d\tau\left[\frac{2E_{\text{kin}}(\tau)}{3Nk_BT}-1\right]$$

Nosé-Hoover

Integral Controller

Macromolecules as linked rigid bodies

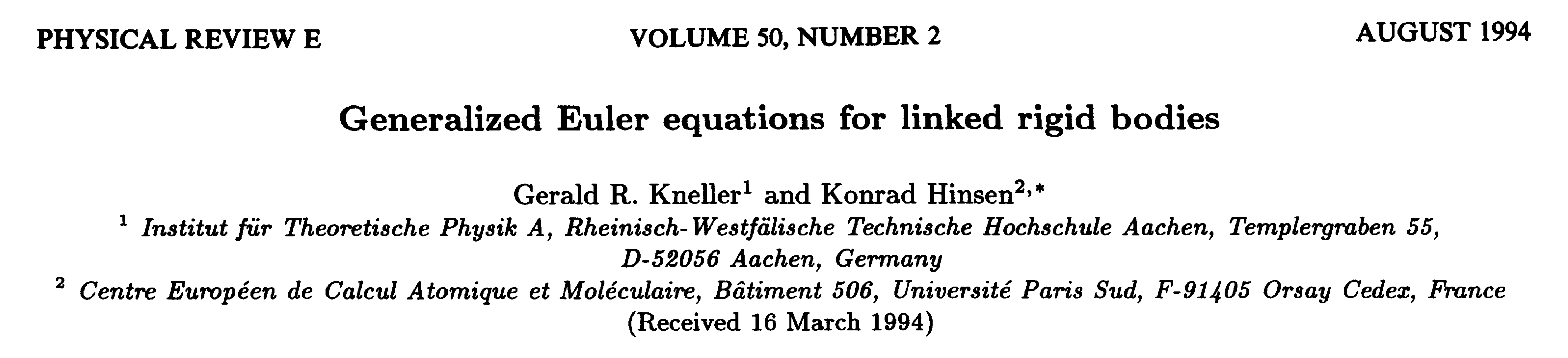

PHYSICAL REVIEW E VOLUME 50, NUMBER 2 AUGUST 1994

Generalized Euler equations for linked rigid bodies

Gerald R. Kneller[1] and Konrad Hinsen[2,*]

[1] *Institut für Theoretische Physik A, Rheinisch-Westfälische Technische Hochschule Aachen, Templergraben 55, D-52056 Aachen, Germany*

[2] *Centre Européen de Calcul Atomique et Moléculaire, Bâtiment 506, Université Paris Sud, F-91405 Orsay Cedex, France*

(Received 16 March 1994)

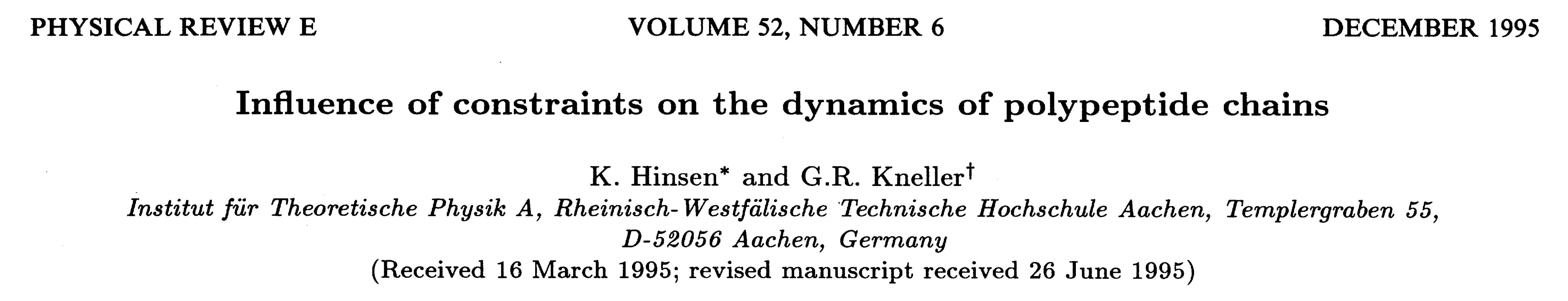

PHYSICAL REVIEW E VOLUME 52, NUMBER 6 DECEMBER 1995

Influence of constraints on the dynamics of polypeptide chains

K. Hinsen* and G.R. Kneller†

Institut für Theoretische Physik A, Rheinisch-Westfälische Technische Hochschule Aachen, Templergraben 55, D-52056 Aachen, Germany

(Received 16 March 1995; revised manuscript received 26 June 1995)

Planar peptide bond

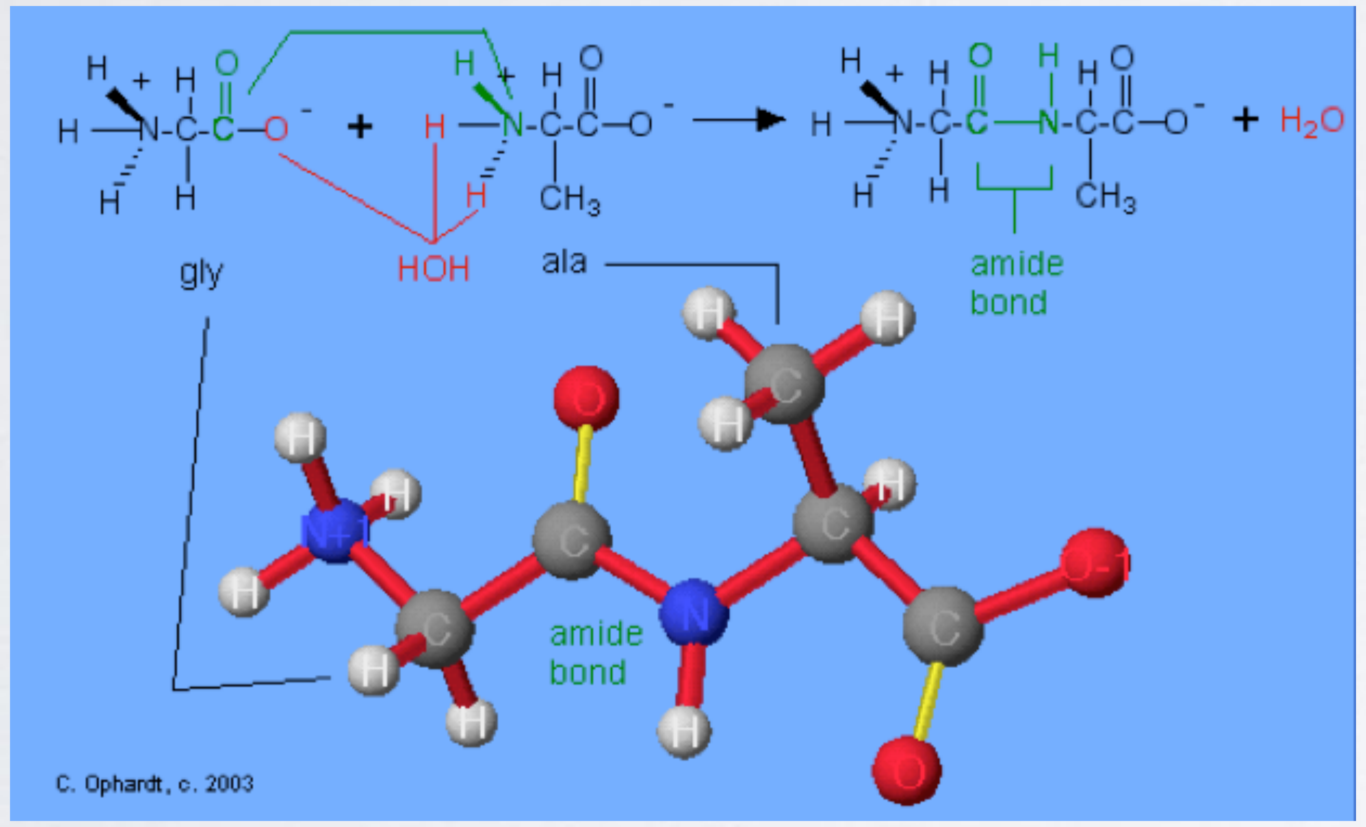

C. Ophardt, c. 2003

Macromolecular chain with rigid peptide planes

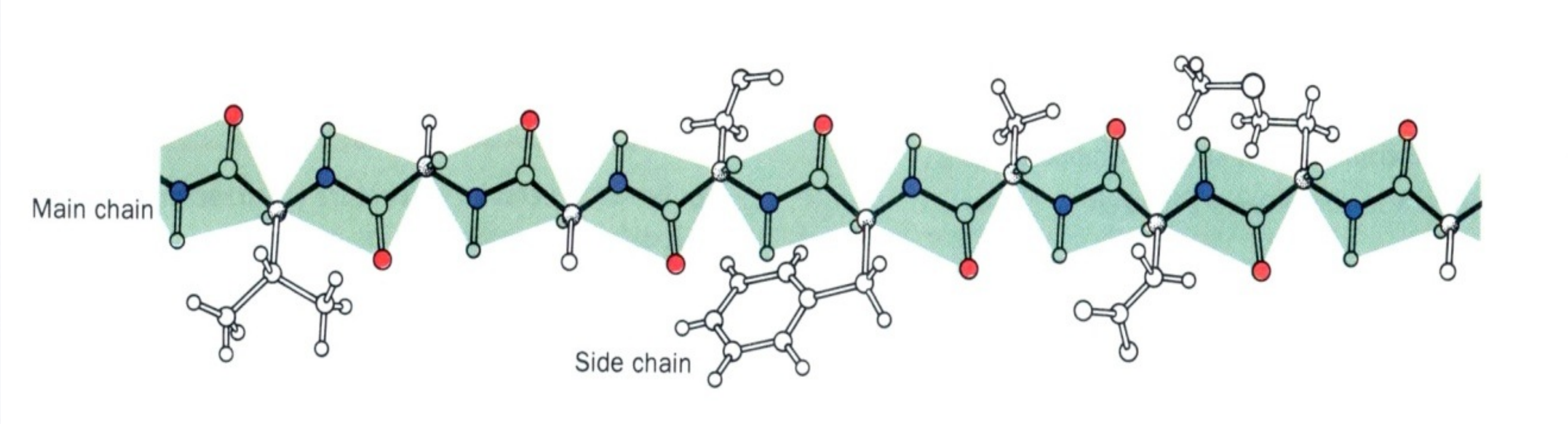

Dynamics of 16-polyalanine with different constraints

K. Hinsen and G. R. Kneller, Phys Rev E, vol. 52, no. B, pp. 6868–6874, 1995.

SHAKE (f=199)

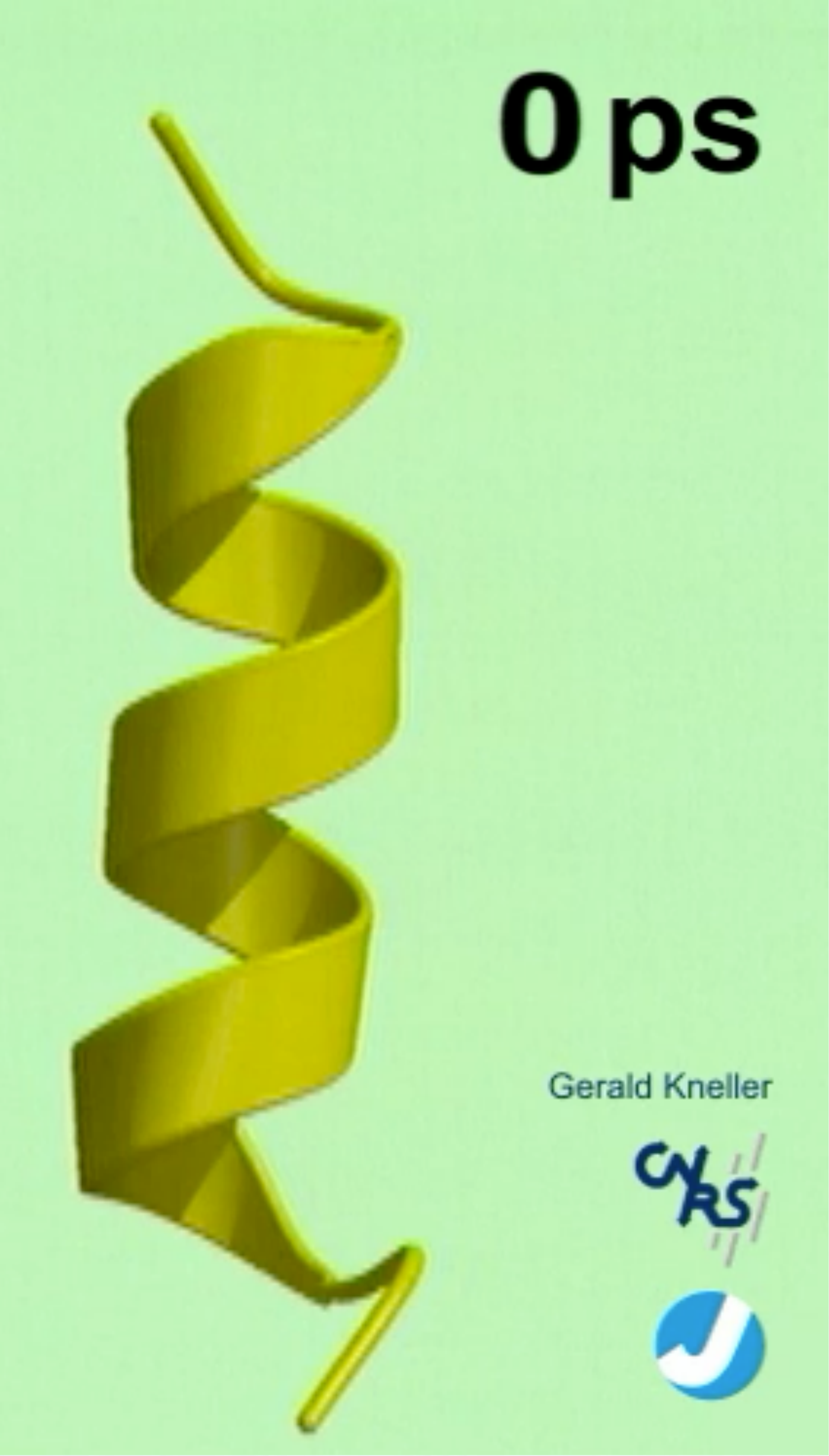

Rigid peptide planes (f=150)

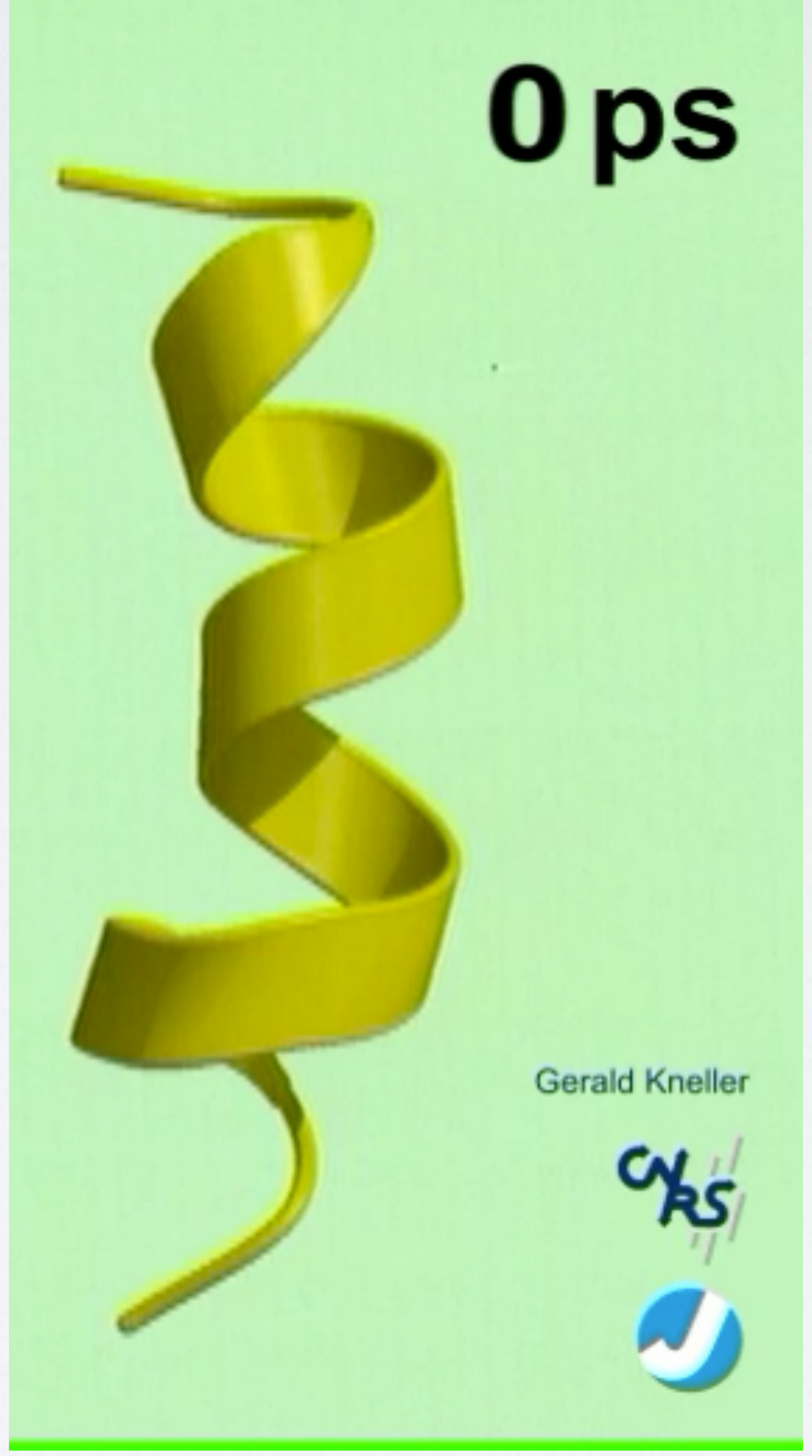

Torsional angle space (f=38)

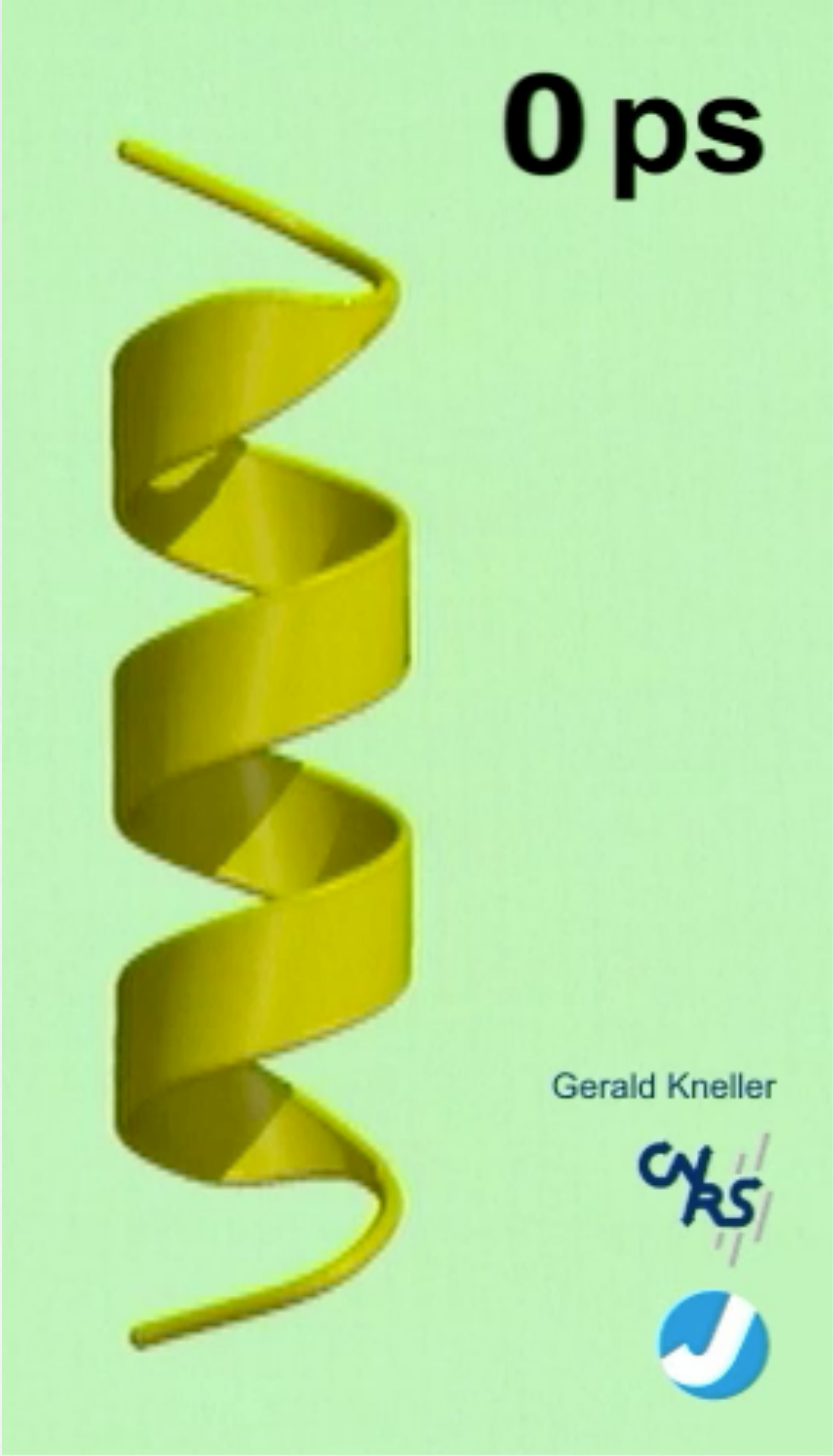

Mean squared displacement W(t)

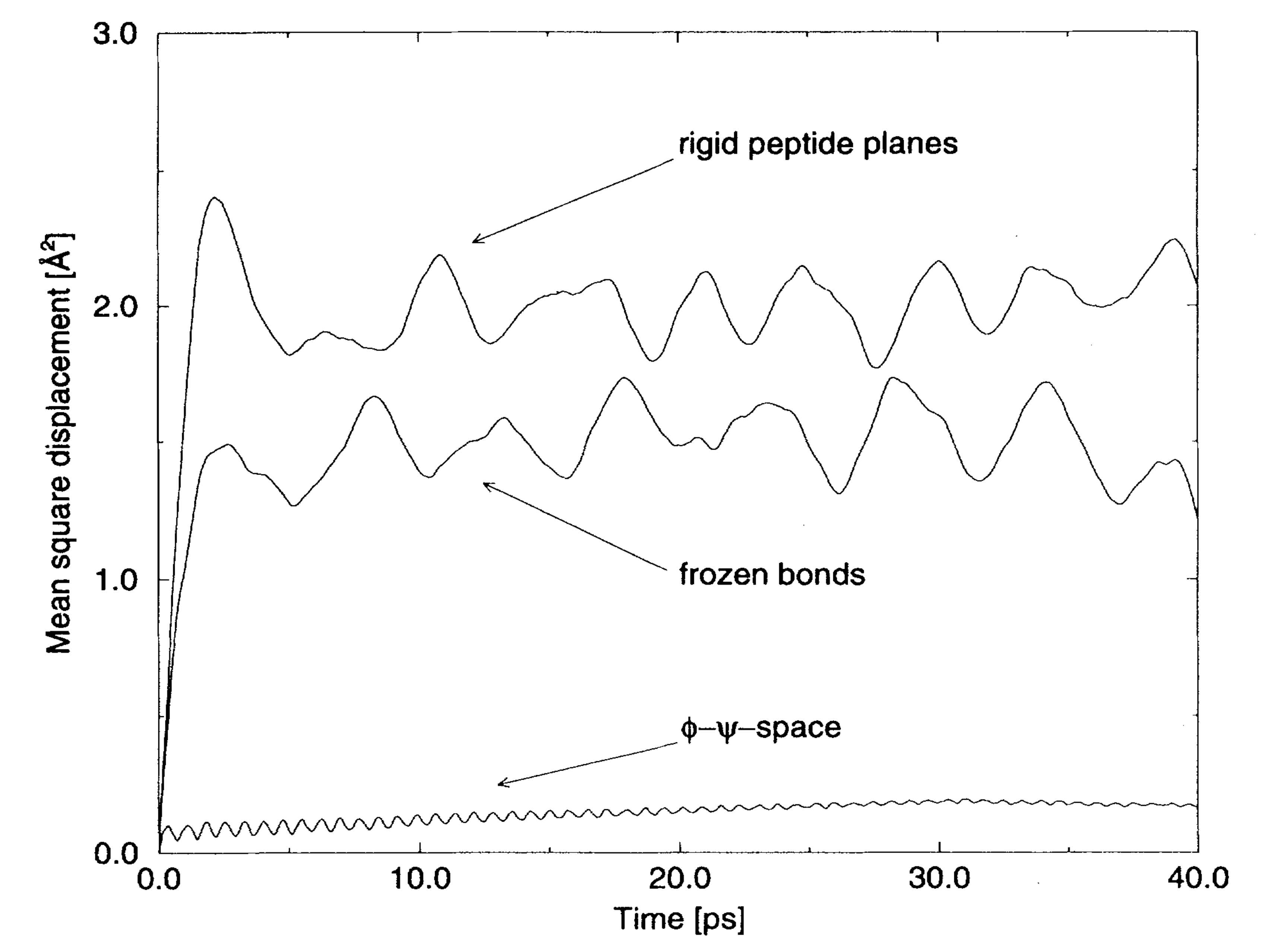

Average velocity power spectrum P(ω)

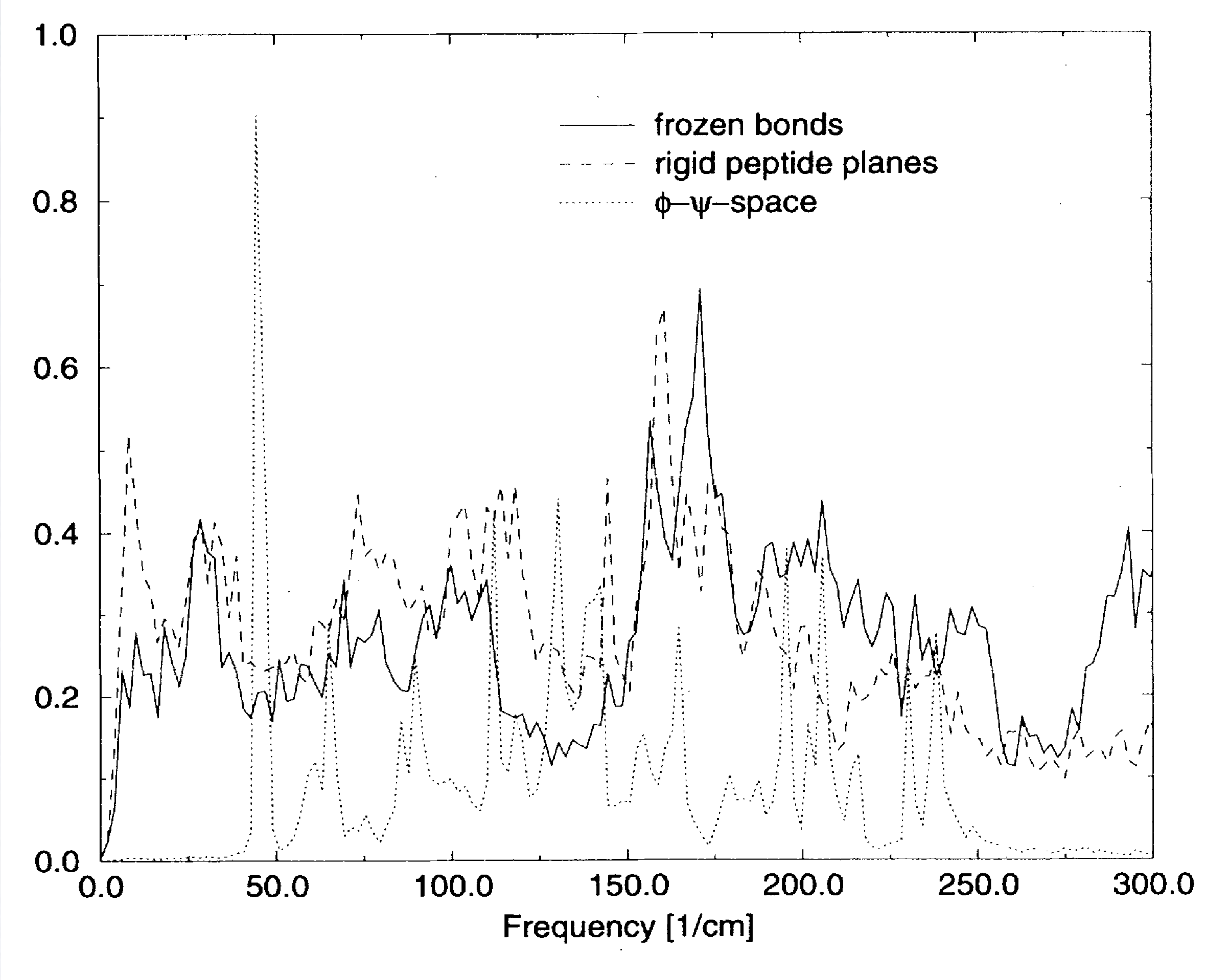

Low frequencies contribute most!

$$\boxed{W(t) = \frac{2}{\pi} \int_{-\infty}^{\infty} d\omega \, \frac{1}{\omega^2} P(\omega) \, (1 - \cos \omega t)}$$

Statistical physics of a toy system - 256 water molecules in a cubic box

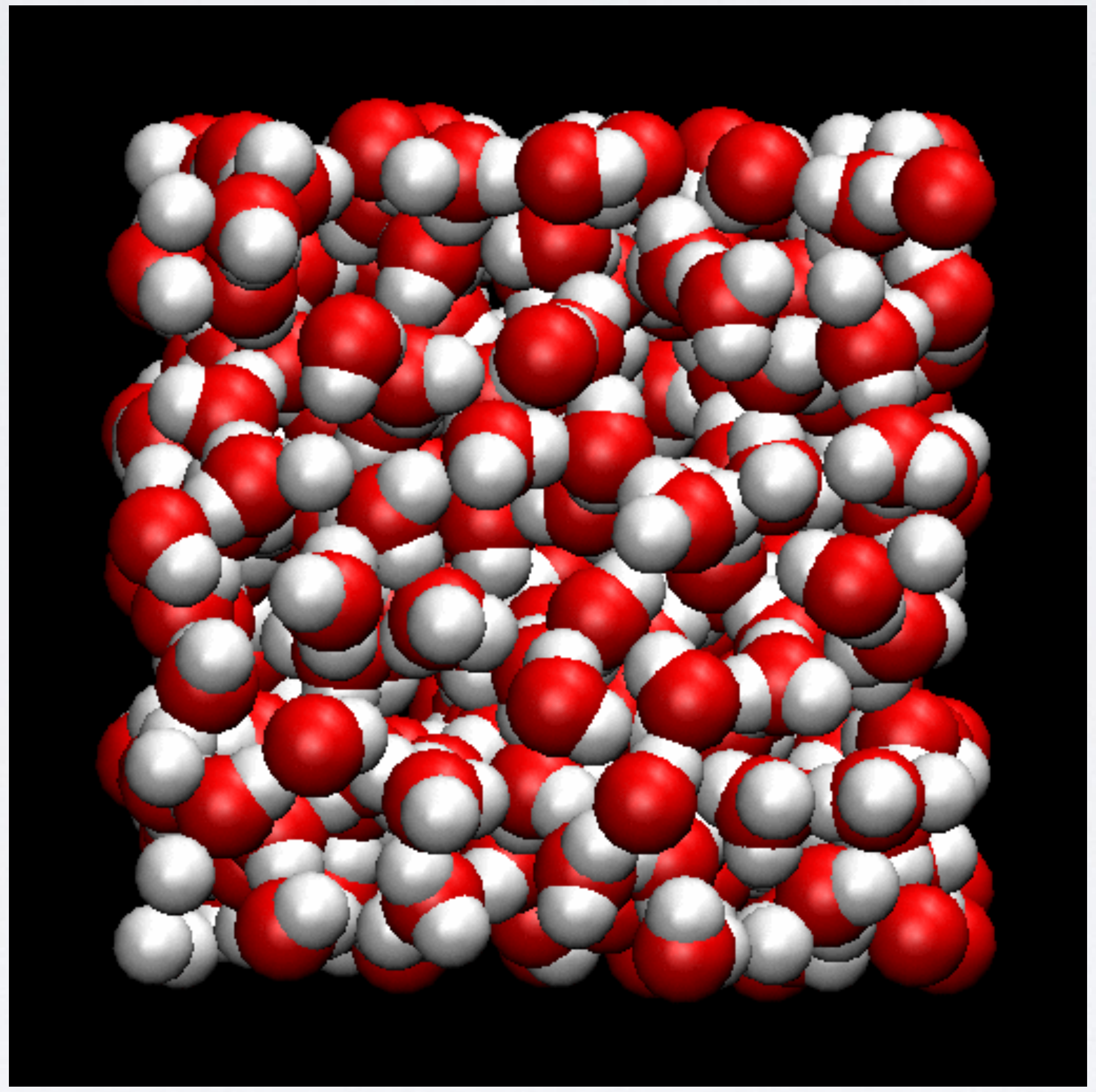

☞ MD trajectoires contain information about the structural dynamics of the simulated system which is largely unexploited.

Static site pair correlation functions of water

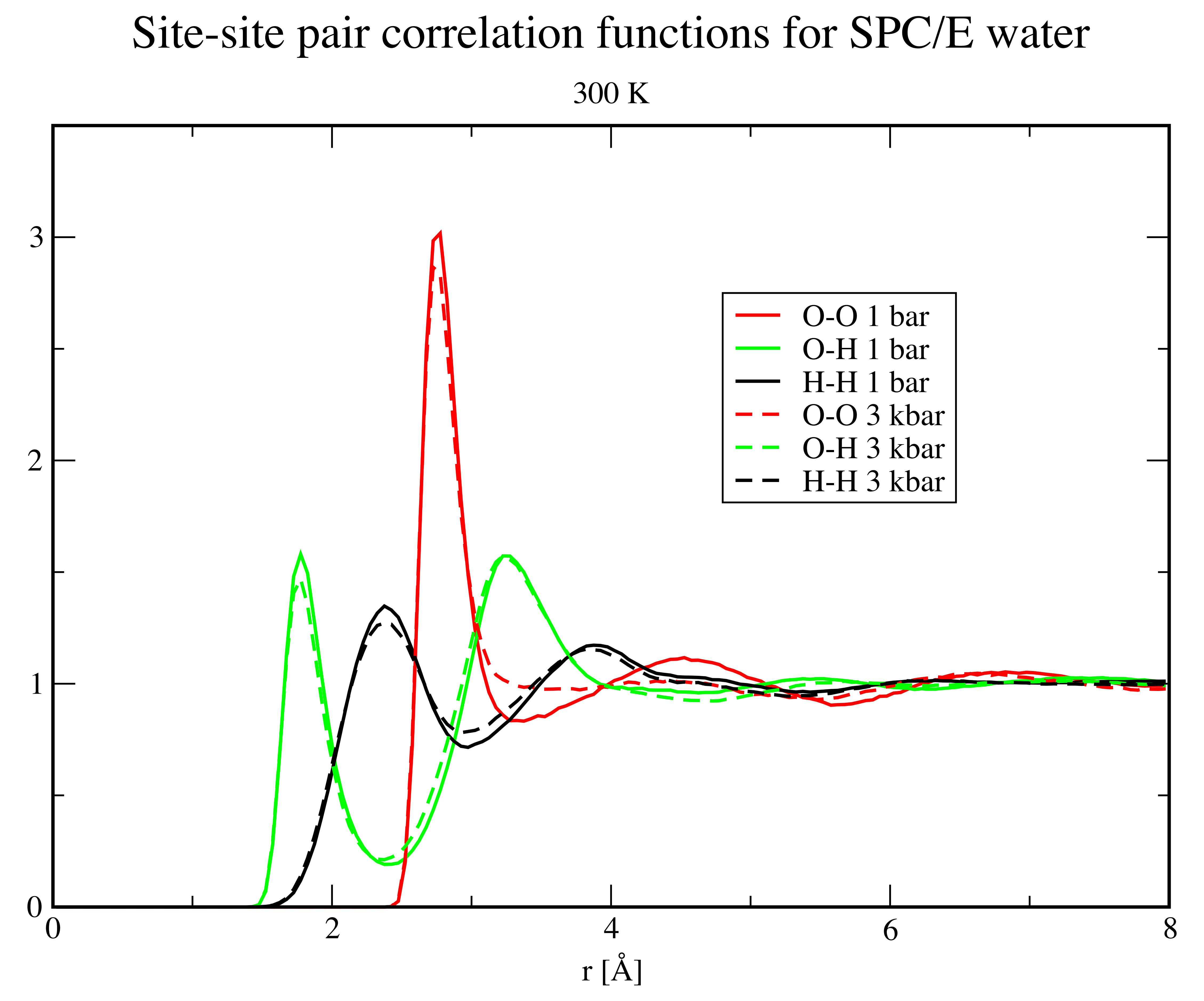

$$g(r) = \frac{1}{4\pi r^2 \rho} \frac{1}{N} \sum_{\alpha} \sum_{\beta \neq \alpha} \langle \delta(r - |R_\alpha - R_\beta|) \rangle$$

Diffusion of water molecules by MD simulation

$$W(t) = \langle (\mathbf{x}(t) - \mathbf{x}(0)^2 \rangle$$

Molecular dynamics simulation
SPC/E model, T = 300 K, p = 1 atm

$$W(n) \approx \frac{1}{N_t - |n|} \sum_{k=0}^{N_t - |n| - 1} |\mathbf{x}(k+n) - \mathbf{x}(k)|^2$$

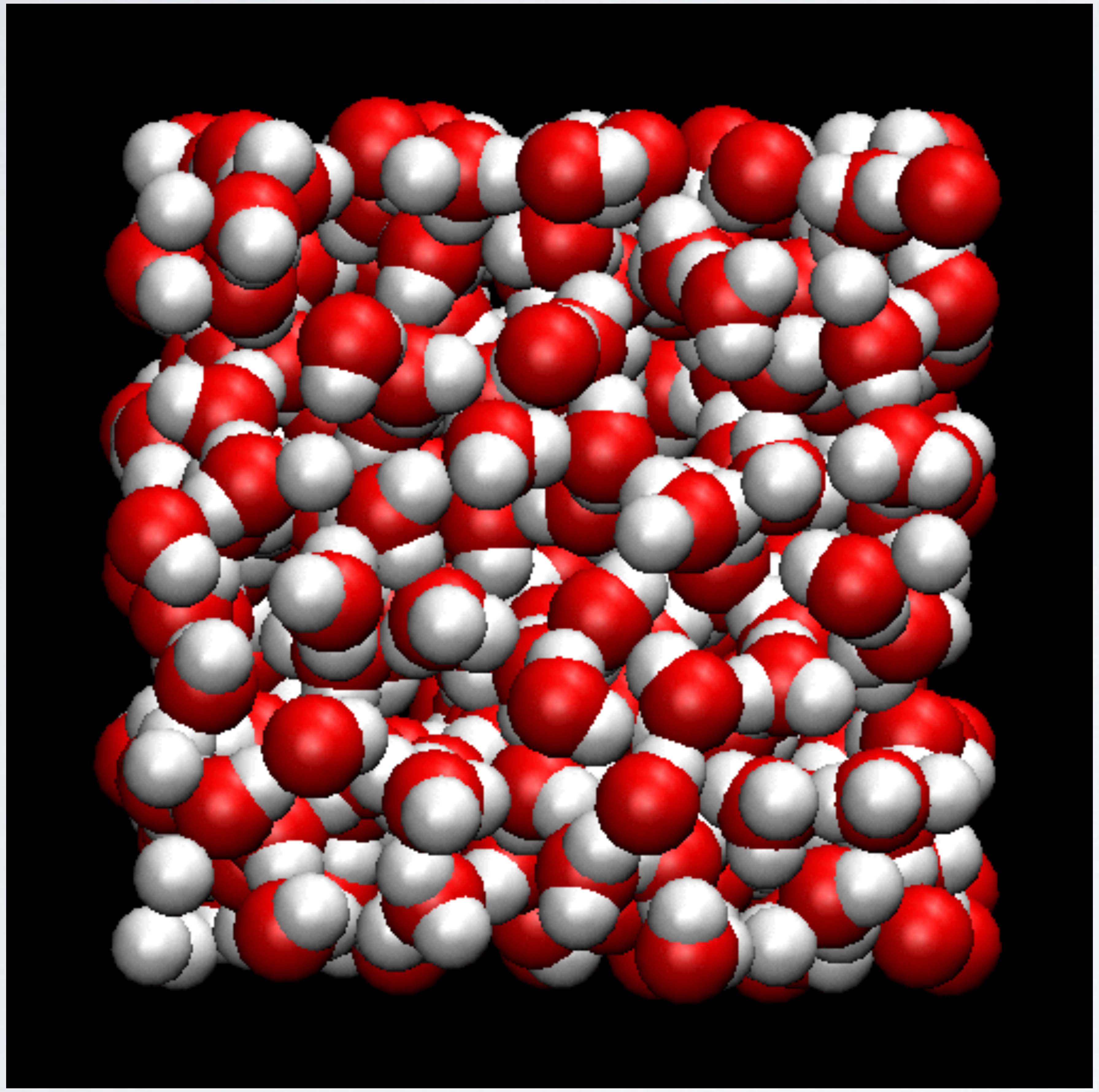

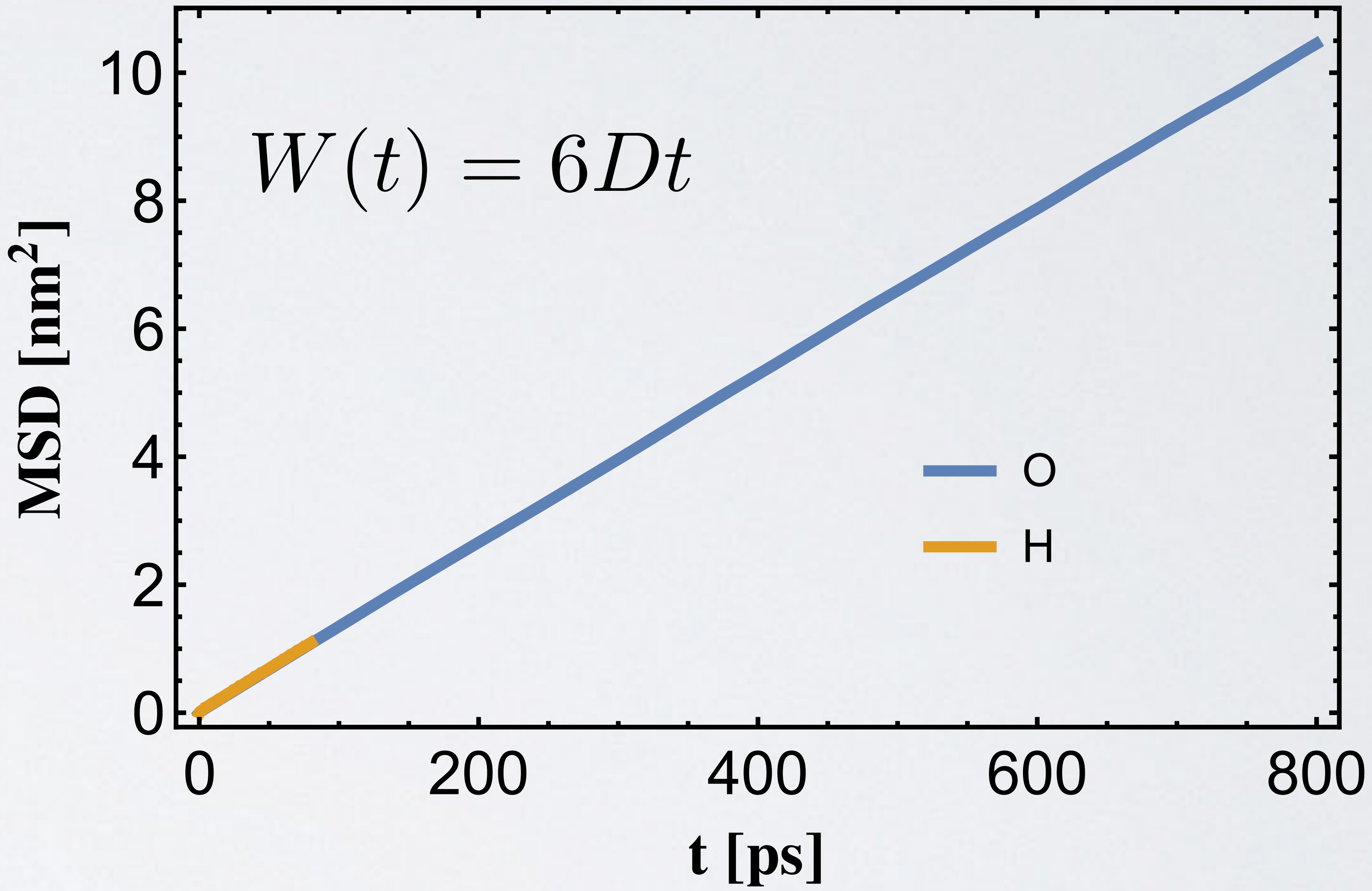

$$D = 2.17 \times 10^{-5} \mathrm{cm}^2/\mathrm{s}$$

$$D_{\mathrm{exp}} = 2.30 \times 10^{-5} \mathrm{cm}^2/\mathrm{s}$$ [1]

HJC. Berendsen, J. R. Grigera, and T. P. Straatsma,
J Phys Chem, vol. 91, no. 24, pp. 6269–6271, 1987.

[1] K. Krynicki, C. D. Green, and D. W. Sawyer, Faraday Discuss. Chem. Soc. 66, 199, (1978)

Remove first jumps due to p.b.c. !

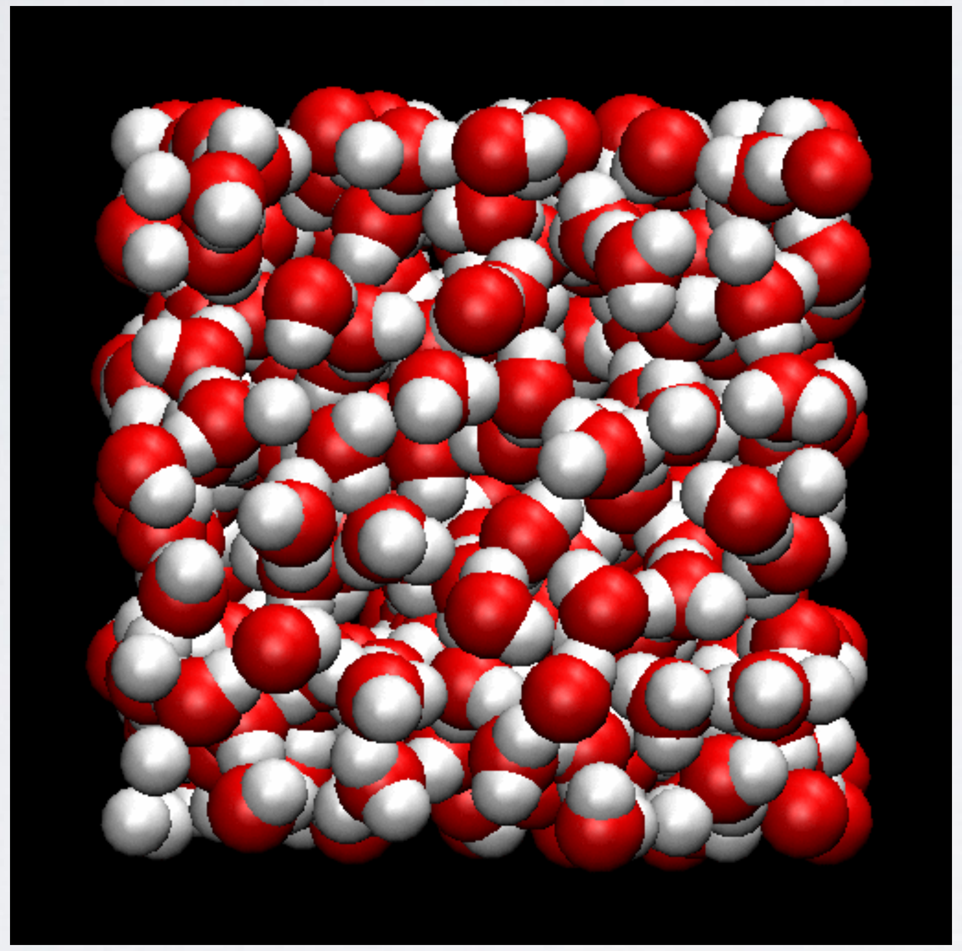

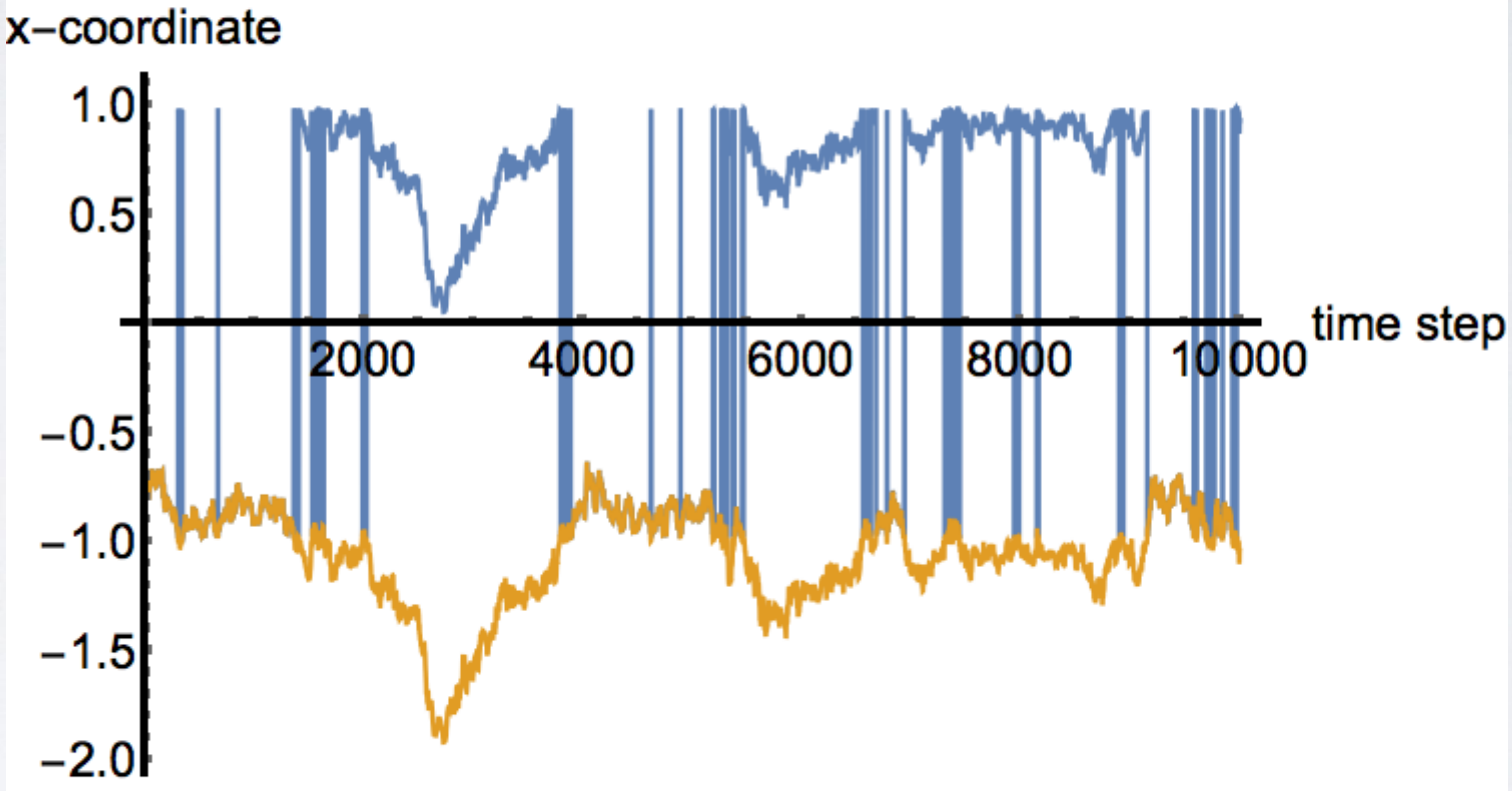

Diffusion models

Diffusion equation

$$\frac{\partial}{\partial t} f(\boldsymbol{r},t) = D\Delta f(\boldsymbol{r},t)$$

A. Fick, Annalen der Physik, vol. 170, no. 1, pp. 59–86, 1855.

A. Einstein, Annalen Der Physik 322, 549 (1905).

M. Von Smoluchowski, Annalen Der Physik 326, 756 (1906).

Mean squared deviation : $\sigma^2(t) = 2Dt$

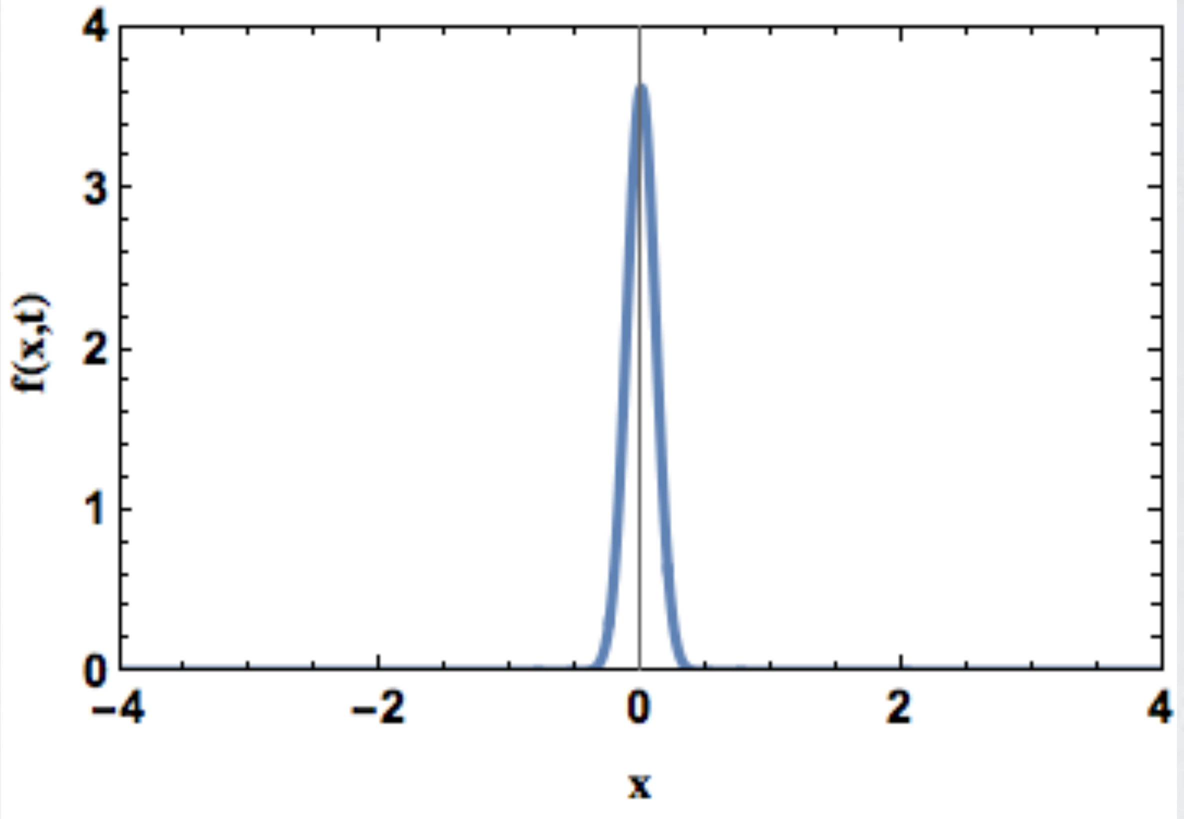

Stochastic process

N. Wiener, Journal of Mathematics and Physics 2, 131 (1923).

Mean squared displacement : $\langle (x(t) - x(0))^2 \rangle = 2Dt$

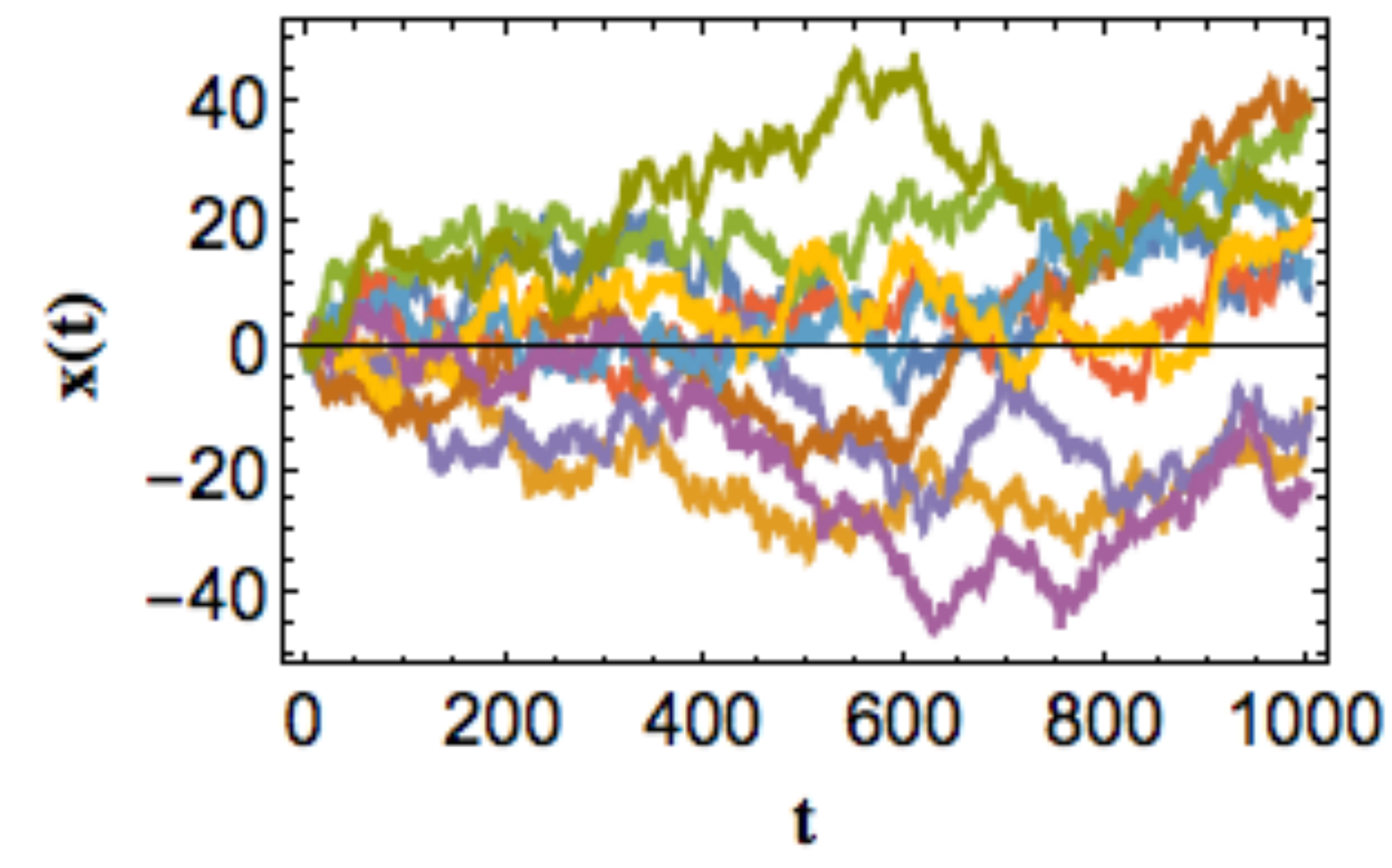

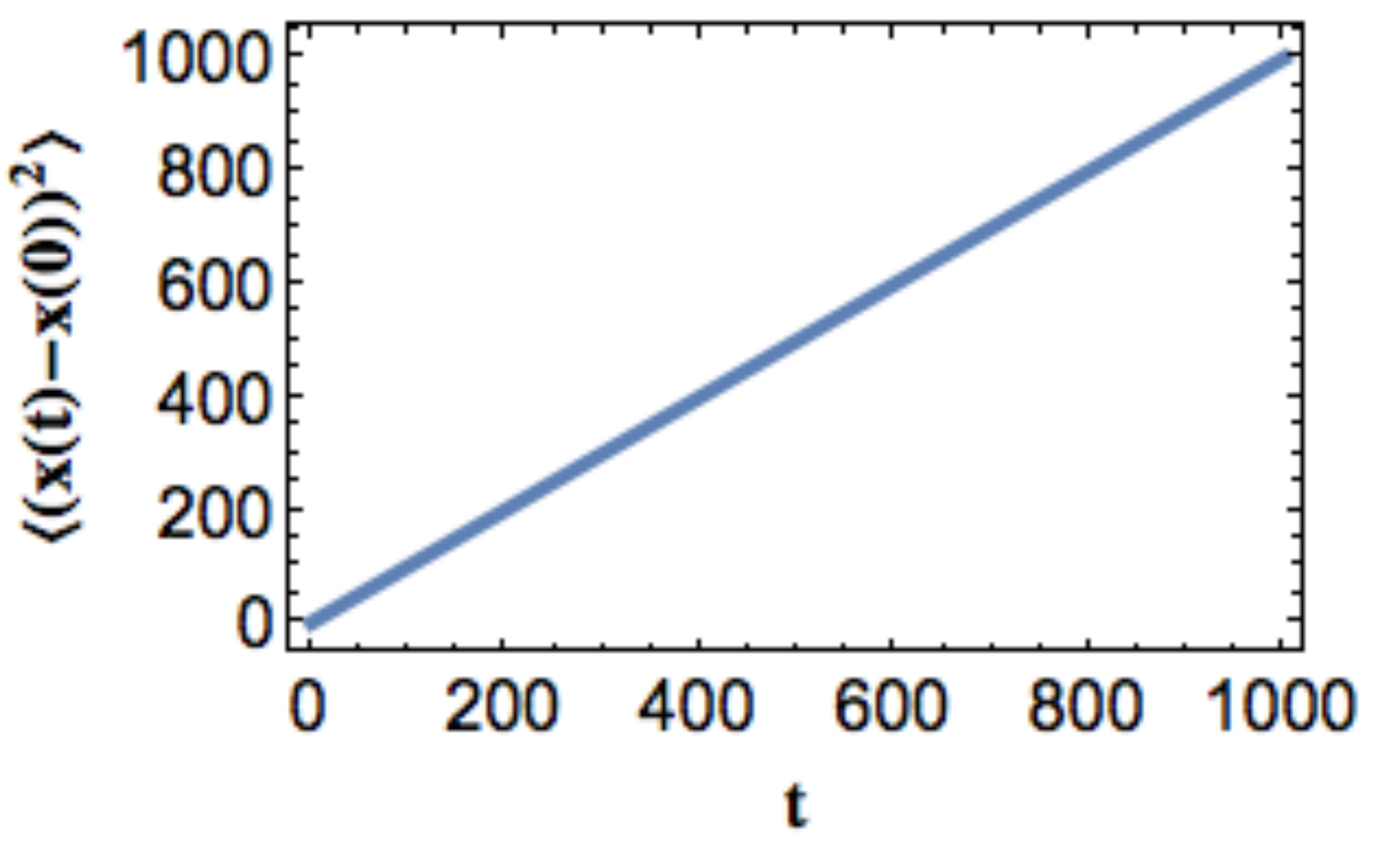

Velocity autocorrelation function (oxygen)

Trajectory

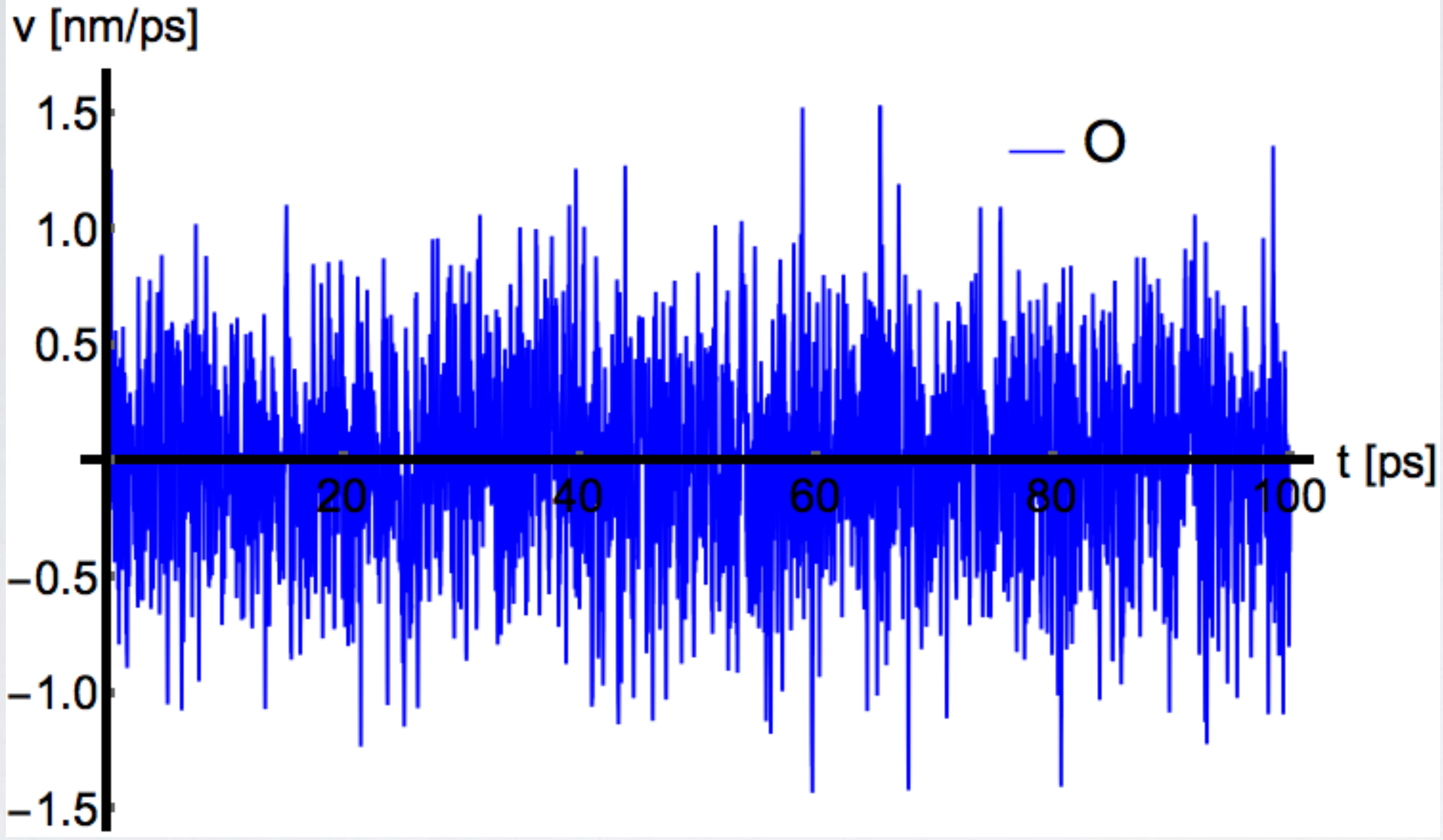

Maxwell distribution

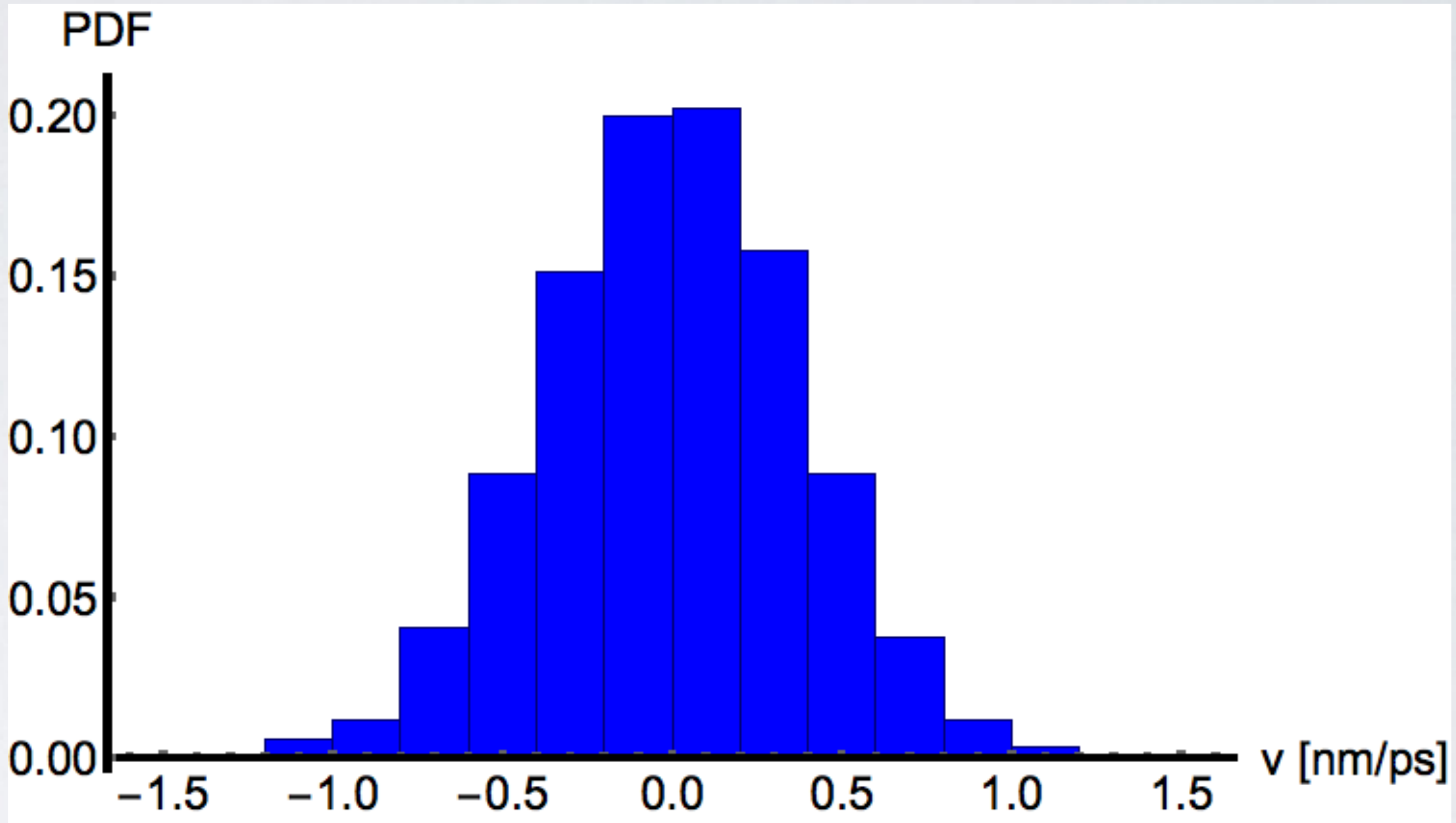

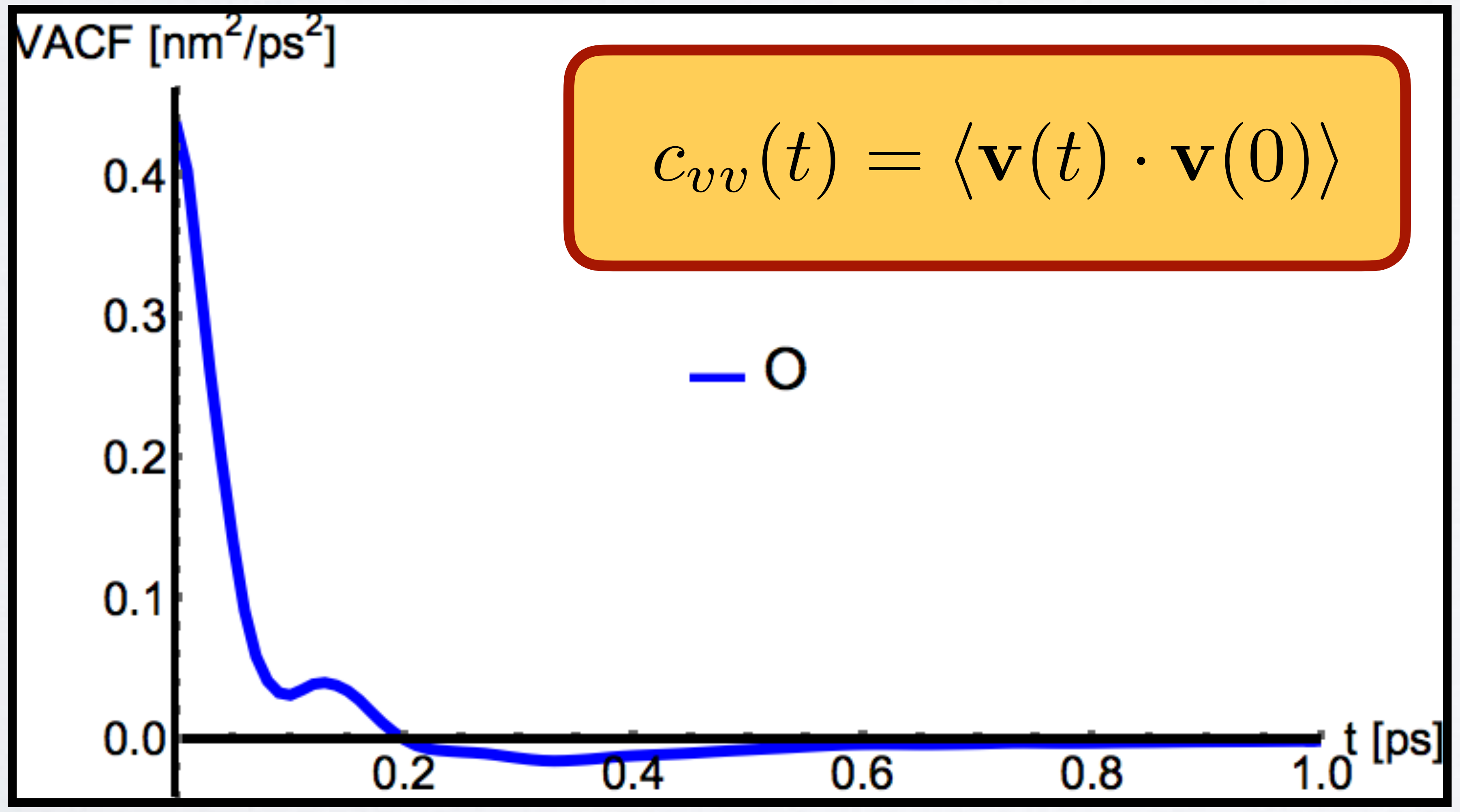

$$c_{vv}(t) = \langle \mathbf{v}(t) \cdot \mathbf{v}(0) \rangle$$

$$c_{vv}^{(\alpha)}(n) \approx \frac{1}{N_t - |n|} \sum_{k=0}^{N_t-|n|-1} \mathbf{v}^{(\alpha)}(k) \cdot \mathbf{v}^{(\alpha)}(k+n)$$

$$c_{vv}(n) = \tfrac{1}{N} \textstyle\sum_{\alpha=1}^{N} c_{vv}^{(\alpha)}(n)$$

Velocity autocorrelation function (hydrogen)

Trajectory

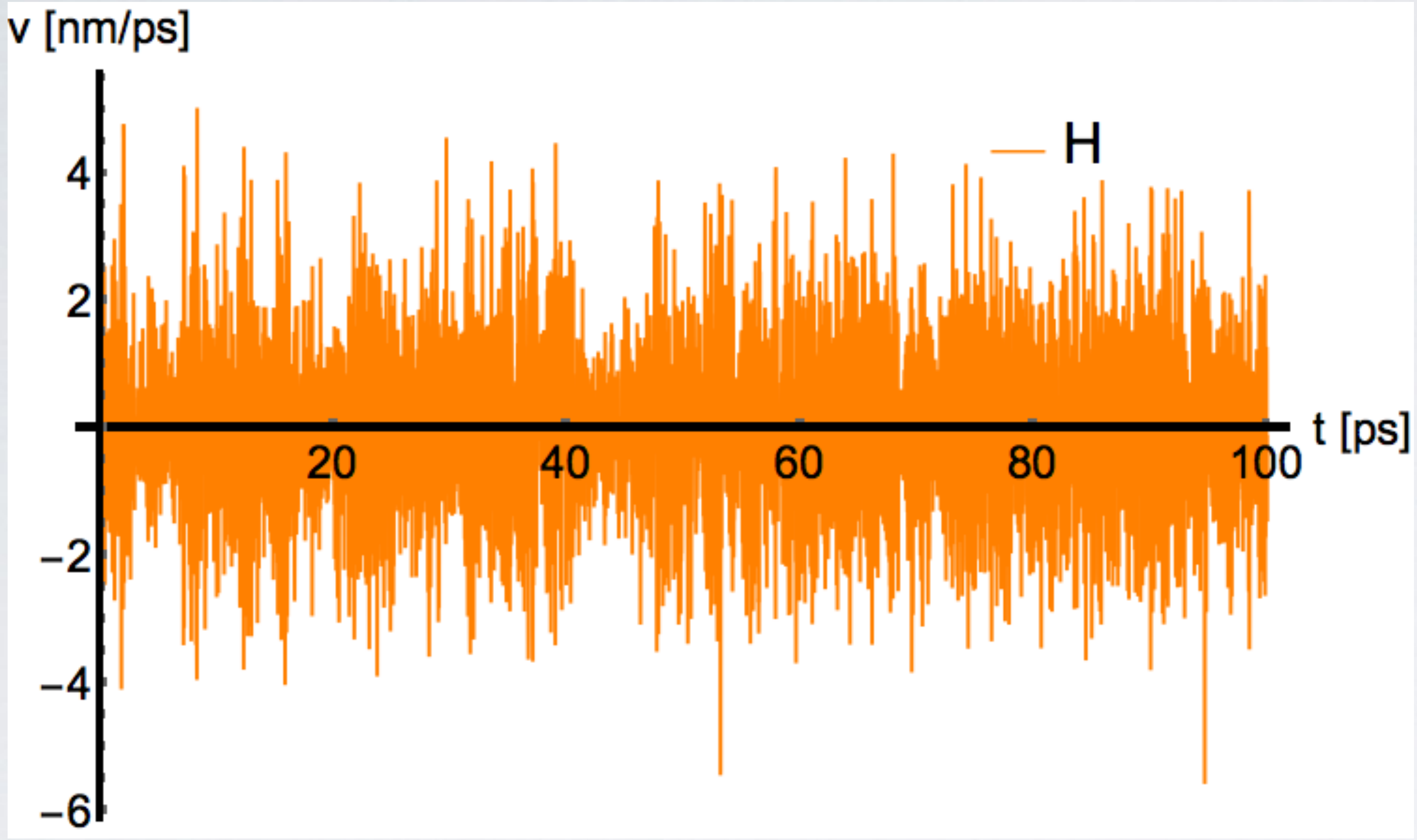

Maxwell distribution

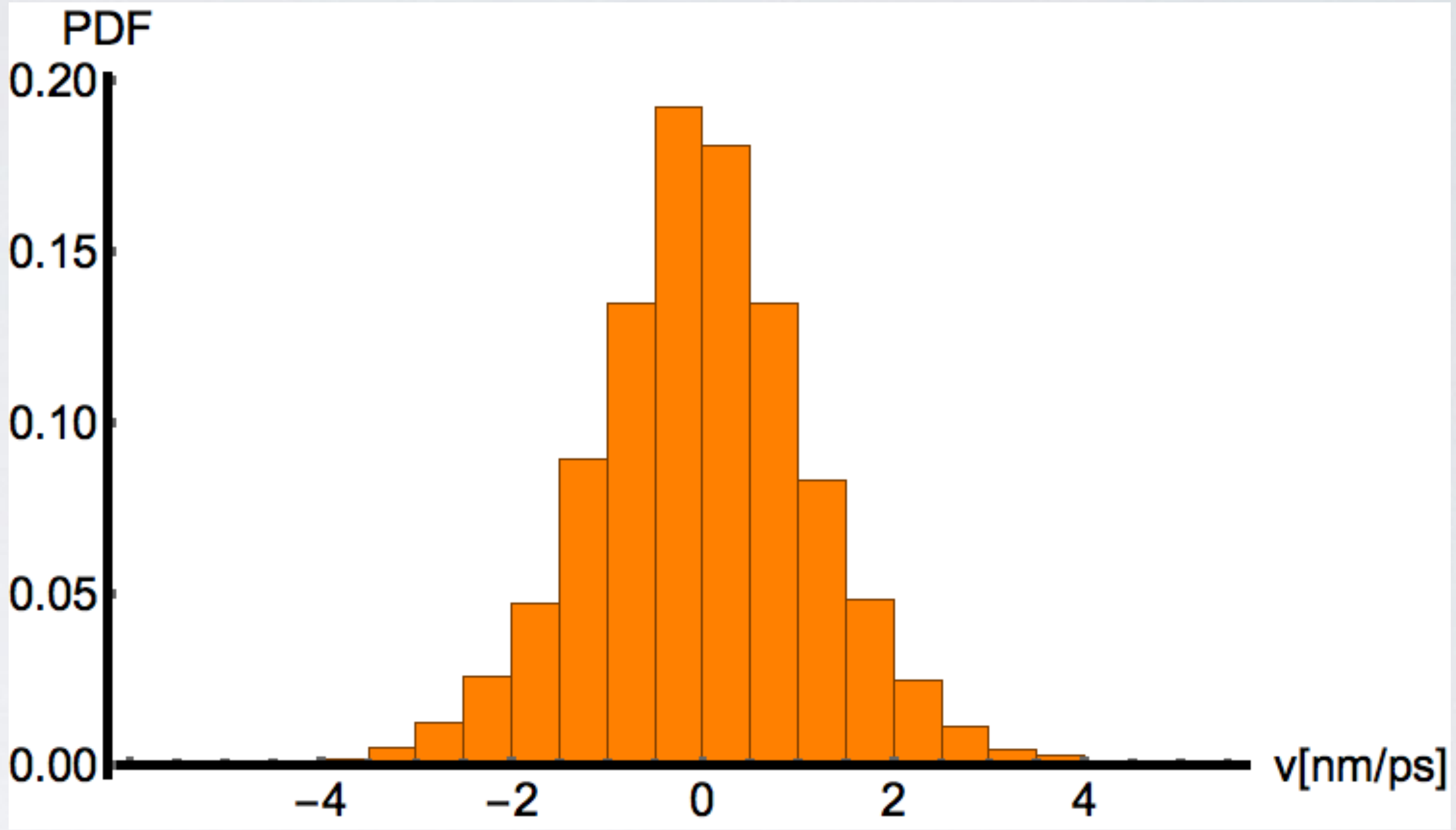

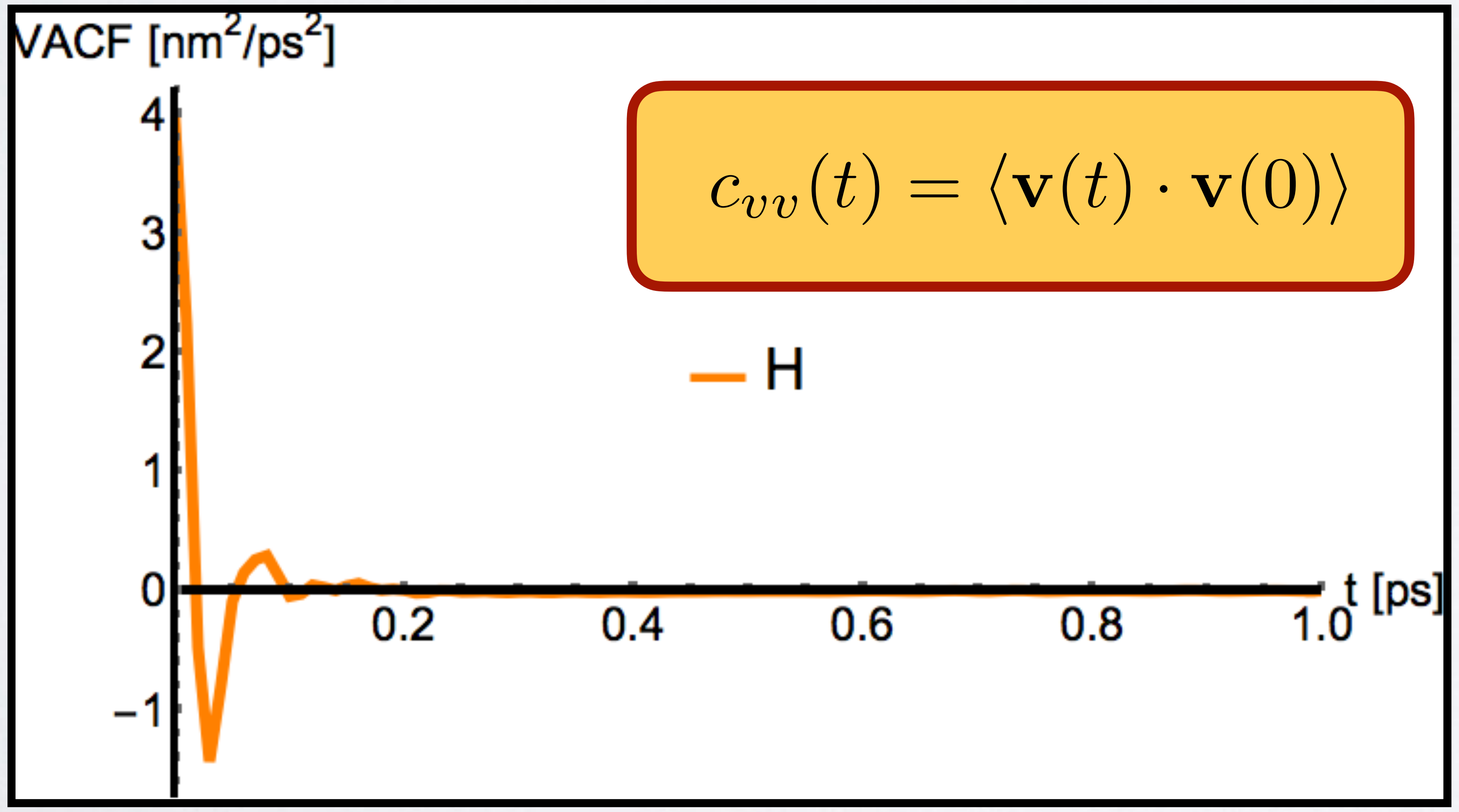

$$c_{vv}(t) = \langle \mathbf{v}(t) \cdot \mathbf{v}(0) \rangle$$

$$c_{vv}^{(\alpha)}(n) \approx \frac{1}{N_t - |n|} \sum_{k=0}^{N_t - |n| - 1} \mathbf{v}^{(\alpha)}(k) \cdot \mathbf{v}^{(\alpha)}(k+n)$$

$$c_{vv}(n) = \tfrac{1}{N} \textstyle\sum_{\alpha=1}^{N} c_{vv}^{(\alpha)}(n)$$

Relating diffusion to microscopic dynamics

$$x(t) - x(0) = \int_0^t dx(\tau) \overset{v(t)=\dot{x}(t)}{=} \int_0^t d\tau v(\tau)$$

➡

$$\boxed{\underbrace{\langle (x(t) - x(0))^2 \rangle}_{W(t)} = 2 \int_0^t d\tau \, (t - \tau) \, \underbrace{\langle v(\tau) v(0) \rangle}_{c_{vv}(\tau)}}$$

The Fourier-transformed VACF (Density of States=**DOS**)

$$g(\omega) \equiv \int_0^\infty dt \, \cos \omega t \, \langle v(t) v(0) \rangle$$

is accessible by **neutron scattering** and **MD « experiments »**

Density of states and diffusion coefficient

$$c_{vv}(t) = \langle v(0)v(t)\rangle$$

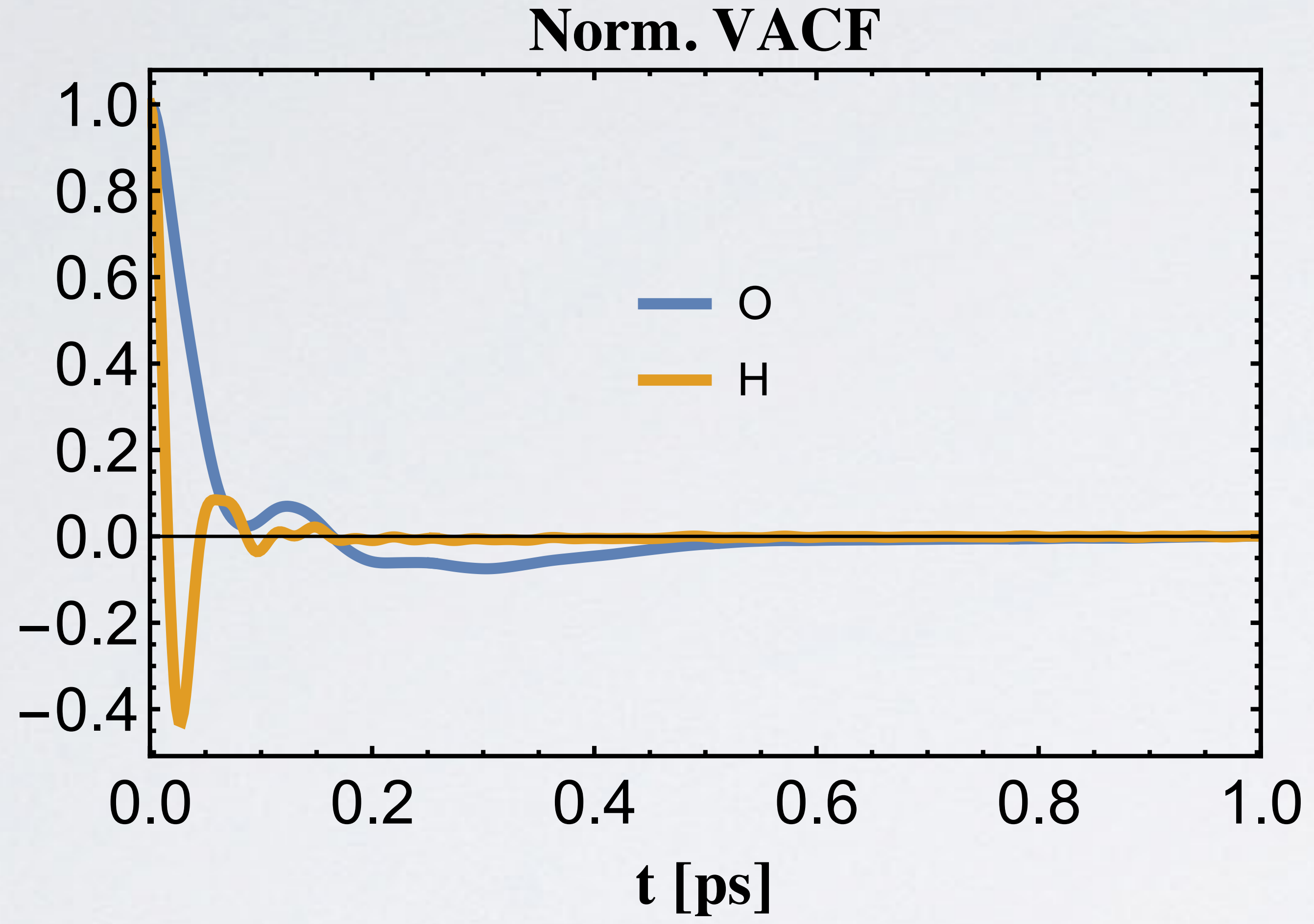

$$D = \int_0^\infty c_{vv}(t) = g(0)$$

$$D_O \approx 2.8 \times 10^{-5}\mathrm{cm}^2/\mathrm{s}$$

$$D_H \approx 3.3 \times 10^{-5}\mathrm{cm}^2/\mathrm{s}$$

$$D_{MSD} \approx 2.17 \times 10^{-5}\mathrm{cm}^2/s$$

$$g(\omega) \equiv \int_0^\infty dt\ \cos\omega t\, c_{vv}(t)$$

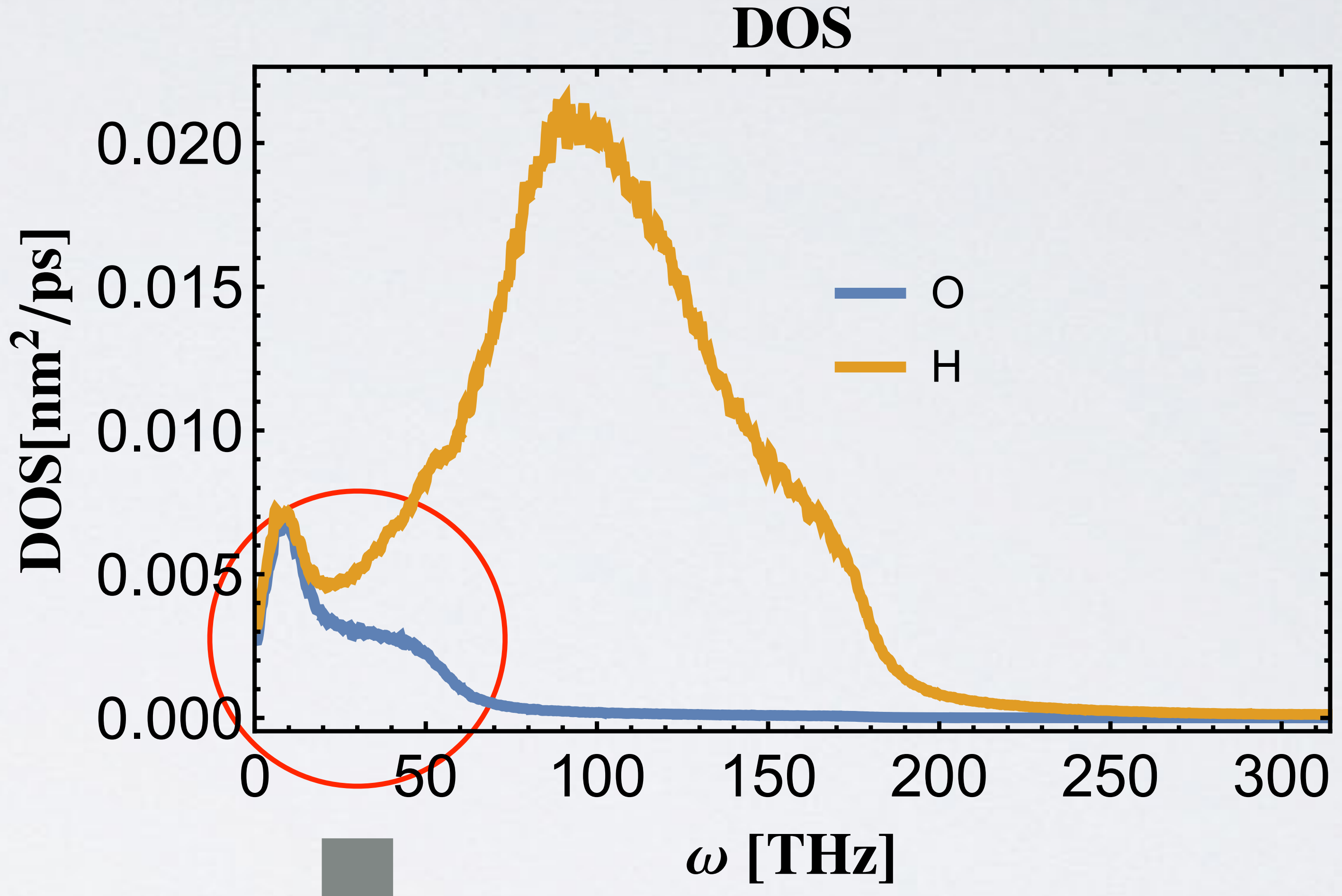

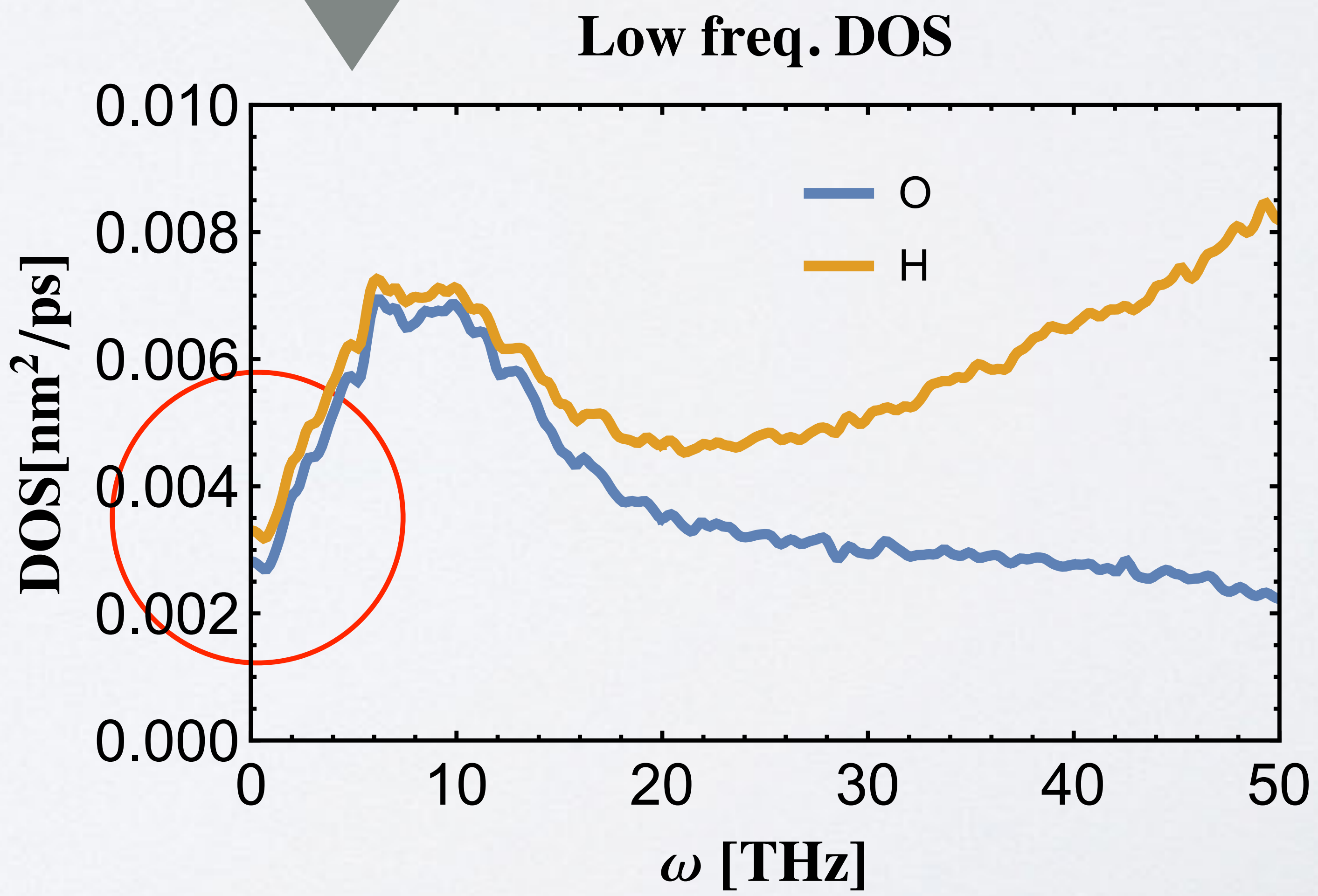

Anomalous diffusion of molecules in a lipid bilayer

- S. Stachura and G. R. Kneller, Mol. Simulat., vol. 40, no. 1– 3, pp. 245–250, 2014.
- S. Stachura and G. R. Kneller, J. Chem. Phys., vol. 143, p. 191103, 2015.

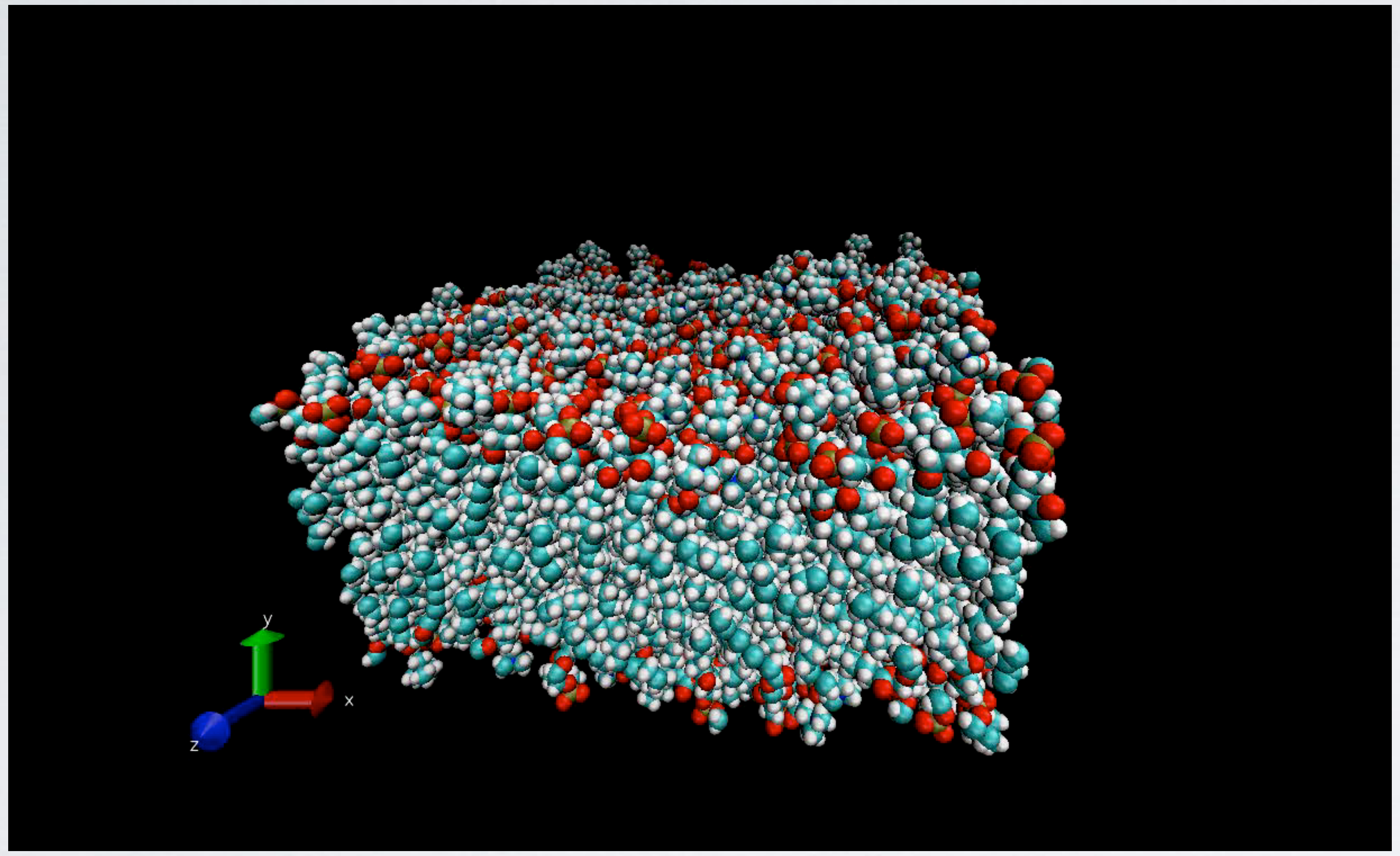

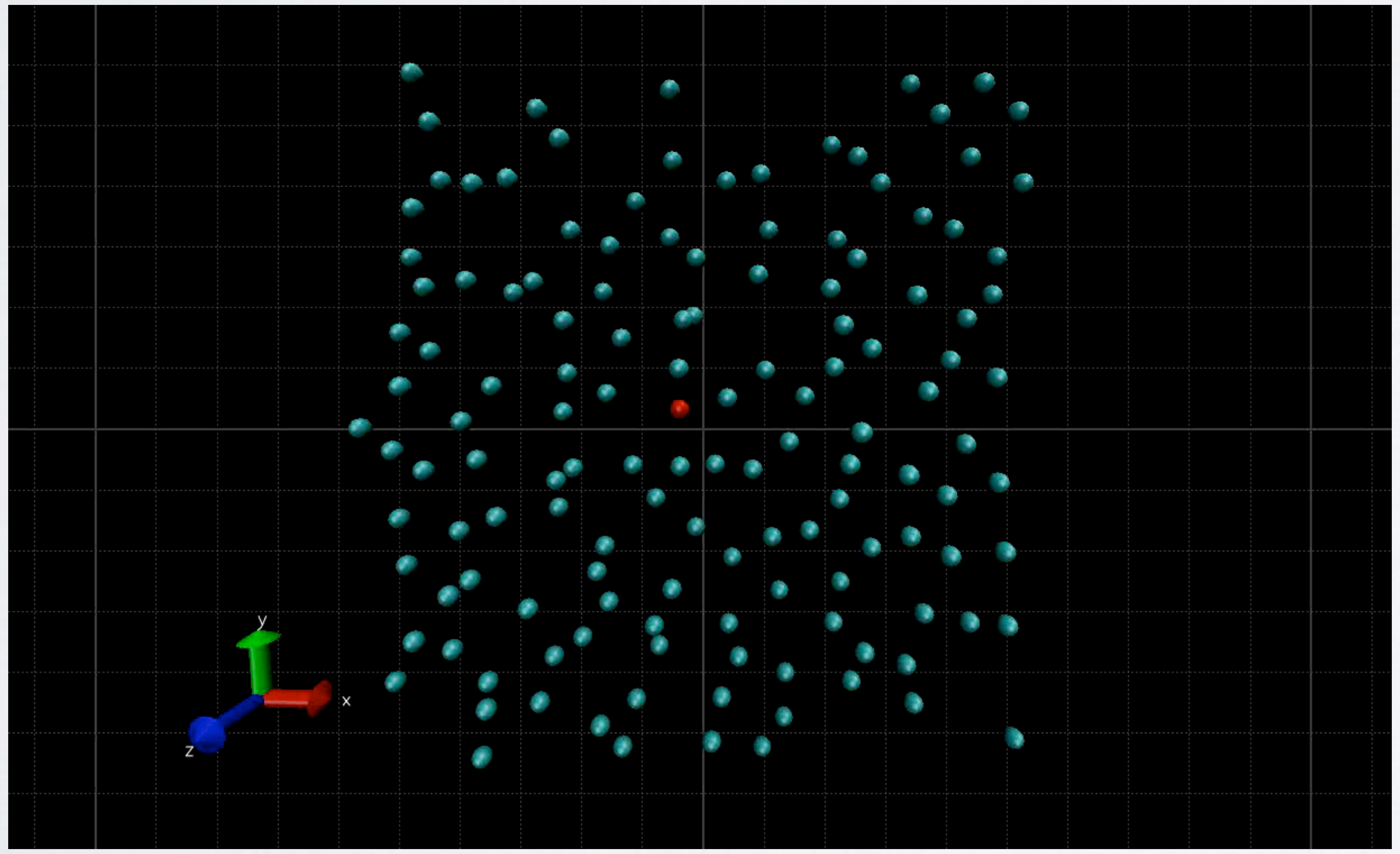

- 2x137 POPC molecules (10 nm × 10 nm in the XY-plane)
- 10471 water molecules (fully hydrated)
- OPLS force field
- T=310 K

MSD for lateral diffusion

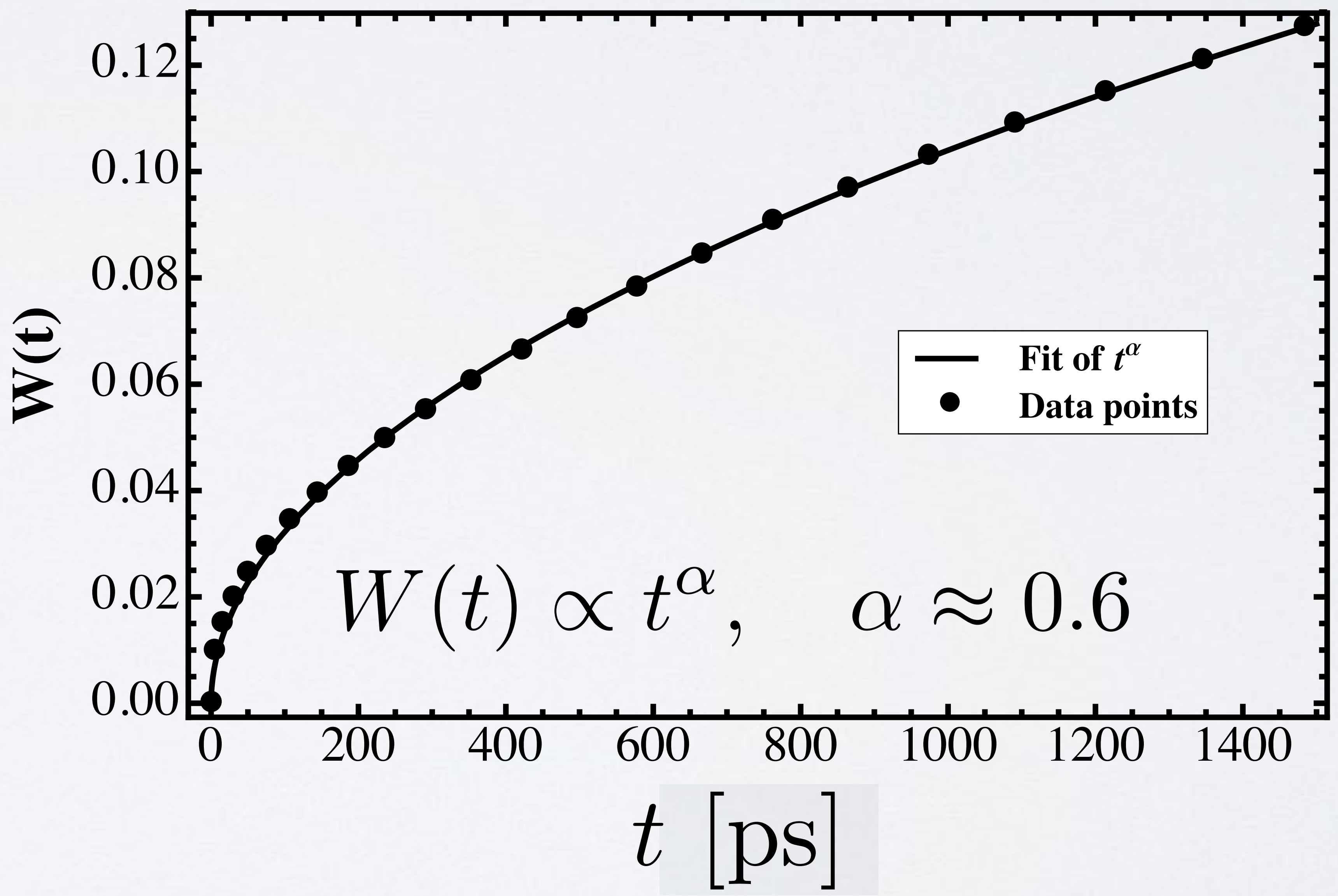

ps to ns time scale

See also

E. Flenner, J. Das, M. Rheinstädter, and I. Kosztin, Phys Rev E 79, 11907 (2009).
G.R. Kneller, K. Baczynski, and M. Pasenkiewicz-Gierula, J Chem Phys 135, 141105 (2011).
J.H. Jeon, H. Monne, M. Javanainen, and R. Metzler, Phys Rev Lett (2012).

Anomalous diffusion is known since long time

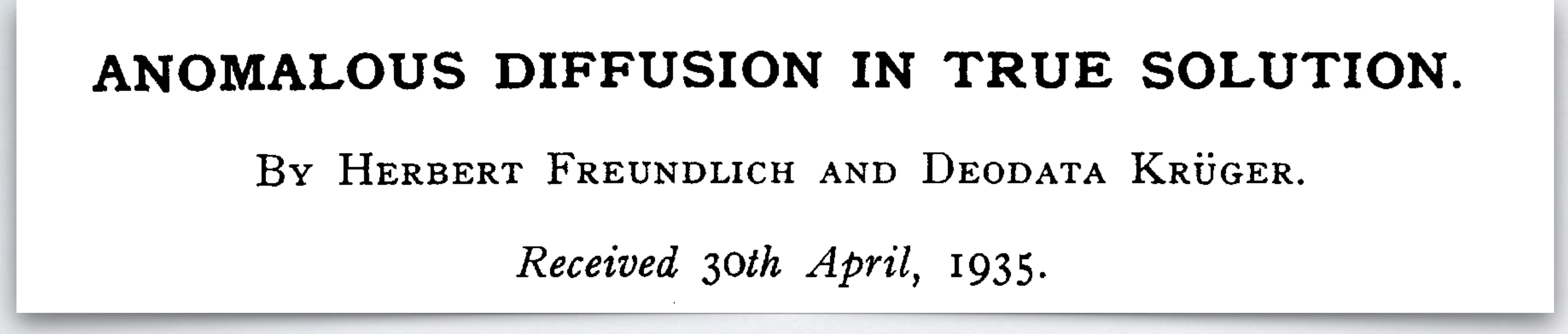

ANOMALOUS DIFFUSION IN TRUE SOLUTION.

By HERBERT FREUNDLICH AND DEODATA KRÜGER.

Received 30th April, 1935.

H. Freundlich and D. Krüger, Trans. Faraday Soc. 31, 906 (1935).

$$\sigma^2(t) := \frac{\int d^n r \, |\mathbf{r}|^2 f(\mathbf{r}, t)}{\int d^n r \, f(\mathbf{r}, t)}$$

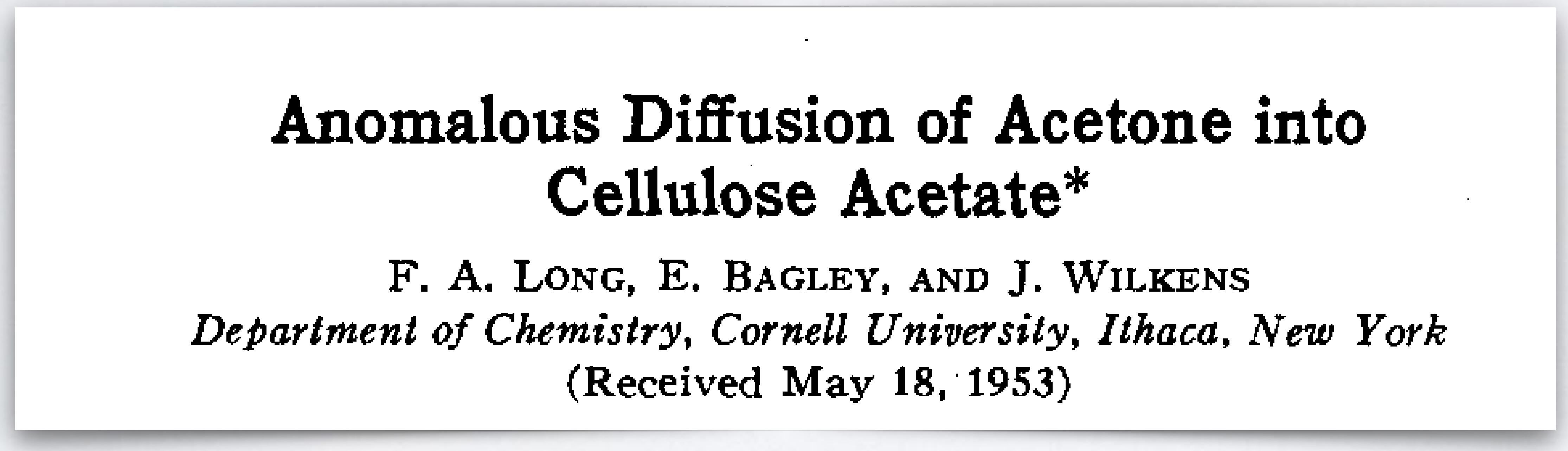

Anomalous Diffusion of Acetone into Cellulose Acetate*

F. A. LONG, E. BAGLEY, AND J. WILKENS

Department of Chemistry, Cornell University, Ithaca, New York

(Received May 18, 1953)

F.A. Long, E. Bagley, and J. Wilkens,
The Journal of Chemical Physics 21, 1412 (1953).

$$\boxed{\sigma^2(t) \propto t^\alpha}$$

$$0 < \alpha < 1$$

(subdiffusion)

Subdiffusion of lipids observed by FCS

P. Schwille, J. Korlach, and W. Webb, Cytometry 36, 176 (1999).

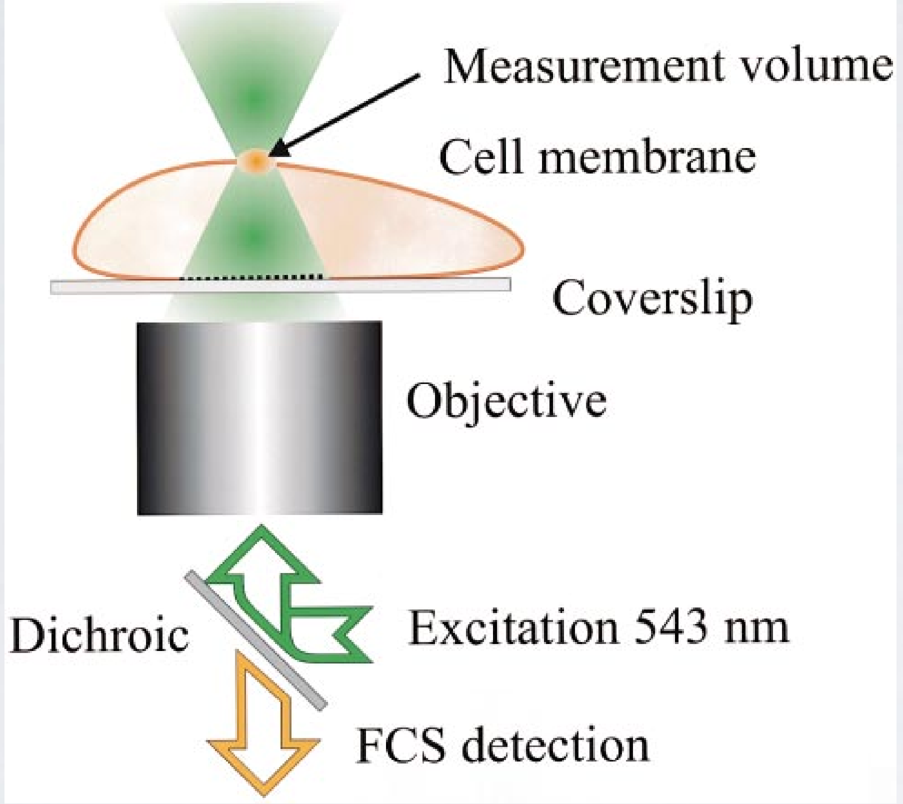

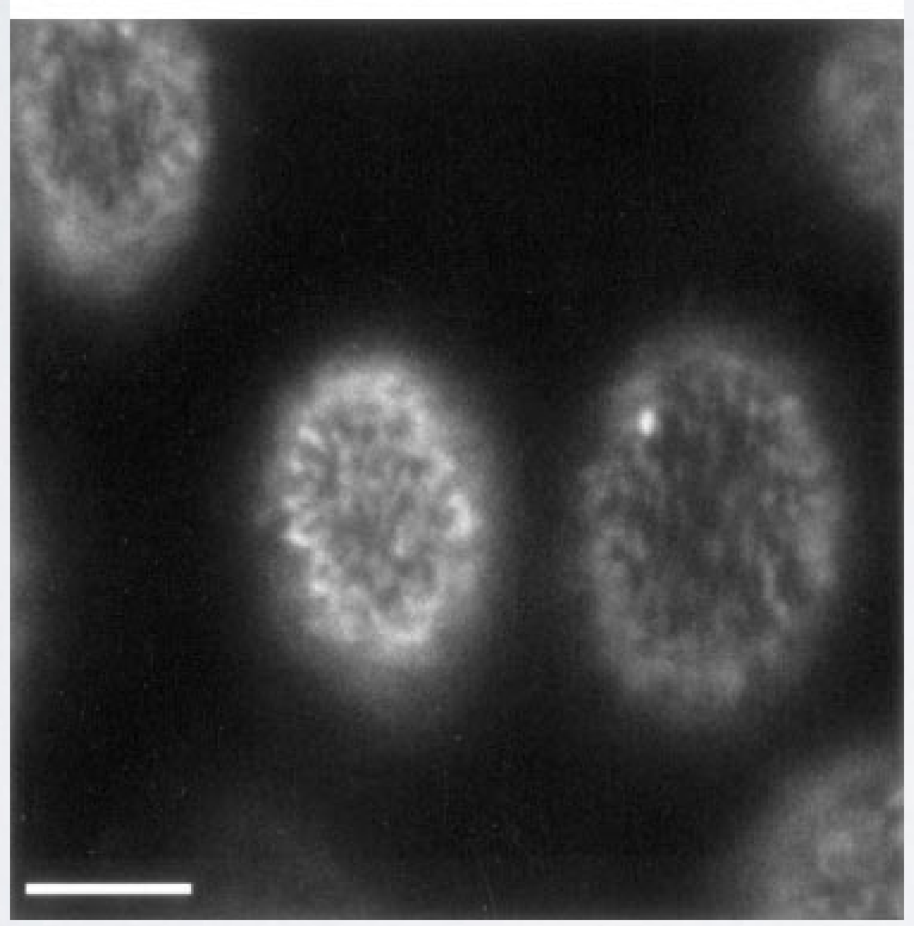

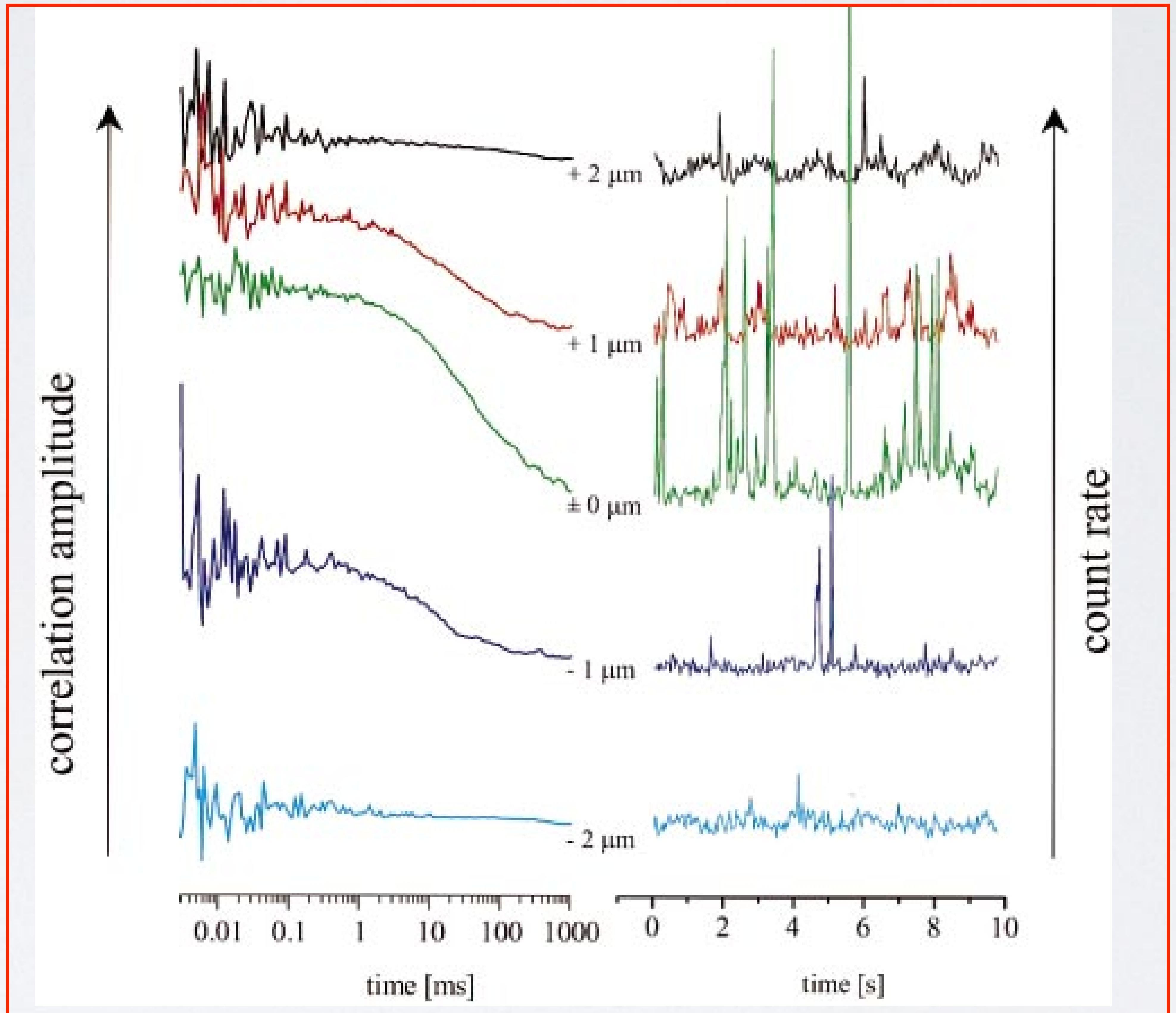

$$\sigma^2(t) \propto t^\alpha$$

ms to s time scale

Asymptotic analysis of anomalous diffusion

G. R. Kneller, J Chem Phys, vol. 134, p. 224106, 2011.

Generalized Langevin equation

R. Zwanzig, *Nonequilibrium statistical mechanics*. Oxford University Press, 2001.

$$\dot{\mathbf{v}}(t) = -\int_0^t dt'\,\kappa(t-t')\mathbf{v}(t') + \mathbf{f}^{(+)}(t)$$

Memory kernel

$$\langle \mathbf{v}(t)\cdot\mathbf{f}^{(+)}(t')\rangle = 0.$$

$$\partial_t c_{vv}(t) = -\int_0^t dt'\, c_{vv}(t-t')\kappa(t').$$

$$\boxed{\kappa(t)\equiv\Omega^2} \Rightarrow \boxed{c_{vv}(t) = \langle v^2\rangle\cos\Omega t}$$

oscillatory «rattling»
motions in the «cage» of
nearest neighbors

Journal für die Reine und Angewandte Mathematik (Crelle's Journal) **1931,** 27–39 (1931).

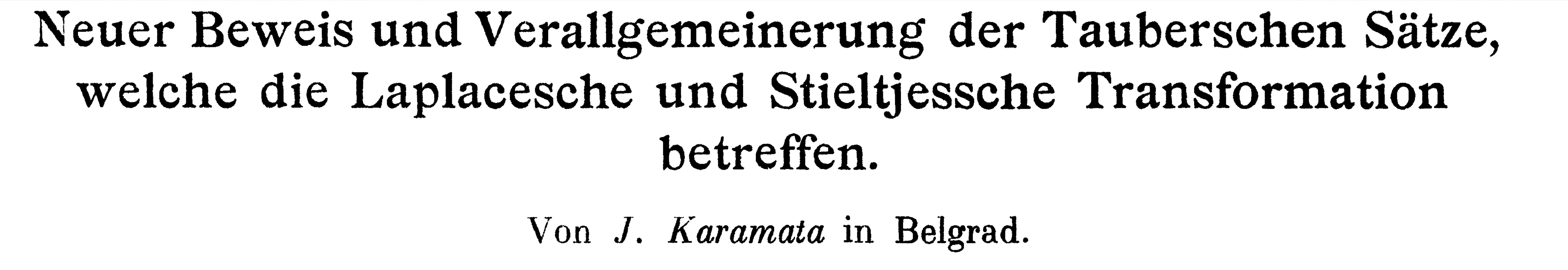

Neuer Beweis und Verallgemeinerung der Tauberschen Sätze, welche die Laplacesche und Stieltjessche Transformation betreffen.

Von *J. Karamata* in Belgrad.

$$h(t) \overset{t\to\infty}{\sim} L(t)t^{\rho} \Leftrightarrow \hat{h}(s) \overset{s\to 0}{\sim} L(1/s)\frac{\Gamma(\rho+1)}{s^{\rho+1}} \quad (\rho > -1).$$

$\hat{h}(s) = \int_0^{\infty} dt\ \exp(-st)h(t) \quad (\Re\{s\} > 0)$ Laplace transform

$\lim_{t\to\infty} L(\lambda t)/L(t) = 1$, with $\lambda > 0$. Slowly growing function

Combining

1. Mathematics (Tauberian theorem)

$$W(t) \overset{t\to\infty}{\sim} 2D_\alpha L(t)t^\alpha \longleftrightarrow \hat{W}(s) \overset{s\to 0}{\sim} 2D_\alpha L(1/s)\frac{\Gamma(\alpha+1)}{s^{\alpha+1}}.$$

$$\lim_{t\to\infty} L(t) = 1 \qquad \lim_{t\to\infty} t\frac{dL(t)}{dt} = 0$$

$$\hat{W}(s) = \int_0^\infty dt\, \exp(-st)W(t)$$

2. Physics

$$W(t) = 2\int_0^t d\tau\,(t-\tau)c_{vv}(\tau)$$

$$\frac{dc_{vv}(t)}{dt} = -\int_0^t d\tau\,\kappa(t-\tau)c_{vv}(\tau)$$

$$\Longrightarrow$$

$$\hat{W}(s) = \frac{2\boxed{\hat{c}_{vv}(s)}}{s^2} = \frac{2\langle v^2\rangle}{s^2(s+\boxed{\hat{\kappa}(s)})}$$

Necessary conditions for long-time tails

$$c_{vv}(t) \overset{t\to\infty}{\sim} D_\alpha \alpha(\alpha-1)L(t)t^{\alpha-2},$$

also sufficient for $1 < \alpha < 2$

$$\kappa(t) \overset{t\to\infty}{\sim} \frac{\langle \mathbf{v}^2\rangle}{D_\alpha}\frac{\sin(\pi\alpha)}{\pi\alpha}\frac{1}{L(t)}t^{-\alpha}.$$

also sufficient for $0 < \alpha < 1$

$$\alpha(\alpha-1)$$

$$\frac{\sin(\pi\alpha)}{\pi\alpha}$$

Signs of the long time tails

Generalized Kubo relation

$$D_\alpha = \frac{1}{\Gamma(1+\alpha)} \int_0^\infty dt \;\; {}_0\partial_t^{\alpha-1} c_{vv}(t).$$

Fractional derivative of order α-1

$${}_0\partial_t^{\alpha-1} f(t) = \frac{d}{dt} \int_0^t du \, \frac{(t-u)^{1-\alpha}}{\Gamma(2-\alpha)} f(u)$$

Kneller, G. R. , J Chem Phys 134, 224106 (2011).

Simple model for free diffusion

model memory function

$$\kappa_f(t) = \Omega^2 M(\alpha, 1, -t/\tau)$$

Kummer function

$$\hat{\kappa}_f(s) = \Omega^2 \left\{ \frac{\tau^\alpha}{s^{1-\alpha}} \frac{1}{(s\tau+1)^\alpha} \right\}$$

asymptotic form

$$\kappa_f(t) \overset{t\to\infty}{\sim} \begin{cases} \Omega^2 \frac{(t/\tau)^{-\alpha}}{\Gamma(1-\alpha)}, & \alpha \neq 1, \\ \Omega^2 \exp(-t/\tau), & \alpha = 1. \end{cases}$$

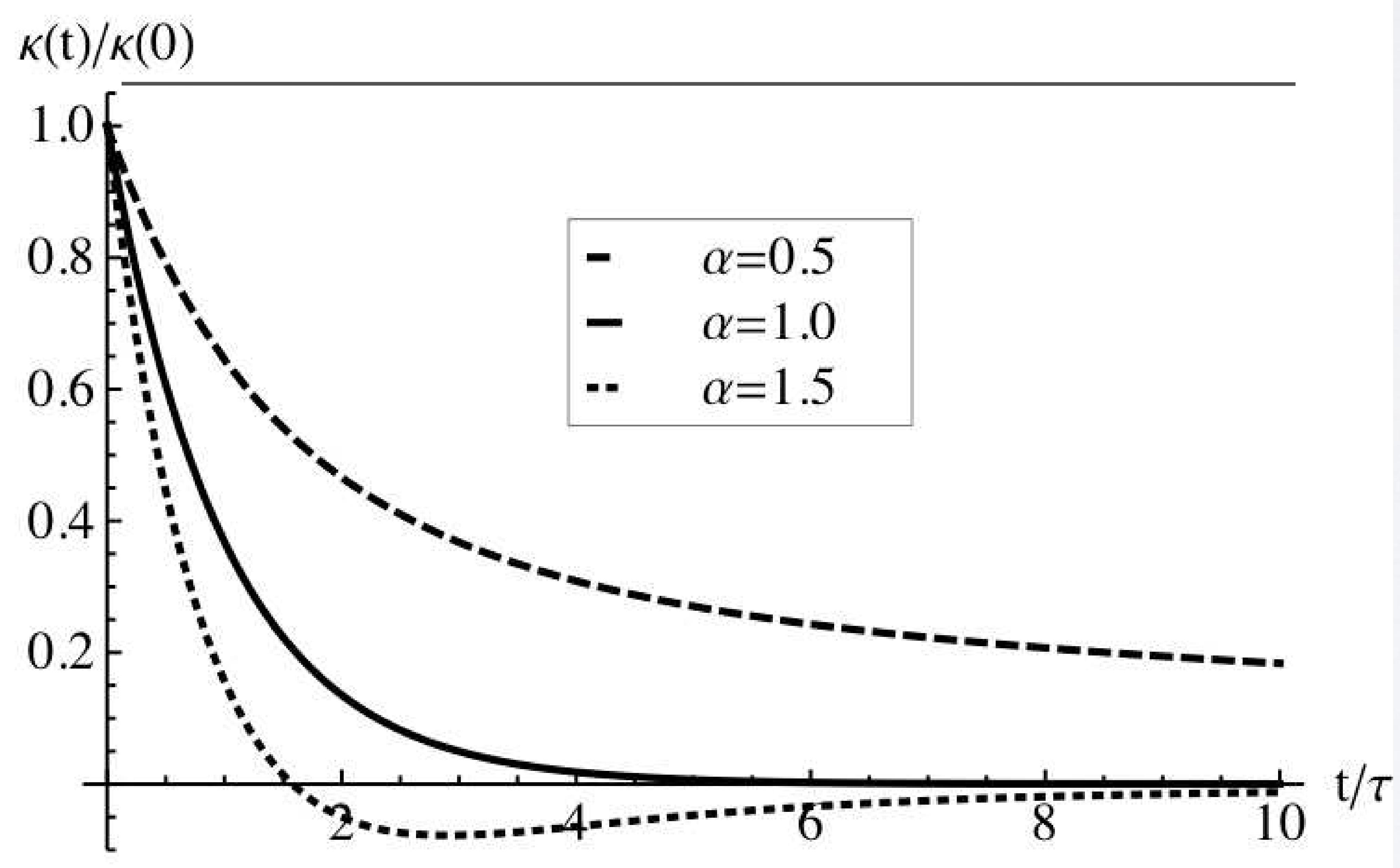

G. Kneller, *J. Chem. Phys.*, vol. 134, p. 224106, 2011.

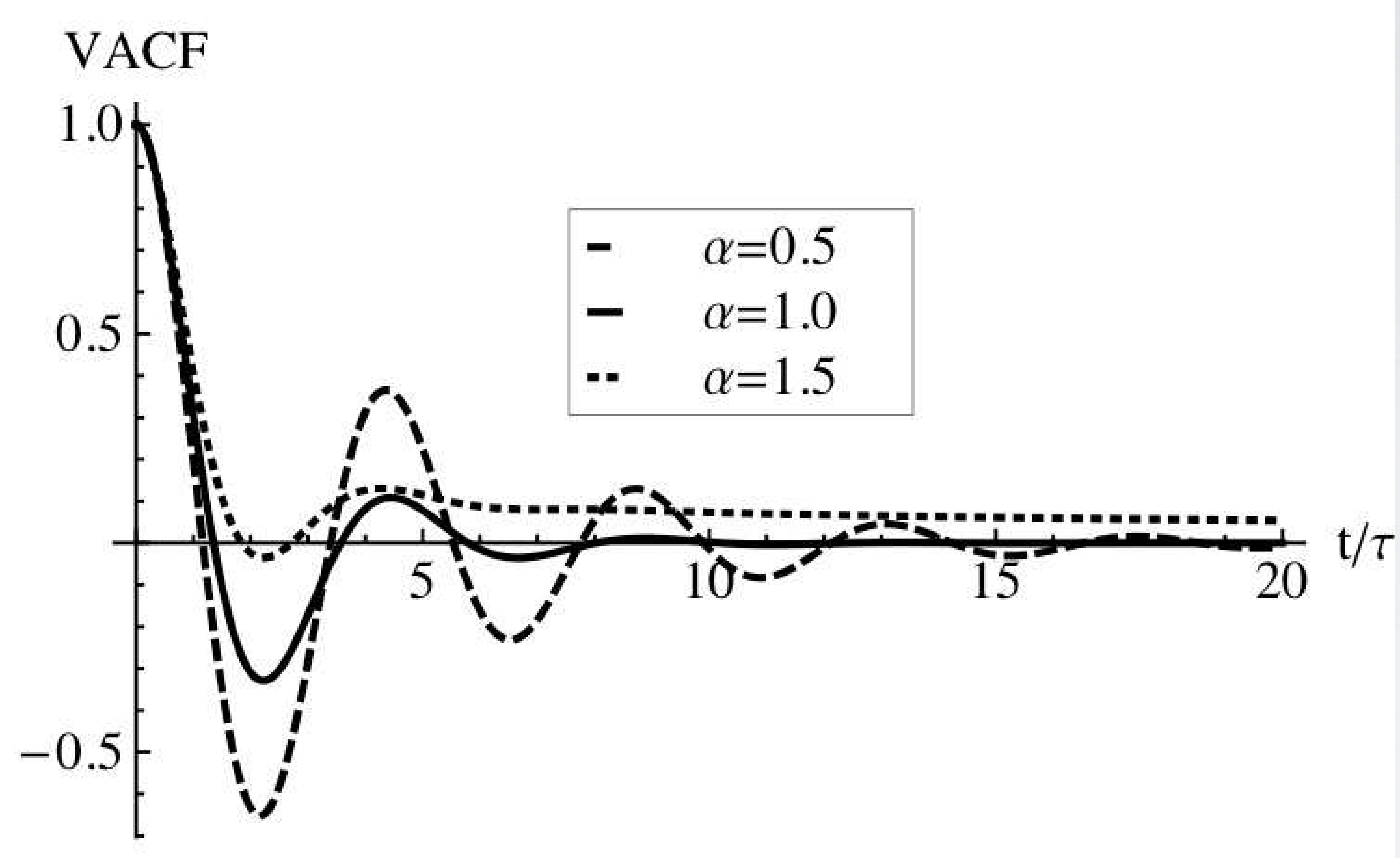
VACF
1.0
0.5
−0.5
5
10
15
20
t/τ
α=0.5
α=1.0
α=1.5

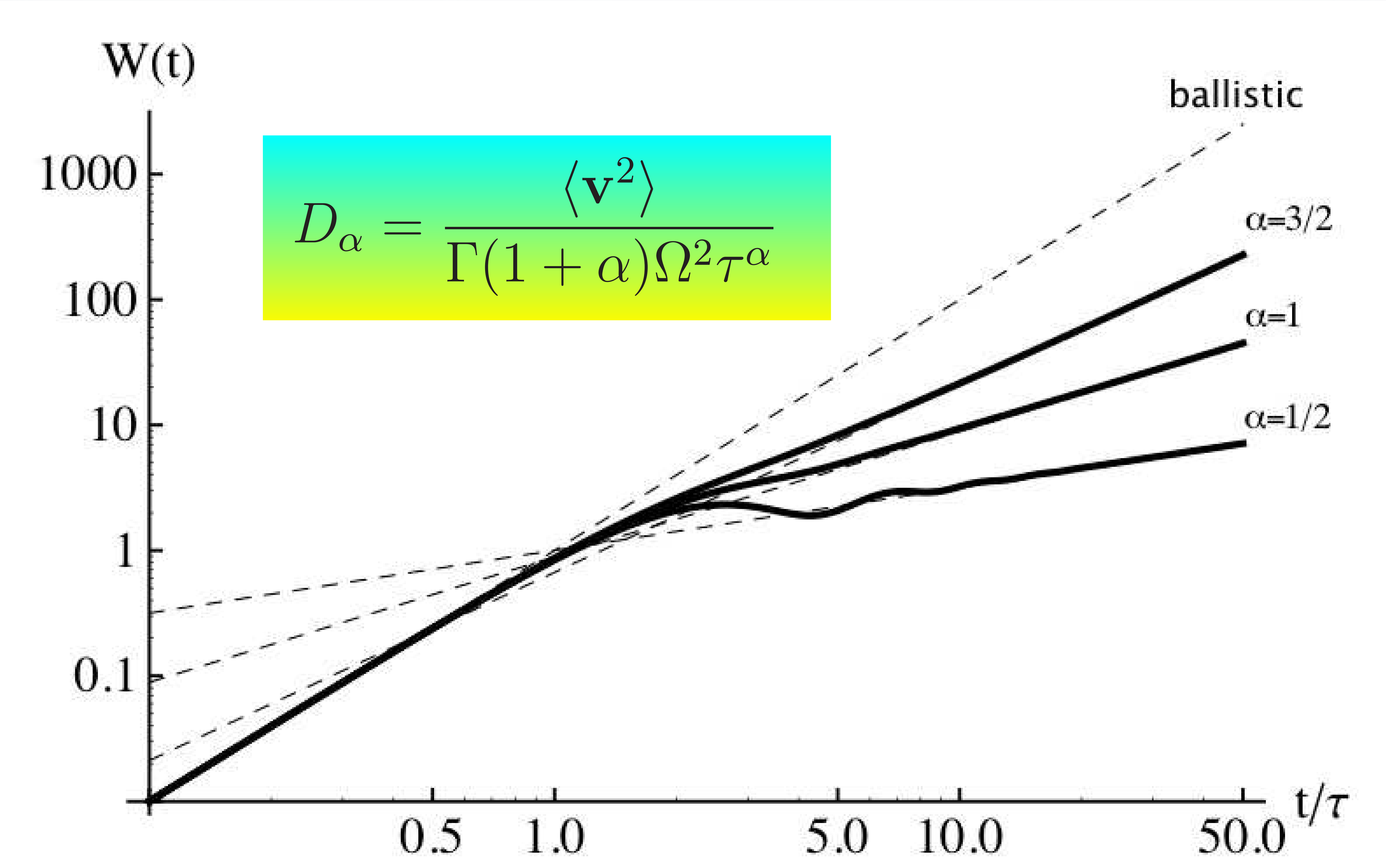

$$D_\alpha = \frac{\langle \mathbf{v}^2 \rangle}{\Gamma(1+\alpha)\Omega^2\tau^\alpha}$$

Asymptotic model for Confined anomalous diffusion (α=0)

$$W(t) \overset{t\to\infty}{\sim} 2D_0 L(t), \quad \text{with} \quad D_0 = \langle (\mathbf{x} - \langle \mathbf{x} \rangle)^2 \rangle$$

$$c_{vv}(t) \overset{t\to\infty}{\sim} D_\alpha \alpha(\alpha - 1) L(t) t^{\alpha-2},$$

$$\kappa(t) \overset{t\to\infty}{\sim} \frac{\langle \mathbf{v}^2 \rangle}{D_\alpha} \frac{\sin(\pi\alpha)}{\pi\alpha} \frac{1}{L(t)} t^{-\alpha}.$$

α=0

$$c_{vv}(t) \overset{t\to\infty}{\sim} 0,$$

$$\kappa(t) \overset{t\to\infty}{\sim} \frac{\langle \mathbf{v}^2 \rangle}{D_0} \frac{1}{L(t)}$$

No long time tail

The memory function tends to a plateau value

Low-frequency DOS

☞

$$\boxed{g(\omega) = \int_0^\infty dt\, \cos(\omega t) c_{vv}(t) \overset{\omega\to 0}{\sim} \omega^{1-\alpha} \sin\left(\frac{\pi\alpha}{2}\right) \Gamma(1+\alpha) D_\alpha}$$

$$\omega\tau_v \ll 1, \quad \text{with} \quad \tau_v = \left(\frac{D_\alpha}{\langle|\mathbf{v}^2|\rangle}\right)^{\frac{1}{2-\alpha}}$$

in the ps regime

S. Stachura and G. R. Kneller, J. Chem. Phys., vol. 143, p. 191103, 2015

DOS from neutron scattering experiments

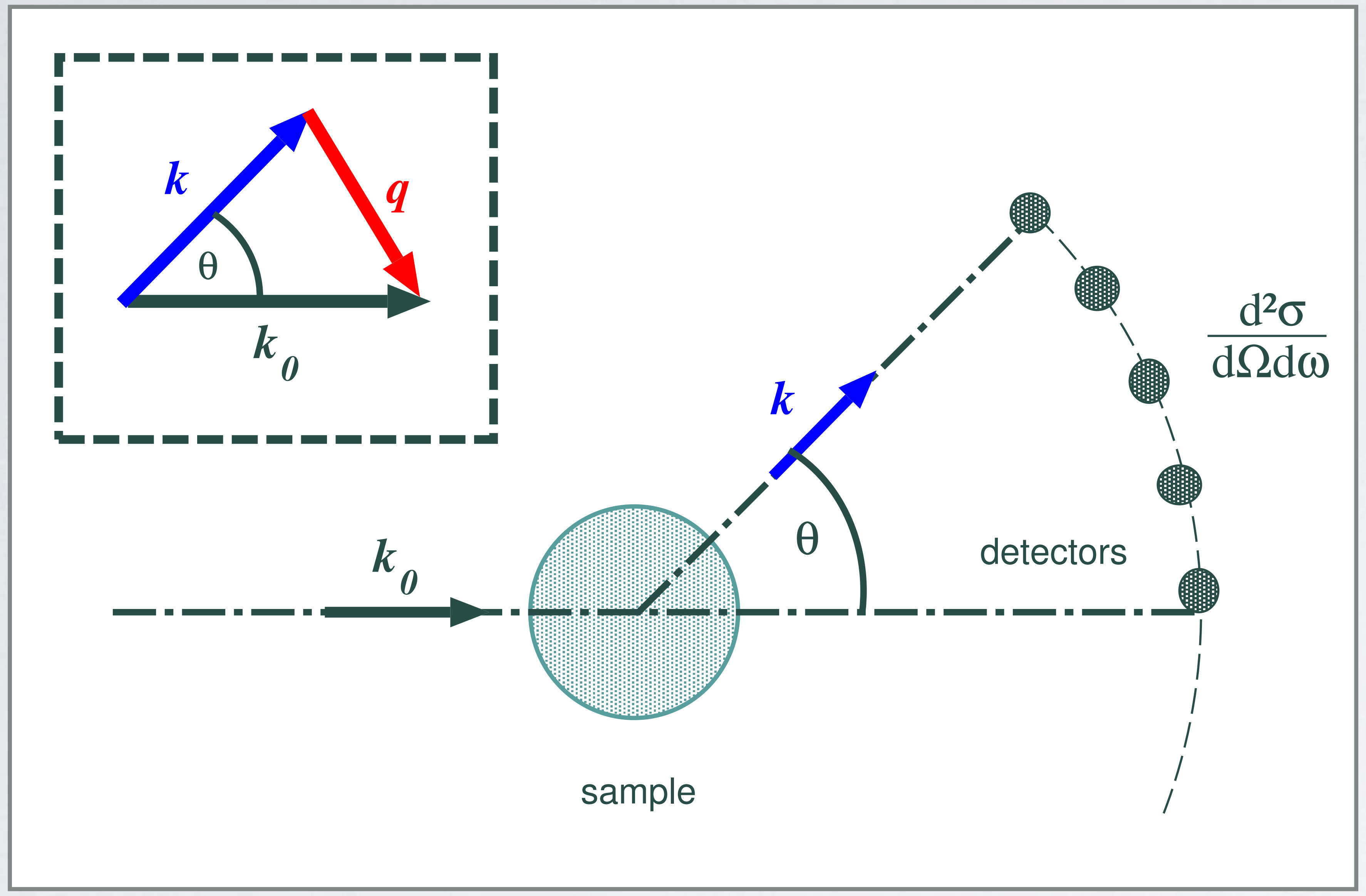

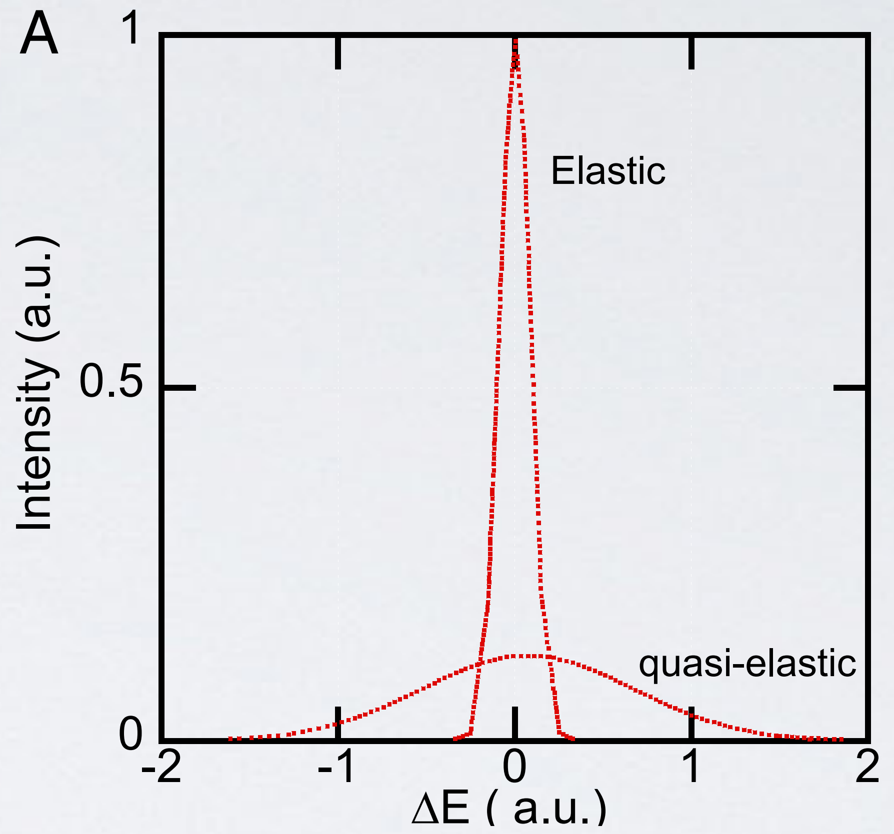

momentum transfer:

$$\mathbf{q} = \mathbf{k}_0 - \mathbf{k} = (\mathbf{p}_0 - \mathbf{p})/\hbar$$

energy transfer:

$$\omega = (E_0 - E)/\hbar$$

$$\frac{d^2\sigma}{d\Omega d\omega} = \frac{k}{k_0} S(\mathbf{q}, \omega)$$

$$g(\omega) = \lim_{q \to 0} \frac{\omega^2}{q^2} S(q, \omega)$$

$$S(\mathbf{q}, \omega) \approx \frac{1}{2\pi} \int_{-\infty}^{+\infty} dt\, e^{-i\omega t} \left\langle e^{-i\mathbf{q}\cdot(\mathbf{r}(t) - \mathbf{r}(0))} \right\rangle$$

GHz-THz freq. scale
ps-ns time scale

VACF long time tails from neutron scattering experiments

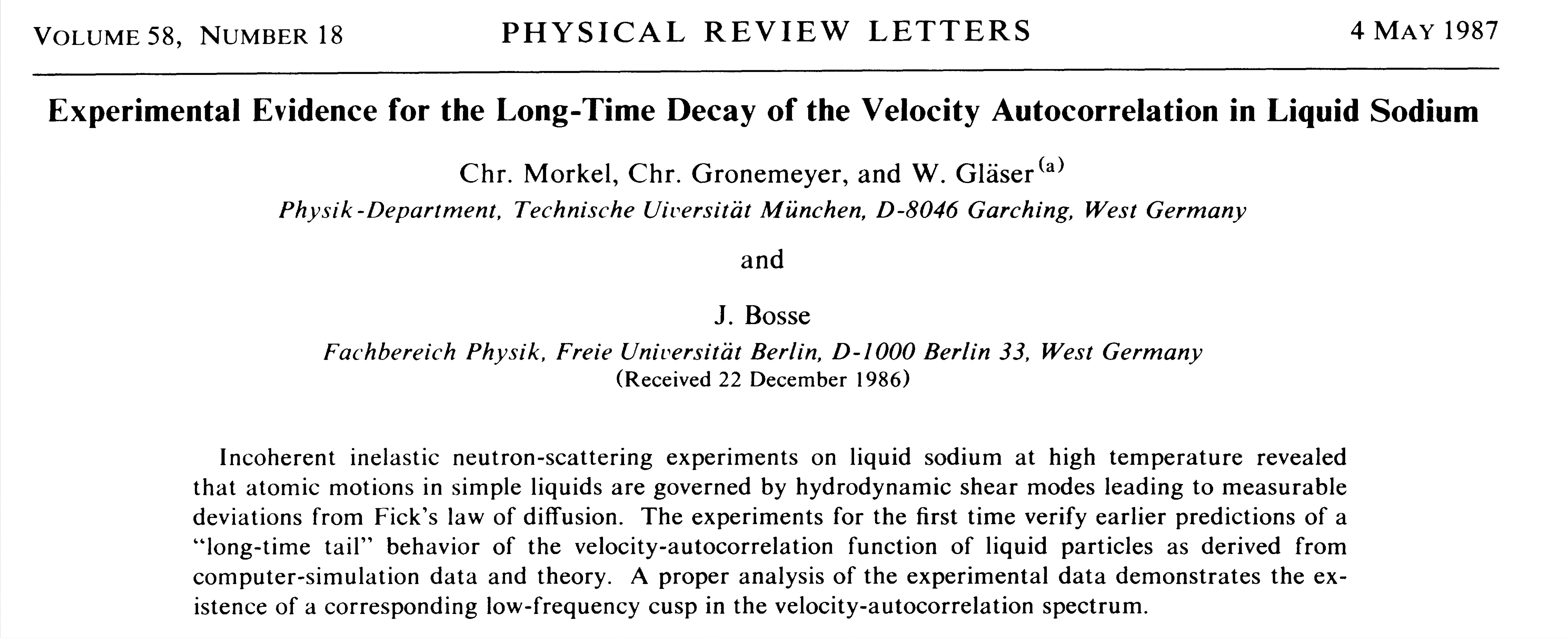

VOLUME 58, NUMBER 18 PHYSICAL REVIEW LETTERS 4 MAY 1987

Experimental Evidence for the Long-Time Decay of the Velocity Autocorrelation in Liquid Sodium

Chr. Morkel, Chr. Gronemeyer, and W. Gläser[(a)]
Physik-Department, Technische Universität München, D-8046 Garching, West Germany

and

J. Bosse
Fachbereich Physik, Freie Universität Berlin, D-1000 Berlin 33, West Germany

(Received 22 December 1986)

Incoherent inelastic neutron-scattering experiments on liquid sodium at high temperature revealed that atomic motions in simple liquids are governed by hydrodynamic shear modes leading to measurable deviations from Fick's law of diffusion. The experiments for the first time verify earlier predictions of a "long-time tail" behavior of the velocity-autocorrelation function of liquid particles as derived from computer-simulation data and theory. A proper analysis of the experimental data demonstrates the existence of a corresponding low-frequency cusp in the velocity-autocorrelation spectrum.

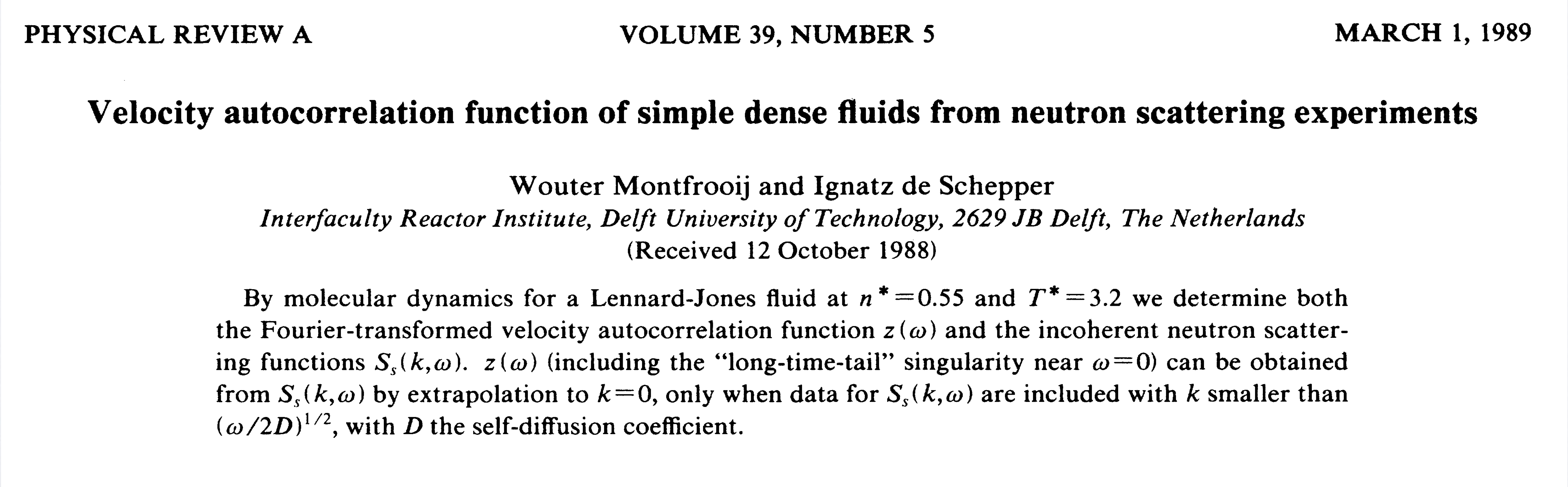

PHYSICAL REVIEW A VOLUME 39, NUMBER 5 MARCH 1, 1989

Velocity autocorrelation function of simple dense fluids from neutron scattering experiments

Wouter Montfrooij and Ignatz de Schepper
Interfaculty Reactor Institute, Delft University of Technology, 2629 JB Delft, The Netherlands

(Received 12 October 1988)

By molecular dynamics for a Lennard-Jones fluid at $n^*=0.55$ and $T^*=3.2$ we determine both the Fourier-transformed velocity autocorrelation function $z(\omega)$ and the incoherent neutron scattering functions $S_s(k,\omega)$. $z(\omega)$ (including the "long-time-tail" singularity near $\omega=0$) can be obtained from $S_s(k,\omega)$ by extrapolation to $k=0$, only when data for $S_s(k,\omega)$ are included with k smaller than $(\omega/2D)^{1/2}$, with D the self-diffusion coefficient.

MD simulations of lipid bilayers with all-atom and coarse-grained force fields

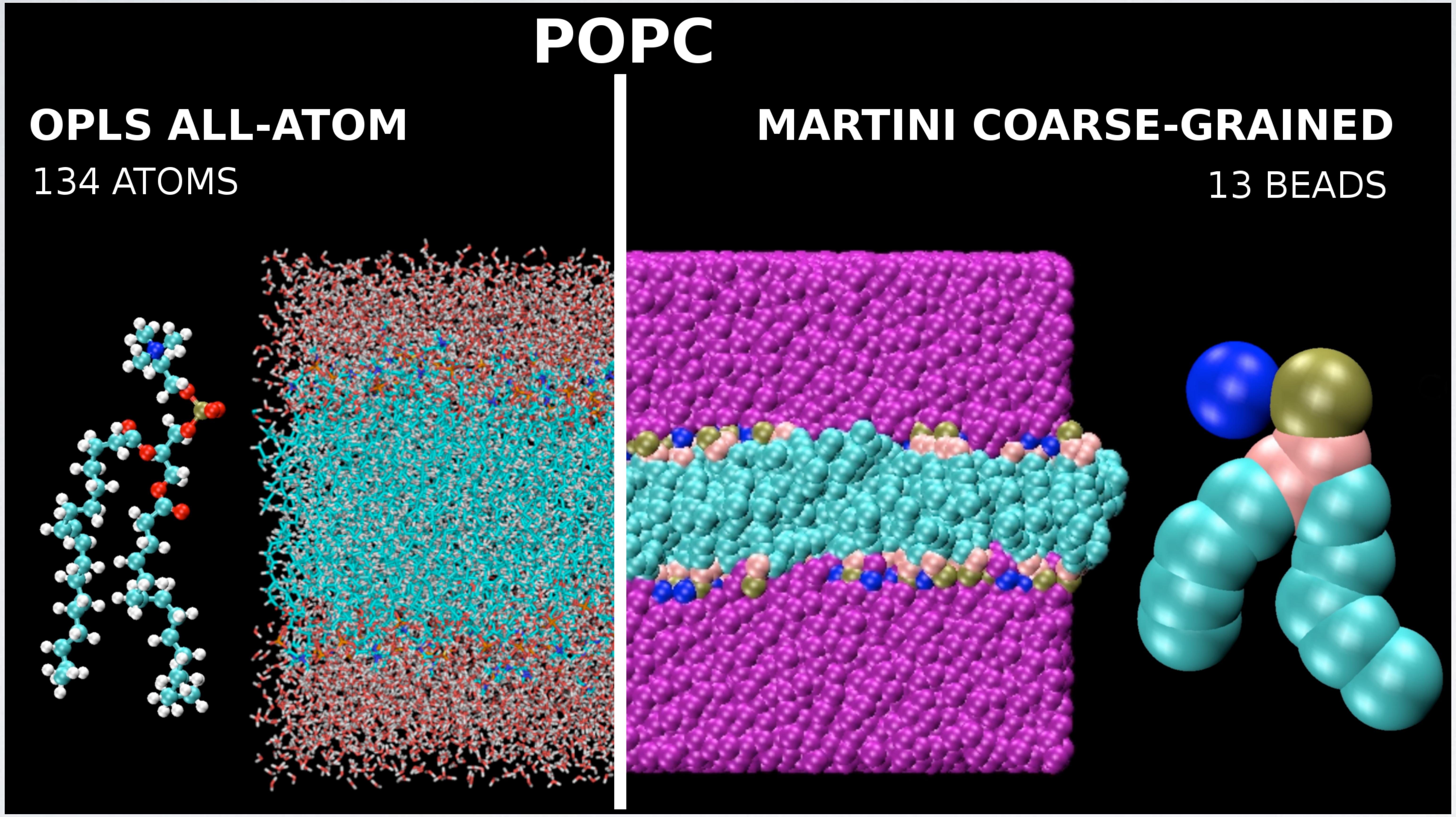

[1] S. Stachura and G. R. Kneller, Mol Simulat, vol. 40, no. 1– 3, pp. 245–250, 2014.

[2] S. Stachura and G. R. Kneller, *J. Chem. Phys.* Vol. 143, pp 191103, 2015.

T = 310 K, p = 1 atm, 150 ns,

274 POPC lipid molecules
+ 10471 water molecules

T = 320 K, p = 1 atm, 600 ns,

2033 POPC lipid molecules
+ 231808 water molecules

Precise calculation of the low-frequency DOS

S. Stachura and G.R. Kneller, J .Chem. Phys., vol. 143, p. 191103, 2015.

$$\boxed{g(\omega) = \int_0^\infty dt\ \cos(\omega t) c_{vv}(t) \overset{\omega \ll 1/\tau_v}{\sim} D_\alpha\, \omega^{1-\alpha} \sin\left(\frac{\pi\alpha}{2}\right)}$$

Compare the low freq. DOS for POPC simulations with an all-atom (OPLS) and a coarse-grained (MARTINI) force field:

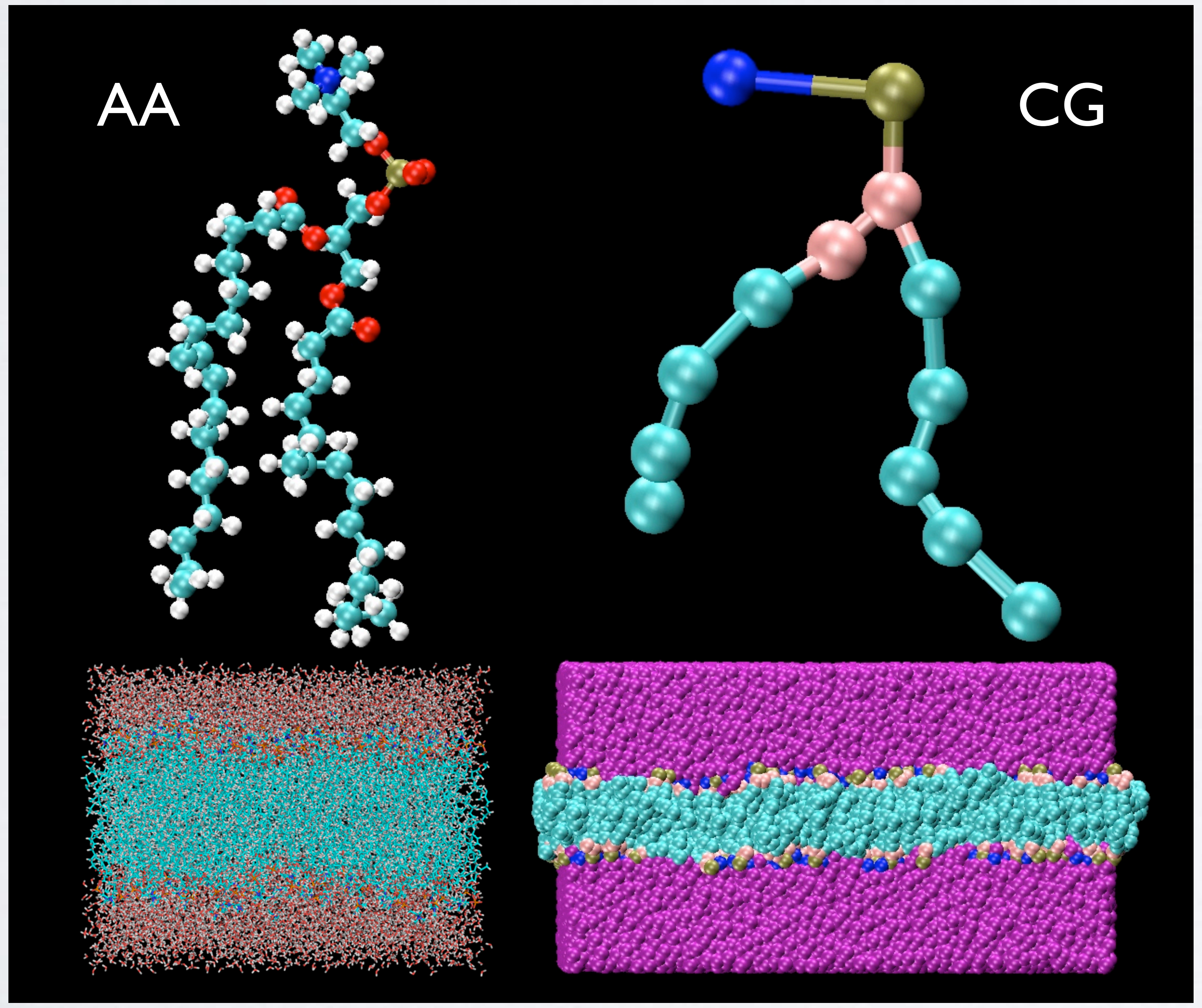

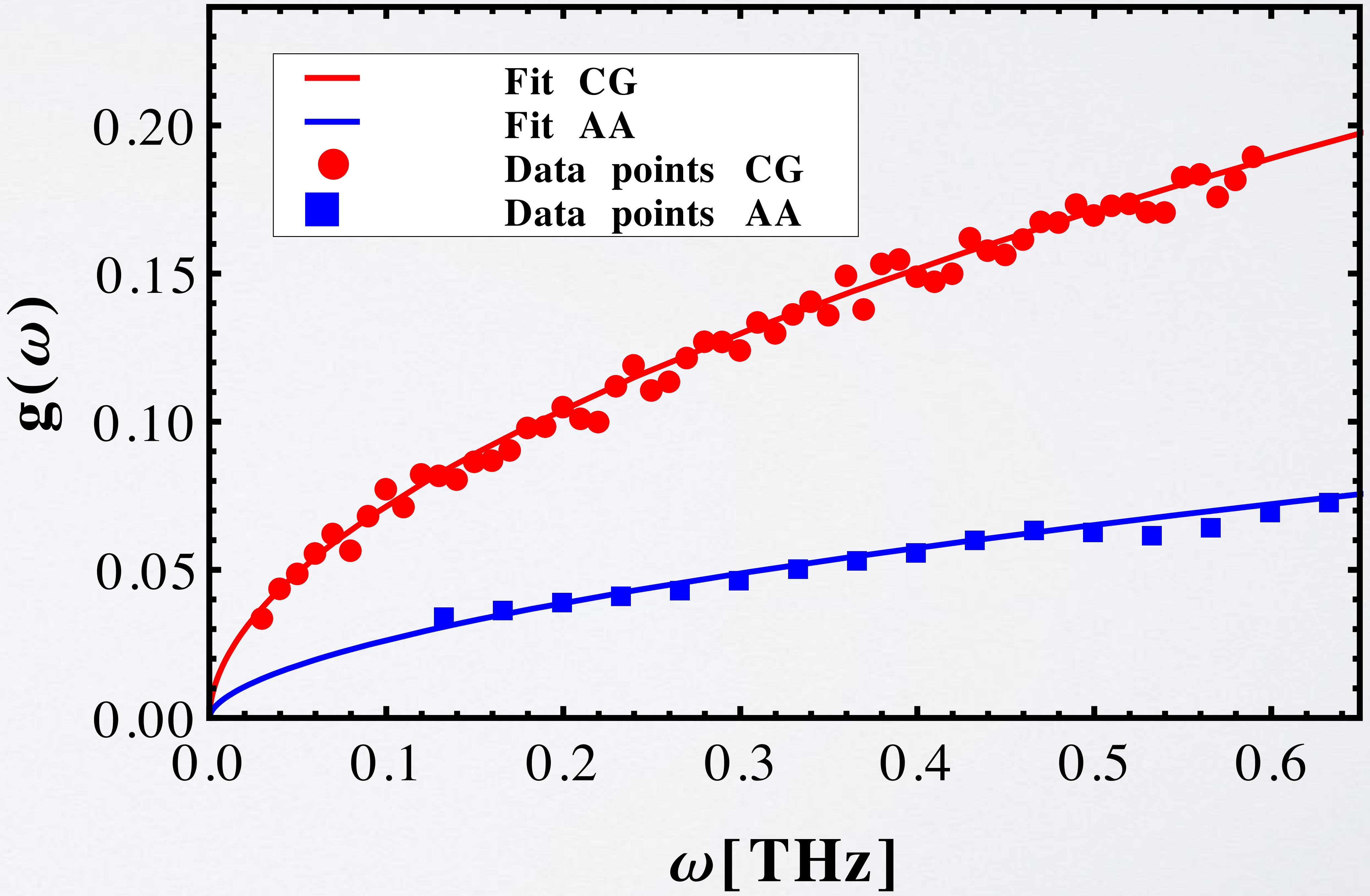

Mean square displacement (log-log)

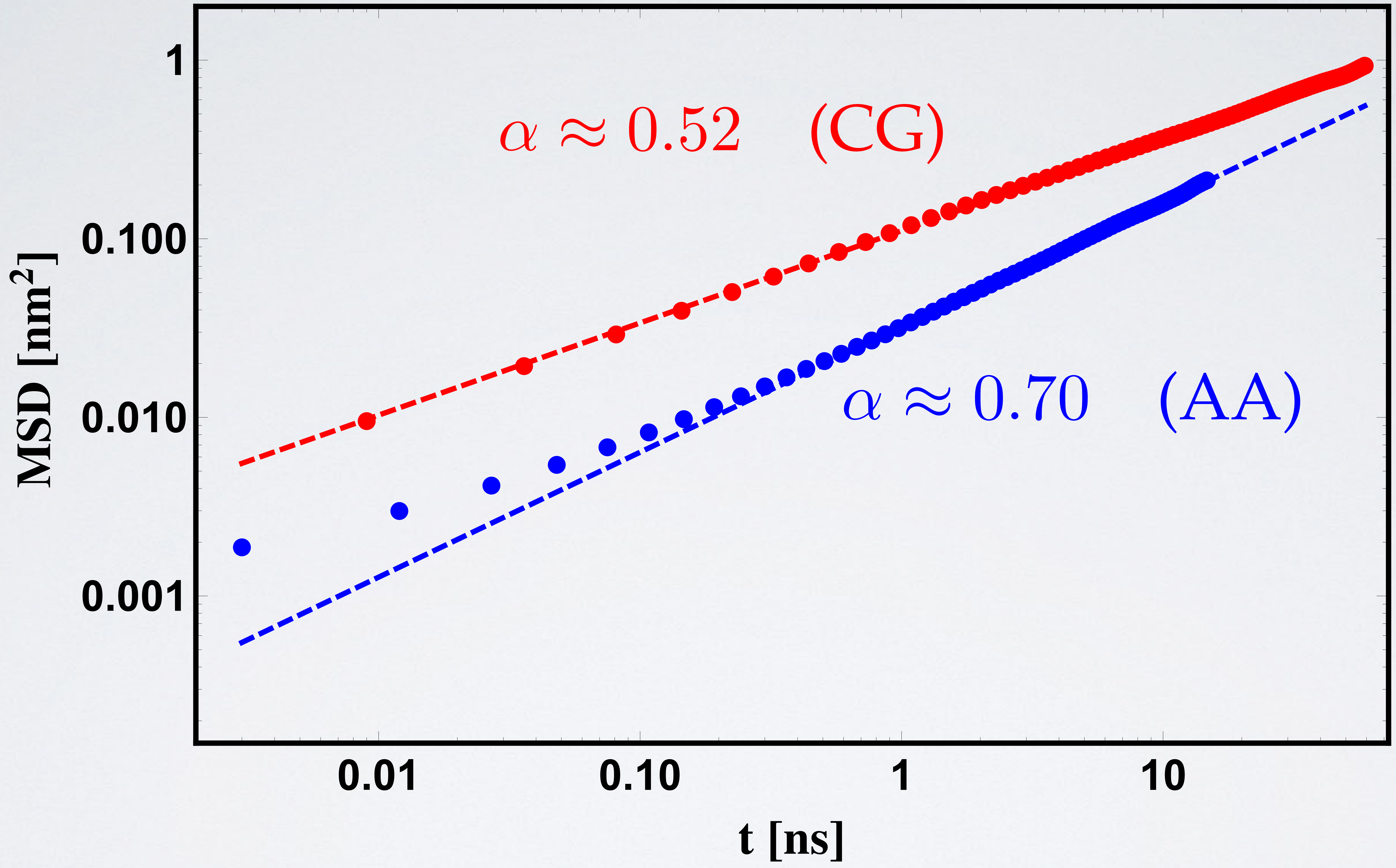

DOS by windowed discrete fast Fourier transform (FFT)

$$g(n) \approx \frac{\Delta t}{2} \sum_{k=-(N_t-1)}^{N_t-1} e^{-\frac{2\pi i n k}{2N_t-1}} w(k) c_{vv}(k)$$

$$w(t) = \exp\left(-t^2/(2\sigma_t^2)\right)$$

DOS by maximum entropy estimation

$$v(n) = \sum_{j=1}^{P} a_j^{(P)} v(n-j) + \epsilon(n)$$

Autoregressive process

$$\langle \epsilon(n) \epsilon(k) \rangle = \sigma_P^2 \delta_{nk}$$

$$g(\omega) \approx \frac{\sigma_P^2 \Delta t}{2 \left| 1 - \sum_{k=1}^{P} a_k^{(P)} \exp(-i\omega k \Delta t) \right|^2}$$

Compare FFT (thin lines) and ME estimation (thick lines)

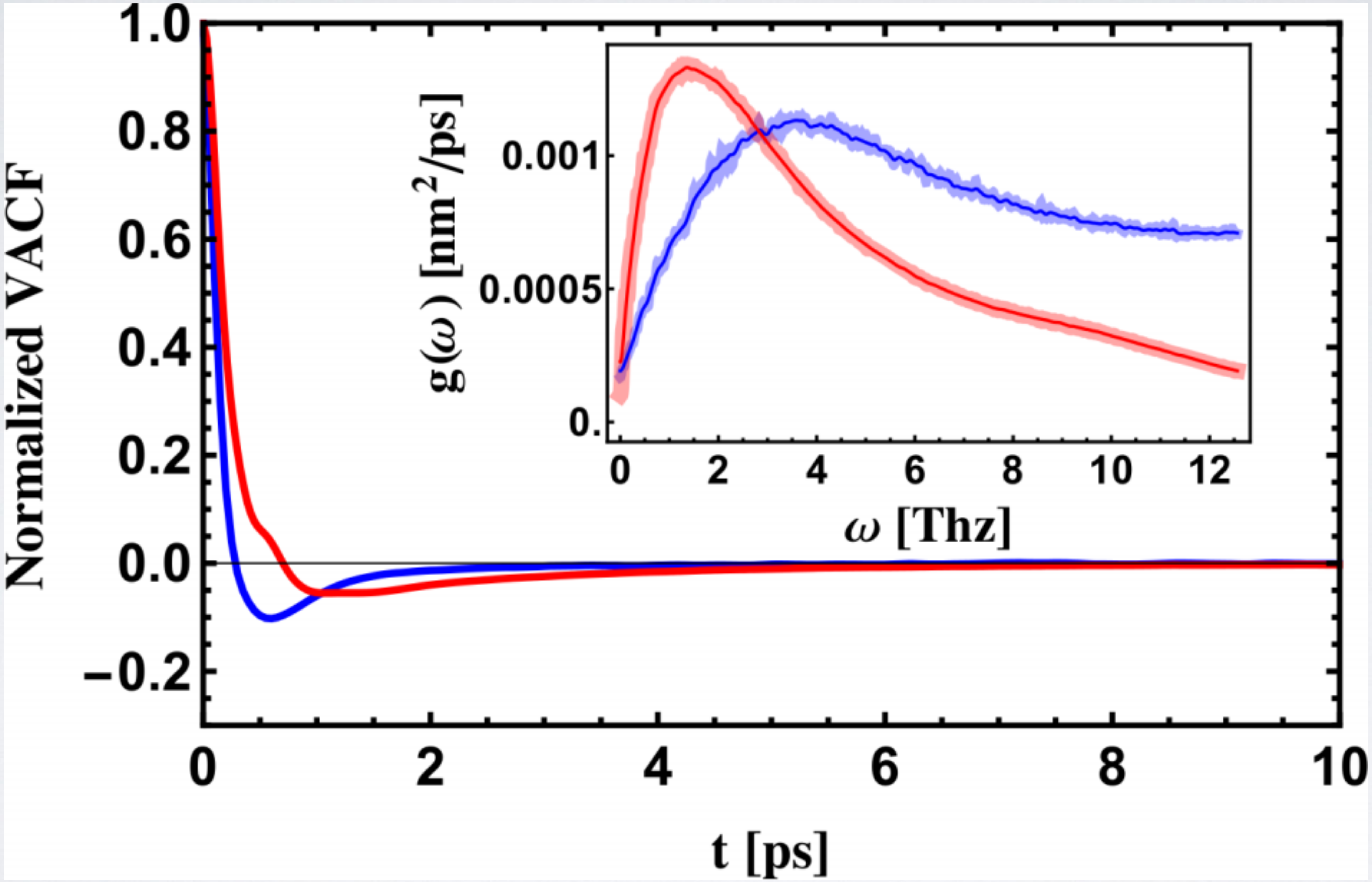

Low frequency DOS - FFT versus MEM estimation

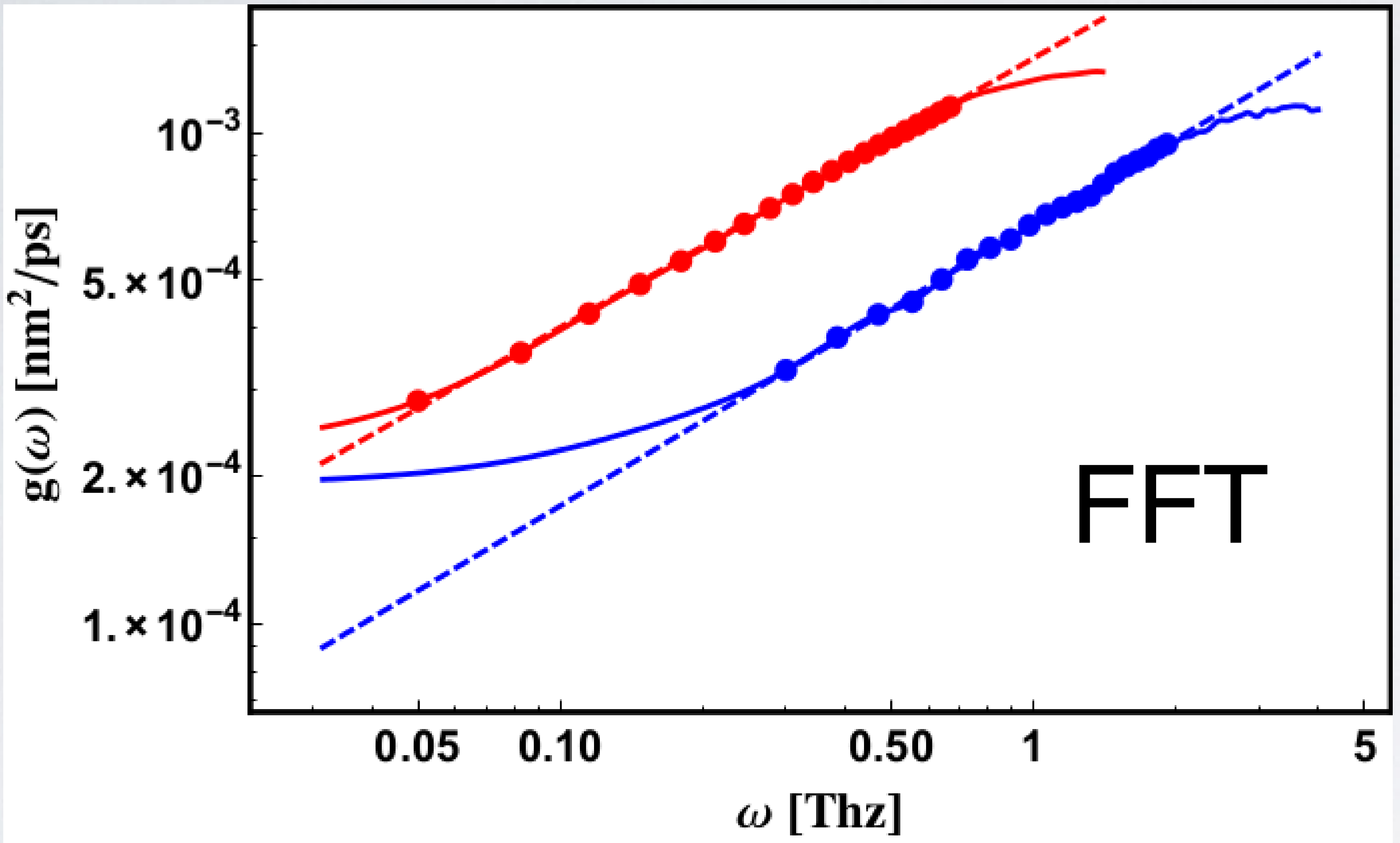

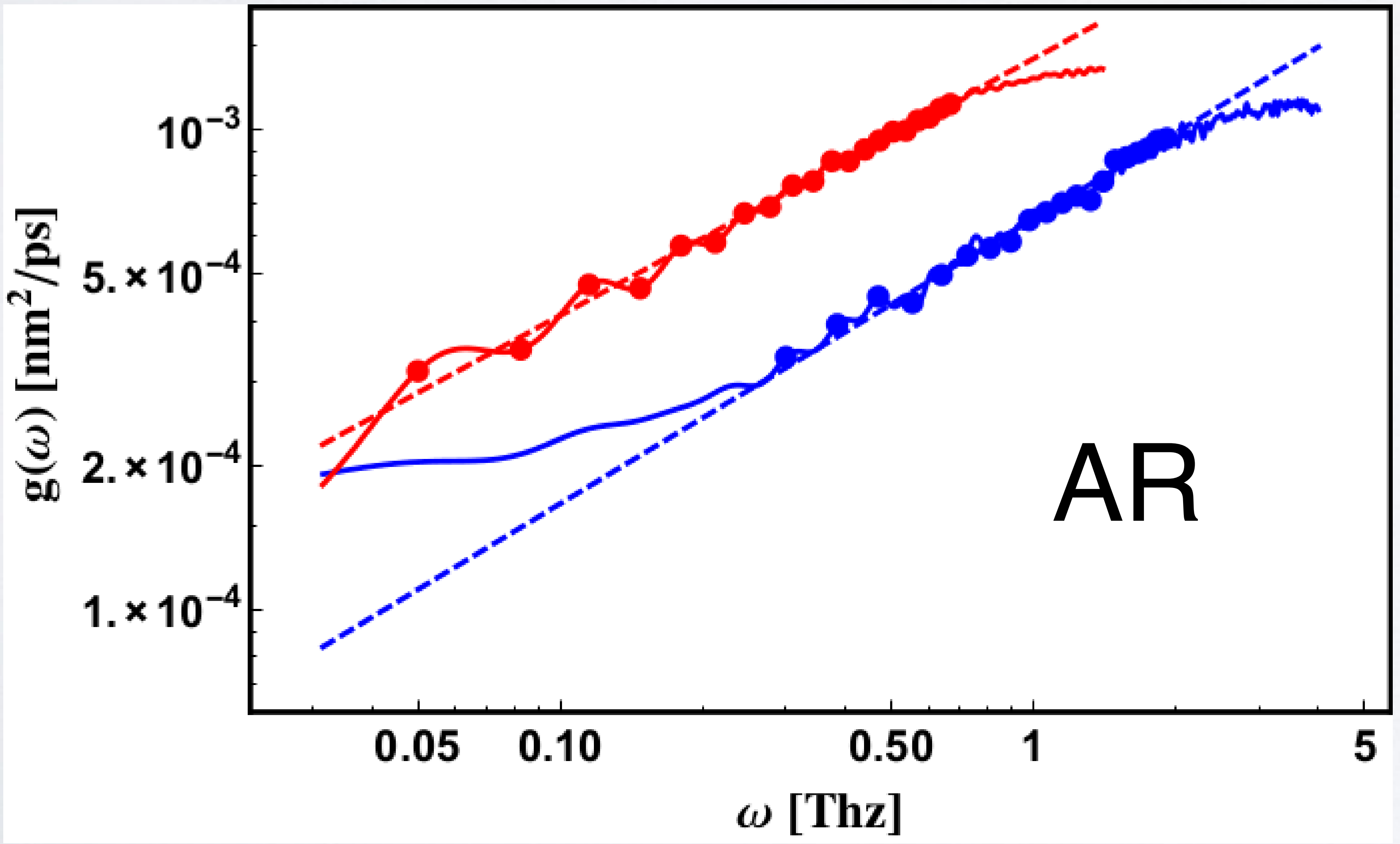

Precision in the lose-frequency regime matters!

Both FFT and AR estimations give very similar results

Long-time tails for DOPC lipid bilayers

G. R. Kneller, K. Baczynski, and M. Pasenkiewicz-Gierula. *J. Chem. Phys.*, 135(14):141105, 2011.

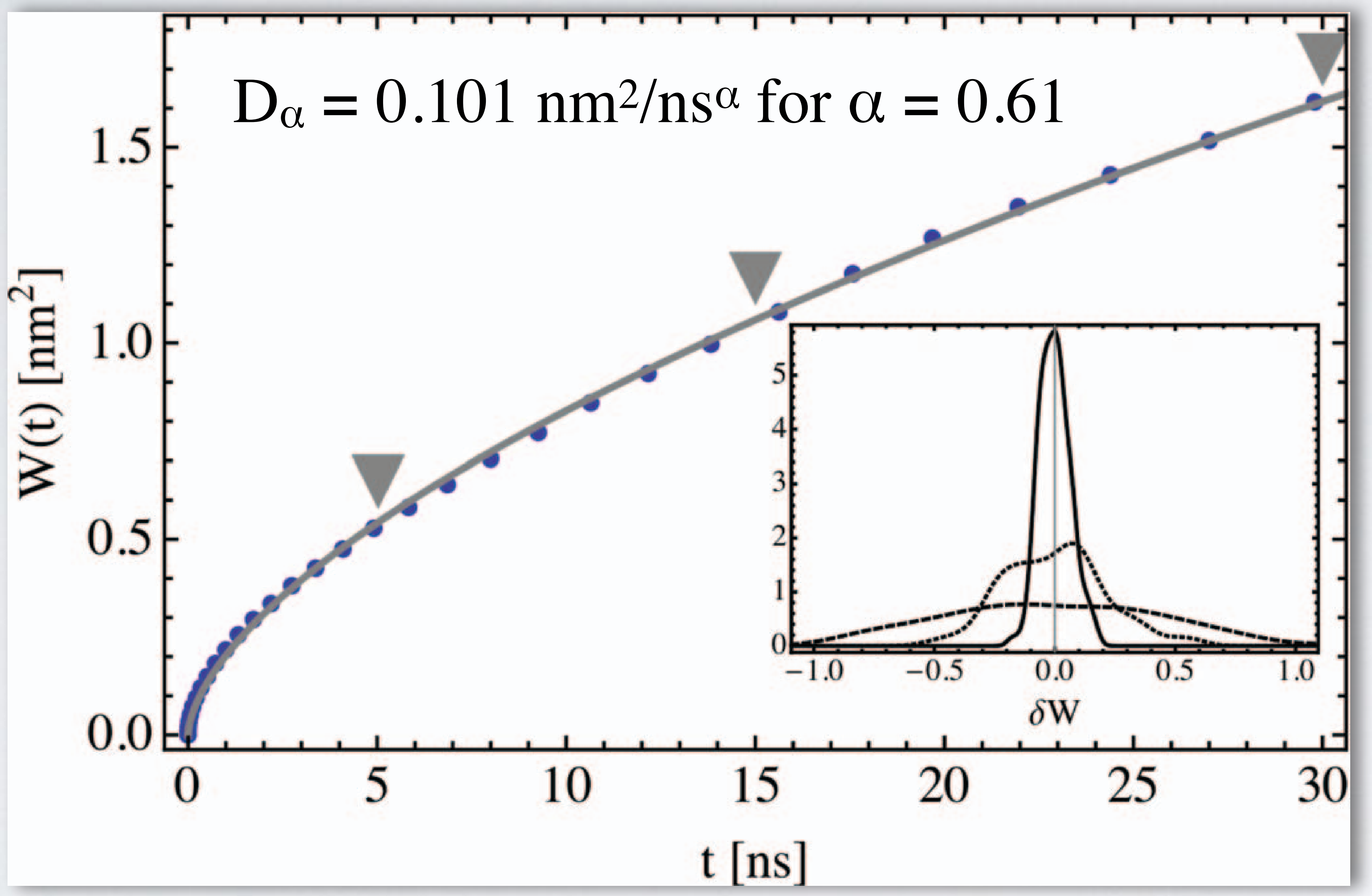

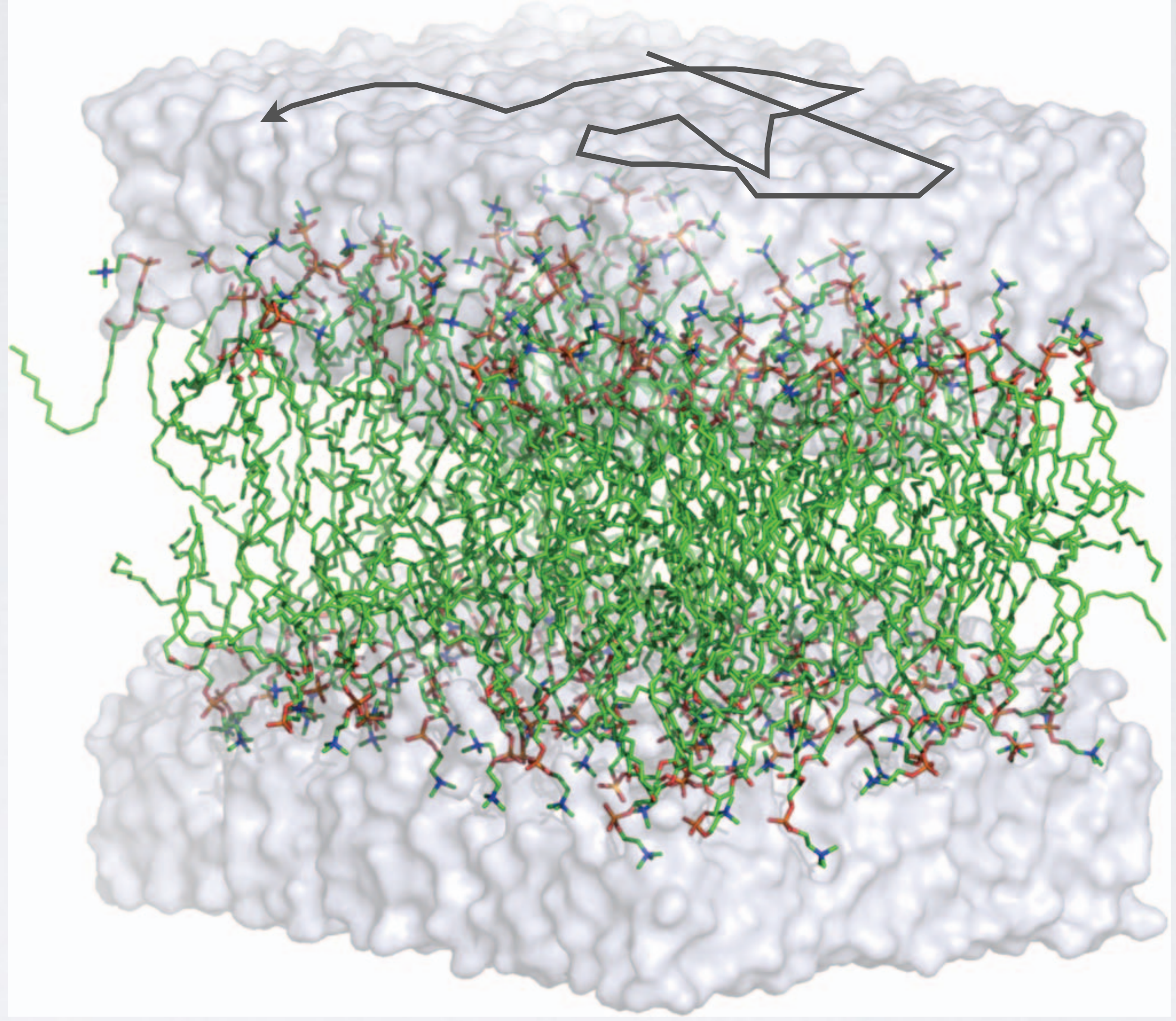

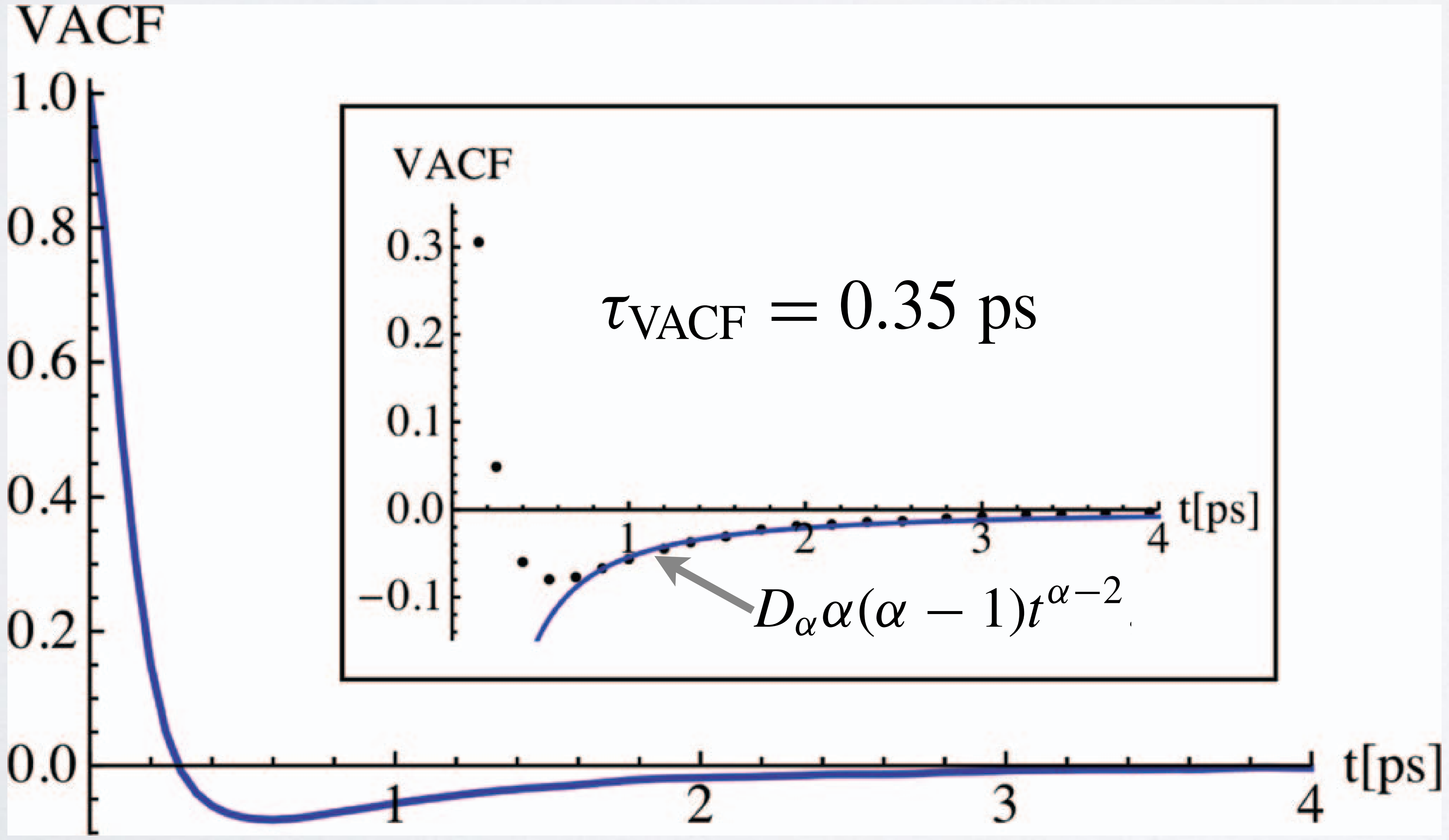

Characteristic time scale:

$$\tau_{\text{VACF}} = \left(\frac{D_\alpha}{\langle \mathbf{v}^2 \rangle}\right)^{1/(2-\alpha)}$$

Memory function and long-time tail

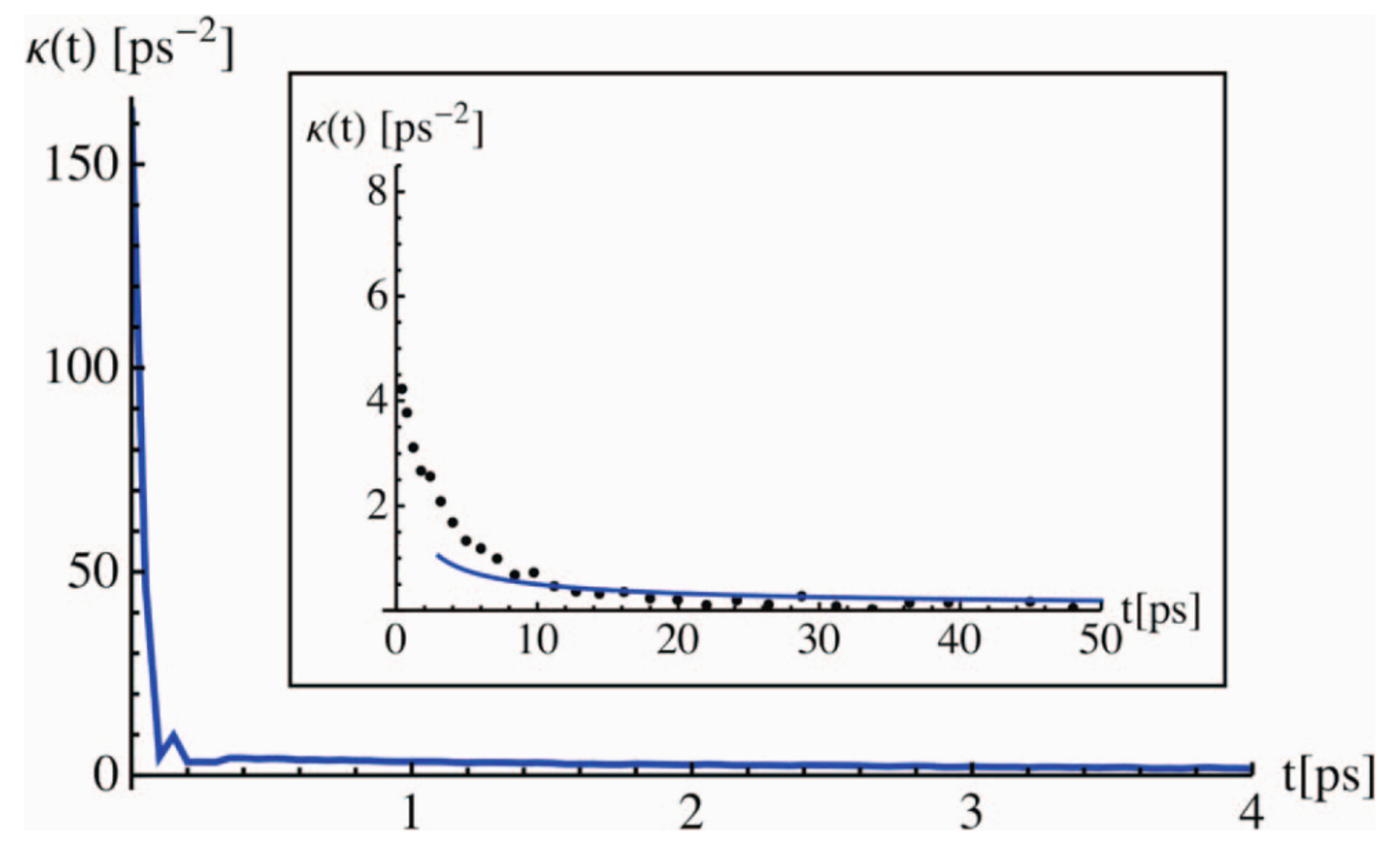

Ongoing work

with Jeremy Smith & Sheeba Malik, Oakridge National Laboratory, USA

MSD, VACF, DOS, and memory function for diffusion of lipids in DMPC at 324 K

Velocity autocorrelation function

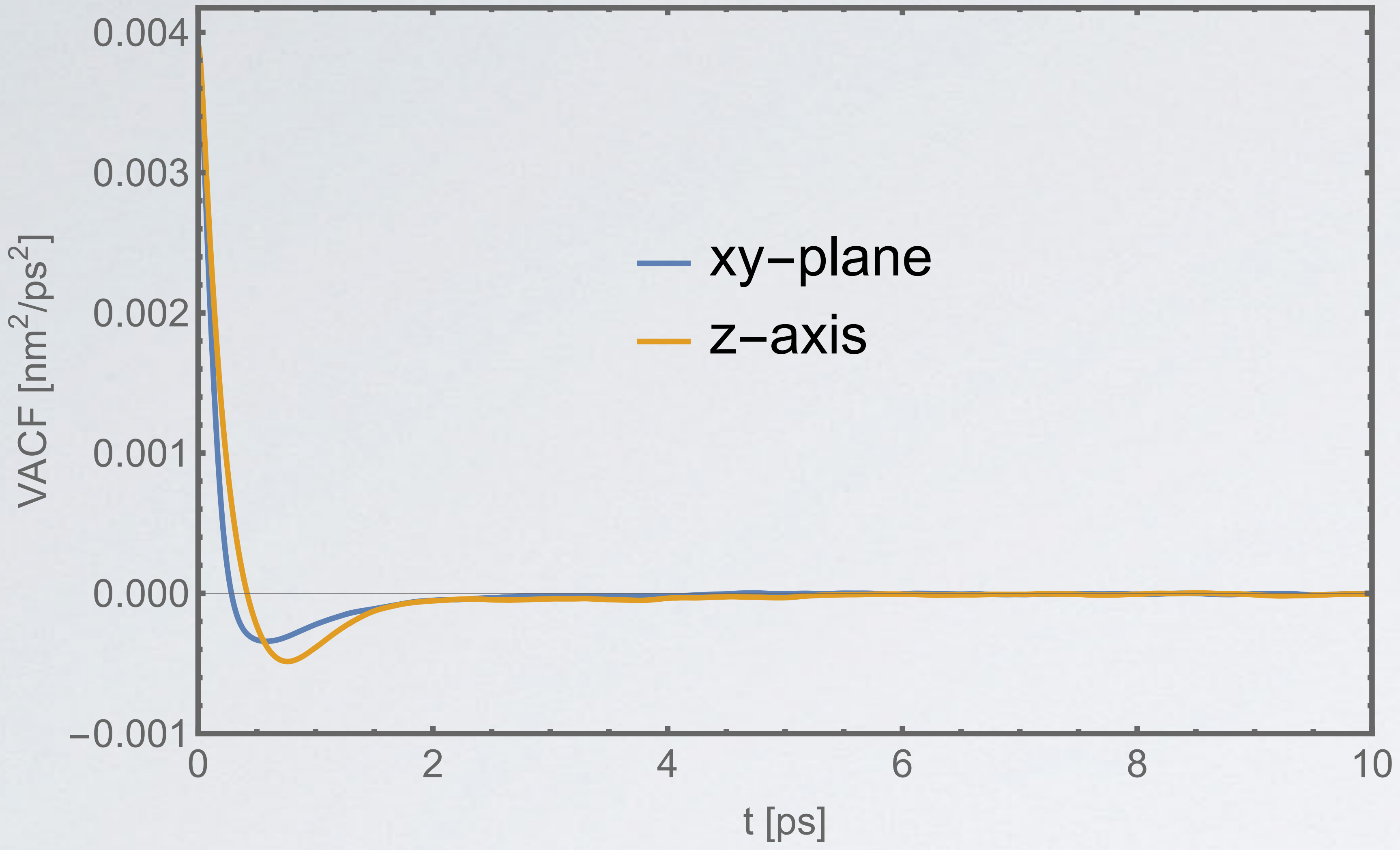

Mean-squared displacement

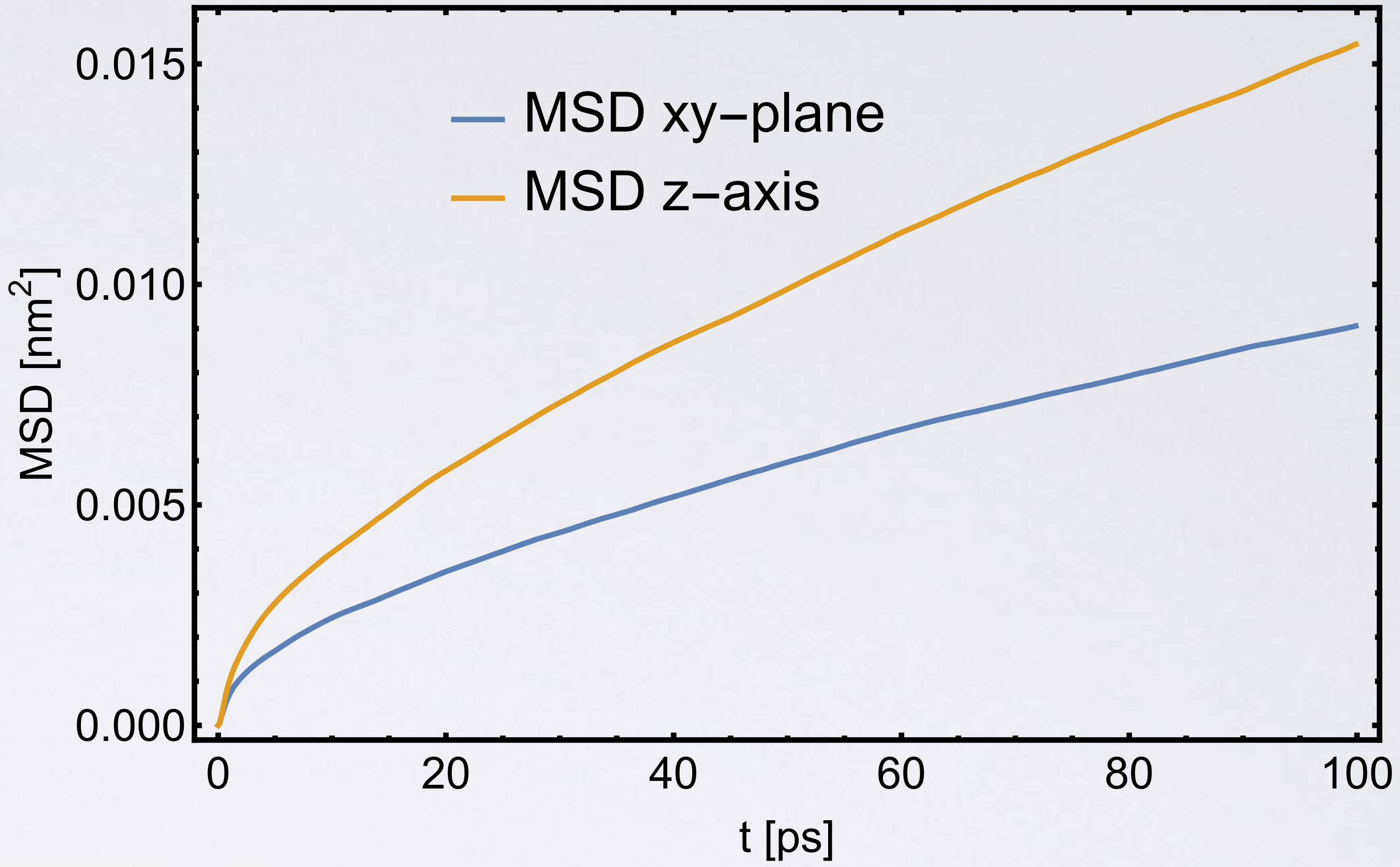

Density-of-states

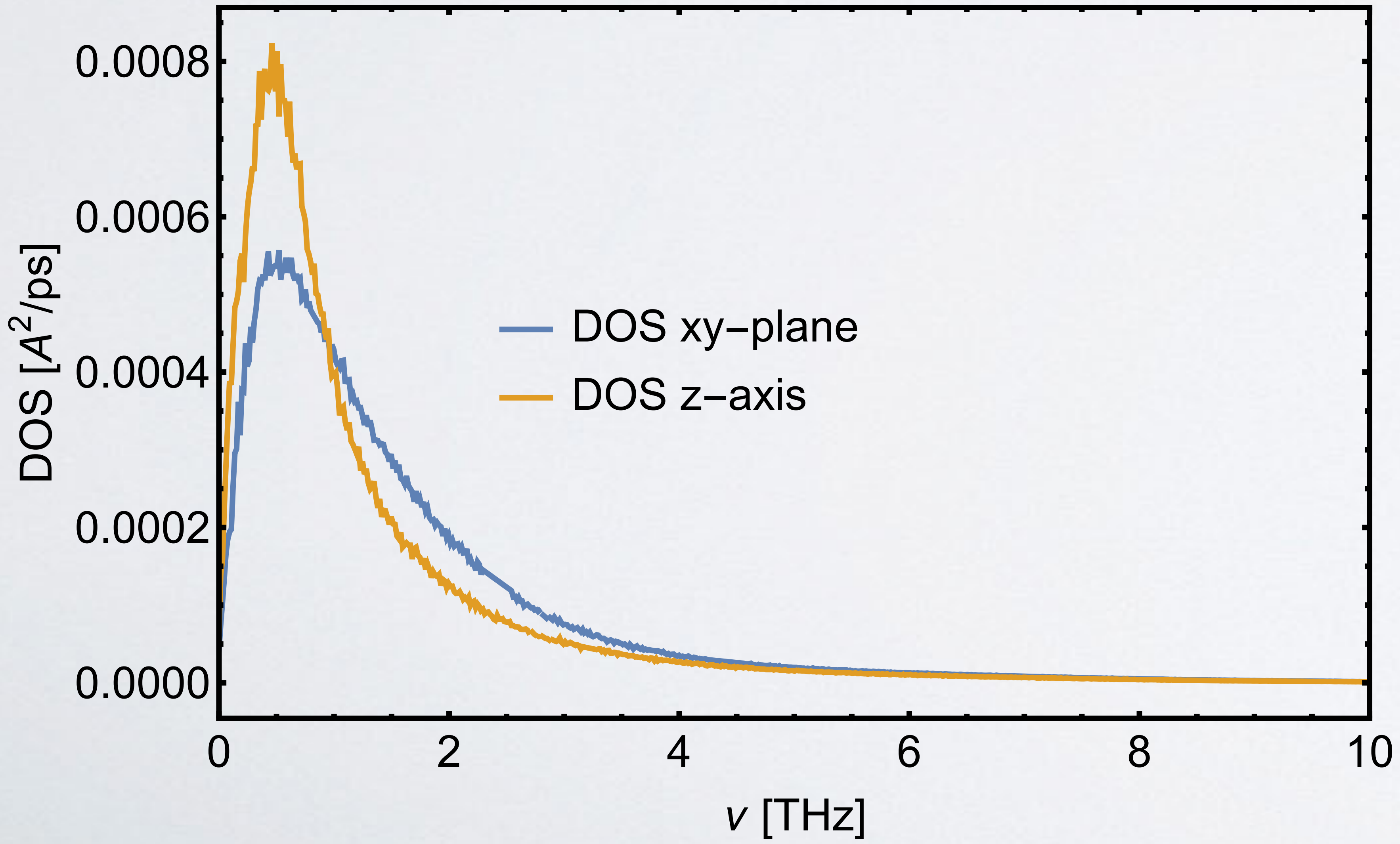

Memory kernel of the VACF

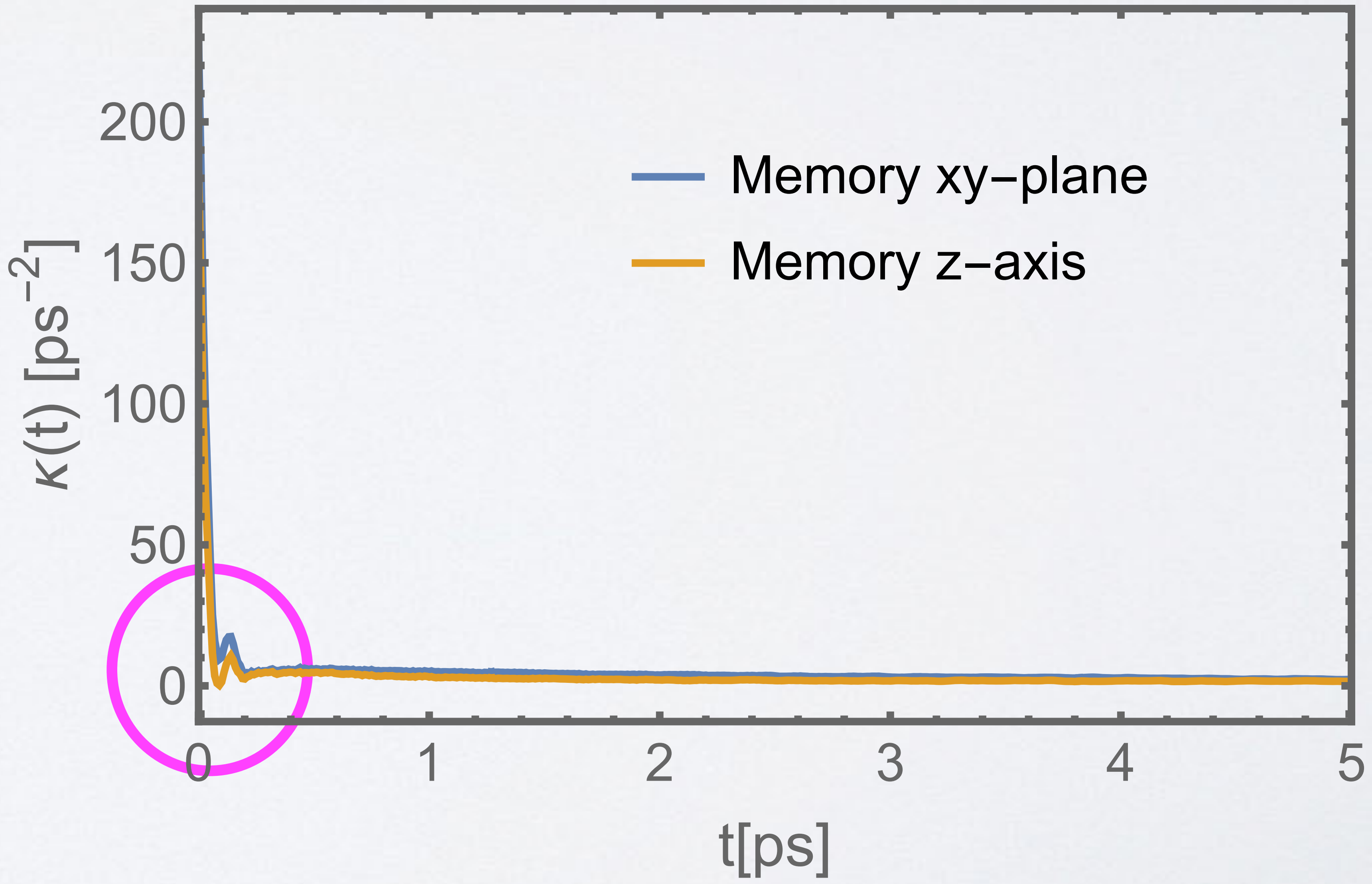

Asymptotic regimes

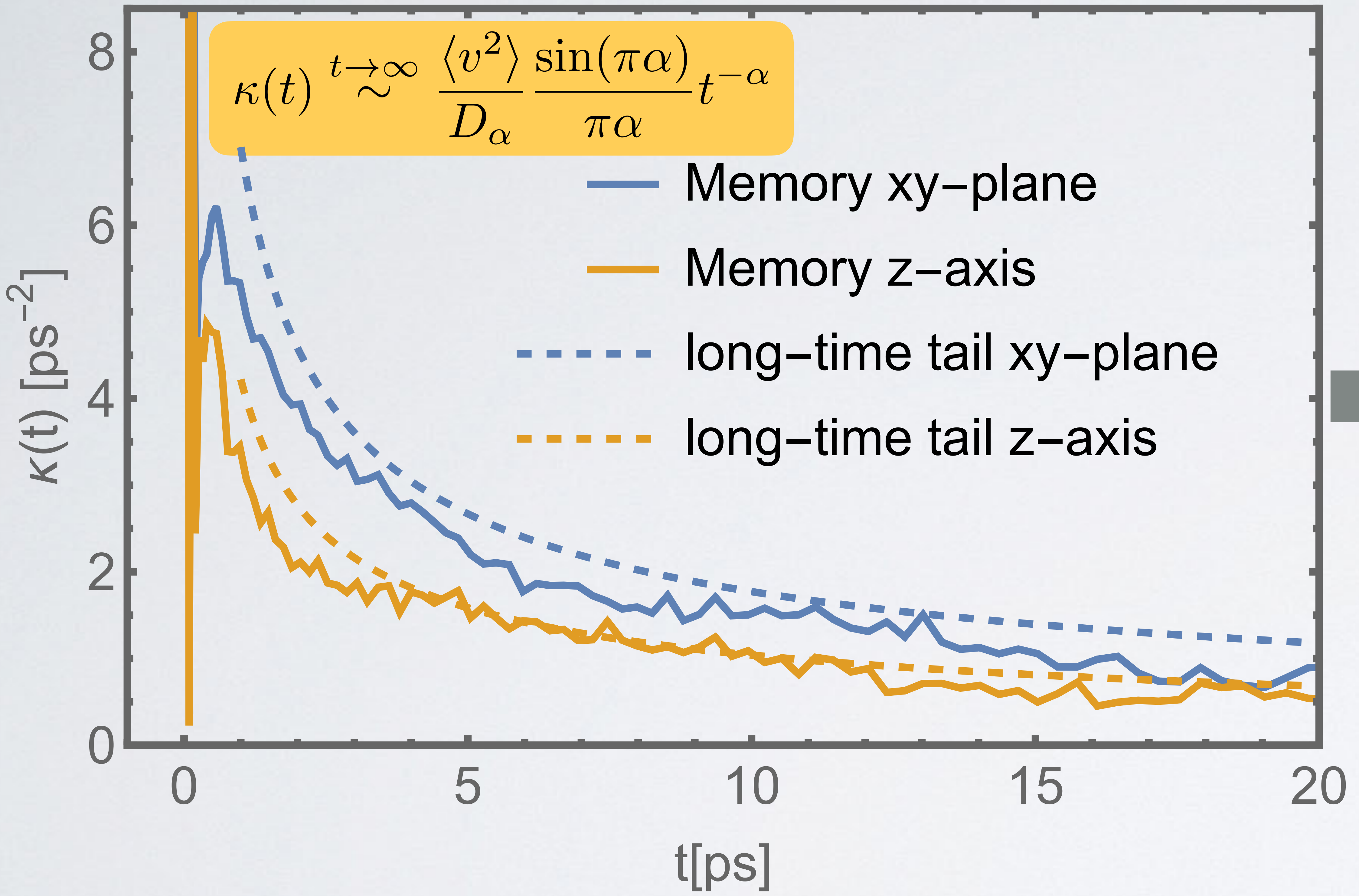

$$\kappa(t) \overset{t\to\infty}{\sim} \frac{\langle v^2\rangle}{D_\alpha}\frac{\sin(\pi\alpha)}{\pi\alpha}t^{-\alpha}$$

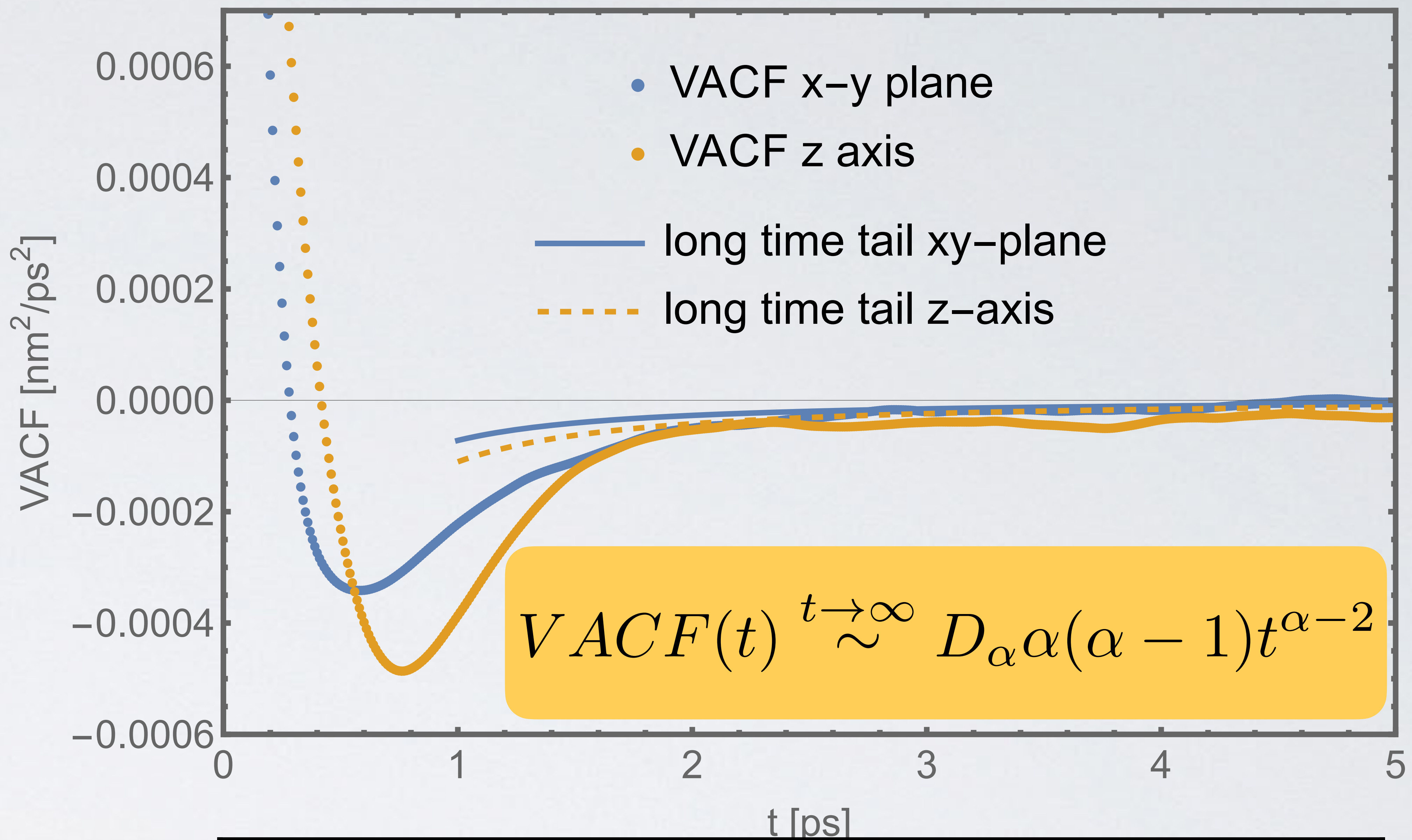

$$VACF(t) \overset{t\to\infty}{\sim} D_\alpha\alpha(\alpha-1)t^{\alpha-2}$$

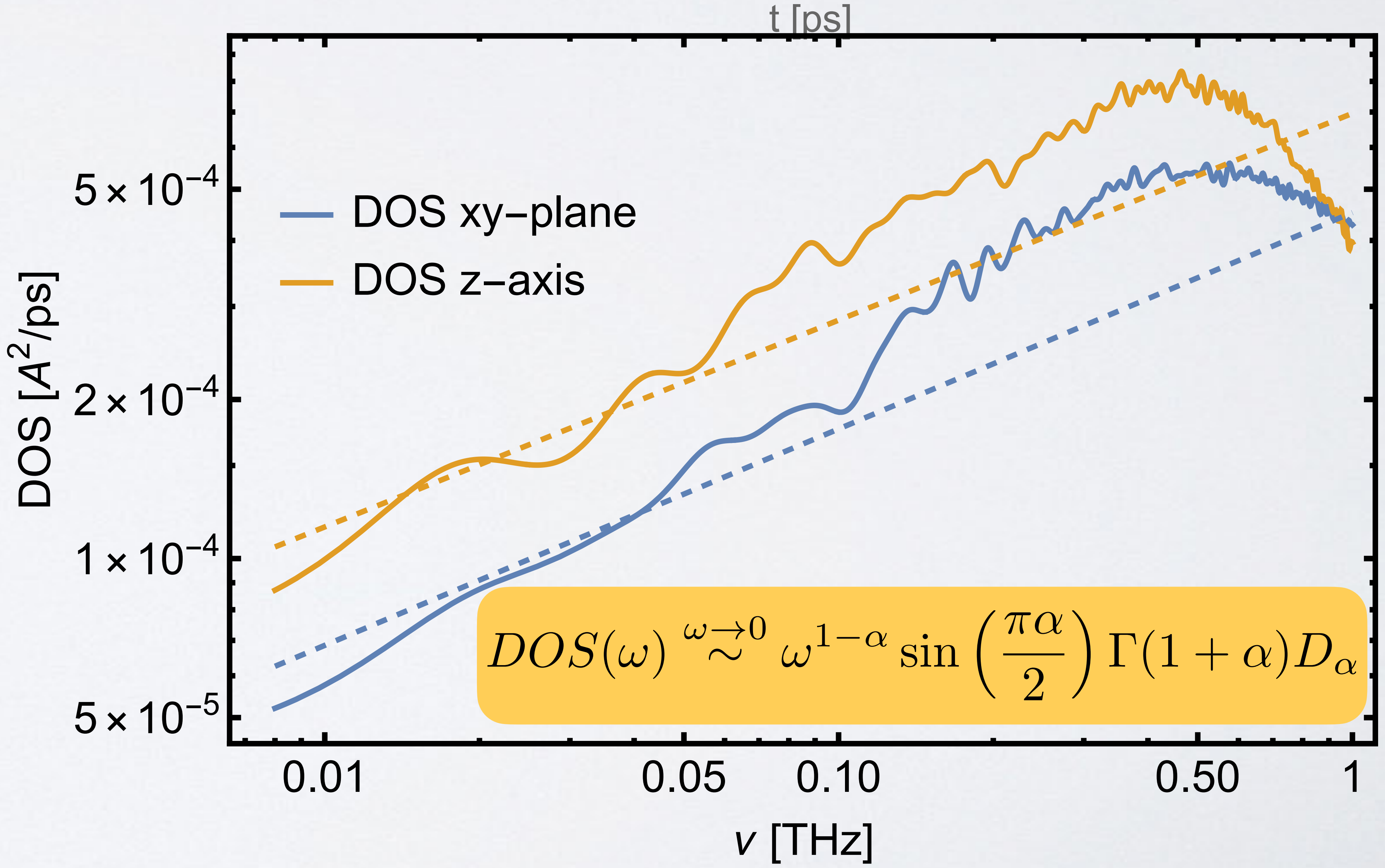

$$DOS(\omega) \overset{\omega\to 0}{\sim} \omega^{1-\alpha}\sin\left(\frac{\pi\alpha}{2}\right)\Gamma(1+\alpha)D_\alpha$$

Memory function at different temperatures

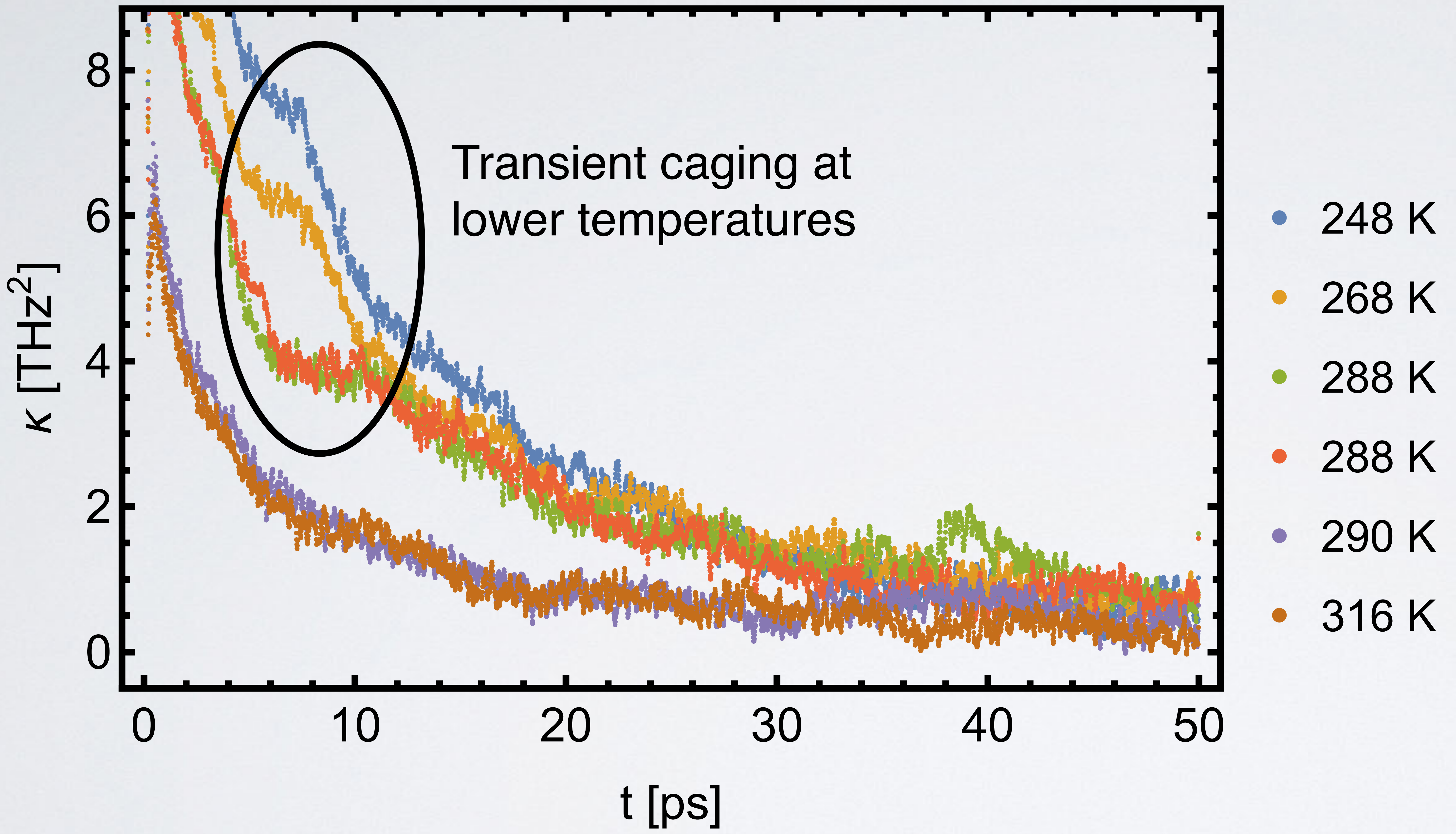

Some algorithms

Calculation of time correlation functions - an « efficient detour » via Fourier space

The correlation theorem of the Fourier transform reads

$$\int_{-\infty}^{+\infty} dt\, f(t+\tau)g^*(\tau) = \frac{1}{2\pi}\int_{-\infty}^{+\infty} d\omega\, \tilde{f}(\omega)\tilde{g}^*(\omega)e^{i\omega t}$$

where

$$\tilde{f}(\omega) = \int_{-\infty}^{+\infty} d\omega\, f(t)e^{-i\omega t},$$

$$f(t) = \frac{1}{2\pi}\int_{-\infty}^{+\infty} d\omega\, \tilde{f}(\omega)e^{i\omega t},$$

is the Fourier transform pair of f.

Computing autocorrelation functions efficiently by FFT

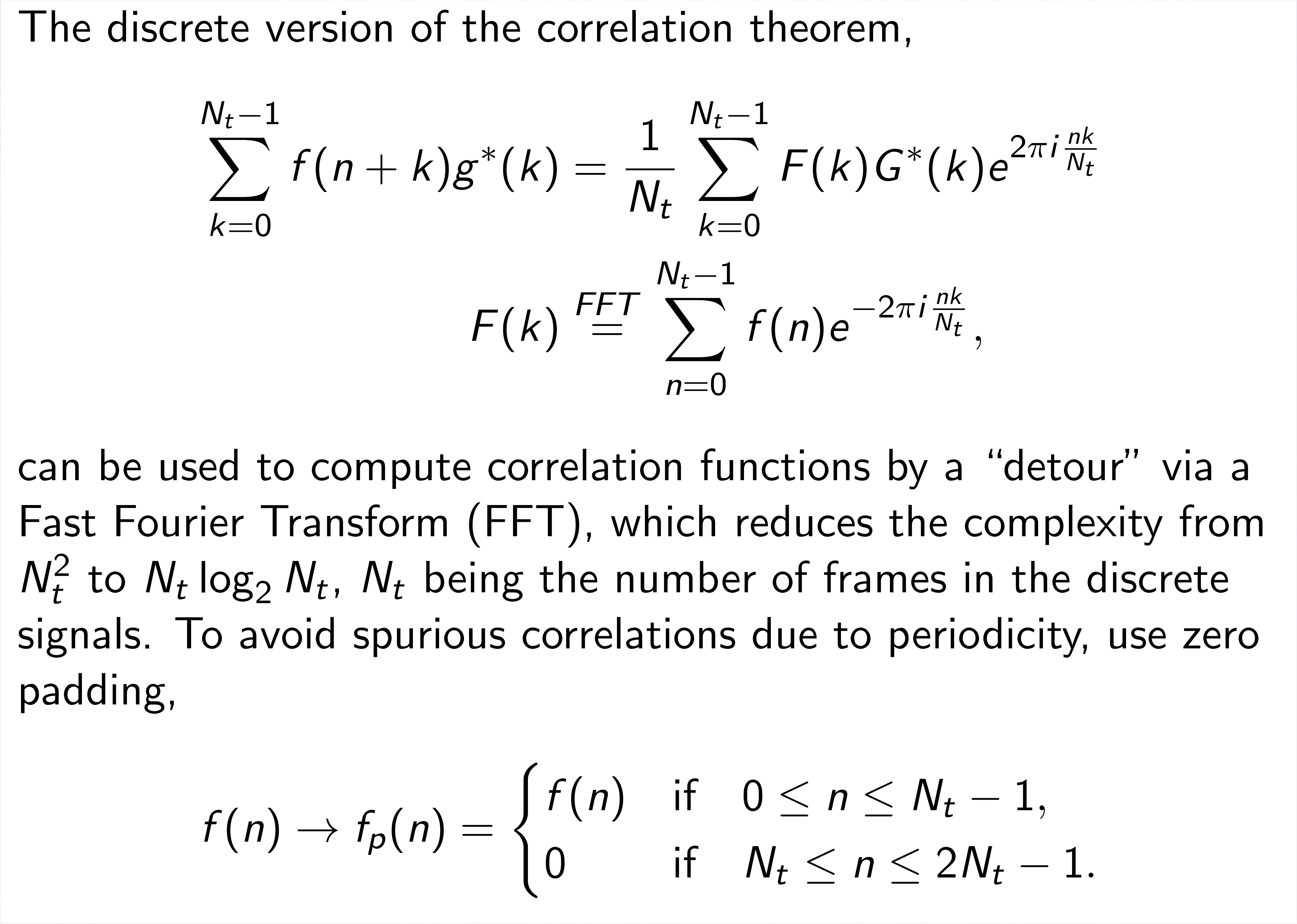

The discrete version of the correlation theorem,

$$\sum_{k=0}^{N_t-1} f(n+k)g^*(k) = \frac{1}{N_t}\sum_{k=0}^{N_t-1} F(k)G^*(k)e^{2\pi i\frac{nk}{N_t}}$$

$$F(k) \overset{FFT}{=} \sum_{n=0}^{N_t-1} f(n)e^{-2\pi i\frac{nk}{N_t}},$$

can be used to compute correlation functions by a "detour" via a Fast Fourier Transform (FFT), which reduces the complexity from N_t^2 to $N_t \log_2 N_t$, N_t being the number of frames in the discrete signals. To avoid spurious correlations due to periodicity, use zero padding,

$$f(n) \to f_p(n) = \begin{cases} f(n) & \text{if} \quad 0 \le n \le N_t - 1, \\ 0 & \text{if} \quad N_t \le n \le 2N_t - 1. \end{cases}$$

$N_t \log(N_t)$ versus N_t^2

Autocorrelation of a discrete and equidistantly sampled signal

```
In[2]:= AC = Function[{x}, Module[{Nt, xp, yp, ac}, Nt = Length[x];
            xp = PadRight[x, 2 * Nt];
            yp = Fourier[xp, FourierParameters → {1, -1}];
            ac = Re[InverseFourier[Conjugate[yp] * yp, FourierParameters → {1, -1}]]]];
```

Computing MSDs

Use here that [6]

$$\left\langle (x(n+k)-x(k))^2 \right\rangle = 2\boxed{\underbrace{\langle x(n+k)x(k)\rangle}_{\text{FCA}}} + \underbrace{\langle x(n+k)^2\rangle}_{\text{recursively}} + \underbrace{\langle x(k)^2\rangle}_{\text{recursively}} .$$

$N_t \log(N_t)$ versus N_t^2

MSD of a discrete and equidistantly sampled trajectory

```
In[3]:= MSD = Function[{x}, Module[{Nt, Sab, SumSq, dsq, msd}, Nt = Length[x];
        dsq = x ^ 2;
        SumSq = 2 * x.x;
        Sab = AC[x];
        msd = Table[0., {i, 1, Nt}];
        Do[SumSq = SumSq - dsq⟦m⟧ - dsq⟦Nt - 2 - m⟧;
         msd⟦m⟧ = (SumSq - 2 Sab⟦m⟧) / (Nt + 1 - m), {m, 2, Nt}];
        msd]];
```

---

[6] G.R. Kneller *et al.*, Comput Phys Commun 91, 191 (1995).

Autoregressive time series model

$$v(n) \equiv v(n\Delta t), \quad n \in \mathbb{Z}.$$

time series

$$\boxed{v(n) = \sum_{k=1}^{P} a_k^{(P)} v(n-k) + \epsilon_P(n)}$$

AR model of order P

$$\begin{aligned} \langle \epsilon_P(n) \rangle &= 0, \\ \langle \epsilon_P(n) \epsilon_P(n') \rangle &= \sigma_P^2 \delta_{nn'}. \end{aligned}$$

"white noise"

parameters of the model: $\alpha_1^{(P)}, \ldots, \alpha_P^{(P)}, \sigma_P$

Wiener-Hopf equations for the coefficients

$$\langle \epsilon_P(n) v(n-k) \rangle = 0 \qquad (k = 1, \ldots, P)$$

$$\boxed{\sum_{k=1}^{P} c_{vv}(|j-k|) a_k^{(P)} = c_{vv}(j), \qquad j = 1 \ldots P}$$

yields the coefficients $a_k^{(P)}$

$$\boxed{\sigma_P^2 = c_{vv}(0) - \sum_{k=1}^{P} a_k^{(P)} c_{vv}(k)}$$

Wiener-Khintchin theorem for discrete signals

- Finite sample of a signal

$$v_M(n) = \begin{cases} v(n) & \text{si} \quad -M \leq n \leq M \\ 0 & \text{sinon} \end{cases}$$

- z-Transform

$$f(n) = \frac{1}{2\pi i} \oint_C dz\, z^{n-1} F_{(>)}(z) \longleftrightarrow \begin{aligned} F(z) &= \sum_{n=-\infty}^{+\infty} f(n) z^{-n}. \\ F_>(z) &= \sum_{n=0}^{\infty} f(n) z^{-n}. \end{aligned}$$

$$(f \circ g)(n) = \sum_{j=-\infty}^{+\infty} f(n+j) g^*(j) \longleftrightarrow F(z) G^*(1/z^*)$$

- Correlation function

$$c_{vv}(n) = \lim_{M \to \infty} \frac{1}{2M+1} \sum_{k=-M}^{M} v(n+k) v^*(k)$$

➡

$$\boxed{C_{vv}(z) = \lim_{M \to \infty} \frac{1}{2M+1} V_M(z) V_M^*(1/z^*)}$$

Analytical form of the z-transformed correlation function

AR model

$$V(z) = \frac{\mathcal{E}_P(z)}{1 - \sum_{k=1}^{P} a_k^{(P)} z^{-k}}$$

$$\lim_{M\to\infty} \frac{1}{2M+1} V(z) V^*(1/z^*) = \frac{\lim_{M\to\infty} \frac{1}{2M+1} \mathcal{E}_P(z) \mathcal{E}_P^*(1/z^*)}{\left(1 - \sum_{k=1}^{P} a_k^{(P)} z^{-k}\right)\left(1 - \sum_{l=1}^{P} a_l^{(P)} z^{l}\right)}$$

$$C_{vv}^{(AR)}(z) = \frac{C_{\epsilon\epsilon}(z)}{\left(1 - \sum_{k=1}^{P} a_k^{(P)} z^{-k}\right)\left(1 - \sum_{l=1}^{P} a_l^{(P)} z^{l}\right)}$$

$$C_{vv}^{(AR)}(z) = \frac{\sigma_P^2}{\left(1 - \sum_{k=1}^{P} a_k^{(P)} z^{-k}\right)\left(1 - \sum_{l=1}^{P} a_l^{(P)} z^{l}\right)}$$

“all pole”
model

Maximum entropy estimation of Fourier transforms

$$\tilde{c}_{vv}^{(AR)}(\omega) = \Delta t \sum_{n=-\infty}^{+\infty} c_{vv}^{(AR)}(n) \exp[-in\omega\Delta t] \approx \tilde{c}_{vv}(\omega)$$

$$\Downarrow$$

$$\tilde{c}_{vv}^{(AR)}(\omega) = \Delta t \, C_{vv}^{(AR)}(\exp(i\omega\Delta t))$$

Estimation which is independent from the standard method by FFT!

Application 1: A simple liquid (argon)

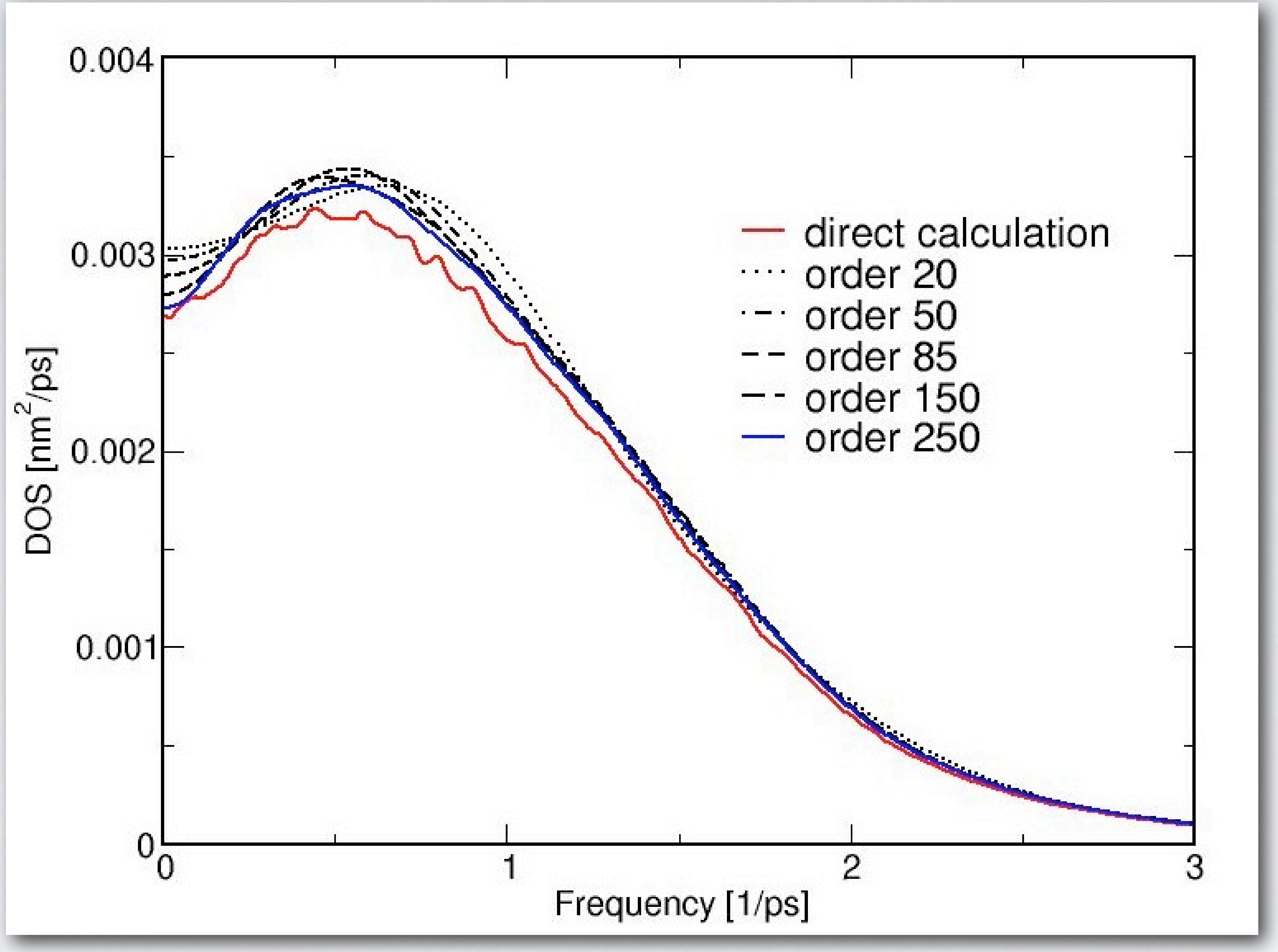

G.R. Kneller and K. Hinsen. *J*. *Chem*. *Phys*., 115(24):11097–11105, 2001.

nMoldyn

http://dirac.cnrs-orleans.fr/nMOLDYN.html

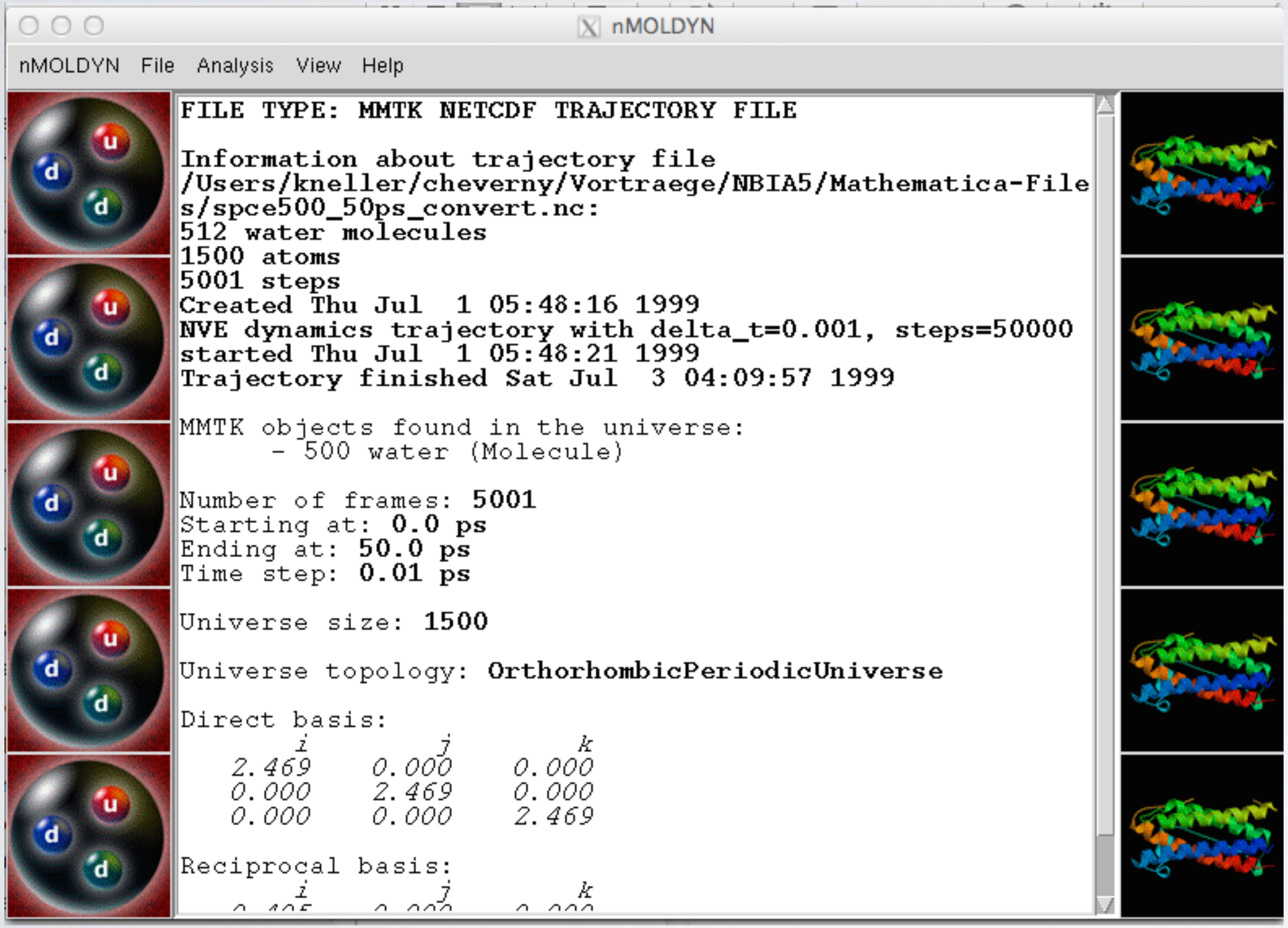

```
FILE TYPE: MMTK NETCDF TRAJECTORY FILE

Information about trajectory file
/Users/kneller/cheverny/Vortraege/NBIA5/Mathematica-File
s/spce500_50ps_convert.nc:
512 water molecules
1500 atoms
5001 steps
Created Thu Jul  1 05:48:16 1999
NVE dynamics trajectory with delta_t=0.001, steps=50000
started Thu Jul  1 05:48:21 1999
Trajectory finished Sat Jul  3 04:09:57 1999

MMTK objects found in the universe:
     - 500 water (Molecule)

Number of frames: 5001
Starting at: 0.0 ps
Ending at: 50.0 ps
Time step: 0.01 ps

Universe size: 1500

Universe topology: OrthorhombicPeriodicUniverse

Direct basis:
           i           j           k
      2.469       0.000       0.000
      0.000       2.469       0.000
      0.000       0.000       2.469

Reciprocal basis:
           i           j           k
```

- Mean squared displacements
- Velocity auto correlation function (VACF)
- Dynamic and static scattering functions (F(q,t), S(q), EISF(q))
- Memory functions (VACF, F(q,t))
- Fourier spectra of time correlation functions by FFT and ME estimation (VACF, F(q,t))
- Rigid-body motions
- Angular velocity ACF
- Reorientational ACFs

References

1. G.R. Kneller, V. Keiner, M. Kneller, and M. Schiller, Comp. Phys. Commun. 91, 191 (1995).
2. T. Rog, K. Murzyn, K. Hinsen, and G.R. Kneller, J Comp. Chem. 24, 657 (2003).
3. V. Calandrini, E. Pellegrini, P. Calligari, K. Hinsen, and G.R. Kneller, Collection SFN 12, 201 (2011).
4. K. Hinsen, E. Pellegrini, S. Stachura, and G.R. Kneller, J Comp. Chem. 33, 2043 (2012).

RÉPUBLIQUE FRANÇAISE
Liberté
Égalité
Fraternité

anr® agence nationale de la recherche
AU SERVICE DE LA SCIENCE

Simulating experiments on protein structure and dynamics – SPUTNIK

with M. Johnson, ILL

Be creative — the core code is extremely compact !

Wolfram Mathematica® code

Remove periodic boundary conditions

```
In[1]:= RemovePBC =
          Function[{x, box}, Module[{dx, dxCorr, xout, Nt, i}, dx = Differences[x];
            dxCorr = Table[Which[dx⟦i⟧ > box⟦i⟧ / 2, dx⟦i⟧ - box⟦i⟧, dx⟦i⟧ < -box⟦i⟧ / 2, dx⟦
                 i⟧ + box⟦i⟧, -box⟦i⟧ / 2 ≤ dx⟦i⟧ ≤ box⟦i⟧ / 2, dx⟦i⟧], {i, 1, Length[dx]}];
            xout = Accumulate[dxCorr] + x⟦1⟧]];
```

Autocorrelation of a discrete and equidistantly sampled signal

```
In[2]:= AC = Function[{x}, Module[{Nt, xp, yp, ac}, Nt = Length[x];
            xp = PadRight[x, 2 * Nt];
            yp = Fourier[xp, FourierParameters → {1, -1}];
            ac = Re[InverseFourier[Conjugate[yp] * yp, FourierParameters → {1, -1}]]]];
```

MSD of a discrete and equidistantly sampled trajectory

```
In[3]:= MSD = Function[{x}, Module[{Nt, Sab, SumSq, dsq, msd}, Nt = Length[x];
            dsq = x ^ 2;
            SumSq = 2 * x.x;
            Sab = AC[x];
            msd = Table[0., {i, 1, Nt}];
            Do[SumSq = SumSq - dsq⟦m⟧ - dsq⟦Nt - 2 - m⟧;
             msd⟦m⟧ = (SumSq - 2 Sab⟦m⟧) / (Nt + 1 - m), {m, 2, Nt}];
            msd]];
```

Corresponding Jupyter notebooks

https://gchevrot.github.io/WebNmoldyn/

Coherent intermediate scattering function

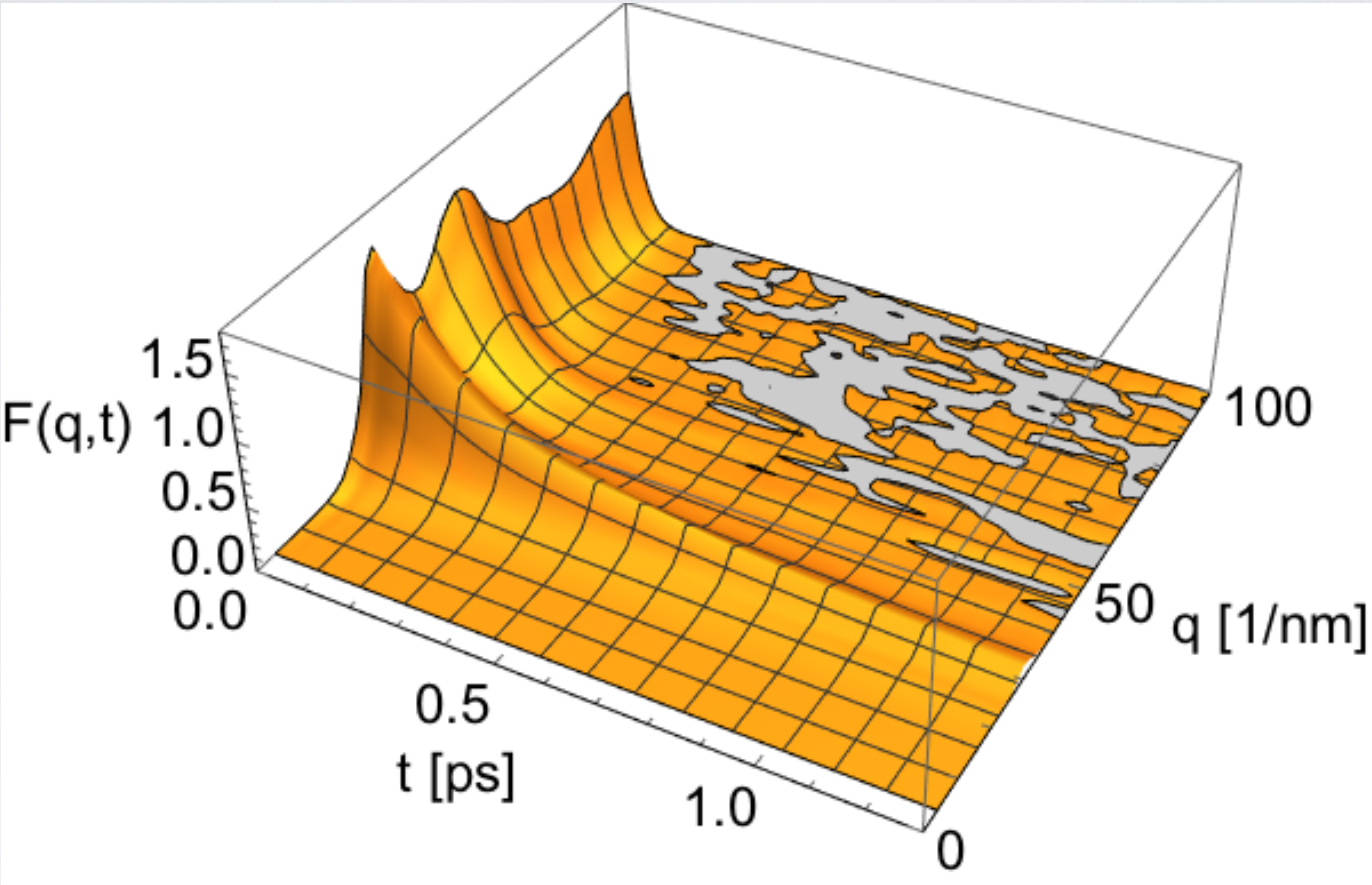

Coherent dynamic structure factor

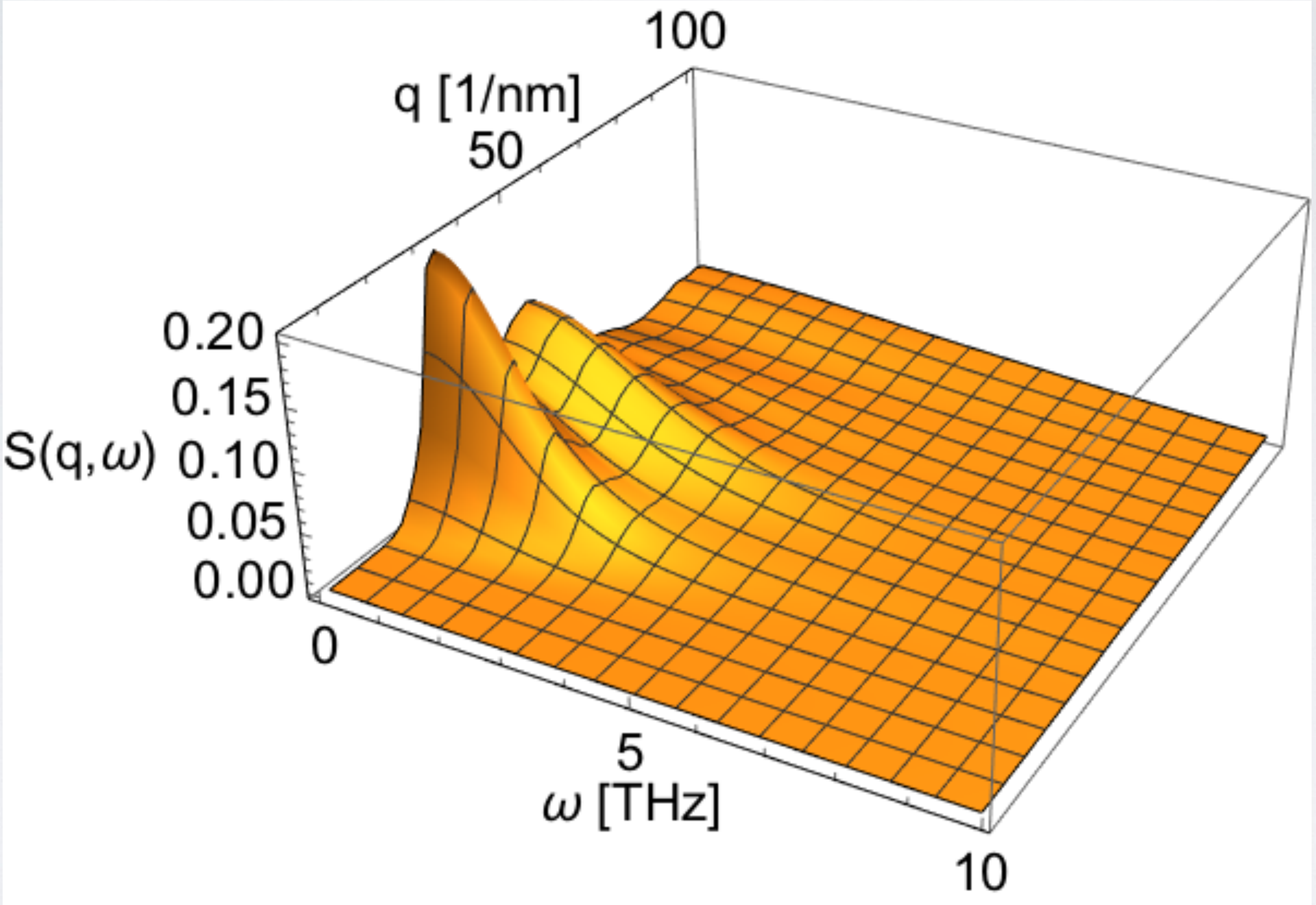

Asymptotic forms of the VACF and its memory function

Kneller, G. R. , J Chem Phys 134, 224106 (2011).

1. Mathematics (Tauberian theorem)

$$W(t) \overset{t\to\infty}{\sim} 2D_\alpha L(t) t^\alpha$$

$$0 < \alpha < 2$$

$$\lim_{t\to\infty} L(t) = 1$$

2. Physics

$$W(t) = 2\int_0^t d\tau\,(t-\tau)c_{vv}(\tau)$$

$$\frac{dc_{vv}(t)}{dt} = -\int_0^t d\tau\,\kappa(t-\tau)c_{vv}(\tau)$$

Memory function

$$c_{vv}(t) \overset{t\to\infty}{\sim} D_\alpha \alpha(\alpha-1)L(t)t^{\alpha-2},$$

$$\kappa(t) \overset{t\to\infty}{\sim} \frac{\langle \mathbf{v}^2\rangle}{D_\alpha}\frac{\sin(\pi\alpha)}{\pi\alpha}\frac{1}{L(t)}t^{-\alpha}.$$